ANALYSIS OF THE CYCLIC CHARACTER OF SILICICLASTIC SEDIMENTS AT THE NEW JERSEY CONTINENTAL SHELF USING ULTRA-HIGH RESOLUTION 3D SEISMIC AND WELL DATA

by

Masoud Aali

Submitted in partial fulfilment of the requirements
for the degree of Doctor of Philosophy

at

Dalhousie University
Halifax, Nova Scotia
October 2020

TABLE OF CONTENTS

LIST OF FIGURES

ABSTRACT

This dissertation describes the development and application of geophysical techniques to understand the impact of eustasy on the deposition of shallow-marine stratigraphic sequences at the New Jersey margin − one of the best places to study eustasy in sedimentary records. At this margin, eustasy has been the leading driver for sedimentary processes due to smooth thermal subsidence, continuous sediment supply, and stable tectonic history since the Oligocene. This study analyzes 564 km^2 of 3D multi-channel seismic (MCS) data from the research cruise MGL1510 together with the IODP Expedition 313 well data to answer the following questions about the margin evolution: 1) What was the influence of eustatic changes on the shelf sedimentary structure during the late Miocene? 2) What was the impact of well-established orbital parameters on the spatial and temporal variations in processes controlling Miocene stratigraphic sequences?

I developed the Geometrical Breakdown Approach (GBA) to systematically identify seismic packages based on their geometrical characteristics. The GBA facilitates an objective analysis of stratal patterns and brings the resolution of sequence stratigraphic analysis up to the resolution of the input seismic data. Implementing GBA to the 3D MCS data has resulted in identification of ~40% more structure within the Miocene sequences than previously determined. The new structural model provides the framework for estimating spatial patterns of petrophysical properties within clinothems, which may act as a heterogeneous conduit barrier system to fluid flow in offshore fresh-water aquifers and hydrocarbon reservoirs. The integrated methodology used in this research results in an unprecedented 3D model that dissects and characterizes the Miocene sedimentary record at a significantly higher resolution (~5 m laterally) than previously achieved (~100s of m).

Spectral analysis of the cyclicity of these sediments yields local spectral peaks at a wide range of periods, from 25 Kyr to 2.5 Myr, that correspond to the cyclicity observed in insolation due to changes in the Earth's orbital parameters. The onshore-offshore movements of sequences show a 42% correlation with their contemporary insolation. These findings suggest that even short-period orbitally-driven eustatic changes had a direct impact on the Miocene sedimentary record of the margin.

LIST OF ABBREVIATIONS AND SYMBOLS USED

DFB	Downstepping-Forestepping-Backstepping
DFF	Downstepping-Forestepping-Forestepping
FSST	Falling Stage Systems Tract
HST	Highstand Systems Tract
Kyr	Thousand Years
LST	Lowstand Systems Tract
MRS	Maximum Regressive Surface
MTS	Maximum Transgressive Surface
Mya	Million Years Ago
Myr	Million Years
SB	Sequence Boundary
TST	Transgressive Systems Tract
UBB	Upstepping-Backstepping-Backstepping
UBF	Upstepping-Backstepping-Forestepping
δA	Rate of Accommodation Creation
δS	Rate of Sediment Flux

ACKNOWLEDGEMENTS

My Ph.D. research started with an expedition and has evolved into a learning journey, one that carries on beyond this dissertation. I would like to express my appreciation to a number of people who have been great companions during my Ph.D. research. The completion of this dissertation would not have been possible without their assistance, support, and encouragement.

I am grateful to Prof. Mladen Nedimović, for his continuous support, thoughtfulness, and supervision during my Ph.D. research. I would like to express my appreciation to Dr. Craig Fulthorpe, Dr. Gregory Mountain, Dr. Vittorio Maselli, Dr. David Reynolds, Dr. Martin Gibling, and Dr. Jamie Austin for their contributions, insightful comments, and constructive criticism. I would like to extend my sincere thanks to Mr. Bill Richards for the invaluable discussions and unwavering guidance during our meetings. I wish to express my gratitude to Dr. Nick Culshaw and Rebecca (Becky) Jameson for their rewarding courses during the first year of my program, and Dr. Grant Wach for his positivity and support during my professional competitions. Special thanks to Dr. James Brenan, Ms. Darlene Van de Rijt, and Ms. Norma Keeping, the department's chair and administration staff for their warm and supportive attitude during my studies in the Department of Earth and Environmental Sciences at Dalhousie University. Lastly, I would like to acknowledge the support of the Transatlantic Ocean System Science and Technology (TOSST) program at Dalhousie University for generously supporting this research.

CHAPTER 1. INTRODUCTION

1.1 Rifted continental margins and associated geohazards

Rifted margins - also known as Atlantic type, trailing-edge, passive, or divergent margins - have existed somewhere on our planet almost persistently since 2.7 billion years ago (Bradley, 2008). These margins are products of continental breakup or rifting followed by seafloor spreading. They are comprised of sedimentary wedges that lie on top of transitional plate sections found at the contact zone between thinned continental and accreted oceanic crust (Bradley, 2008; Mann, 2015).

Continental rifts have dissected several supercontinents throughout the Earth's history. Almost 250 million years ago, fragmentation of the most recent supercontinent Pangea has commenced moulding much of the present shape of the continents (Figure 1.1) (Brune, 2016; Müller et al., 2008). Today, the length of active continental rifts is only a small fraction of the length of plate boundaries around the world. Nevertheless, as inheritance from the breakup of Pangea, rifted margins are considered as the most common type of crustal boundaries on the planet (Mann, 2015) covering over 105,000 km, which is longer than the length of convergent plate boundaries (53,000 km) or seafloor spreading ridges (65,000 km) (Bradley, 2008).

Two key geohazards humans face at rifted margins are sea-level rise and tsunami waves caused by submarine landslides (Brune, 2016; Camargo et al., 2019). While public's awareness of the impacts of sea-level rise on all coastal regions appear to be well developed, their perception of the effects of tsunamis seems to be tied to subduction zones only. This is likely because the subduction earthquakes are well known to trigger tsunamis, which are a relatively common occurrence with far-reaching consequences. However, submarine mass movements at oceanic volcanoes and rifted margins can also be tsunamigenic (e.g. Boulila et al., 2011; Ruffman & Hann, 2006).

Although characterized by far less shaking than convergent margins, rifted continental margins are subjected to release of tectonic stress by fault slip and earthquakes (Heidbach et al., 2010). For example, in the mid to high latitude regions, the main driver for tectonic stress buildup often are the ongoing lithospheric adjustments due to deglaciation. In northern Fennoscandia, removal

of ice sheets caused non-isostatic compressive stresses that have triggered local and regional earthquakes along massive faults up to 150 km in length and with displacement of fault blocks of up to 15 m (Arvidsson, 1996). In the North Atlantic region, lithospheric adjustments and post-glacial rebound still reactivate the pre-existing faults generated by older tectonic events, specifically those inherited from the margin rift phase (Brune, 2016; Wu, 1998). Such a process is believed to have triggered an earthquake with magnitude M=7.3 in Baffin Bay in 1933 which is known as one of the largest intraplate events and the largest earthquake ever recorded north of the Arctic Circle (Stein et al., 1979).

Ground shaking caused by tectonic stress release can mobilize accumulated unconsolidated sediments at rifted margins and result in their relocation through submarine slumps, debris flows, and turbidity currents (e.g., Behrmann et al., 2003; Brune et al., 2010; Clarke et al., 2014; Harbitz et al., 2014; Korup, 2012; Leynaud et al., 2009; Løvholt et al., 2012; Moore & Normark, 1994; Tinti et al., 2004). In 1929, a magnitude M=7.2 earthquake offshore Newfoundland disrupted more than 200 km^3 of unconsolidated slope sediments to generate the largest submarine landslide in Canada; the landslide disintegrated sediments into turbidity currents with a speed of 60-100 km/h that carried the sediments up to 1000 km away from the source (Schulten et al., 2018). The submarine landslide and ensuing turbidity currents, that heavily damaged the inter-continental telecommunication cables along the seafloor, generated tsunami waves that reportedly killed 28 people in nearby coastal areas (Fine et al., 2005; Schulten et al., 2018).

Inducing significant submarine slope failure requires two main initial conditions: first, a large quantity of sediments must be depositing on a critical slope; and second, a stimulator must trigger the mass movement of sediments (Hampton et al., 1996). At the New Jersey margin, for example, subaqueous fans show that the mouths of nearby rivers supplied sediments to the continental margin with an average rate of 80 meters per million years; the gravitational load caused by the ongoing sediment deposition continuously increased the applied stresses and excess pore pressure of the sediments below gradually reducing their inner strength (Rieke & Chilingarian, 1974; Swarbrick et al., 2002). For slopes that are deemed unstable in this area, small perturbations or earthquakes can theoretically initiate tsunamigenic submarine landslides, as has been observed at other rifted margins (e.g., Schulten et al., 2018).

Characterizing unconsolidated sediments is crucial to locate areas prone to slump and estimate tsunami potential of a region. This can, for example, be done by: 1) sampling the deposited sediments; 2) imaging fault scarps and basement slopes; 3) determining the thickness and volume of failed sediments in existing slumps; 4) determining the kinematics of slope failures (instantaneous or retrogressive) (Mountjoy et al., 2009; Schulten et al., 2018). The key information needed for locating and characterizing potential sediment-failure areas is obtained by high-resolution seismic imaging and drilling.

Continental margins have received increasing public attention in recent years due to sea-level rise that threatens coastal population and infrastructure (Kulp & Strauss, 2016; Micheal et al., 2019). With about 200 million people settled within coastal floodplains less than 1 meter above current sea-level (Stern & Herbert, 2015), sea-level rise, driven by climate change and non-climatic factors, and its effects on the low-lying areas represents a globally significant socio-economic hazard that needs to be studied, particularly now during the period of accelerated ice-cover melting (Shepherd et al., 2020). The current global sea-level projections predict up to 1.2 m of sea-level rise by 2100 and 2.8 m by 2200 (Kopp et al., 2014); By the end of 21st century, houses of approximately 650 million people are estimated to be below sea level or subject to recurrent flooding. The global warming discussions put the spotlight on the impact of sea-level rise at the land-sea boundary. In 2018, the Intergovernmental Panel on Climate Change (2018) announced that sea-level rise has become an inevitable consequence of global warming and a major concern globally (Intergovernmental Panel on Climate Change, 2018). Many experts have argued that the predictions of future sea-level rise are too conservative and do not adequately reflect uncertainty (Kulp & Strauss, 2016; Oppenheimer et al., 2007; Pfeffer et al., 2008; Solomon et al., 2008).

One possible way to reduce the current uncertainties in sea-level predictions is to combine available numerical climate models with field observations and geological records to better constrain and understand sea-level variations in the past under varying climate conditions. The climatic transition that happened in the Miocene epoch is a relevant example. The Middle Miocene Climatic Optimum (~17-15 Mya) is a period in the Earth's history when the climate was warmer and the East Antarctic ice sheet was smaller than presently (Goldner et al., 2016; Pekar & DeConto, 2006). This was followed by the Middle Miocene Climate Transition, in

which the earth experienced major Antarctic ice sheet expansion and global cooling (~15–13 Ma) (Knorr & Lohmann, 2014). The geological records of the Miocene epoch show the planet's response to global climate change (Frigola et al., 2018; Herold et al., 2011; Micheels et al., 2009) and has the potential to be used as an analog for the modern climate models.

In addition to global sea level, shoreline position is a function of several other controlling factors like sediment supply, lithospheric cooling, isostasy, flexural loading, and mantle dynamics. Consequently, the actual local sea-level rise or fall might be much higher or lower than what global eustatic projections indicate; for instance, while glacial rebound in Scandinavia is moving the shoreline seaward, subsidence due to sediment compaction is sinking Venice and moving the shoreline in the opposite direction (Steffen & Kaufmann, 2005; Tosi et al., 2013).

It is generally accepted that human population situated at rifted margins is subject to socio-economic geohazards such as earthquakes, landslides, tsunamis, and flooding; difficulties in assessing and quantifying the risk this population faces call for more research to better characterize these events and processes, and broaden and deepen our insight into their magnitude and recurrence rate.

1.2 Processes that shape sedimentary structures at rifted margins

At rifted continental margins, sedimentary sequences are shaped by the available accommodation and rate of sedimentation (Matenco & Haq, 2020). The primary factors controlling the amount of available accommodation are eustasy (long-term sea level fluctuations), tectonics, and pre-existing structure (JERVEY, 1988). The rate of sedimentation is mostly governed by sediment transport. Eustasy is often thought to dominantly shape the sedimentary record. However, other primary controlling factors can have a similar impact on the development of a sedimentary section. Determining which factor is the dominant contributor to shaping sedimentary record at any particular margin is challenging because the listed primary factors tend to act concurrently. Moreover, multiple primary controlling factors can be driven by a single process. For example, insolation is the key driver for climate change, which at global scale has a strong effect on eustacy and locally affects erosion and sediment transport. Similarly, individual primary controlling factors can be driven by more than one process. For example, eustasy is affected in a major way by both climate change and plate tectonics, just at different time scales.

Eustasy controls the accommodation available for deposition (Reynolds et al., 1991). Over geological time, eustasy either results from a change in the bulk volume of oceanic basins, or from a change in the water volume in the oceans (Guillaume et al., 2016). Assembly and dispersal of continents, and growth and decay of continental ice sheets have been primary drivers for change in the bulk volume of oceanic basins and the volume of water in the oceans, respectively (e.g Miller & Mountain, 1996; Rohling et al., 2013). Vail et al. (1977) suggested that eustasy forms stratigraphic sequences with six temporal orders, from a couple of hundred of million years (first order) to tens of thousands of years (sixth order) (Table 1.1). However, further research has shown that the timing and amplitude of eustatic oscillations are challenging to estimate, and that making any assumptions based on the relative differences between the amplitude of eustatic events can be misleading and incorrect (Boulila et al., 2011; Miller et al., 2005, 2018; Miller & Mountain, 1996). In addition to the challenges associated with determining the amplitude of eustatic oscillations, limitations of dating techniques in providing high-resolution age constraints make it difficult to identify and classify third to sixth order stratigraphic sequences. Incorporating several dating techniques to improve the resolution of available age models, and quantifying the contribution of controlling mechanisms on eustasy can lead to better constraints of the timing and environmental conditions that shaped the sedimentary structure of rifted margins (Boulila et al., 2011).

Tectonic processes such as flexural and Airy loading of sediments (Karner & Watts, 1982), thermal subsidence, folding, and faulting potentially overprint the impact of eustasy on sedimentary strata, even at rifted margins (Browning et al., 2006). The sediment load during the deposition phase causes isostatic compensation, depresses the lithosphere, and compacts the underlying sediments (e.g. Beaumont, 2007; Karner & Watts, 1982; Keen & Beaumont, 1990; Watts & Steckler, 1979). Furthermore, this load compacts the prograding clinoforms and dewaters the underlying strata, leading to lateral variation in thickness and preservability of sequences (Browning et al., 2006), rotation underneath the prograding strata, and formation of an anticlinal closure (Steckler et al., 1993); features that have been observed frequently in the clinoforms at the shelf break of the New Jersey margin. The impact of thermal subsidence might be small and uniform, but sediment compaction and isostasy can intensify the total subsidence rate by a few orders of magnitude (Steckler et al., 1993).

Sediment transport processes such as traction and wave reworking, diffusion, slope avalanche and by-pass (Karner & Driscoll, 1997) determine where the sediments are deposited or eroded (Steckler et al., 1993; Swift & Thorne, 2009). Interaction of advective and diffusive processes responsible for carrying deposits within the margin vary throughout a given sea-level cycle (Karner & Driscoll, 1997; M. D. Matthews & Perlmutter, 2009; Perlmutter et al., 1995). When the ratio of advection to diffusion is high, sediment transport complexes efficiently carry the deposits basinward across the continental shelf. On the other hand, while the ratio of advection to diffusion is low, sediment transport complexes carry the deposits along the shelf rather than across it (Karner & Driscoll, 1997). Fluvial systems and channel-levee complexes are good analogies that show how the ratio of advection to diffusion affects sediment transport processes. In these environments, the distributary role evolves from a braided to a meandering system as the advection to diffusion rate decreases in a sediment transport process (Hoyal & Sheets, 2009).

Margin's pre-existing structure controls the height and slope of clinoforms and sedimentary bypass (Reynolds et al., 1991; Steckler et al., 1993; Watts & Steckler, 1979). Steckler et al. (1993) argued that the pre-existing margin geometry can have substantial influence on stacking patterns in stratigraphic sequences overprinting the effect of eustasy and sediment supply. In their back-stripping analysis for late Miocene sediments, the clinoform height doubles over the interval of 25.5 Mya to 21 Mya, followed by an increase in the maximum slope of the front of clinoforms. The maximum stable dip of the clinoform slope for the depositing sediments limits the prograding deposition in shelf break as new sediments overload the clinoform slope, slump off the clinoform, and form a downslope ramp. This sequence of events may have been repeated several times during the Miocene offshore the New Jersey margin.

The presence of all these processes at a margin make it difficult, if not impossible, to quantify the impact of eustasy on creation or reduction of accommodation. This range of controlling factors, from eustasy to sediment intake can also generate cyclic patterns within the stratigraphic records (Figure 1.2) (Galloway, 1989; Pitman III & Golovchenk, 1983; Jervey, 1988; Reynolds et al., 1991; Steckler et al., 1993; Watts & Steckler, 1979; Watts & Thorne, 1984). Depending on how the influential mechanisms on a margin are interacting, the timing of systems tracts (Catuneanu et al., 2009) and sequence boundaries formation may differ substantially in a sea-level cycle. A study by Tesson et al. (1990) on Pleistocene sediments of the Rhône continental shelf is a prime example; while the high-resolution dating of sediments in the Late Quaternary

shows several period of global high sea-level (Murray-Wallace & Woodroffe, 2014), the seismic images of this section comprise mostly a series of transgressive and lowstand systems tracts in the glacial cycles. Several other studies have quantified this time lag between eustatic level (i.e., long-term global sea-level changes) and geometry of deposited sequences, as well as how climate, total subsidence, tectonics, sedimentary flux, and flexural isostasy can amplify the time lag (Jervey, 1988; Matthews & Perlmutter, 2009; Reynolds et al., 1991; Steckler et al., 1993). The phase of forming systems tract and the absolute sea level (in sea-level cycle) can differ by ±90 degrees (Angevine, 1989). Therefore, the eustatic changes that two margins have experienced over time are identical, but the correlated systems tracts and sequence boundaries (i.e. those formed contemporarily) may have up to 180 degrees of phase lag relative to the eustatic cycle. Consequently, a correlation between the timing of sequence boundaries and the phase in the eustatic cycle within a rifted margin can only be valid in an environment where the contribution of other controlling mechanisms is known to be negligible or can be estimated with a high degree of accuracy.

1.2.1 Footprint of insolation on sedimentary record

Insolation has an indirect impact on both accommodation and the rate of sedimentation by influencing climate, periods of glaciation, and change in the volume of ice caps on a global scale (Carlson, 2011; Ruddiman, 2003). Insolation causes fluctuation in the global climate and imposes cyclicity in stratigraphic records (Hays et al., 1976; Hinnov, 2013; Naish et al., 2009; Strasser et al., 2006).

Insolation on the earth surface is primarily controlled by a series of quasi-periodic orbital parameters over the geological time. Gravitational motion of planets in their elliptical orbit, rotation along their own axis, and their inter-planetary interactions are known as orbital parameters eccentricity, obliquity, and climatic precession respectively. The eccentricity of the Earth's elliptical orbit changes with a major period of ~100 kyr; the obliquity of the Earth’s axis has a period of ~41 kyr; and the climatic precession, which has the shortest periodicity, oscillates at 23 kyr (Milanković, 1920). These fluctuations consequently induce global climatic changes over geological time scales (Hays et al., 1976; Imbrie et al., 1984). Interference of these events also results in the resonance of their effect with longer periods as low frequency cycles modulating the amplitude of precession and obliquity (Abels, 2008). Orbital solutions for the

Earth's paleoclimate and eccentricity also show 0.97 Myr and 2.4 Myr cycles (for details see Laskar et al., 2004; Abels, 2008) in the last 40 Myr. Over this period, changes in obliquity amplitude are modulated by low-frequency components of 172 kyr and 1.2 Myr. Interference of eccentricity and obliquity also result in an astronomical tuning with a cycle of 405 kyr, which is considered as the most secure basis for calibrating the geological age with astronomical parameters (Laskar et al., 2004a; Shackleton et al., 2000).

In the late Cenozoic icehouse, high-resolution O^{18} isotope records demonstrate consistency between episodes of climate change with quasi-periodic orbital parameters (Miller et al., 2020). A spectral analysis of the logged O^{18} isotopes in 5.5 Myr of sediment records within late Oligocene to early Miocene (Zachos et al., 2001) revealed variance of the isotope values at all Milanković frequencies (Milanković, 1920). In another study, Holbourn et al., (2007) used O^{18} isotope as a climate proxy to analyze astronomically-tuned climatic transition with a fine resolution (1-9 kyr) in the middle Miocene. The footprint of orbital forces is not limited to high-frequency events, as several workers in the field have correlated the timing of glacioeustatic events with the 405 kyr, 1.2 Myr, and ~2.4 Myr cyclicity observed in astronomical parameters (e.g., K. Matthews & Al-Husseini, 2010; Matthews & Perlmutter, 2009; Pälike et al., 2004; Wade & Pälike, 2004). Studying the impact of orbital forces on climate, eustasy, and consequently on the sedimentary records and their geometry may shed light on how orbital parameters influence processes on the shelfs of rifted margins.

1.3 Paleo-climate studies at New Jersey continental margin

The New Jersey rifted continental margin has several peculiar properties that make it a natural laboratory to study paleoclimate and a prime location to investigate the history and dynamics of eustatic changes since the Oligocene (Miller & Mountain, 1996): 1) since early Jurassic rifting, the margin has experienced a smooth thermal subsidence (Steckler & Watts, 1978; Watts & Steckler, 1979), 2) substantial sediment supply since Oligocene resulted in a thick (hundreds of meters) record of sediments resolvable in seismic profiles (Miller et al., 1998; Poag & Sevon, 1989), 3) the margin's mid-latitude setting provides an optimal geochronologic control (MGL1510 expedition Proposal, 2011), 4) the margin has a relatively stable tectonic history (Miller et al., 2014), and 5) more than four decades of scientific research has provided a wealthy

repository of supporting data and information. Therefore, while regional controlling factors have contributed to the shoreline movements of this rifted margin, the eustatic change has been the dominant player.

1.3.1 Geological structure and history of the New Jersey margin

Separation of the North American and African plates began in Late Triassic and was followed by a period of rifting of the margin in Lower Jurassic. Seafloor spreading began off the coast of Georgia in the lower Jurassic and progressively extended northward along the Atlantic margin in the Middle Jurassic (Withjack et al., 1998). A 200 million year history of sedimentation in the US middle Atlantic region that accompanied the rifting and drifting resulted in a large accumulation of sediments that locally reach thickness of up to 16 km (Grow & Sheridan, 1988). The rifting process was associated with a diachronous post rifting unconformity that set apart the active rifting stage of the margin from the structurally quiescent drifting stage (Miller et al., 2014). Since the beginning of the drifting stage, eustatic change, thermal subsidence, lithosphere flexure, mantle dynamics, and sediment compaction became the dominant processes forming the margin history until the Plio-Pleistocene (Miller & Mountain, 1994; Mountain et al., 2007; Reynolds et al., 1991; Rowley et al., 2011; Watts, A. B. & Steckler, 1981; Watts & Steckler, 1979). During the major Pleistocene glacials, continental ice sheets in the northern hemisphere reached northern New Jersey. As a result, the near-field glacial isostatic adjustments influenced sedimentation within the margin (Miller et al., 2014). The Paleocene-Pleistocene sediments at the margin do not form a continuous record, which makes them challenging to date (Miller et al., 1998).

Over the past 100 Myr, the New Jersey margin sedimentary facies record eight depositional regimes (Browning et al., 2008): 1) Cretaceous riverine environment with warm climate, high sediment input, and high sea level; 2) Cenomanian-early Turonian marine-dominated sediments deposited during high sea-level with minor deltaic influence; 3) late Turonian-Coniacian non-marine delta system during a long period of low sea level; 4) Santonian-Campanian wave-dominated marine environment with strong deltaic influence; 5) Maastrichtian-middle Eocene starved marine ramp associated with high sea level, but low sediment input from the hinterland; 6) Eocene-Oligocene starved siliciclastic shelf environment; 7) early-middle Miocene prograding marine shelf with a strong wave-dominated deltaic influence, during which the New Jersey

margin experienced multiple eustatic fluctuations; and 8) late Miocene-recent eroded coastal system with a long period of low sea level and low sediment supply due to bypassing (Browning et al., 2008).

In the Early to Middle Miocene, the amplitude of million-year–scale relative sea-level change seen at the New Jersey margin is as high as 50 m (Katz et al., 2013). These events are considered eustatic variations, because they occur on a shorter time interval than epeirogenic influences (Kominz et al., 2016). The sedimentary record from several IODP wells drilled onshore (legs 150X and 174AX), in outer shelf (leg 150), and continental slope (leg 174A) has shown strong correlation between the timing of sequence boundaries and spikes in O^{18}-isotopes in the Miocene deep-sea sedimentary record (Browning et al., 2008; Miller & Mountain, 1996), suggesting that the observed change in relative sea-level is primarily caused by variation of climate and ice growth and decay.

The modern New Jersey margin is starving as the estuaries block sediments from reaching the offshore areas (Miller et al., 2014). Coarse sand, resulted from reworked coastal plain sediments during the Holocene transgression, overshadowed the modern shelf processes (Emery, 1968). The Appalachian Mountains are considered the ultimate source for the modern quartz sand; however, during the Holocene transgression, these sediments were majorly reworked from coastal plains and nearshore zones (Pazzaglia & Gardner, 1994) and subsequently redeposited in a modern hydrodynamic equilibrium (Miller et al., 2014).

Today, the magnitude of seafloor slope gradient separates the New Jersey continental margin into the continental shelf, slope and rise; the gradients of the slope are less than 1:1000 (0.06°), greater than 1:40 (>1.4°), and ~ 1:100 (~ 0.6°) for the continental shelf, continental slope and continental rise, respectively (Emery, 1968; Heezen et al., 1959). The continental shelf extends up to more than 150 km offshore, with an average water depth of ~135 meters at the shelf-slope break (Heezen et al., 1959). The shelf itself can be divided into the inner shelf (0-40 m), middle shelf (40-100 m) and outer shelf (>100 m) (Goff et al., 1999; Miller et al., 2014).

1.3.2 Previous research on the New Jersey margin

Because of its accessibility, the New Jersey margin has been the main target for marine geoscientists studying the US middle Atlantic region since the beginning of the twentieth century. Their work has led to the definition of fundamental terms in ocean floor studies such as

shelf, slope, and rise (Heezen et al., 1959). The fever of oil exploration reached the margin in the early 1970s, resulting in the drilling of 32 exploration wells on the distal parts of the continental shelf and slope, and several stratigraphic test wells at the margin (Miller et al., 2014; Poag & Sevon, 1989; Scholle, 1980). Despite the failure in discovering economical hydrocarbon prospects, the margin remained until present as one of the focal points for studying stratigraphy of continental margins and paleo-sea-level changes.

The international research community has found an extraordinary value in the Neogene clinoform shelf sediments offshore the New Jersey margin to study the processes that shape the sedimentary record at rifted margins, and to investigate links between stratigraphic records and eustasy (Fulthorpe & Austin, 2008; Monteverde et al., 2000; Mountain et al., 2007; Watkins & Mountain, 1988). In a community effort to evaluate the relationship among eustatic change, climate, stratigraphic sequences, supply of sediments, and variation in subsidence rate at a rifted continental margin, a series of boreholes were drilled along the New Jersey Sea-Level Transect, starting from the onshore New Jersey coastal plain across the continental shelf to the slope and rise (Figure 1.3) (Miller et al., 1998; Miller & Mountain, 1994). The objective of drilling a transect of boreholes was to estimate the amplitude of relative eustatic changes associated with the sequences (Miller & Mountain, 1994), as well as the age of sequence boundaries to correlate the age of sequences and the timing of major eustatic events with sufficient (<<1 Myr) chronostratigraphic precision.

Expedition 313 was the IODP's first attempt to provide the scientific community with direct samples from the Neogene clinoforms of the New Jersey continental shelf. The three sites M27, M28, and M29, which were drilled in ~35-40 m of water and offshore distance of 45 to 65 km, continuously cored and logged at three locations targeting: 1) the youngest topset sediment of the sequences, 2) the oldest bottomset sediments of the sequences at the clinoform toe, and 3) farther seaward sediments, where the sequences are less reworked and samples are more suitable for age control (Fulthorpe et al., 2008). This approach yielded reliable measurements of seaward variation in facies, paleo-water depth (Katz et al., 2013), sediments composition (Hendra, 2010; Mountain et al., 2010), and age of sediments (Browning et al., 2013) along the key surfaces. Excellent core recovery of ~80% resulted in 1311 m of cores from the three sites. Downhole logging, multi-sensor track measurements of unsplit cores, and various other studies done on the samples sum up to more than 150 types of measurements and analysis. The main objectives of

these studies were to 1) correlate the seismically imaged sequence boundaries in the late Paleogene-Neogene with eustatic variations implied by oxygen isotope fluctuations - as a global proxy for glacioeustasy (Browning et al., 2013; Katz et al., 2013; Miller, Mountain, et al., 2013), 2) estimate the amplitude, rate, and mechanism of eustatic change in this period (Miller, Mountain, et al., 2013; Miller et al., 2014), 3) estimate the stratigraphic response of the margin, such as changes in the geometry of facies and their succession in eustatic variations (McCarthy et al., 2013; Mountain et al., 2009; Proust et al., 2018), and 4) improve models to better predict the influence of active processes on the sedimentary record of the continental shelf (Miller et al., 2018). Paleontologic zonation combined with Sr-isotope dating of the facies sampled in all three sites show a continuous record of sea level cycles from 22 to 12 Mya (Katz et al., 2013, Kominz et al, 2016). Paleobathymetric analysis of benthic foraminifera revealed changes in paleowater depth from below 20 m up to more than 120 m in topset beds of clinoforms (Katz et al., 2013).

In the seismic profiles of the margin, stratal surfaces form the major reflections (Miller, Browning, et al., 2013). Most of these boundaries in the Eocene - Miocene interval show a strong correlation between the timing of glacioeustatic falls and increases in O^{18} isotope (Miller et al., 1998; Miller & Mountain, 1996). Previous studies show that the margin has gone through several cycles of eustatic changes, with an amplitude of ~20-85 m - in line with climate proxies (Katz et al., 2013a; Kominz et al., 1998; Kominz & Pekar, 2001). Reconstruction of depositional settings through backstripping of the transgressive-regressive sequences in coastal plains revealed the following stratigraphic records of sea-level cycles at the margin: 15-17 sequences in the Late Cretaceous, 6 in the Paleocene, 12 in the Eocene, 7 in the Oligocene, and 18-20 in the Miocene (Greenlee et al., 1992; Miller et al., 2014; Miller & Mountain, 1994; Mountain et al., 2006; Steckler et al., 1999). Backstripping has helped estimate the amplitude of eustatic changes for the Oligocene sediments with an accuracy of ±10 m. In the Cretaceous-Eocene, and Neogene, the eustatic cycles were not recorded continuously (Browning et al., 2008; Miller et al., 2005); however, biostratigraphic analysis of the core samples has been used to estimate the timing and amplitude of eustatic changes during these times (Greenlee et al., 1992; Katz et al., 2013).

Despite all the contributions made by IODP, deconvolving the factors involved in the generation of sequences in geological time is limited by sparse direct samples, the resolution of seismic data, and the unknowns outnumbering the constrained controlling factors - leaving a lot of room for subjective interpretation. Moreover, uncertainties regarding the margins stratigraphic

evolution and the processes influencing clinoform formation still exist. For instance, paleobathymetric analyses show that the paleo-water depth dropped to less than 20 m in the topset area, but no shoreline features or incised valleys were recognized on the 2D seismic data. By moving seaward, core samples from the clinoform toe comprise several intervals of debris flow deposits. However, no strong evidence of sediment transport exists in 2D seismic sections, neither up-dip nor along strike.

1.4 Aim, scope, and structure of this thesis

The top of clinoform rollovers in the paleo-shelf are among the most sensitive sedimentary features to post-Oligocene eustatic change (Mountain et al., 2009). Only the preserved shallow water continental shelf sediments form successions of facies bounded by regional unconformities. Neither onshore nor continental slope drilling could constrain these sediment records fully. The onshore area is far updip to have a comprehensive record of lowstand sediments, and the inland wells are too sparse and lack seismic profiles to determine the stratigraphic architecture as well as facies distribution of post-Oligocene sediments. The scientific community also understood from the ODP Leg 150 samples that, even though the stratigraphic record for the continental slope is nearly continuous, the paleowater depth is too deep to give insight into the role of eustatic changes in forming facies and sequence successions (Mountain et al., 1996).

Expedition 313 provided the scientific community with direct samples from the topset, foreset and toeset of Neogene clinoforms of the New Jersey continental shelf and yielded reliable measurements of lateral variation in facies, paleo-water depth (Katz et al., 2013), sediments composition (Hendra, 2010; Mountain et al., 2010), and age of sediments (Browning et al., 2013) along the key surfaces. However, due to the lack of 3D multichannel seismic (MCS) data, mapping the drilled sequences in 3D and studying the footprints of local sedimentary processes within these sequences, which are crucial to deconvolve the factors that generate them, has not yet been possible.

In 2015, I joined R/V Marcus G. Langseth research cruise MGL1510 which ran an ultra-high resolution 3D MCS survey on the New Jersey continental shelf covering an area encompassing the Expedition 313 drill sites. We covered ~564 km^2 using a hybrid configuration of 24 rows of

50 m long high-resolution P-cables and one 3 km long 2D MCS streamer to optimize seismic velocity analysis. The research cruise had several objectives including: 1) image shifts in the paleo-shoreline trajectory in the clinoform topset, as well as the potential incisions that might develop in response to drop in paleo-sea level, 2) document changes in morphology of depositional environment and processes imageable seismically in dip and strike directions over geological time. Integrating characteristics of shallow water facies changes from Expedition 313 with their 3D architecture and geometry could provide insight about the detailed processes near paleo shelf edge and add the missing spatial imaging needed to test and confirm findings of the Expedition 313. Ultimately, rendering an integrated model to define the spatial variation of the measured properties may link them with the geomorphological features and the depositional/erosional processes imaged by the 3D seismic data. My doctoral research was chosen strategically to make the most out of these newly available data by analyzing them together with the well (M27-M29) data from the IODP Expedition 313.

1.4.1 Research objectives

The focus of this PhD thesis study is to (a) understand how stratigraphic sequences of the New Jersey margin have responded to processes that shape the sedimentary record in the shallow water environment and (b) define a relationship between sequence development and these controlling processes. These goals are achieved by integrating the results from Expedition 313 and the recently acquired 3D seismic reflection volume to resolve the main ambiguities of the Neogene stratigraphic evolution offshore the New Jersey rifted continental margin. The main research questions and the linked hypotheses are as follows:

1) What was the influence of eustatic changes on the paleo-shelf landward of clinoform rollovers during the known sea-level low stands in late Oligocene-Miocene? Linked hypothesis: In response to an increase in the amplitude of eustatic changes since the Oligocene, the chance of paleo-shelf exposure has subsequently increased. Increasing paleo-shelf exposure may result in a growing number of fluvial incisions and mass transport systems during low sea-level. Incised valleys are crucial indicators of paleo-water depth at the boundary between sequences; observing these incisions at the topset or seaward of a clinothem yield a reliable measure of sea-level at the time of their formation.

Previous studies on the margin continental shelf have found a limited number of incised valleys landward of clinoforms rollovers, and lowstand wedges seaward of clinoforms in the early Miocene, suggesting a low amplitude base level change (Gallegos, 2017; Miller et al., 2018; Monteverde et al., 2008). By moving up to the younger sediments in mid-Miocene, several intervals of erosion have been imaged with seismic profiles in the foreset area, suggesting high amplitude base level falls at the time (Miller & Mountain, 1994). Using seismic attribute analysis to map these incisions through time in three dimensions, combined with findings of Expedition 313, may yield constraints on the shoreline position and an estimate of the amplitude of eustatic changes in the Miocene interval.

2) What are the mechanisms of sediment transport seaward of clinoform rollovers and how do they fit in the current stratigraphic models? Linked hypothesis: Despite the complexity of the factors shaping the morphology of a clinoform front, gravity flow and turbidity currents are the main processes delivering sediments seaward of clinoform toes at the New Jersey margin.

In their classic model of sequences deposited at the shelf break, Van Wagner et al. (1988) point to slope fans seaward of clinoform's toes as mainly responsible for sediment bypass and transport of coarse grain sediments seaward during high amplitude sea-level fall. These mass transport deposits, sampled by Expedition 313, are comprised of glauconitic sand and highly mature quartz with grains up to gravel size (Ando et al., 2014; Mountain et al., 2010). The resulting slope apron deposits form sedimentary units up to a few hundred meters thick extending for 10s of kilometers along-strike on a sole with two degrees gradients seaward of clinoform rollovers. However, little evidence exists to define the mechanisms responsible for transporting these sediments across the New Jersey shelf (Greenlee et al., 1992; Poulsen et al., 1998). Correlating the timing of these slope apron depositions with eustatic changes may give insight about the forcing factors that controlled the evolution of clinoforms.

Identifying possible failure scars near clinoform rollovers, if any, or transport channels that carried mass flow basinward would help further research on sediment transport pathways. The current sequence stratigraphic models, that include fans and laterally widespread onlap, rely on sediments coming from a point source (Karner & Driscoll, 1997). Previous studies in the middle-late Miocene sequences of New Jersey margin show that the eroded paleo-shelf topsets are not associated with lowstand accumulation seaward of clinoform toes (e.g. Fulthorpe et al., 2000).

One speculation is that these deposits may have been transported farther seaward or along the strike in the margin. Australia's Northwestern Shelf (Sanchez et al., 2012a, 2012b; Tagliaro et al., 2018) and the Canterbury basin in New Zealand (Carter et al., 2004; Lu et al., 2003, 2005) are analogues that have undergone similar processes in Miocene. In Australia's Northwestern Shelf, changes to oceanic circulation in the Indian Ocean caused along-strike sediment transport superimposing on progradation changes in Miocene sediments (Tagliaro et al., 2018). Measurements of the along-strike (migration) and down-dip (progradation) movement of these deltas are well documented by Sanchez et al. (2012a, 2012b). While the lowstand wedges are missing in Miocene shelf depositional setting of Canterbury basin, the along-strike currents were strong enough to control the sequence thickness, and cause a largely elongated sediment drift; the current erosion in drift moats create anachronous unconformities (Carter et al., 2004). Shallowness and scarcity of New Jersey's mid-late Miocene shelf canyons are in favour of Fulthrope et al.'s (2008) hypothesis that waves and currents in paleo shelf diffused the fluvial point sources deposits into a linear delivery of sediments to the clinoform front (Fulthorpe & Austin, 2008). As the result, individual point sources failed to overcome along strike forces to form lobate depocenters seaward of clinoform rollovers (Fulthorpe, 1991). The absence of prominent point sources and lobate fans, contrary to the existence of slope aprons in the New Jersey continental shelf, may challenge the standard sequence model for shallow continental shelves. However, supporting these speculations requires detailed imaging and documentation of mass transport systems at the margin (Helland-Hansen & Hampson, 2009; Henriksen et al., 2009; Patruno et al., 2015).

3) What was the sedimentary response of the margin to the global mid-Miocene climate change - the transition from a relative warmth or so-called Miocene Climatic Optimum to a steady period of cooling that re-established the ice sheets globally? Linked hypothesis: a globally significant change in climate had direct impact on the onshore-offshore movement of the Miocene sedimentary sequences, that also influenced the lithology of facies and the geometry of the clinoforms.

The mid-Miocene climate transition is contemporary with a substantial increase in the influx of siliciclastic sediments into many continental margins such as: the Angola margin (Lavier et al., 2001), the Gulf of Mexico (Galloway, 2008; Galloway et al., 2000), the Canterbury basin in New Zealand (Lu et al., 2005), the Maltese Islands margin (John et al., 2003), the Northern Carnarvon

basin on Northwestern Shelf of Australia (Sanchez et al., 2012b, 2012a), and the New Jersey margin (Poag & Sevon, 1989; Steckler et al., 1999). This increase in the mid-Miocene influx of siliciclastic sediments has been correlated to the alteration in climate patterns noted by a $\delta^{18}O$ increase in the Pacific, Southern and Atlantic Oceans (Miller & Fairbanks, 1983; Tagliaro et al., 2018). Changes in key oceanic gateways and rejuvenation of heat flow in the Pacific and African superplume likely resulted in the disruption of global equatorial/polar oceanic circulation and accelerated plate motion respectively, triggering a chain of events that evolved the climate and reshaped the earths surface in the late Cenozoic (Potter & Szatmari, 2009).

Beside climate, global tectonic processes as well as dropping paleo-sea level also amplified the influx of sediments by exhuming the exposed shelf to above the base level and, therefore, exposing it to erosion. However, the contribution of these processes was not enough to increase the influx of terrigenous sediments by 20-fold in the Miocene, as reconstruction and back-stripping the stratigraphic records suggest for the New Jersey continental shelf (Steckler et al., 1999). The modest 100-200 m of change in sea-level was not sufficient to generate a considerable amount of sediments, but it was the main process for distribution and redistribution of sediments along the margin (Galloway, 1989; Poag & Sevon, 1989). The other proposed mechanisms focus on processes in the hinterland: 1) Change in precipitation in elevated terrain because of high-amplitude climate changes late in Cenozoic (Molnar, 2004) - As higher aridity and vegetation change resulting from climate change would lead to more large-magnitude floods and an increase in bedload transport that doubled the incision rates in elevated areas (Molnar, 2001); 2) Tectonic uplift of the hinterland (Pazzaglia & Brandon, 1996) - Episodic uplift of source terrains of Appalachian Highlands abruptly accelerated sediment accumulation and influx rate in the middle Miocene that lasted for ~7 million years (Poag & Sevon, 1989).

4) What was the impact of orbital forces on the spatial and temporal processes controlling Miocene sedimentary cycles? Link hypothesis: Quasi-periodic variations in the Earth's orbital parameters, and its rotation relative to the Sun, yielded changes in the total insolation and induced cyclicity in the global climate change; consequently, this cyclicity must have been documented in the Miocene stratigraphic records.

Studying the recorded fluctuation of the Earth's orbital parameters in stratigraphic records (cyclostratigraphy) has led to invaluable discoveries about the Earth's history (Hinnov, 2000;

Strasser et al., 2006). Since Hays et al. (1976) discovered the Milanković periodicity in Pleistocene paleoclimate records, the scientific community has been eager to find evidence of orbitally-forced events throughout geological time (Hinnov & Ogg, 2007; Houghton et al., 1996; Lourens & Tuenter, 2009; Pisias & Shackleton, 1984; Prokopenko et al., 2006). Henry & Ran, (1994) used pollen records to study paleoclimate changes in the Late Pliocene-Pleistocene; Williams et al. (2010) studied sedimentary records of biogenic silica as a proxy to estimate the climate response to the insolation during the past 5 Myr; Olsen (1997) used ca. 40 Myr-long Late Triassic–Early Jurassic Newark Basin sedimentary records to detect pervasive sedimentary cyclicity produced by Milanković-type forcing of climate; Kutterolf et al. (2013 & 2018) detected Milanković frequencies in the global volcanic activity and tephra records.

The distribution of facies and the spatial geometry of stratigraphic sequences reflect the autocyclic interbasinal (local mechanism) or extra-basinal allocyclic processes (regional to global mechanisms) that have influenced the sedimentary records. In other words, physical and environmental limits in a depositional setting may result in repeated buildup/shutdown or transgression/retrogradation patterns. Peritidal carbonates, turbidites, tempestites, and switching delta lobes are some of the sedimentary facies in which autocyclic depositional mechanisms can induce cyclicity (Einsele et al., 1991, 1996; Hinnov, 2000).

In Miocene siliciclastic sediments on the New Jersey continental margin, orbitally-forced eustatic change might be the strongest control on the sequence cyclicity. Even though many authors have suggested a correspondence between ~1.2 Myr obliquity modulation cycles and third order sequences (Boulila et al., 2011; Miller et al., 1998; Miller, Sugarman, et al., 2013; Mountain et al., 2007), spectral analysis of 12 Myr record of sequence cyclicity in the margin would give insight about the control of other orbital forces with shorter periodicity.

1.5 Thesis outline

This thesis comprises 5 chapters that are organized as follows:

Chapter 1 starts with a short overview of rifted continental margins, their distribution, characteristics, and importance, especially with respect to related geohazards and impacts on humans. Next introduced is the New Jersey rifted continental margin and why it has become the focal place for studying paleoclimate and global sea-level change over the past several decades.

This is followed by the early geological history of the New Jersey margin and its oceanographic setting with additional information on why this margin was chosen as the study area for this Ph.D. research. The chapter ends with the main scientific questions and related testable hypotheses that are addressed in the following chapters.

Chapter 2 introduces development of Geometrical Breakdown Approach (GBA) to facilitate objective analysis of stratal patterns in shallow marine environments. The introduced approach is centered on rigorous terminology based on the upward-downward and landward-seaward trajectories of clinoform inflection points and stratal terminations, respectively. The results are captured in three-letter acronyms, providing an efficient way of recording repetitive spatial and temporal patterns. I test this approach on synthetic and field data. The results demonstrate that the proposed geometrical criteria are a reliable tool for accurate recognition of systems tracts within the strata and that their application is a step forward to separating observation and interpretation in sequence stratigraphic analysis. Comparison of the stratigraphic models based on the proposed GBA and existing approaches reveals that, although the examined approaches are fundamentally different, the final interpretations are in general agreement. Nevertheless, the GBA differs from earlier approaches by the greater level of detail extracted that can bring the resolution of sequence stratigraphic analysis to the resolution of the input seismic data.

Chapter 3 describes analyses of the variation of sedimentary parameters in the Miocene clinothems using the ultra-high-resolution seismic data. The identified sequences and systems tracts are incorporated to isolate sedimentary packages deposited in each phase of sea level cycle to predict sedimentological properties in shallow marine sediments at a significantly higher resolution (~5 m laterally) than previously achieved (~100s of m). By using seismic inversion and multi-attribute linear regression processes, relationship is established between the identified stratigraphic sequences and quantitative seismic interpretation to obtain a distinct trend of variation in density, P-wave velocity and, consequently, volume of clay in systems tracts within each sequence. The estimated properties in 3D space give insight on the sedimentary processes and variation of lithofacies in response to changes in the depositional setting. Further, the observed spatially repeating pattern of petrophysical properties within clinothems can act as a heterogeneous conduit barrier system to fluid flow in siliciclastic sedimentary aquifers and hydrocarbon reservoirs. Characterizing the channelized sediments, especially those which formed during the eustatic changes, aids in understanding of the mechanisms of fluid migration

(low salinity water in offshore fresh-water aquifers or hydrocarbons in petroleum systems) along the clinoforms.

Chapter 4 establishes a quantitative link between the identified periods in stratigraphic imprints of eustatic cycles and Milanković cycles, which are quasi-periodic variations in the Earth's orbital parameters and its rotation relative to the sun. I use the detailed sequence stratigraphic model from Chapter 3 to identify fourth order and fifth order cyclicities in sediment records from Oligocene to Late Miocene. The reconstructed log for stratigraphic events and the systems tracts over time is then spectrally decomposed and correlated with the change in the total insolation and induced cyclicity in paleoclimate change. The correlation in the cyclicity between the two series sheds new light on the interaction between orbital forces, climate, and changes in paleo depositional setting.

Chapter 5 summarizes the highlights of the important outcomes of this thesis research and provides an outlook for future research in the field.

Order of Eustatic cycle	Nomenclature	Duration (Ma)	
		Range	Mode
First	Megasequence	50–100+	80
Second	Supersequence	5–50	10
Third	Sequence	0.5-5	1
Fourth	Parasequence Set	0.1-0.5	0.45
Fifth	Parasequence	0.01-0.1	0.04
Sixth	punctuated aggradational cycle	0.01<	-

Table 1.1: Duration and nomenclature for the first to fifth order eustatic cycles. Modified from Goodwin et al., 1986; Mitchum & Van Wagoner, 1991.

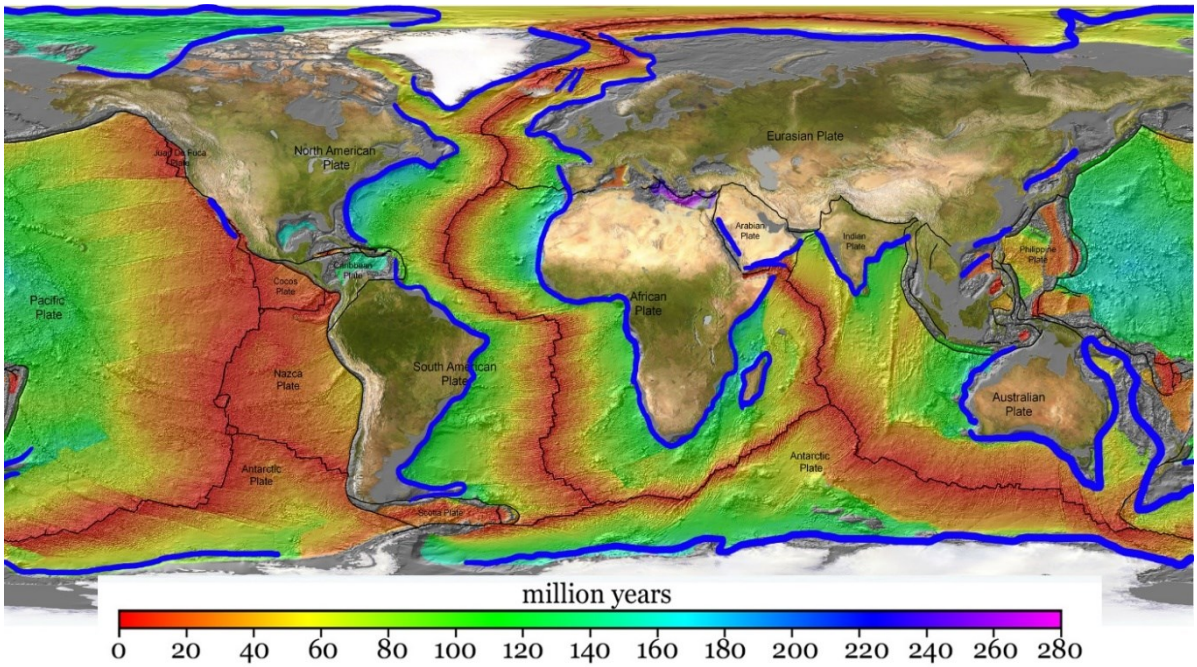

Figure 1.1: World map showing the current rifted margins (blue lines). Base map, from NOAA National Geophysical Data Center (NGDC), represents the age of oceanic lithosphere. Modified from Müller et al., (2008).

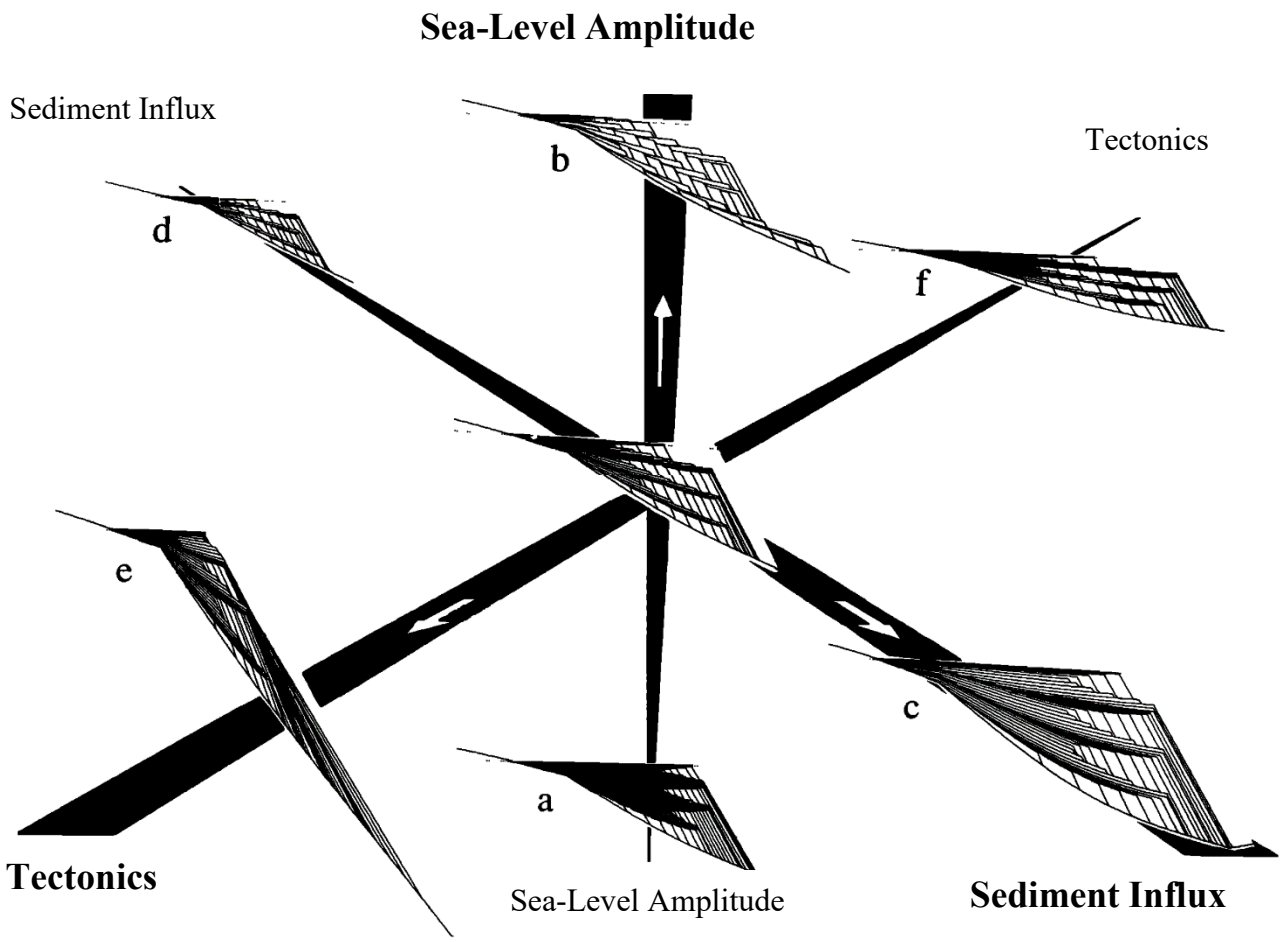

Figure 1.2: Perspective view of the change in sequence architecture as a function of sea level, sediment flux, and tectonics. The models represent 100 time-steps in 10 Myr of deposition. Arrows show the direction of increase in influence of each parameter; all the plots are presented at the same scale. Modified from Reynolds et al. (1991).

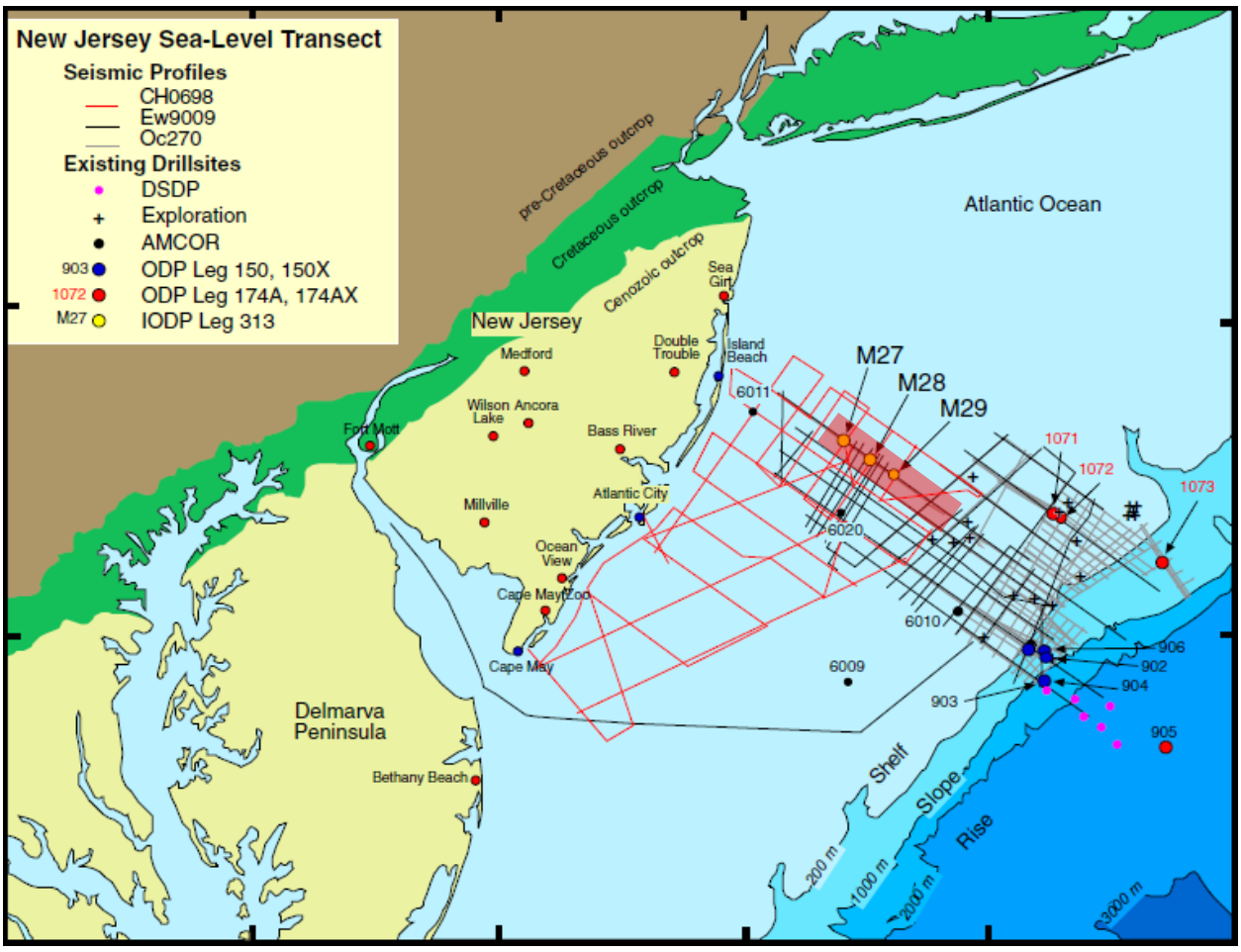

Figure 1.3: Location map of the New Jersey and Mid-Atlantic Margin sea-level transect, as well as the seismic profiles acquired across the margin. The red rectangle indicates is the 3D seismic survey carried out during the research cruise MGL1510. Modified from Browning et al. (2013).

1.6 References

Abels, H. A. (2008). *Long-period orbital climate forcing [PhD Thesis]* (Issue 297). Utrecht University.

Ando, H., Oyama, M., & Nanayama, F. (2014). Data report: grain size distribution of Miocene successions, IODP Expedition 313 Sites M0027, M0028, and M0029, New Jersey shallow shelf. *Proceedings of the Integrated Ocean Drilling Program*, *313*. https://doi.org/10.2204/iodp.proc.313.201.2014

Angevine, C. L. (1989). Relationship of Eustatic Oscillations to Regressions and Transgressions on Passive Continental Margins. In *Origin and Evolution of Sedimentary Basins and Their Energy and Mineral Resources* (pp. 29–35). American Geophysical Union (AGU). https://doi.org/10.1029/GM048p0029

Arvidsson, R. (1996). Fennoscandian Earthquakes : Whole Crustal Rupturing Related to Postglacial Rebound. *Science*, *274*(5288), 744–746. http://www.jstor.org/stable/2891742

Beaumont, C. (2007). The evolution of sedimentary basins on a viscoelastic lithosphere: Theory and examples. In *Geophysical Journal of the Royal Astronomical Society* (Vol. 55). https://doi.org/10.1111/j.1365-246X.1978.tb04283.x

Behrmann, S. K. J., Völker, D., Stipp, M., Berndt, C., Urgeles, R., Chaytor, J. D., & Huhn, K. (2003). *Submarine Mass Movements and Their Consequences* (Vol. 19). https://doi.org/10.1007/978-94-010-0093-2

Boulila, S., Galbrun, B., Miller, K. G., Pekar, S. F., Browning, J. V., Laskar, J., & Wright, J. D. (2011). On the origin of Cenozoic and Mesozoic "third-order" eustatic sequences. *Earth-Science Reviews*, *109*(3–4), 94–112. https://doi.org/10.1016/j.earscirev.2011.09.003

Bradley, D. C. (2008). Passive margins through earth history. *Earth-Science Reviews*, *91*(1–4), 1–26. https://doi.org/10.1016/j.earscirev.2008.08.001

Browning, J. V., Miller, K. G., McLaughlin, P. P., Kominz, M. A., Sugarman, P. J., Monteverde, D., Feigenson, M. D., & Hernández, J. C. (2006). Quantification of the effects of eustasy, subsidence, and sediment supply on Miocene sequences, mid-Atlantic margin of the United States. *Bulletin of the Geological Society of America*, *118*(5–6), 567–588. https://doi.org/10.1130/B25551.1

Browning, J. V., Miller, K. G., Sugarman, P. J., Barron, J. A., McCarthy, F. M. G. G., Kulhanek, D. K., Katz, M. E., & Feigenson, M. D. (2013). Chronology of Eocene–Miocene sequences on the New Jersey shallow shelf: Implications for regional, interregional, and global correlations. *Geosphere*, *9*(6), 1434–1456. https://doi.org/10.1130/GES00853.1

Browning, J. V., Miller, K. G., Sugarman, P. J., Kominz, M. A., Mclaughlin, P. P., Kulpecz, A. A., & Feigenson, M. D. (2008). 100 Myr record of sequences, sedimentary facies and sea level change from Ocean Drilling Program onshore coreholes, US Mid-Atlantic coastal plain. *Basin Research*, *20*(2), 227–248. https://doi.org/10.1111/j.1365-2117.2008.00360.x

Brune, S. (2016). Rifts and Rifted Margins: A Review of Geodynamic Processes and Natural Hazards. *Plate Boundaries and Natural Hazards*, 11–37. https://doi.org/10.1002/9781119054146.ch2

Brune, S., Babeyko, A. Y., Ladage, S., & Sobolev, S. V. (2010). Landslide tsunami hazard in the Indonesian Sunda Arc. *Natural Hazards and Earth System Science*, *10*(3), 589–604. https://doi.org/10.5194/nhess-10-589-2010

Camargo, J. M. R., Silva, M. V. B., Júnior, A. V. F., & Araújo, T. C. M. (2019). Marine geohazards: A bibliometric-based review. *Geosciences (Switzerland)*, *9*(2). https://doi.org/10.3390/geosciences9020100

Carlson, A. (2011). Ice sheets and sea level in Earth's past. *Nature Education Knowledge*, *3*.
Carter, R. M., Fulthorpe, C. S., & Lu, H. (2004). Canterbury drifts at Ocean Drilling Program site 1119, New Zealand: Climatic modulation of southwest Pacific intermediate water flows since 3.9 Ma. *Geology*, *32*(11), 1005–1008. https://doi.org/10.1130/G20783.1
Catuneanu, O., Abreu, V., Bhattacharya, J. P., Blum, M. D., Dalrymple, R. W., Eriksson, P. G., Fielding, C. R., Fisher, W. L., Galloway, W. E., Gibling, M., Giles, K. A., Holbrook, J. M., Jordan, R., Kendall, ; Christopher G. St. C., Macurda, B., Martinsen, O. J., Miall, A., Neal, J. E., Nummedal, D., … Winker, C. (2009). Towards the standardization of sequence stratigraphy. *Earth-Science Reviews*, *92*(1–2), 1–33. https://doi.org/10.1016/j.earscirev.2008.10.003
Clarke, S., Hubble, T., Airey, D., Yu, P., Boyd, R., Keene, J., Exon, N., Gardner, J., & Ward, S. (2014). Morphology of Australia's eastern continental slope and related tsunami hazard. *Advances in Natural and Technological Hazards Research*, *37*(July), 529–538. https://doi.org/10.1007/978-3-319-00972-8_47
Einsele, G., Chough, S. K., & Shiki, T. (1996). Depositional events and their records - an introduction. *Sedimentary Geology*, *104*(1–4), 1–9. https://doi.org/10.1016/0037-0738(95)00117-4
Einsele, G., Ricken, W., & Seilacher, A. (1991). *Cycles and Events in Stratigraphy*.
Emery, K. O. (1968). *Positions of empty pelecypod valves on the continental shelf*. *38*(4), 1264–1269.
Fine, I. V., Rabinovich, A. B., Bornhold, B. D., Thomson, R. E., & Kulikov, E. A. (2005). The Grand Banks landslide-generated tsunami of November 18, 1929: Preliminary analysis and numerical modeling. *Marine Geology*, *215*(1-2 SPEC. ISS.), 45–57. https://doi.org/10.1016/j.margeo.2004.11.007
Frigola, A., Prange, M., & Schulz, M. (2018). Boundary conditions for the Middle Miocene Climate Transition (MMCT v1.0). *Geoscientific Model Development*, *11*(4), 1607–1626. https://doi.org/10.5194/gmd-11-1607-2018
Fulthorpe, C. S. (1991). Geological controls on seismic sequence resolution. *Geology*, *19*(1), 61–65. https://doi.org/10.1130/0091-7613(1991)019<0061:GCOSSR>2.3.CO;2
Fulthorpe, C. S., & Austin, J. A. (2008). Assessing the significance of along-strike variations of middle to late Miocene prograding clinoformal sequence geometries beneath the New Jersey continental shelf. *Basin Research*, *20*(2), 269–283. https://doi.org/10.1111/j.1365-2117.2008.00350.x
Fulthorpe, C. S., Austin, J. A., & Mountain, G. S. (2000). Morphology and distribution of Miocene slope incisions of New Jersey: Are they diagnostic of sequence boundaries? *Bulletin of the Geological Society of America*, *112*(6), 817–828. https://doi.org/10.1130/0016-7606(2000)112<817:MADOMS>2.0.CO;2
Fulthorpe, C. S., Miller, K. G., Droxler, A. W., Hesselbo, S. P., Camoin, G. F., & Kominz, M. A. (2008). Drilling to decipher long-term sea-level changes and effects - A joint consortium for ocean leadership, ICDP, IODP, DOSECC, and Chevron Workshop. *Scientific Drilling*, *6*, 19–28. https://doi.org/10.2204/lodp.sd.6.02.2008
Gallegos, G. (2017). Lower Miocene (ca . 20-18 Ma) New Jersey Sequence Stratigraphy : Architecture and Onshore-Offshore Correlations. *MSc Dissertation*.
Galloway, W. E. (1989). Genetic stratigraphic sequences in basin analysis II: application to northwest Gulf of Mexico Cenozoic basin. *American Association of Petroleum Geologists Bulletin*, *73*(2), 143–154. https://doi.org/10.1306/703C9AFA-1707-11D7-

8645000102C1865D
Galloway, W. E. (2008). Chapter 15 Depositional Evolution of the Gulf of Mexico Sedimentary Basin. In *Sedimentary Basins of the World* (Vol. 5, Issue C). Elsevier. https://doi.org/10.1016/S1874-5997(08)00015-4
Galloway, W. E., Ganey-Curry, P. E., Li, X., & Buffler, R. T. (2000). Cenozoic depositional history of the Gulf of Mexico basin. *AAPG Bulletin*, *11*(11), 1743–1774. https://doi.org/10.1306/8626C37F-173B-11D7-8645000102C1865D
Goff, J. A., Swift, D. J. P. P., Duncan, C. S., Mayer, L. A., & Hughes-Clarke, J. (1999). High-resolution swath sonar investigation of sand ridge, dune and ribbon morphology in the offshore environment of the New Jersey margin. *Marine Geology*, *161*(2–4), 307–337. https://doi.org/10.1016/S0025-3227(99)00073-0
Goldner, A., Ramstein, G., Favre, E., Utescher, T., Hamon, N., Munhoven, G., Erdei, B., Krapp, M., Dury, M., Henrot, A.-J., François, L., & Herold, N. (2016). Middle Miocene climate and vegetation models and their validation with proxy data. *Palaeogeography, Palaeoclimatology, Palaeoecology*, *467*, 95–119. https://doi.org/10.1016/j.palaeo.2016.05.026
Greenlee, S. M., Devlin, W. J., Miller, K. G., Mountain, G. S., & Flemings, P. B. (1992). Integrated sequence stratigraphy of Neogene deposits, New Jersey continental shelf and slope: comparison with the Exxon model. *Geological Society of America Bulletin*, *104*(11), 1403–1411. https://doi.org/10.1130/0016-7606(1992)104<1403:ISSOND>2.3.CO;2
Grow, J. A., & Sheridan, R. E. (1988). U.S. Atlantic Continental Margin; A typical Atlantic-type or passive continental margin. In R. E. Sheridan & J. A. Grow (Eds.), *The Atlantic Continental Margin*. Geological Society of America. https://doi.org/10.1130/DNAG-GNA-I2.1
Guillaume, B., Pochat, S., Monteux, J., Husson, L., & Choblet, G. (2016). Can eustatic charts go beyond first order? Insights from the Permian-Triassic. *Lithosphere*, *8*(5), 505–518. https://doi.org/10.1130/L523.1
Hampton, M. A., Lee, H. J., & Locat, J. (1996). Submarine landslides. *Reviews of Geophysics*, *34*(1), 33–59. https://doi.org/10.1029/95RG03287
Harbitz, C. B., Løvholt, F., & Bungum, H. (2014). Submarine landslide tsunamis: How extreme and how likely? *Natural Hazards*, *72*(3), 1341–1374. https://doi.org/10.1007/s11069-013-0681-3
Hays, J. D., Imbrie, J., & Shackleton, N. J. J. (1976). Variations in the Earth ' s Orbit : Pacemaker of the Ice Ages. *Science*, *194*(4270). https://doi.org/10.1126/science.194.4270.1121
Heezen, B. C., Tharp, M., & Ewing, M. (Eds.). (1959). *The Floors of the Oceans: I. The North Atlantic*. https://doi.org/10.1130/SPE65
Heidbach, O., Tingay, M., Barth, A., Reinecker, J., Kurfeß, D., & Müller, B. (2010). Global crustal stress pattern based on the World Stress Map database release 2008. *Tectonophysics*, *482*(1–4), 3–15. https://doi.org/10.1016/j.tecto.2009.07.023
Helland-Hansen, W., & Hampson, G. J. (2009). Trajectory analysis: Concepts and applications. *Basin Research*, *21*(5), 454–483. https://doi.org/10.1111/j.1365-2117.2009.00425.x
Hendra, W. (2010). Lithofacies and Depositional Environment Spanning the Cretaceous-Paleogene Boundary on the New Jersey Coastal Plain. *MSc Dissertation*, *5*(1976), 265–288.
Henriksen, S., Hampson, G. J., Helland-Hansen, W., Johannessen, E. P., & Steel, R. J. (2009). Shelf edge and shoreline trajectories, a dynamic approach to stratigraphic analysis. *Basin*

Research, *21*(5), 445–453. https://doi.org/10.1111/j.1365-2117.2009.00432.x
Henry, H., & Ran, E. (1994). Late Pliocene-Pleistocene high resolution pollen sequence of Colombia: An overview of climatic change. In *Quaternary International* (Vol. 21). https://doi.org/10.1016/1040-6182(94)90021-3
Herold, N., Huber, M., & Müller, R. D. (2011). Modeling the Miocene Climatic Optimum. Part I: Land and Atmosphere*. *Journal of Climate*, *24*(24), 6353–6372. https://doi.org/10.1175/2011jcli4035.1
Hinnov, L. A. (2000). *NEW PERSPECTIVES ON ORBITALLY FORCED STRATIGRAPHY*. *12*(8), 727–732. https://doi.org/10.1177/0741713604268894
Hinnov, L. A. (2013). Cyclostratigraphy and its revolutionizing applications in the earth and planetary sciences. *Bulletin of the Geological Society of America*, *125*(11–12), 1703–1734. https://doi.org/10.1130/B30934.1
Hinnov, L. A., & Ogg, J. G. G. (2007). Cylostratigraphy and the Astronomical Time Scale. *Beyond the GSSP: New Developments in Chronostratigraphy*, 239–251.
Holbrook, J. M., Kuhnt, W., Schulz, M., Flores, J. A., & Andersen, N. (2007). Orbitally-paced climate evolution during the middle Miocene "Monterey" carbon-isotope excursion. *Earth and Planetary Science Letters*, *261*(3–4), 534–550. https://doi.org/10.1016/j.epsl.2007.07.026
Houghton, J. T., L.G. Meira Filho, B.A. Callander, N. H., Maskell, A. K. and K., & K. (1996). *The science of climate change. contribution of working group 1 to the second assessment report of the intergovernmental panel*. 588. https://doi.org/10.1017/CBO9781107415324.004
Hoyal, D. C. J. D., & Sheets, B. A. (2009). Morphodynamic evolution of experimental cohesive deltas. *JOURNAL OF GEOPHYSICAL RESEARCH*, *114*(January), 1–18. https://doi.org/10.1029/2007JF000882
Imbrie, J., Hays, J. D., Martinson, D. G., McIntyre, A., Mix, A. C., Morley, J. J., Pisias, N. G., Prell, W. L., & Shackleton, N. J. (1984). The orbital theory of Pleistocene climate: Support from a revised chronology of the marine d18O record. *Milankovitch and Climate: Understanding the Response to Astronomical Forcing*, *1*(January), 269–305. https://doi.org/-
Intergovernmental panel on climate change. (2018). *Intergovernmental panel on climate change (IPCC) report*. *June*.
JERVEY, M. T. (1988). Quantitative Geological Modeling of Siliciclastic Rock Sequences and Their Seismic Expression. In C. K. Wilgus, B. S. Hastings, H. Posamentier, J. Van Wagoner, C. A. Ross, & C. G. S. C. Kendall (Eds.), *Sea-Level Changes* (pp. 47–69). SEPM (Society for Sedimentary Geology). https://doi.org/10.2110/pec.88.01.0047
John, C. M., Mutti, M., & Adatte, T. (2003). Mixed carbonate-siliciclastic record on the North African margin (Malta) - Coupling of weathering processes and mid Miocene climate. *Bulletin of the Geological Society of America*, *115*(2), 217–229. https://doi.org/10.1130/0016-7606(2003)115<0217:MCSROT>2.0.CO;2
Karner, G. D., & Driscoll, N. W. (1997). Three-dimensional interplay of advective and diffusive processes in the generation of sequence boundaries. *Journal of the Geological Society*, *154*(3), 443–449. https://doi.org/10.1144/gsjgs.154.3.0443
Karner, G. D., & Watts, A. B. (1982). On isostasy at Atlantic type margins. *Journal of Geophysical Research*, *87*, 2923–2984.
Katz, M. E., Browning, J. V., Miller, K. G., Monteverde, D. H., Mountain, G. S., & Williams, R.

H. (2013). Paleobathymetry and sequence stratigraphic interpretations from benthic foraminifera: Insights on New Jersey shelf architecture, IODP Expedition 313. *Geosphere*, *9*(6), 1488–1513. https://doi.org/10.1130/GES00872.1

Keen, C. E., & Beaumont, C. (1990). Geodynamics of Rifted Continental Margins. In M. J. Keen & G. L. Williams (Eds.), *Geology of the Continental Margin of Eastern Canada*. Geological Society of America. https://doi.org/10.1130/DNAG-GNA-I1.391

Knorr, G., & Lohmann, G. (2014). Climate warming during Antarctic ice sheet expansion at the Middle Miocene transition. *Nature Geoscience*, *7*(5), 376–381. https://doi.org/10.1038/ngeo2119

Kominz, M. A., Miller, K. G., & Browning, J. V. (1998). Long-term and short-term global Cenozoic sea-level estimates. *Geology*, *7613*(4), 311–314. https://doi.org/10.1130/0091-7613(1998)026<0311

Kominz, M. A., Miller, K. G., Browning, J. V., Katz, M. E., & Mountain, G. S. (2016). Miocene relative sea level on the New Jersey shallow continental shelf and coastal plain derived from one-dimensional backstripping: A case for both eustasy and epeirogeny. *Geosphere*, *12*(5), 1437–1456. https://doi.org/10.1130/GES01241.1

Kominz, M. A., & Pekar, S. F. (2001). Oligocene eustasy from two-dimensional sequence stratigraphic backstripping. *Bulletin of the Geological Society of America*, *113*(3), 291–304. https://doi.org/10.1130/0016-7606(2001)113<0291:OEFTDS>2.0.CO;2

Kopp, R. E., Horton, R. M., Little, C. M., Mitrovica, J. X., Oppenheimer, M., Rasmussen, D. J., Strauss, B. H., & Tebaldi, C. (2014). Probabilistic 21st and 22nd century sea-level projections at a global network of tide-gauge sites. *Earth's Future*, *2*(8), 383–406. https://doi.org/10.1002/2014EF000239

Korup, O. (2012). Earth's portfolio of extreme sediment transport events. *Earth-Science Reviews*, *112*(3–4), 115–125. https://doi.org/10.1016/j.earscirev.2012.02.006

Kulp, S., & Strauss, B. H. (2016). Global DEM Errors Underpredict Coastal Vulnerability to Sea Level Rise and Flooding. *Frontiers in Earth Science*, *4*(April), 1–8. https://doi.org/10.3389/feart.2016.00036

Kutterolf, S., Jegen, M., Mitrovica, J. X., Kwasnitschka, T., Freundt, A., & Huybers, P. J. (2013). A detection of Milankovitch frequencies in global volcanic activity. *Geology*, *41*(2), 227–230. https://doi.org/10.1130/G33419.1

Kutterolfa, S., Schindlbeckb, J. C. C., Jegena, M., Freundta, A., & Straubc, S. M. M. (2018). Milankovitch frequencies in tephra records at volcanic arcs: The relation of kyr-scale cyclic variations in volcanism to global climate changes. *Quaternary Science Reviews*. https://doi.org/10.1080/09654313.2014.916254

Laskar, J., Roboutel, P., Joutel, F., Gastineau, M., Correia, A. C. M., & Levrard, B. (2004). Long-term solution for the insolation quantities of the Earth. *Proceedings of the International Astronomical Union*, *2*(14), 465. https://doi.org/10.1017/S1743921307011404

Lavier, L. L., Steckler, M. S., & Brigaud, F. (2001). Climatic and tectonic control on the Cenozoic evolution of the West African margin. *Marine Geology*, *178*(1–4), 63–80. https://doi.org/10.1016/S0025-3227(01)00175-X

Leynaud, D., Mienert, J., & Vanneste, M. (2009). Submarine mass movements on glaciated and non-glaciated European continental margins: A review of triggering mechanisms and preconditions to failure. *Marine and Petroleum Geology*, *26*(5), 618–632. https://doi.org/10.1016/j.marpetgeo.2008.02.008

Lourens, L., & Tuenter, E. (2009). The Role of Variations of the Earth's Orbital Characteristics

in Climate Change. *Climate Change*. https://doi.org/10.1016/B978-0-444-53301-2.00005-1
Løvholt, F., Kühn, D., Bungum, H., Harbitz, C. B., & Glimsdal, S. (2012). Historical tsunamis and present tsunami hazard in eastern Indonesia and the southern Philippines. *Journal of Geophysical Research: Solid Earth*, *117*(9), 1–19. https://doi.org/10.1029/2012JB009425
Lu, H., Fulthorpe, C. S., & Mann, P. (2003). Three-dimensional architecture of shelf-building sediment drifts in the offshore Canterbury Basin, New Zealand. *Marine Geology*, *193*(1–2), 19–47. https://doi.org/10.1016/S0025-3227(02)00612-6
Lu, H., Fulthorpe, C. S., Mann, P., & Kominz, M. A. (2005). Miocene-recent tectonic and climatic controls on sediment supply and sequence stratigraphy: Canterbury basin, New Zealand. *Basin Research*, *17*(2), 311–328. https://doi.org/10.1111/j.1365-2117.2005.00266.x
Mann, P. (2015). Passive Plate Margin. *Encyclopedia of Marine Geosciences*. https://doi.org/10.1007/978-94-007-6644-0_100-1
Matthews, M. D., & Perlmutter, M. A. (2009). Global Cyclostratigraphy: An Application to the Eocene Green River Basin. In *Orbital Forcing and Cyclic Sequences* (pp. 459–481). Blackwell Publishing Ltd. https://doi.org/10.1002/9781444304039.ch28
Matthews, R., & Al-Husseini, M. (2010). Orbital-forcing glacio-eustasy: A sequence-stratigraphic time scale. *GeoArabia*, *15*(3), 155–167.
McCarthy, F. M. G. G., Katz, M. E., Kotthoff, U., Browning, J. V., Miller, K. G., Zanatta, R., Williams, R. H., Drljepan, M., Hesselbo, S. P., Bjerum, C., & Mountain, G. S. (2013). Sea-level control of new jersey margin architecture: Palynological evidence from integrated ocean drilling program expedition 313. *Geosphere*, *9*(6), 1457–1487. https://doi.org/10.1130/GES00853.1
MGL1510 expedition Proposal. (2011). *MGL1510 Proposal-Collaborative Research : Community-Based 3D Imaging that Ties Clinoform Geometry to Facies Successions and Neogene Sea-Level Change*. *fall*.
Micheal, O., Glavovic, B., Hinkel, J., Roderik, van, Magnan, A., Abd-Elgawad, A., Rongshu, C., Miguel, C.-J., Robert, D., Ghosh, T., Hay, J., Ben, M., Meyssignac, B., Sebesvari, Z., A.J., S., Dangendorf, S., & Frederikse, T. (2019). *Sea Level Rise and Implications for Low Lying Islands, Coasts and Communities*.
Micheels, A., Bruch, A., & Mosbrugger, V. (2009). MIOCENE CLIMATE MODELLING SENSITIVITY EXPERIMENTS FOR DIFFERENT CO 2 CONCENTRATIONS Arne Micheels , Angela Bruch , and Volker Mosbrugger. *Palaeontologia Electronica*, *12*(2), 5A. http://palaeo-electronica.org/2009_2/172/index.html
Milanković, M. (1920). *Théorie Mathématique des Phénomènes Thermiques Produits par la Radiation Solaire*. Gauthier-Villars et Cie.
Miller, K. G., Browning, J. V., John Schmelz, W., Kopp, R. E., Mountain, G. S., & Wright, J. D. (2020). Cenozoic sea-level and cryospheric evolution from deep-sea geochemical and continental margin records. *Science Advances*, *6*(20). https://doi.org/10.1126/sciadv.aaz1346
Miller, K. G., Browning, J. V., Mountain, G. S., Bassetti, M. A., Monteverde, D. H., Katz, M. E., Inwood, J., Lofi, J., & Proust, J. N. (2013). Sequence boundaries are impedance contrasts: Core-seismic-log integration of Oligocene-Miocene sequences, New Jersey shallow shelf. *Geosphere*, *9*(5), 1257–1285. https://doi.org/10.1130/GES00858.1
Miller, K. G., Browning, J. V., Mountain, G. S., Sheridan, R. E., Sugarman, P. J., Glenn, S., & Christensen, B. A. (2014). Chapter 3 History of continental shelf and slope sedimentation

on the US middle Atlantic margin. *Geological Society, London, Memoirs*, *41*(1), 21–34. https://doi.org/10.1144/M41.3

Miller, K. G., & Fairbanks, R. G. (1983). Evidence for Oligocene–Middle Miocene abyssal circulation changes in the western North Atlantic. *Nature*, *306*, 250. https://doi.org/10.1038/306250a0

Miller, K. G., Kominz, M. A., Browning, J. V., Wright, J. D., Mountain, G. S., Katz, M. E., Sugarman, P. J., Cramer, B. S., Christie-Blick, N., & Pekar, S. F. (2005). The phanerozoic record of global sea-level change. *Science*, *310*(5752), 1293–1298. https://doi.org/10.1126/science.1116412

Miller, K. G., Lombardi, C. J., Browning, J. V., Schmelz, W. J., Gallegos, G., Mountain, G. S., & Baldwin, K. E. (2018). Back To Basics of Sequence Stratigraphy: Early Miocene and Mid-cretaceous Examples from the New Jersey Paleoshelf. *Journal of Sedimentary Research*, *88*(1), 148–176. https://doi.org/10.2110/jsr.2017.73

Miller, K. G., & Mountain, G. S. (1994). Global Sea-Level Change and the New Jersey Margin. *Proceedings of the Ocean Drilling Program, Initial Reports*, *150*, 11–20.

Miller, K. G., & Mountain, G. S. (1996). Drilling and Dating New Jersey Oligocene-Miocene Sequences: Ice Volume, Global Sea Level, and Exxon Records. *Science*, *271*(5252), 1092–1095. https://doi.org/10.1126/science.271.5252.1092

Miller, K. G., Mountain, G. S., Browning, J. V., Katz, M. E., Monteverde, D. H., Sugarman, P. J., Ando, H., Bassetti, M. A., Bjerum, C., Hodgson, D. M., Hesselbo, S. P., Karakaya, S., Proust, J. N., & Rabineau, M. (2013). Testing sequence stratigraphic models by drilling Miocene foresets on the New Jersey shallow shelf. *Geosphere*, *9*(5), 1236–1256. https://doi.org/10.1130/GES00884.1

Miller, K. G., Mountain, G. S., Browning, J. V., Kominz, M. A., Sugarman, P. J., Christie-Blick, N., Katz, M. E., & Wright, J. D. (1998). Cenozoic global sea level, sequences, and the New Jersey transect: Results from coastal plain and continental slope drilling. *Reviews of Geophysics*, *36*(4), 569–601. https://doi.org/10.1029/98RG01624

Miller, K. G., Sugarman, P. J., Browning, J. V., Sheridan, R. E., Kulhanek, D. K., Monteverde, D. H., Wehmiller, J. F., Lombardi, C., & Feigenson, M. D. (2013). Pleistocene sequence stratigraphy of the shallow continental shelf, offshore New Jersey: Constraints of integrated ocean drilling program Leg 313 core holes. *Geosphere*, *9*(1), 74–95. https://doi.org/10.1130/GES00795.1

Molnar, P. (2001). Climate change, flooding in arid environments, and erosion rates. *Geology*, *29*(12), 1071–1074. https://doi.org/10.1130/0091-7613(2001)029<1071:CCFIAE>2.0.CO

Molnar, P. (2004). LATE CENOZOIC INCREASE IN ACCUMULATION RATES OF TERRESTRIAL SEDIMENT: How Might Climate Change Have Affected Erosion Rates? *Annual Review of Earth and Planetary Sciences*, *32*(1), 67–89. https://doi.org/10.1016/j.matcom.2017.10.010

Monteverde, D. H., Miller, K. G., & Mountain, G. S. (2000). Correlation of offshore seismic profiles with onshore New Jersey Miocene sediments. *Sedimentary Geology*, *134*(1–2), 111–127. https://doi.org/10.1016/S0037-0738(00)00016-6

Monteverde, D. H., Mountain, G. S., & Miller, K. G. (2008). Early Miocene sequence development across the New Jersey margin. *Basin Research*, *20*(2), 249–267. https://doi.org/10.1111/j.1365-2117.2008.00351.x

Moore, J. G., & Normark, W. R. (1994). GIANT HAWAIIAN LANDSLIDES. *Annual Review of Earth and Planetary Science*, *22*.

Mountain, G. S., Burger, R. L., Delius, H., Fulthorpe, C. S., Austin, J. A., Goldberg, D. S., Steckler, M. S., Mchugh, C. M., Miller, K. G., Monteverde, D. H., Orange, D. L., & Pratson, L. F. (2007). The long-term stratigraphic record on continental margins. *Continental Margin Sedimentation: From Sediment Transport to Sequence Stratigraphy*, 381–458. https://doi.org/10.1002/9781444304398.ch8

Mountain, G. S., Miller, K. G., Blum, P., Poag, C. W., Twichell, D. ., & Aubry, M.-P. (1996). Data report: Eocene to upper Miocene calcareous nannofossil stratigraphy. *Proc. ODP, Sci. Results, 150*, 70–71.

Mountain, G. S., Miller, K. G., Christie-blick, N., Peter, J., & Fulthorpe, C. S. (2006). Shallow-Water Drilling of the New Jersey Continental Shelf: Determining the Links Between Sediment Architecture and Sea-Level Change. *Research Proposal*.

Mountain, G. S., Proust, J.-N., & McInroy, D. (2009). *Shallow-water drilling of the New Jersey continental shelf: global sea level and architecture of passive margin sediments*. *313*. https://doi.org/10.2204/iodp.sp.313.2009

Mountain, G. S., Proust, J. N. J.-N., & Expedition 313 Science Party. (2010). The New Jersey margin scientific drilling project (IODP expedition 313): Untangling the record of global and local sea-level changes. *Scientific Drilling*, *10*(10), 26–34. https://doi.org/10.2204/iodp.sd.10.03.2010

Mountjoy, J. J., Mckean, J., Barnes, P. M., & Pettinga, J. R. (2009). Terrestrial-style slow-moving earth fl ow kinematics in a submarine landslide complex. *Marine Geology*, *267*(3–4), 114–127. https://doi.org/10.1016/j.margeo.2009.09.007

Müller, R. D., Sdrolias, M., Gaina, C., & Roest, W. R. (2008). Age, spreading rates, and spreading asymmetry of the world's ocean crust. *Geochemistry, Geophysics, Geosystems*, *9*(4), 1–19. https://doi.org/10.1029/2007GC001743

Murray-Wallace, C. V, & Woodroffe, C. D. (2014). *Quaternary Sea-Level Changes: A Global Perspective*. Cambridge University Press. https://doi.org/10.1017/CBO9781139024440

Naish, T., Powell, R., Levy, R., Wilson, G., Scherer, R., Talarico, F., Krissek, L., Niessen, F., Pompilio, M., Wilson, T., Carter, L., DeConto, R., Huybers, P., McKay, R., Pollard, D., Ross, J., Winter, D., Barrett, P., Browne, G., … Williams, T. (2009). Obliquity-paced Pliocene West Antarctic ice sheet oscillations. *Nature*, *458*(7236), 322–328. https://doi.org/10.1038/nature07867

Olsen, P. E. (1997). Stratigraphic Record of the Early Mesozoic Breakup of Pangea in the Laurasia-Gondwana Rift System. *Annual Review of Earth and Planetary Sciences*, *25*(1), 337–401. https://doi.org/10.1146/annurev.earth.25.1.337

Oppenheimer, M., O'Neil, B. C., Webster, M., & Agrawala, S. (2007). The Limits of Consensus The Limits of Consensus. *Science*, *Spetember*.

Pälike, H., Laskar, J., & Shackleton, N. J. (2004). Geologic constraints on the chaotic diffusion of the solar system. *Geology*, *32*(11), 929–932. https://doi.org/10.1130/G20750.1

Patruno, S., Hampson, G. J., & Jackson, C. A. L. (2015). Quantitative characterisation of deltaic and subaqueous clinoforms. *Earth-Science Reviews*, *142*, 79–119. https://doi.org/10.1016/j.earscirev.2015.01.004

Pazzaglia, F. J., & Brandon, M. T. (1996). Macrogeomorphic evolution of the post-TriassicAppalachian mountains determined by deconvolutionof the offshore basin sedimentary record. *Basin Research*, *8*(1996), 1–24. file:///Users/lstevens/Papers2/Articles/1996/Unknown/Unknown/1996_.pdf%5Cnpapers2://publication/uuid/7EBAB4BB-024D-4383-B73C-43E20BCCD91C

Pazzaglia, F. J., & Gardner, W. (1994). Late Cenozoic flexural deformation of the middle U.S. Atlantic passive margin. *Atlantic*, *99*.
Pekar, S., & M. DeConto, R. (2006). Pekar, S. F. & DeConto, R. M. High-resolution ice-volume estimates for the early Miocene: evidence for a dynamic ice sheet in Antarctica. Palaeogeog. Palaeoclimatol. Palaeoecol. 231, 101-109. *Palaeogeography, Palaeoclimatology, Palaeoecology*, *231*, 101–109. https://doi.org/10.1016/j.palaeo.2005.07.027
Perlmutter, M. A., Brennan, P. A., Hook, S. C., Dempster, K., & Pasta, D. (1995). Global cyclostratigraphic analysis of the Seychelles Southern Shelf for potential reservoir, seal and source rocks. *Sedimentary Geology*, *96*(1–2), 93–118. https://doi.org/10.1016/0037-0738(94)00128-H
Pfeffer, W. T., Harper, J. T., & O'Neel, S. (2008). Kinematic Constraints on Glacier Contributions to 21st-Century Sea-Level Rise. *Science*, *311*(January), 212–216.
Pisias, N. G., & Shackleton, N. J. (1984). Modelling the global climate response to orbital forcing and atmospheric carbon dioxide changes. *Nature*, *310*, 757. https://doi.org/10.1038/310757a0
Pitman, W. I. I. I., & Golovchenk, X. (1983). The effect of sea-level change on the shelf edge and slope of passive margins. *SEPM Special Publication*, *33*, 41–58.
Poag, C. W., & Sevon, W. D. (1989). A record of Appalachian denudation in postrift Mesozoic and Cenozoic sedimentary deposits of the U.S. Middle Atlantic continental margin. *Geomorphology*, *2*(1–3), 119–157. https://doi.org/10.1016/0169-555X(89)90009-3
Potter, P. E., & Szatmari, P. (2009). Global Miocene tectonics and the modern world. *Earth-Science Reviews*, *96*(4), 279–295. https://doi.org/10.1016/j.earscirev.2009.07.003
Poulsen, C. J., Flemings, P. B., Robinson, R. A. J. J., & Metzger, J. M. (1998). Three-dimensional stratigraphic evolution of the Miocene Baltimore Canyon region: Implications for eustatic interpretations and the systems tract model. *Bulletin of the Geological Society of America*, *110*(9), 1105–1122. https://doi.org/10.1130/0016-7606(1998)110<1105:TDSEOT>2.3.CO;2
Prokopenko, A. A., Hinnov, L. A., Williams, D. F., & Kuzmin, M. I. (2006). Orbital forcing of continental climate during the Pleistocene: a complete astronomically tuned climatic record from Lake Baikal, SE Siberia. *Quaternary Science Reviews*, *25*(23–24), 3431–3457. https://doi.org/10.1016/j.quascirev.2006.10.002
Proust, J. N., Pouderoux, H., Ando, H., Hesselbo, S. P., Hodgson, D. M., Lofi, J., Rabineau, M., & Sugarman, P. J. (2018). Facies architecture of Miocene subaqueous clinothems of the New Jersey passive margin: Results from IODP-ICDP Expedition 313. *Geosphere*, *14*(4), 1564–1591. https://doi.org/10.1130/GES01545.1
Reynolds, D. J., Steckler, M. S., & Coakley, B. J. (1991). The role of the sediment load in sequence stratigraphy: The influence of flexural isostasy and compaction. *Journal of Geophysical Research: Solid Earth*, *96*(B4), 6931–6949. https://doi.org/10.1029/90JB01914
Rieke, H. H., & Chilingarian, G. V. (1974). Chapter 4 Effect of Compaction on Some Properties of Argillaceous Sediments. *Developments in Sedimentology*, *16*(C), 123–217. https://doi.org/10.1016/S0070-4571(08)70774-X
Rohling, E. J., Haigh, I. D., Foster, G. L., Roberts, A. P., & Grant, K. M. (2013). A geological perspective on potential future sea-level rise. *Scientific Reports*, *3*. https://doi.org/10.1038/srep03461
Rowley, D. B., Forte, A. M., Moucha, R., Mitrovica, J. X., Simmons, N. A., & Grand, S. P.

(2011). *Dynamic Topography Change of the Eastern US since 4 Ma: Implications for Sea Level and Stratigraphic Architecture of Passive Margins*.
Ruddiman, W. F. (2003). Orbital insolation, ice volume, and greenhouse gases. *Quaternary Science Reviews*, *22*, 1597–1629. https://doi.org/10.1016/S0277-3791(03)00087-8
Ruffman, A., & Hann, V. (2006). The Newfoundland Tsunami of November 18 , 1929 : An Examination of the Twenty-eight Deaths of the " South Coast Disaster ." *Newfoundland and Labrador Studies*, *21*(1), 1719–1726.
Sanchez, C. M., Fulthorpe, C. S., & Steel, R. J. (2012a). Middle Miocene-Pliocene siliciclastic influx across a carbonate shelf and influence of deltaic sedimentation on shelf construction, Northern Carnarvon Basin, Northwest Shelf of Australia. *Basin Research*, *24*(6), 664–682. https://doi.org/10.1111/j.1365-2117.2012.00546.x
Sanchez, C. M., Fulthorpe, C. S., & Steel, R. J. (2012b). Miocene shelf-edge deltas and their impact on deepwater slope progradation and morphology, Northwest Shelf of Australia. *Basin Research*, *24*(6), 683–698. https://doi.org/10.1111/j.1365-2117.2012.00545.x
Scholle, P. A. (1980). Geological studies of the COST No. B-3 Well, United States Mid-Atlantic continental slope area. In *Circular*. https://doi.org/10.3133/cir833
Schulten, I., Mosher, D. C., Krastel, S., Piper, D. J. W., Kienast, M., By, N. S., & Kiel, C. (2018). Surficial sediment failures due to the 1929 Grand Banks Earthquake , St Pierre Slope Natural Resources Canada , Bedford Institute of Oceanography , 1 Challenger. *The Geological Society of London*.
Shackleton, N. J., Hall, M. A., Raffi, I., Tauxe, L., & Zachos, J. (2000). Astronomical calibration age for the Oligocene-Miocene boundary. *Geology*, *28*(5), 447–450. https://doi.org/10.1130/0091-7613(2000)028<0447:ACAFTO>2.3.CO;2
Shepherd, A., Ivins, E., Rignot, E., Smith, B., van den Broeke, M., Velicogna, I., Whitehouse, P., Briggs, K., Joughin, I., Krinner, G., Nowicki, S., Payne, T., Scambos, T., Schlegel, N., A, G., Agosta, C., Ahlstrøm, A., Babonis, G., Barletta, V. R., … Team, T. I. (2020). Mass balance of the Greenland Ice Sheet from 1992 to 2018. *Nature*, *579*(7798), 233–239. https://doi.org/10.1038/s41586-019-1855-2
Solomon, S., Alley, R., Gregory, J., Lemke, P., & Manning, M. (2008). A Closer Look at the IPCC Report. *Science*, *319*(5862), 409 LP – 410. https://doi.org/10.1126/science.319.5862.409c
Steckler, M. S., Mountain, G. S., Miller, K. G., & Christie-Blick, N. (1999). Reconstruction of Tertiary progradation and clinoform development on the New Jersey passive margin by 2-D backstripping. *Marine Geology*, *154*(1–4), 399–420. https://doi.org/10.1016/S0025-3227(98)00126-1
Steckler, M. S., Reynolds, D. J., Coakley, B. J., Swift, B. A., & Jarrard, R. (1993). Modelling Passive Margin Sequence Stratigraphy. In *Sequence Stratigraphy and Facies Associations*. https://doi.org/10.1002/9781444303810
Steckler, M. S., & Watts, A. B. (1978). Subsidence of the Atlantic-type continental margin off New York. *Earth and Planetary Science Letters*, *41*(1), 1–13. https://doi.org/10.1016/0012-821X(78)90036-5
Steffen, H., & Kaufmann, G. (2005). Glacial isostatic adjustment of Scandinavia and northwestern Europe and the radial viscosity structure of the Earth's mantle. *Geophysical Journal International*, *163*(2), 801–812. https://doi.org/10.1111/j.1365-246X.2005.02740.x
Stein, S., Sleep, N. H., Geller, R. J., Wang, S.-C., & Kroeger, G. C. (1979). EARTHQUAKES ALONG THE PASSIVE MARGIN OF EASTERN CANADA Seth. *Geophysical Research*

Letters, *6*(7).
Stern, N., & Herbert, N. (2015). Stern Review: The Economics of Climate Change. *Cambridge University Press*. https://doi.org/10.1257/aer.98.2.1
Strasser, A., Hilgen, F. J., & Heckel, P. H. (2006). Cyclostratigraphy – concepts, definitions, and applications. *Newsletters on Stratigraphy*, *42*(2), 75–114. https://doi.org/10.1127/0078-0421/2006/0042-0075
Swarbrick, R., Osborne, M., & Yardley, G. (2002). Comparison of overpressure magnitude resulting from the main generating mechanisms. In *AAPG Memoir* (pp. 1–12).
Swift, D. J. P., & Thorne, J. A. (2009). Sedimentation on Continental Margins, I: A General Model for Shelf Sedimentation. In *Shelf Sand and Sandstone Bodies* (pp. 1–31). John Wiley & Sons, Ltd. https://doi.org/10.1002/9781444303933.ch1
Tagliaro, G., Fulthorpe, C. S., Gallagher, S. J., McHugh, C. M., Kominz, M. A., & Lavier, L. L. (2018). Neogene siliciclastic deposition and climate variability on a carbonate margin: Australian Northwest Shelf. *Marine Geology*, *403*(June), 285–300. https://doi.org/10.1016/j.margeo.2018.06.007
Tesson, M., Gensous, B., Allen, G. P., & Ravenne, C. (1990). Late Quaternary deltaic lowstand wedges on the Rhône continental shelf, France. *Marine Geology*, *91*(4), 325–332. https://doi.org/https://doi.org/10.1016/0025-3227(90)90053-M
Tinti, S., Maramai, A., & Graziani, L. (2004). The New Catalogue of Italian Tsunamis. *Natural Hazards*, *33*, 439–465. https://www.fool.com/investing/2016/06/04/3-reasons-comcast-bought-dreamworks.aspx?source=iedfolrf0000001
Tosi, L., Teatini, P., & Strozzi, T. (2013). Natural versus anthropogenic subsidence of Venice. *Scientific Reports*, *3*(1), 2710. https://doi.org/10.1038/srep02710
Van Wagoner, J., Posamentier, H. W., Mitchum, R., Vail, P. R., Sarg, J. F. F., Loutit, T. S., & Hardenbol, J. (1988). An overview of the fundamentals of sequence stratigraphy and key definitions. *The Society of Economic Paleontologists and Mineralogists*, *42*, 39–45. https://doi.org/10.2110/pec.88.01.0039
Wade, B. S., & Pälike, H. (2004). Oligocene climate dynamics. *Paleoceanography*, *19*(4), 1–16. https://doi.org/10.1029/2004PA001042
Watkins, J. S., & Mountain, G. S. (1988). *The Role of ODP Drilling in the Inverstigation of Global Changes in Sea Level*.
Watts, A. B., & Steckler, M. S. (1981). Subsidence and tectonics of Atlantic-type continental margins. *Oceanologica ACTA*, 143–154.
Watts, A. B., & Steckler, M. S. (1979). *Subsidence and eustasy at the continental margin of eastern North America* (pp. 218–234). https://doi.org/10.1029/ME003p0218
Watts, A. B., & Thorne, J. A. (1984). Tectonic global changes in sea-level and their relationship to stratigraphic sequences at the U.S. Atlantic continental margin. *Mar. Petrol Geol.*, *1(4)*(1977), 319–339. https://doi.org/10.1016/0264-8172(84)90134-X
Williams, D. F., Peck, J., Karabanov, E. B., A. A. Prokopenko, V. Kravchinsky, King, J., & Kuzmin, M. I. (2010). *Lake Baikal Record of Continental Climate Response to Orbital Insolation During the Past 5 Million Years Lake Baikal Record of Continental Climate Response to Orbital Insolation During the Past 5 Million Years*. *1114*(1997), 1114–1117. https://doi.org/10.1126/science.278.5340.1114
Withjack, M. O., Schlische, R. W., & Olsen, P. E. (1998). Diachronous rifting, drifting, and inversion on the passive margin of central eastern North America: an analog for other passive margins. *AAPG Bulletin*, *82*(5 A), 817–835. https://doi.org/10.1306/1D9BC60B-

172D-11D7-8645000102C1865D
Wu, P. (1998). Intraplate earthquakes and Postglacial Rebound in Eastern Canada and Northern Europe. *Dynamics of the Ice Age Earth: A Modern Perspective*, 603–628.
Zachos, J. C., Shackleton, N. J., Revenaugh, J. S., Palike, H., & Flower, B. P. (2001). Climate Response to Orbital ForcingAcross the Oligocene-Miocene Boundary. *Science*, *292*(5515), 274–278. http://www.sciencemag.org/cgi/content/abstract/292/5515/274

CHAPTER 2. GEOMETRICAL BREAKDOWN APPROACH TO INTERPRETATION OF STRATIGRAPHIC CYCLES

2.1 Abstract

Seismic and sequence stratigraphic analyses are important methodologies for interpreting coastal and shallow-marine deposits. Though both methods are based on objective criteria, terminology for reflection/stratal stacking is widely linked to eustatic cycles, which does not adequately incorporate factors such as differential subsidence, sediment supply, and autogenic effects. To reduce reliance on model-driven interpretations, we develop a Geometrical Breakdown Approach (GBA) that facilitates interpretation of horizon-bound reflection packages by systematically identifying upward-downward and landward-seaward trajectories of clinoform inflection points and stratal terminations, respectively, enabling a rigorous characterization of stratal surfaces and depositional units. The results are captured in three-letter acronyms that provide an efficient way of recognizing repetitive stacking patterns. This approach discriminates reflection packages objectively to the maximum level of resolution provided by the data, with subsequent interpretation using selected sequence stratigraphic models based on three/four systems tracts or progradational-retrogradational-aggradational-degradational units. We test this approach using a synthetic analogue model and field data from the New Jersey margin. The results demonstrate that the geometrical criteria constitute a reliable tool for identifying systems tracts and are a step forward in providing an objective and straightforward method for practitioners at all levels of experience. Comparison of GBA with existing approaches shows that, although the interpretations are commonly in general agreement, GBA allows a greater level of detail to be extracted, utilizing more effectively the fine-scale resolution provided by the input seismic data.

2.2 Introduction

Sequence stratigraphy is the study of sedimentary units within a chronostratigraphic framework of genetically related strata bounded by surfaces of deposition (correlative conformities), non-deposition, and erosion (Van Wagoner et al., 1988). The discipline, which evolved from seismic stratigraphy (Vail et al., 1977), characterizes stratal stacking patterns and has been widely used to interpret the depositional history of sedimentary basins at multiple scales, as well as to infer the rate of sediment supply with respect to base-level change (Mitchum et al., 1977b; Posamentier et al., 1988; Helland-Hansen and Gjelberg, 1994), especially in coastal and shelfal environments (e.g. Csato et al., 2013; Eriksson et al., 2013; Fulthorpe et al., 1999; Mountain et al., 2007; Steckler et al., 1999).

Sloss et al. (1949) defined six unconformity-bound depositional cycles in shallow-marine strata across the North American craton, attributed to the long term (first-order) sea-level change resulting from breakup and formation of supercontinents every 200-400 million years (Myr). Researchers working on plate-tectonics theory observed second-order sea-level cycles at 10-100 Myr time scales related to changes in the size of the oceans driven by fluctuations in the volume of magma produced at mid-ocean ridges (Hallam, 1963) and the relative speed of plate motion (Sheridan, 1987). With the advent of multi-channel seismic imaging, discontinuities were identified using physical properties (i.e. reflection terminations), and Peter Vail and others at Esso Production Research (now ExxonMobil) proposed new concepts for interpreting the significance of stratal stacking patterns observed in 2D seismic data on continental shelves, attributing third-order cycles with 0.5 to 5 Myr duration predominantly to glacio-eustasy (Vail et al., 1977; Mitchum et al., 1990). Advances in borehole logging, isotope geochemistry, and dating techniques led to the refinement of paleo sea-level curves (Haq et al., 1987; Miller et al., 2005) and the recognition of fourth and fifth-order cycles with durations of 0.1-0.5 Myr and 0.01-0.1 Myr, respectively (Van Wagoner et al., 1990; 1988). These concepts have been extensively documented in AAPG Memoir 26 (1977), SEPM Special Publication 42 (1988), and several other publications (Catuneanu et al., 2009; Embry & Johannessen, 2017; Miall, 2006; Miller et al., 2018; Posarnentier and Allen, 1999; Zaitlin et al., 1994).

A key development was the recognition of systems tracts, i.e. genetically associated stratigraphic units that form at different phases of a single cycle of sea-level change (Van Wagoner et al.,

1988; Hunt & Tucker, 1992; Jervey, 1988; Plint & Nummedal, 2000). Figure 2.1 summarizes some of the main models that consider stacking patterns as the basic criteria to identify systems tracts within a sequence (Galloway, 1989). The proposed depositional sequence models (Hunt and Tucker, 1992; Miller et al., 2018; Van Wagoner et al., 1988) use the subaerial unconformity (a diachronous surface) and its marine correlative conformity (synchronous surface) as a composite sequence boundary (Catuneanu, 2002). In their models, formation of the subaerial unconformity is assumed contemporary with the stage of base level fall at the shoreline, and the correlative conformity is considered as the sea floor at the end of forced regression. Depositional sequences used by Van Wagoner et al. (1988) and Miller et al. (2018) are similar in concept, except that a falling stage systems tract is recognized in the latter. The transgressive–regressive sequence model (Embry and Johannessen, 1993) is bounded by composite surfaces including subaerial unconformities, ravinement surfaces, and their correlative maximum regressive surfaces (Catuneanu, 2002). In transgressive–regressive model, the correlative conformity is replaced with the marine portion of the maximum regressive surface in shallow marine settings on outcrop or subsurface data.

Precise seismic criteria for identifying the boundaries between systems tracts, however, are often lacking, leading to subjective interpretations and model results that fail to utilize the resolution available using seismic data. For example, the boundary between highstand systems tract and falling stage systems tract is not defined by any specific surface in the four systems tracts model due to the challenge in recognizing the onset of sea level fall. In addition, orbital forces, eustasy, tectonic movements, rate of sediment supply, and autocyclicity (Muto et al., 2007) have all been understood to contribute to depositional cyclicity, leading to uncertainty as to whether, or to what degree, glacio-eustasy can be recognized in the sedimentary record (e.g. Matthews & Al-Husseini, 2010; Matthews & Frohlich, 1998; Strasser et al., 2000) and whether sequence stratigraphy is fractal, with a hierarchal or continuous pattern (e.g. Schlager, 2004).

In order to estimate the timing and partitioning of sediments within sequences, sediment mass balance must be coupled with allogenic controlling mechanisms (e.g. Kendall et al., 1991; Martin et al., 2009; Perlmutter et al., 1997; Weimer and Posamentier, 1993). The accommodation succession method (Neal and Abreu, 2009) links accommodation creation and sediment fill with three observable stratal patterns: progradation-aggradation during which the rate of accommodation creation is less than sediment fill; retrogradation during which the rate of

accommodation creation exceeds sediment fill; and aggradation-progradation-degradation during which the rate of accommodation creation is less than the volume of the supplied sediment, so that accommodation growth is negative. This model explains the initial condition necessary to deposit each stratal package but does not define precise criteria for identifying package boundaries.

The rapid development of seismic and sequence stratigraphy since 1977 has advanced sedimentary geology considerably but has also led to an abundance of overlapping terminology, methods, and models which are often not clearly separated. We find that this makes the task of addressing fundamental scientific questions using large data sets difficult, particularly for new practitioners. This overall problem has been recognized by numerous studies (Catuneanu et al., 2009; Helland-Hansen; 2009; Embry 2009); Burgess et al., 2016; Miller et al., 2018). With a goal to further improve and simplify seismic and sequence stratigraphic work, we develop a new method for systematic identification, characterisation, and interpretation of depositional units that we name Geometrical Breakdown Approach (GBA). The GBA examines the geometry of stratigraphic surfaces relative to older strata and defines objective geometric criteria building on robust aspects of existing methods for stacking patterns and shoreline trajectories to generate an efficient and repeatable interpretation of clinothem external and internal structure. In essence, we characterise each seismically resolvable depositional unit, from a single pair of reflections at close to tuning frequency to groups of reflections with similar geometry, with a three-letter acronym that combines nomenclature for reflection terminations (Part 2 of AAPG Memoir 26; Mitchum et al., 1977b) seismic facies (Part 6 of AAPG Memoir 26; Mitchum et al., 1977a), and shoreline trajectories (Bullimore et al., 2005, Helland-Hansen and Martinsen, 1996; Helland-Hansen and Hampson, 2009). These acronyms effectively characterise the geometry and relative spatial position of every depositional unit imaged (or group of similar units), and they immediately reveal cyclicity, although without any connotation regarding the origin of that cyclicity. The three-letter acronyms can then be used to assign depositional units to model-based interpretations of systems tracts (Posamentier et al., 1988; Plint and Nummedal, 2000) and accommodation successions (Neal & Abreu, 2009; Neal et al., 2016).

We first test the GBA on a synthetic analogue model to evaluate its effectiveness in a known and controlled environment. This is followed by a test on 2D field seismic data collected over the Miocene shelfal clinothems and across three IODP wells offshore the New Jersey margin, with

the initial assumption that variations in subsidence, sediment supply, and along-strike autocyclic processes (e.g. Madof et al., 2016) had a secondary impact on sediment deposition. Earlier results from seismic and sequence stratigraphic analysis of this profile and associated wells provide an excellent opportunity for evaluating the GBA performance. The main goal of the field 2D seismic data test is to identify and characterize depositional units objectively, without contamination by model-driven terms (Miller et al., 2018), and then to analyze eustatic cyclicity via a sequence stratigraphic model integrated with well data.

2.3 Methods

The GBA is a streamlined methodology to interpret seismic reflection data in order to identify and characterize seismic-stratigraphic packages that can then be incorporated into a sequence stratigraphic framework. The approach, which is an evolution of accommodation succession method proposed by Neil and Abreu (2009), is based on the following procedure: 1) identify the landward and seaward terminations (i.e. the coastal (or proximal) onlap and the distal downlap) of each reflection within the interval of interest; 2) identify reflection packages with similar seismic facies (which can be defined following Vail et al., 1977) and geometry (clinothems) and locate the uppermost rollover point for each clinoform (or, if not evident, the mid-point; see definition of Patruno et al., 2015); 3) determine the direction of vertical shift in the uppermost rollover point (or mid-point) relative to the underlying package, and, likewise, the direction of horizontal shift of the uppermost landward and seaward terminations, and assign a three-letter acronym as described below; 4) use the upward succession of acronyms to identify stratigraphic patterns and cycles; 5) interpret factors that govern the patterns using models selected by the interpreter (in our case a conventional model of four systems tracts); and 6) apply steps 1-5 to multiple sequences to define sequence sets and composite sequences (sequences with a lower hierarchal order).

The spatial relationships for a package are defined, relative to the preceding package, by lateral shifts of stratal terminations and successive upward or downward movements of the rollover points for the upper surface. The rollover point typically upsteps (**U**) or downsteps (**D**), although there are instances where it maintains a static level (**S**) - equivalent to toplap - or may have been eroded (**E**) without obvious angularity. The landward and seaward terminations backstep (**B**) or forestep (**F**) (onlap and downlap, as defined in previous studies but adding relative direction). In

our study, U, D, B, and F were typically adequate but S and E are added to maintain flexibility for different environments.

On this basis, the three-letter acronym of each reflection package is derived according to the geometry of its upper surface (Figure 2.2). The first letter defines the relative position of the rollover point with respect to the underlying package, and the second and third letters define the relative position of the landward and seaward terminations, respectively. The stacking patterns are then assigned to systems tracts based on the preferred stratigraphic model (Figure 2.1). For a four systems tract model (Figure 2.3), the stacking patterns are assigned as:

1. Lowstand Systems Tract (LST): a pronounced **DFB** or **DFF** followed by one or more **UBF**s; the basal surface of the DFF or DFB defines the sequence boundary and the base of the LST; a forced regression, expressed by progradation and aggradation.
2. Transgressive Systems Tract (TST): one or successive **UBB**s; the base of the TST is defined by the onset of backstepping for both terminations (BB), with continued upstepping of the rollover point (U); a transgression, expressed as retrogradation.
3. Highstand Systems Tract (HST): two or more successive **UBF**s**;** the base of the HST is defined by the onset of forestepping for seaward termination (F) with continued backstepping of the landward termination (B) and upstepping of the rollover point (U); a normal regression, expressed as progradation and aggradation.
4. Falling Stage Systems Tract (FSST): two or more successive **DFB**s and/or **DFF**s; the base of the FSST is defined by the onset of downstepping of the rollover point (D) and forestepping of the landward (and commonly the seaward) termination point (F); the beginning of a forced regression, expressed by degradation and commonly progradation.
5. The maximum regressive surface (MRS) is marked by the change from UBFs to UBBs, and the maximum transgressive surface (MTS) is marked by the change from UBBs to UBFs.

6. In the case of erosion and/or a complex system of sediment deposition (e.g. along-strike three-dimensional changes), DFB and UFB may be present in the stratal package; determining the systems tract should be performed on a case-by-case basis.

7. Similarly, this style of combined geometric and positional characterization may be used and adapted to depositional systems where different interpretational models may apply or be developed, for example mass transport deposits, turbidites, slope and basin floor systems.

The workflow described here identifies each package uniquely and the sedimentary record emerges as repeated patterns of three-letter acronyms. By relating these patterns to models, it is then possible to integrate the different stacking patters into the sequence stratigraphic model that best supports the interpretation of the data in the specific case. The clear advance of the proposed approach is that it follows simple rules, avoids complex terminology, is repeatable and easy to annotate, and makes the interpretation more methodical.

In essence, we have combined the key nomenclature of reflection terminations, seismic packages with consistent morphology (in multi-reflection packages the acronym of the upper bounding surface is the same as each individual internal surface), and the spatial relationships of back, fore-, up- and down-stepping, while avoiding model-driven terminology. This makes the approach efficient, as only the upper bounding surface of each package needs to be correlated throughout a seismic survey, resulting in a set of single names that convey the key geometric and spatial information. In practice, as is typical in interpretation procedures, the obvious packages and bounding surfaces tend to ‘jump out’ and more subtle features become progressively more apparent.

An application of the GBA to the Miller et al. (2018) clinothem model shows that, while both approaches rely mainly on stratal geometry, the GBA incorporates the landward and seaward terminations to distinguish the interface between successive systems tracts (Figure 2.4). For implementing a rigorous seismic analysis, the GBA does not require the introduction of additional data, as for example the wireline measurements of petrophysical properties used in Miller et al. (2018). These data can be incorporated if available as an independent dataset to better correlate seismic facies with physical properties.

The GBA focuses on the spatial "stepping" relationships between depositional packages rather than their internal features. In other words, in this approach, while internal signatures are an important part of interpreting seismic data, it is the geometry of upper and lower surfaces of each depositional unit on seismic sections that describes a discrete body of rock that is younger than the one below and older than the one above (Vail et al., 1977; Mitchum et al., 1977a). Where seismic artifacts are present, interpretational judgement may be needed to define the bounding reflections, but establishing a framework of interconnecting and truncating surfaces makes the rest of the procedure systematic. The question then arises of how much detail to invest in horizon interpretation. The workflow is applicable at multiple scales, down to Rayleigh's limit of seismic resolution (Kallweit and Wood, 1982) (half the wavelet width), which has been estimated through well calibration and forward modelling. However, separating signal from noise becomes harder as the level of detail increases.

2.4 Data

We apply the GBA to high-resolution synthetic and field data to illustrate and test the approach in forward and inverse directions (i.e., known process to create stratigraphy vs known stratigraphy to recreate process). We first use a synthetic dataset Henceforth XES02 generated by the Experimental EarthScape Facility of St. Anthony Falls Laboratory at University of Minnesota using programmable differential subsidence in a sedimentary basin under lab conditions (Paola et al., 2001). The experimental setup provides full control over influential input mechanisms of base-level change, subsidence, and rate of sediment influx, allowing an analysis of their effect on the depositional environment. Next, as a real-world example, we implement the GBA to analyze Miocene clinothems offshore the New Jersey margin. In doing so, we incorporate the methodological approaches proposed by Neal and Abreu (2009) and Miller et al. (2018), and we identify key surfaces, sequences, systems tracts, and sequence sets only after all the three-letter acronyms have been determined.

2.4.1 Henceforth XES02 Experiment

For the synthetic data test of the GBA, we use the stratigraphic section from the XES02 experiment shown in Figure 2.5A constructed by high-resolution laser and sonar tomography. The XES02 experiment (Figure 2.5A,B) was designed to examine the stratigraphic response of a shallow marine basin to slow, rapid, and superimposed cycles of base-level change under a

constant rate of subsidence, water supply, and sediment supply (Paola et al., 2001). The slow removal of underlying material from the bottom of the apparatus allows continuous sediment deposition during 310 hours of the experiment. Although constant through time at any one locality, the rate of subsidence increased downstream. In this setup, the trend in base-level change strongly influences the change in the ratio of accommodation creation to sediment flux.

The experiment comprised two phases (Figure 2.5B). Phase 1 consisted of two base-level cycles, the first of which started with a steady base level and active subsidence to build an initial deposit, followed by the imposition of a slow cycle of base-level change and a short equilibrium period. A second, rapid base-level cycle was followed by a constant base level to promote a long equilibration period. Phase 1 was designed to study the stratigraphic response to base-level change for comparison with independent records of basin equilibrium time (Paola et al., 2001). Phase 2 consisted of six high frequency base-level cycles that comprised one slow cycle with longer periodicity. It was designed to simulate natural conditions where recorded base-level cycles can have several major periodicities in response to external drivers and mechanisms (Strong and Paola, 2006; Martin et al., 2009). Because of the low overburden pressure, sediment compaction was negligible during the experiment. At the end of the experiment, some of the eight imposed cycles of base-level change had generated an incomplete suite of surfaces due to erosion, whereas other cycles had generated more than one sedimentary unit for the same discordance. As a result, it is challenging to identify all eight base-level cycles in the preserved record, despite the well-controlled setting. However, the sediment mass migration and shoreline movement curves were in phase with the base-level curve throughout the experiment (Figure 2.5B).

2.4.2 New Jersey Rifted Continental Margin

For the field data test of the GBA, we use the offshore New Jersey seismic profile Oc270 line 529 that crosses IODP holes M27, M28, and M29 (Figures 2.6 and 2.7). The New Jersey rifted continental margin is a prime location to investigate the history of eustatic changes since the Oligocene. High sediment influx (Poag and Sevon, 1989; Miller et al., 1998), tectonic stability (Miller et al., 2014), continuous subsidence due to lithospheric cooling, sediment compaction and isostatic adjustment (Steckler and Watts, 1978; Watts and Steckler, 1979; Reynolds et al., 1991), and a wealth of available data (wells, seismic profiles, bathymetry) make it a natural

laboratory to study paleo-climate and eustatic changes (Miller and Mountain, 1996). In a community effort to evaluate the relative influence of controlling mechanisms on the sedimentary record, a series of boreholes (Figure 2.6), including the most recent IODP holes M27, M28, and M29, were drilled along the New Jersey Sea-Level Transect, extending from the onshore New Jersey coastal plain across the continental shelf to the slope and rise (Miller and Mountain, 1994; Miller et al., 1998). The transect of boreholes made it possible to determine 1) the ages of sequence boundaries with a chronostratigraphic precision of ±0.25 Myr to ±0.5 Myr (Browning et al., 2013) to correlate the sequences with major eustatic events, and 2) the amplitude of relative sea-level changes associated with stratigraphic sequences (Miller and Mountain, 1994).

More than 30 seismic profiles and dozens of wells have greatly improved the resolution of the sequence stratigraphic model for the margin (e.g. Greenlee et al., 1992; Kominz et al., 2002; Miller et al., 2013; Mountain et al., 1996, 2007). Nearly continuous records from the Oligocene to middle Miocene form an excellent repository for evaluating chronostratigraphic and paleoenvironmental constraints (Steckler et al., 1999; Kominz et al., 2002; Browning et al., 2013; Katz et al., 2013; McCarthy et al., 2013). Previous studies of the New Jersey rifted margin showed that, since Oligocene times, eustasy, subsidence, sediment supply, and isostasy have contributed to the shoreline movement, with eustatic forcing being predominant (Grow and Sheridan, 1988; Mountain et al., 2010; McCarthy et al., 2013; Miller et al., 2014). Reconstruction of depositional setting through backstripping of the transgressive-regressive sequences deposited on the coastal plain (15-17 Late Cretaceous, 6 Paleocene, 12 Eocene, 7 Oligocene, and 18-20 Miocene sequences) reveals numerous records of sea-level cycles (Greenlee et al., 1992; Miller and Mountain, 1994; Steckler et al., 1999; Mountain et al., 2006; Miller et al., 2014).

2.5 Results

2.5.1 Sequence Stratigraphy of Synthetic Strata Under Known Conditions

The digitized section of Figure 2.5A comprises 101 surfaces formed during the 310 hours of experiment. We focus the most detailed description on the part of the profile outlined by two dashed lines (Figures 2.5C and 2.5D). Above the lower dashed line, which is an unconformity (sequence boundary) generated during Phase 1 after the slow cycle, we observe a downstepping

unit with both landward and seaward terminations are forestepping relative to the lower sequence boundary (DFF). This stratum is followed by a series of upstepping strata, with backstepping landward terminations and forestepping seaward terminations (UBFs). At the top of this package, the UBF trend changes to a UBB trend. The boundary that marks this change in stratal geometry defines the MRS and marks the change from PA to R (or LST to TST). Following a set of UBB packages, an upstepping-backstepping-forestepping (UBF) trend in as the seaward termination begins to forestep, above a boundary that marks the MTS and the change from TST to HST. Although the top of HST is eroded, the lower terminations continue to forestep, indicating no change in environmental dynamics. A series of DFF and DFB strata represent an FSST. The last DFF followed by a series of UBF strata marks the end of the rapid cycle and beginning of the equilibrium period (upper dashed line, which indicates the end of the period chosen for detailed description). The erosional truncation along with the remnant of the HST (UBF strata) marks the sequence boundary at the end of the rapid cycle.

During the long relaxation time of the second part of cycle 2 (Figure 2.5), the base level does not change; however, continuous subsidence tips the basin (setup of the experiment) landward which results in deposition of new strata closer to the source. This means that the rollover point, landward termination, and seaward termination define UBBs. As deltas avulse, backstepping of landward stratal termination (onlap) is associated with prograding packages on the shelf. Strong and Paola (2006) reported that the surface that ultimately serves as the sequence boundary is more widespread than any other prograding upstepping-backstepping surface during the experiment, which increases the chance that the surface will be preserved in the stratigraphic record.

We also identified the geometry of sequences formed during Phase 2, when high-frequency cycles were superimposed on one low-frequency cycle (except cycle 4, which was severely eroded) (Figure 2.5). The sequences show a distinctive progradational, aggradational, and retrogradational stacking pattern (Martin et al., 2009; Neal et al., 2016). On a regional scale, these sequence sets form a genetically related succession representing lowstand, transgressive, highstand, and falling state packages, indicating a long-term fluctuation of the accommodation relative to the sediment flux (Mitchum & Van Wagoner, 1991; Neal & Abreu, 2009; Plint & Nummedal, 2000).

2.5.2 Sequence Stratigraphy of The New Jersey Rifted Continental Margin

Our analysis of seismic profile Oc270 line 529 focuses on several sequences in the Miocene interval (Figure 2.7). Within the ~8-million-years-long succession encompassing the Early to Late Miocene, we picked the rollover points and the landward and seaward terminations for each clinothem. Seismic packages characterized by similar geometry and facies were grouped and annotated using the three-letter acronyms (Figure 2.7), which resulted in 53 systems tracts. At this stage we did not consider the age model of the three wells, and thus we did not discuss any sequence hierarchy.

TSTs, HSTs, and LSTs are observed in most of the identified sequences, with only three FSSTs, two of which observed where the rollover point reaches the local maximum slope gradient. All three FSSTs are followed by relatively thick LSTs. Through time, the rollover point gradually migrates seaward, while the topset strata experience several periods of erosion. In the Late Miocene, the record shows a succession of UBBs and UBFs with a continuous transgression landward. The spectral gamma-ray logs (Figure 2.7) show an overall decrease in amplitude, which is attributed to the deposition of more sandy sediments in the Late Miocene.

2.6 Discussion

Applying the GBA to the synthetic XES02 chronostratigraphic units provides a framework for analyzing the identified seismic packages in the context of controlling mechanisms that influence sediment deposition, allowing the method to be evaluated in a controlled environment. Results from seismic and sequence stratigraphic analysis of field data from two previous studies of the New Jersey margin make possible a comparison with our interpretation based on the GBA. The outcomes of both, the synthetic and the field data study, provide a perspective on applying the GBA to shallow-marine stratigraphic analysis.

2.6.1 Evaluation of the Geometrical Breakdown Approach Application to Synthetic Data

To evaluate the Geometrical Breakdown Approach, we first analyze the key surfaces and systems tracts for the XES02 experimental result. Our analysis is carried out in the context of the most influential input parameter that controlled sediment deposition in the XES02 experiment, base-level (Kim et al., 2014; Martin et al., 2009), that also controlled the rate of accommodation

creation to sediment influx (δA/δS) under constant rate of subsidence and sediment influx (Figure 2.8).

We use equation (1) below from Kim et al. (2014) to compute δA/δS as it defines the rate of accommodation creation to sediment influx as a function of the stratal geometry in a depositional environment. An assumption of XES02 experiment is that the depositional environment experienced negligible loss or gain of sediment and negligible temporal variability in the rate of subsidence.

$$\frac{\delta A}{\delta S} = \frac{(u - s)[\frac{dZ_{bl}}{dt} + \sigma(s)]}{q_{so}} \quad (1)$$

In equation (1), u-s is foreset horizontal length, which is the distance from delta toe (u) to shoreline position or beginning of foreset slope (s), dZbl/dt is base-level change over time (if <0 base level falls), σ(s) is rate of subsidence, and qso is sediment feed rate. Equation (1) implies that the rate of accommodation creation to sediment influx is directly proportional to 1) foreset horizontal length (i.e., the longer the delta toe to top slope foreset the more accommodation is available per unit of sediment influx), and 2) the cumulative sum of base level change and total subsidence. The rate is inversely proportional to sediment feed rate.

The stratigraphic section presented in Figure 2.8 shows that the basin preserved most of sedimentary record from the slow (35-140 hr) and fast (145-165 hr) periods of base-level change in cycles 1 and 2 of Phase 1. The identified systems tracts tie with the respective phases in a δA/δS cycle. During the initial equilibrium period (0 -30 hr), a small rate of subsidence caused a slightly positive δA/δS and, consequently, deposition of UBF strata. As the induced base-level fall reduced the accommodation space, the negative δA/δS resulted in the deposition of DFBs and DFFs (35-50 hr). Later, when the rate of accommodation creation matched the rate of sediment flux, UBF strata generated a lowstand systems tract (50-90 hr) as the δA/δS value increased.

The Phase 2 record of fast cycles superimposed on a long cycle repeats a similar set of systems tracts but with a time lag in relation to the δA/δS cycle. This time lag is as large as 4 hours for some of the systems tracts, which indicates that short-period cycles may be challenging to identify in field data when superimposed on long-period cycles. Additional factors which are normally experienced in real situations, such as compaction and variable rate of sediment supply, had no influence on the lab results. Additionally, the δA/δS log in Figure 2.8 was computed from the instantaneous change in accommodation and may not reflect the impact of the background slow cycle in Phase 2. Nevertheless, observing the relative shift in the location of the rollover point and seaward termination in cycles 4 and 5 (two out of three geometrical criteria for the GBA) seemed sufficient to identify the stacking patterns in partially eroded TSTs and HSTs. More severe erosion and incomplete records from cycles 6 and 7 led to uncertainty in identifying the rollover point and landward termination of strata.

Figure 2.9 summarizes the observed relationship between the timing of systems tract formation and the ratio of accommodation creation to sediment flux. When the rate of accommodation creation exceeds the rate of sediment flux, UBB strata result (TSTs). When the rate of accommodation creation matches the rate of sediment flux, UBF strata result, interpreted as HSTs or LSTs depending on the geometry of the stratal package below. When the rate of accommodation creation is less than the rate of sediment flux, DFF strata result (i.e. FSSTs). Whereas subsequent subaerial erosion or transgressive ravinement often remove the sedimentary record needed to identify FSSTs in field examples (Plint and Nummedal, 2000), we frequently (three quarters of all cycles) identify FSSTs in the synthetic data. This is largely due to the experiment's initial condition of a constant rate of sediment supply: in reality, climatic and tectonic conditions may not only shift the base level but also strongly affect the rate of sediment supply.

2.6.2 Comparison of Stratigraphic Interpretation on The New Jersey Shelf

Figure 2.10 compares the model based on implementing the GBA with the results from previous studies by Katz et al. (2013) and Miller et al. (2013), which benefited from a comprehensive data set that included biofacies and lithologic data from core, as well as seismic data. Using criteria outlined in Miller et al. (2013), the core data highlighted changes in water depth and shallowing and deepening stratal trends, confirming sequences and sequence boundaries identified by observing toplap, onlap, downlap, and erosional truncation features in the seismic data. Miller et al. (2013) classified as TST a succession of deepening upward reflection packages, between an initial transgressive surface and the MTS. Locating the MTS required observing downlap surfaces on seismic profiles and omission surfaces in cores, which can be ambiguous. Observation of benthic foraminifera and abundance of planktonic foraminifera were considered as the strongest biofacies evidence for maximum relative sea-level (Katz et al., 2013), associated with MTS formation in the foreset of a clinoform. This technique has a low vertical resolution as it mainly identifies zones rather than the distinct surfaces designated as MTSs (Loutit et al., 1988). Identification of MTSs was based on a change from deepening-upward (retrogradational) to shallowing-upward (progradational) successions, which relied on the paleo-water depth and may have failed to recognize varied sediment flux, which is the other controlling parameter.

Comparison of the stratigraphic model based on the GBA with the results from previous studies reveals that, despite different approaches, the final interpretations are in general agreement. Figure 2.4 demonstrates the GBA applied to a model of the clinothem developed by Miller et al. (2013). Both clinothem models show a similar internal geometry, but the GBA forces the practitioner to incorporate rollover point and landward and seaward terminations in their seismic analyses. This makes the approach less dependent on well data and direct petrophysical measurements and age dating.

Figure 2.11 and Figure 2.12 show the GBA applied to sequences m5.2 and m5.8. We broke down the progradation of the strata in m5.8, formed in the Late Miocene, into LST, TST, and

HST using the acronym system, and our interpretation agrees with that of Miller et al. (2013) (Figure 2.11). However, for sequence m5.2 (Figure 2.12), the GBA provided a much greater level of detail, including the identification of a ~600 Kyr (Browning et al., 2013) cycle of LST, TST, and HST within strata previously interpreted as a thick HST (~100 m of sediments). The geometrical features observed in seismic data were the primary criteria to classify the sedimentary packages. The resolution of the input seismic data across the section constrained spatial resolutions of the final interpreted model and the precision with which key surfaces, which delineate the onset of systems tracts, are picked.

2.6.3 Advantages of Applying the Geometrical Breakdown Approach

The variety of stratal analysis methods used to study the driving mechanisms for formation of stratigraphic sequences, and the lack of a universal observational seismic framework, have been sources of controversy among practitioners (Neal et al., 2016). Linking the timing of stratigraphic sequence formation to sea-level cycles has contaminated systems tract nomenclature (Miller et al., 2018); in other words, systems tract names do not necessarily reflect accurately sea-level and/or its variation during deposition. This has led to calls for a return to the basics of sequence stratigraphy using seismic, core, and well log data to objectively categorize seismic reflection packages by observing their stratal geometries, stratal terminations, and vertical stacking patterns (Jervey, 1988).

The GBA focuses on geometrical characteristics of reflection packages observed in the sedimentary record. The observed changes in a stratigraphic sequence are attributed to the rate of accommodation creation relative to the rate of sediment flux (Neal et al., 2016), regardless of their driving geological mechanisms (Bohacs, 1998). Our synthetic and field test examples demonstrate that the application of this method is a step forward in separating observation from interpretation, describing stratal surfaces (or packages of conformable surfaces) based on their relative spatial positions before applying systems tract, progradational-retrogradational-aggradational, or transgressive-regressive terminology.

The GBA is less sensitive to the post-depositional tectonic deformation of strata than earlier interpretational approaches because it uses relative locations from three spatially removed points on each reflection package to identify corresponding systems tracts. For each reflection package, two out of the three points are boundary terminations rather than the structural configuration of reflection packages. Tectonic deformation is more likely to change the shape and attitude of reflection packages and, therefore, their internal reflection patterns, which are traditionally used to separate sequences and systems tracts. If clinothems are heavily deformed structurally, or rollover points are unrecognizable, it may still be possible to interpret up- or down-stepping of each reflection (stratal) package relative to the previous package by considering their overall geometry and mid-point locations, although inevitably introducing subjective judgement.

Preservation of strata requires 1) accommodation space, and 2) supply of sediment with hydrodynamic energy needed to generate strata without causing erosion. The sediment type and stratal geometry can be used to understand the balance between these factors, specifically in shallow water environments, but cannot be used to uniquely determine sea-level dynamics. Interpreting geometrical change in sequences based on accommodation succession facilitates stratigraphic analysis away from data control points without speculation about the responsible mechanisms (Bosence et al., 2003; Catuneanu et al., 2010; Obaje, 2013; Williams, 1993; Wilson, 1998).

Existing sequence-stratigraphic approaches limit interpretation of the accommodation successions to the scale of a depositional sequence – the largest stratigraphic unit bounded by sequence boundaries (Neal et al., 2016) on a regional scale. The resolution of seismic data, which is independent of age or regional extent, controls the size of resolvable sedimentary packages (Mitchum et al., 1977b; Neal et al., 2016), but ambiguity and complexity in existing seismic stratigraphic approaches prevents this resolution being reached. The GBA is applicable at multiple levels of detail, down to half-cycle amplitude and phase variations related to lithological changes that have been confirmed through well calibration and forward modelling.

Stratigraphic interpretation based on accommodation succession typically focuses on regional allocyclic changes. However, autogenic processes such as channel avulsion, delta-lobe switching and auto-retreat can induce local changes in accommodation and sediment flux. They may affect part of a conformable unit, in contrast to the regional trend represented by many sequences (Neal and Abreu, 2009; Neal et al., 2016). Interpreting such local events calls for a more detailed framework to categorize features that differ in scale but are the same in nature.

2.7 Conclusion

For shallow-marine strata, the lack of clear separation between observation and interpretation in seismic analysis has frequently hampered the study of stratigraphic sequences and their driving mechanisms. Historically this has been a problem in analysing the relative contribution of allogenic processes (the three "S"s: sea-level, subsidence and sediment supply) and autogenic processes. To mitigate this problem, we introduce the GBA, which follows a simple but rigorous classification of the spatial relationships of depositional units recognized in seismic profiles to identify systems tracts, without any connotation of controlling mechanisms. The approach builds on robust aspects of existing approaches to seismic stratigraphy, while facilitating a more objective analysis of stratal patterns through systematic spatial description. These observations are then used to infer systems tracts, progradational-retrogradational-aggradational trends, and transgressive-regressive terminology.

By applying the GBA to synthetic data and field seismic images, we demonstrate that the proposed geometrical criteria are scale-independent, easy to implement, and a reliable tool for accurate recognition of systems tracts. Comparison with previous approaches shows that, despite differing methodology, the sequence interpretations are commonly in general agreement. However, the GBA can be used to interpret systems tracts and sequences down to the finest resolvable seismic units, a finer resolution than previously possible. While the GBA is tested on a 2D cross-shelf transect that was sensitive to change in the rate of shelfal accommodation creation and sediment fill, its application is readily extendable in 3D and to more proximal and

deeper water settings because it relies simply on capturing the geometry and relative movement of depositional units before addressing their origin. This method could form a basis for automated interpretation of sequences and systems tracts once accurate identification of reflections, reflection connections, and terminations becomes possible through machine learning.

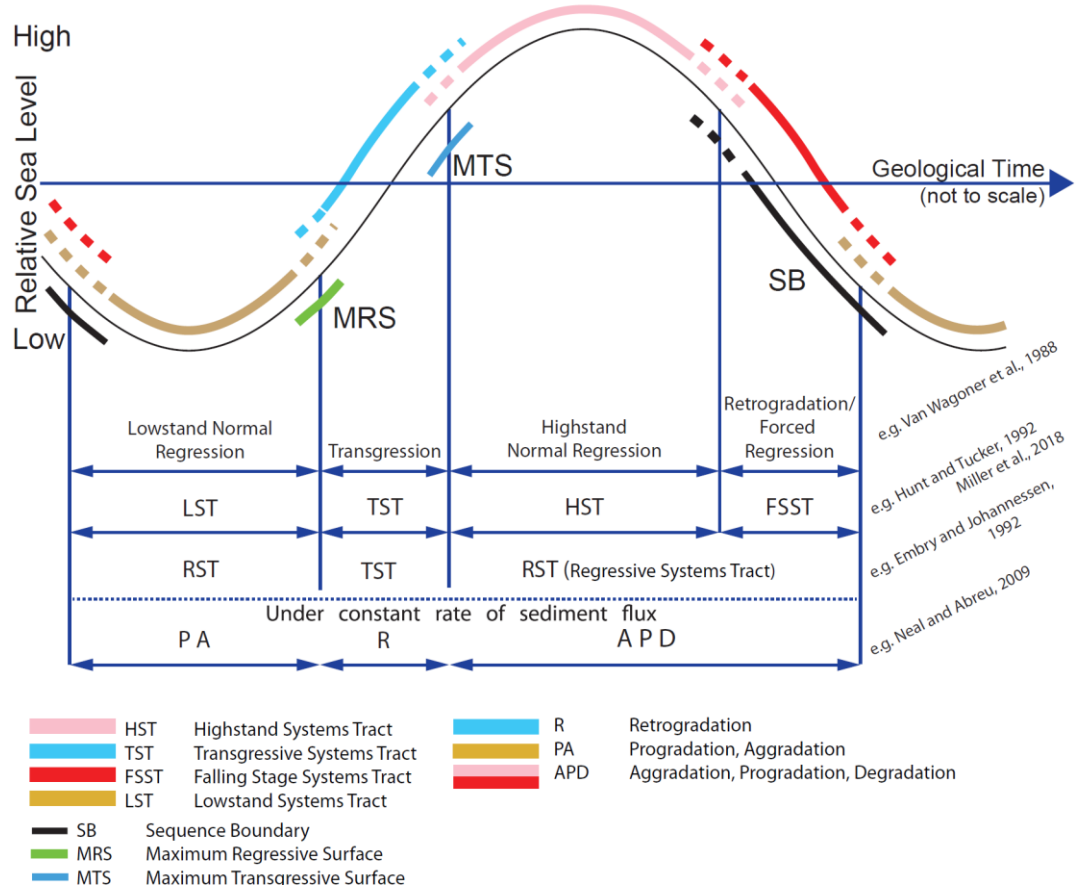

Figure 2.1: Schematic of the common approaches used in seismic sequence stratigraphic interpretation as a function of the relative sea-level cycle proposed by Van Wagoner et al. (1988), Neal and Abreau (2009) and Miller et al. (2018). These complementary approaches focus on different aspects of depositional architecture: (a) stratal stacking patterns like progradation (P), aggradation (A), degradation (D), and retrogradation (R) (Van Wagoner et al., 1988); (b) shoreline trajectories (Helland-Hansen and Martinsen, 1996; Helland-Hansen and Hampson, 2009; Hunt and Tucker, 1992); transgressive–regressive sequence model (Embry and Johannessen, 1992; Jahnson and Murphy, 1984) and (c) accommodation succession stacking (Neal and Abreu, 2009; Neal et al., 2016). LSC – Lowstand Systems Tract, TST – Transgressive Systems Tract, HST – Highstand Systems Tract, FSST – Falling Stage Systems Tract, RST – Regressive Systems Tract, P A – Progradation to Aggradation, P A D – Progradation to Aggradation to Degradation, R – Retrogradation, SB – Sequence Boundary, MRS – Maximum Regressive Surface, MTS – Maximum Transgressive Surface.

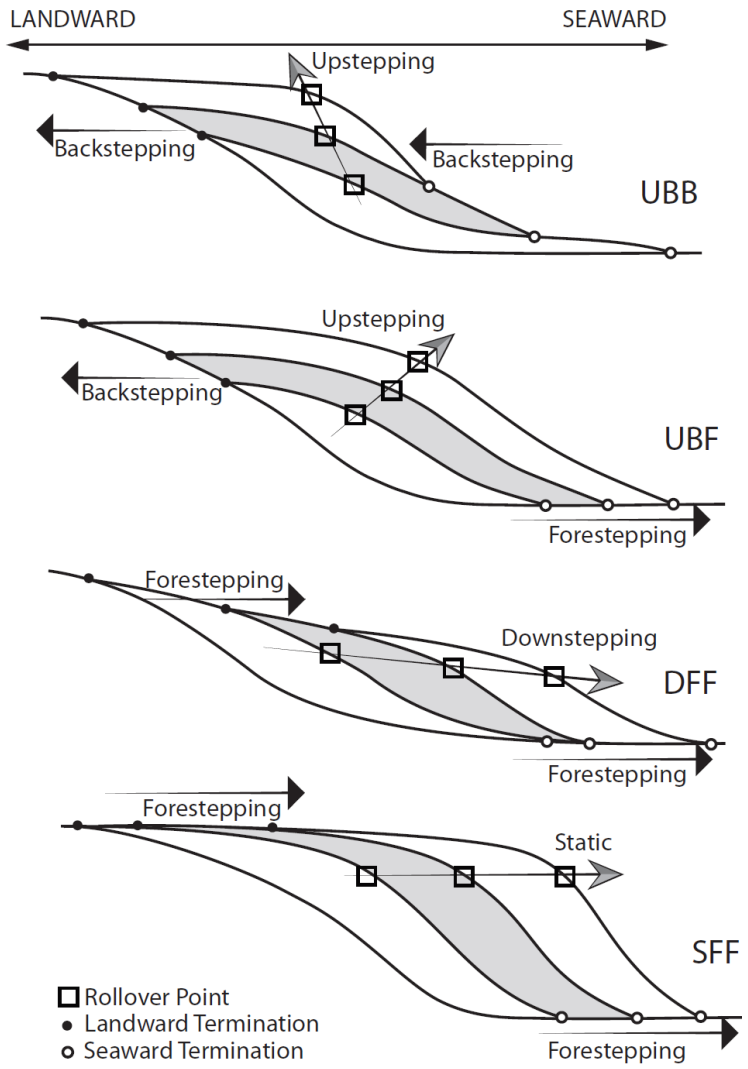

Figure 2.2: The four most common stratal geometries observed in a clinothem body in nature and their corresponding three-letter acronyms defined by the Geometrical Breakdown Approach (GBA). The first letter in the acronym indicates vertical movement (up/down) of the rollover point with respect to the older unit; the second letter defines movement (backstep/forestep) of landward termination of the top surface, and; the third letter defines movement (backstep/forestep) of the seaward termination of the top surface.

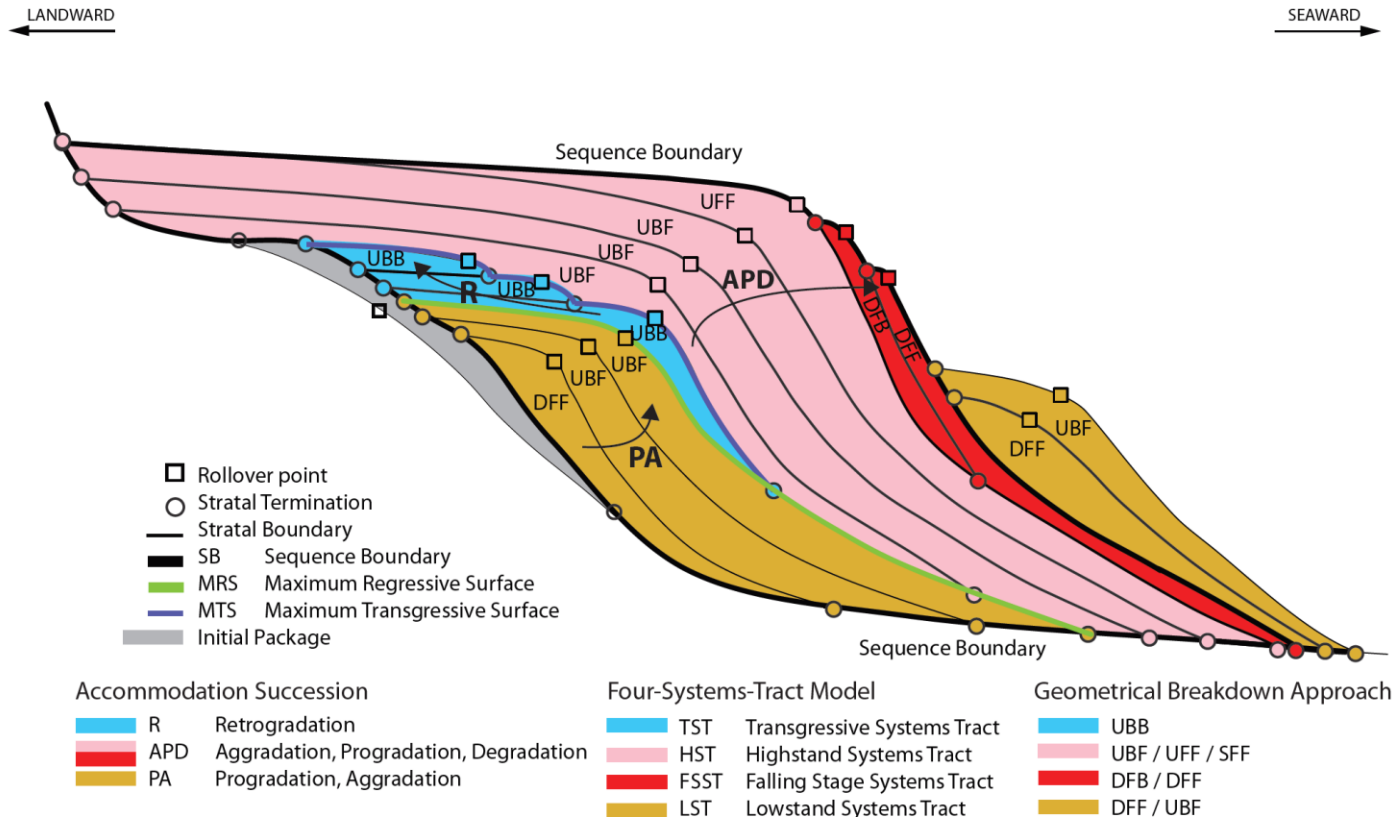

Figure 2.3: Slug diagram of idealized stratal geometries observed in seismic data. The diagram shows a full succession of systems tracts and their associated surfaces.

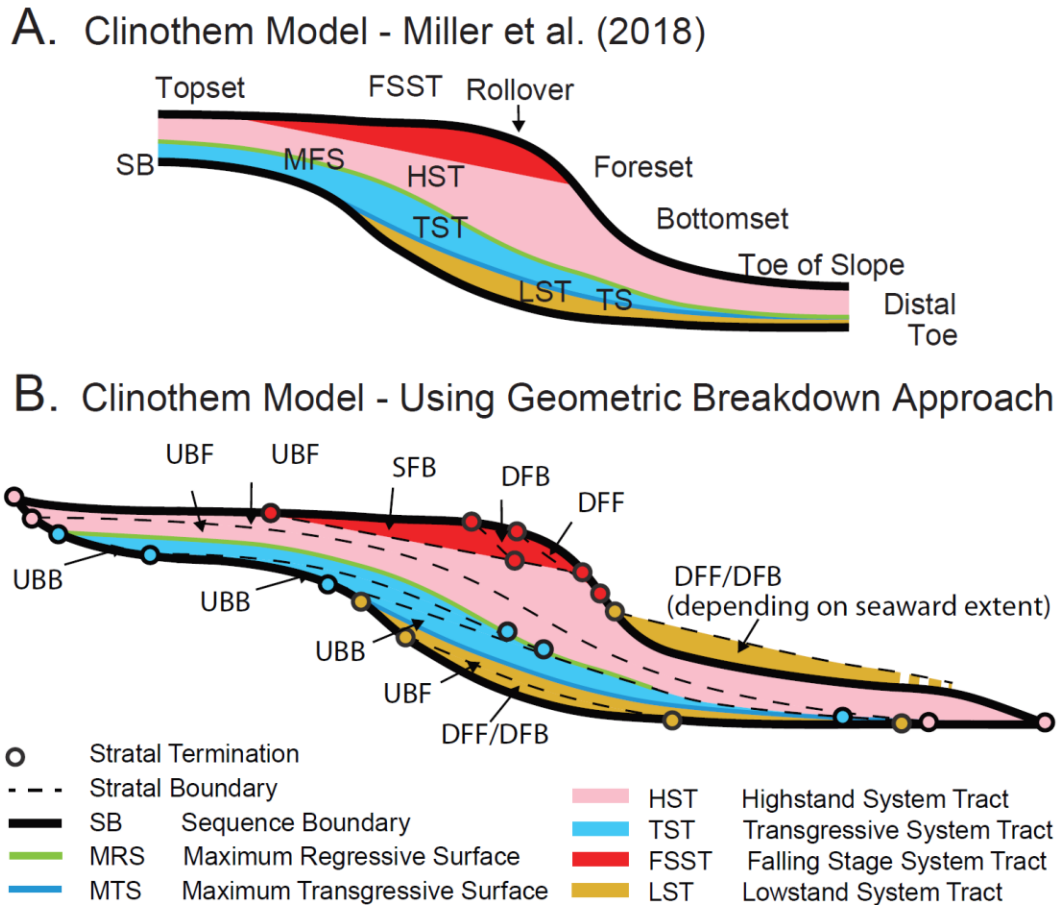

Figure 2.4: Schematic model of clinothem presented by Miller et al. (2018) (A), and the geometrical breakdown of systems tracts using the GBA (B).

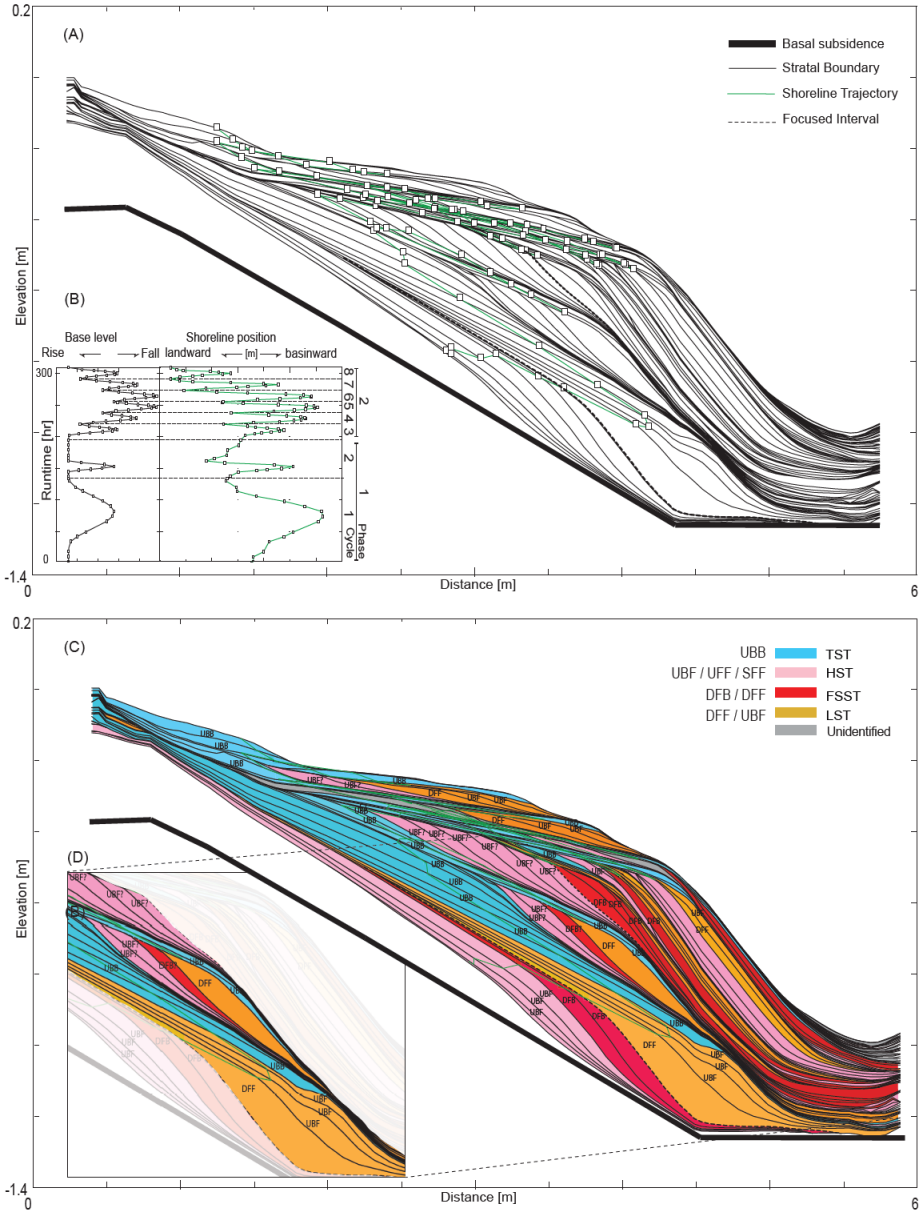

Figure 2.5: Stratigraphic model of the XES02 experiment reconstructed from laser and sonar topographic measurements (A) (image modified from Kim et al., 2014); absolute base-level curve and corresponding shoreline position over the experiment runtime (B); XES02 laser and sonar topographic section shown with the overlain interpretation (C) and the shoreline trajectories (green line). Two dashed lines separate the zone described in Section 4.1 (D).

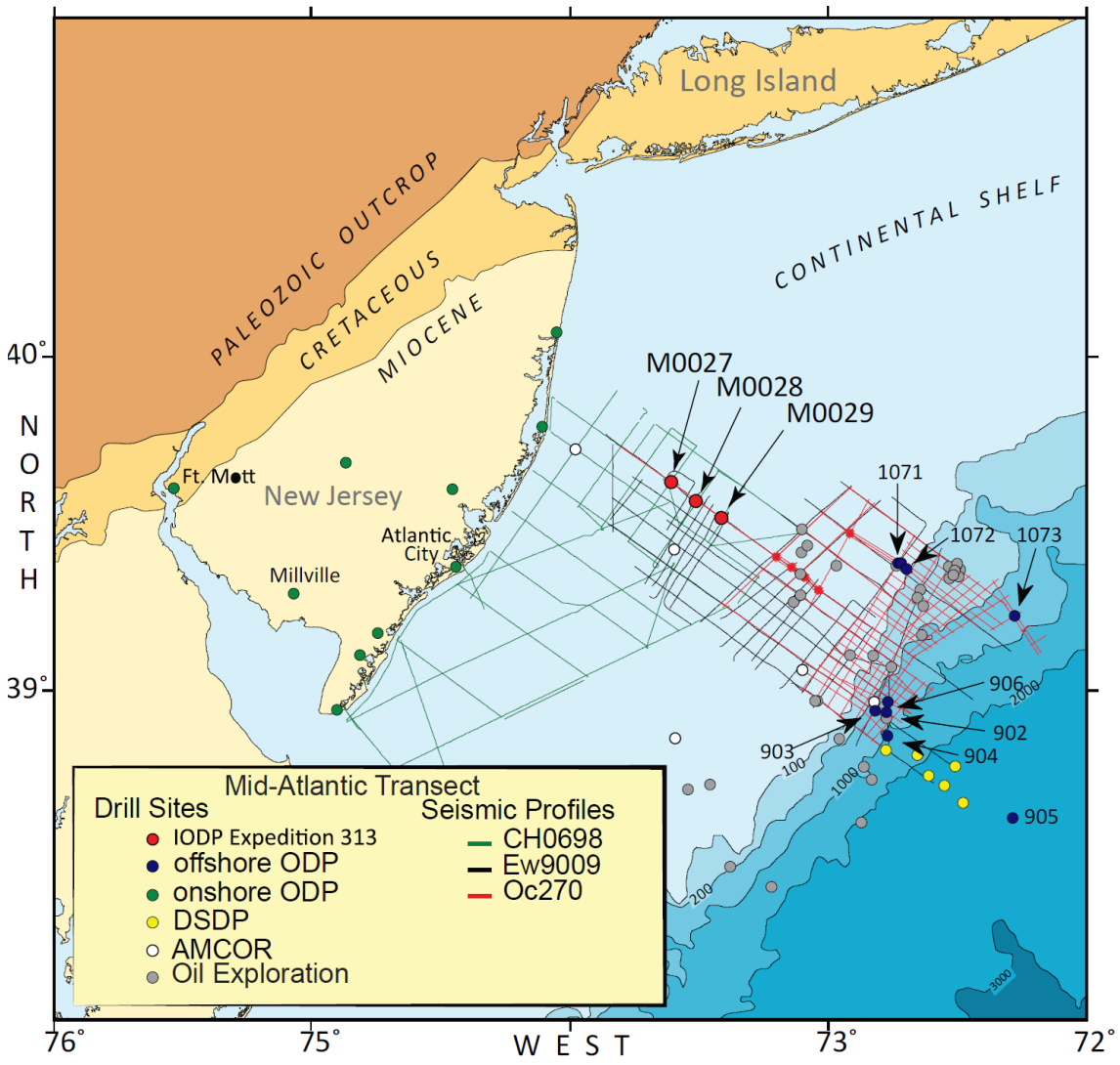

Figure 2.6: Map view of the study area offshore New Jersey continental margin. The seismic data crossing the wells M27, M28, and M29 were used for this study (base map from Mountain et al., 2010).

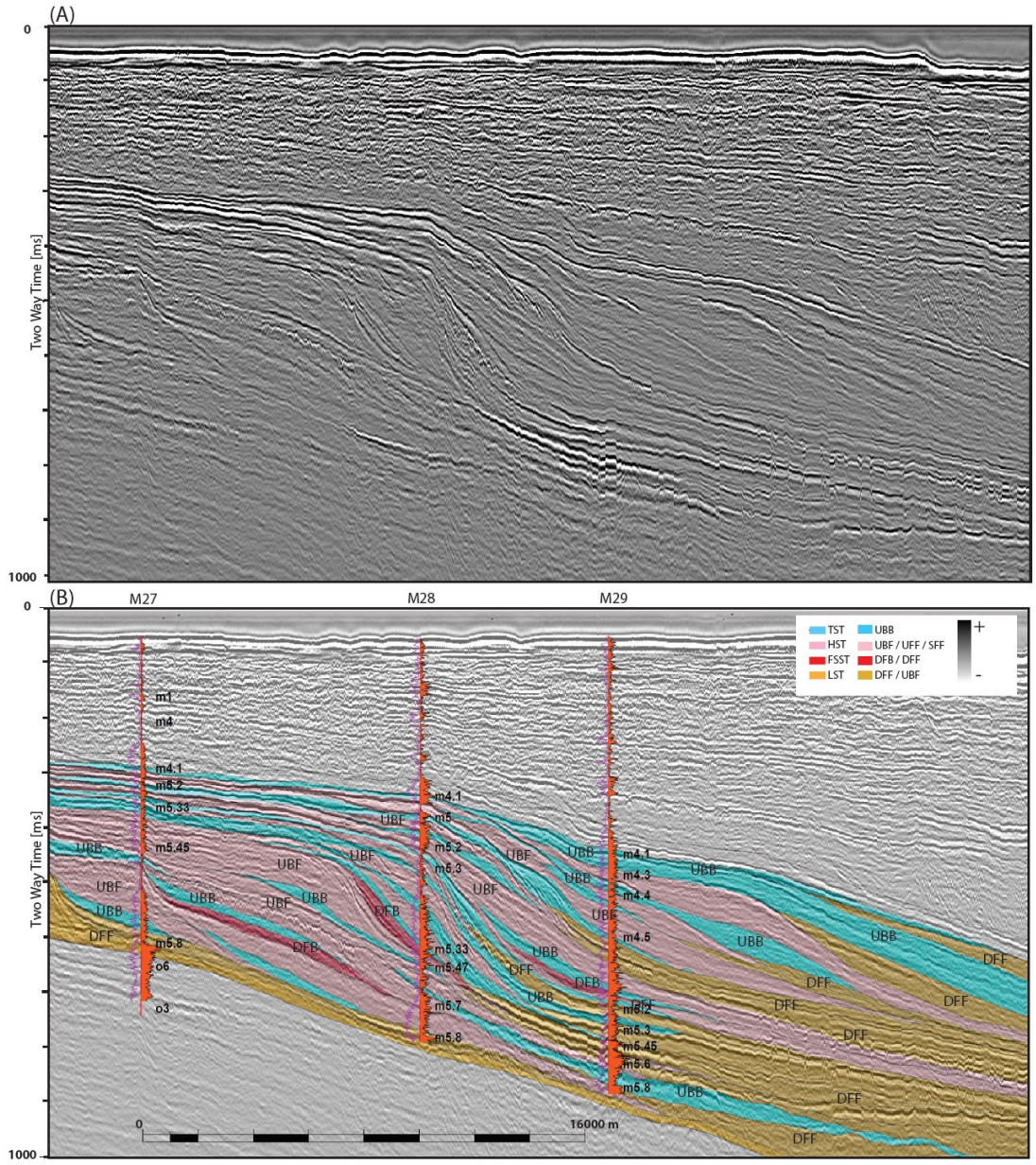

70

Figure 2.7: Seismic profile oc270 line 529 before (A) and after (B) interpretation. Spectral Gamma-ray logs of Thorium (purple log to the left) and Uranium (orange log to the right) are displayed along the IODP wells M27-M29.

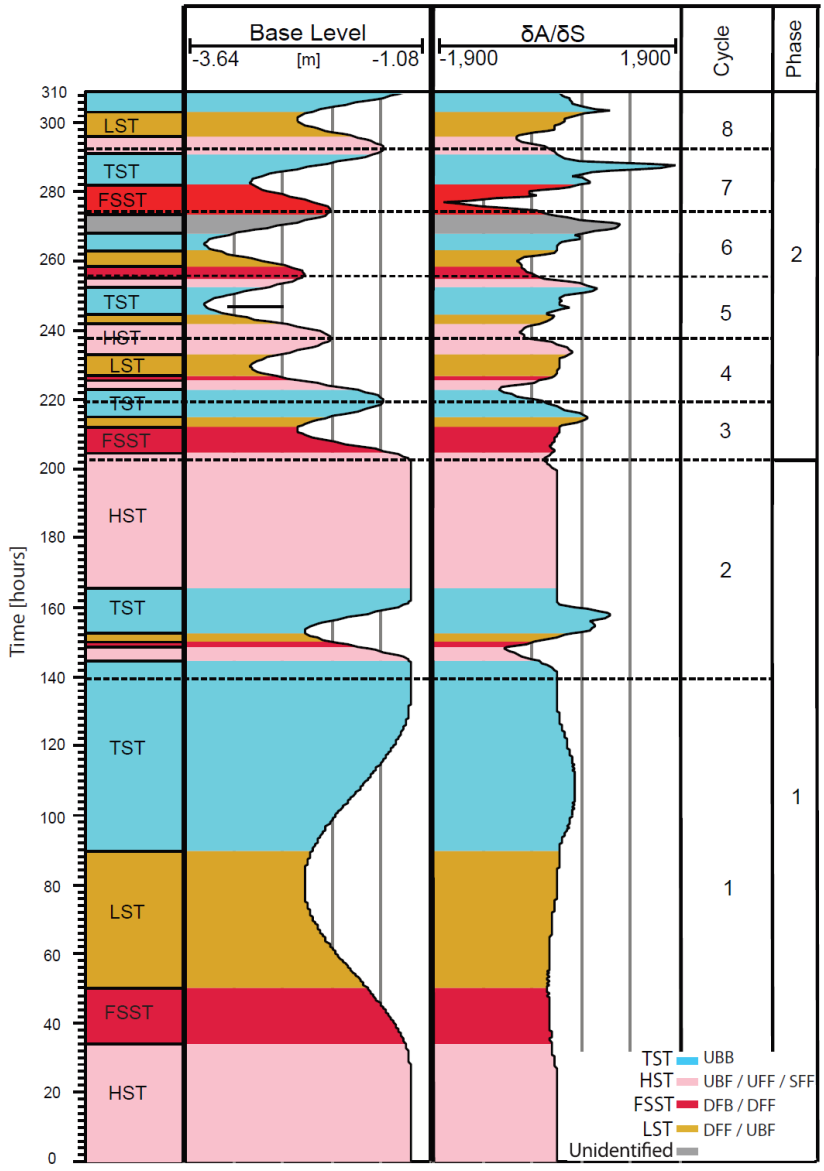

Figure 2.8: Stratigraphic interpretation of the XES02 experiment (color) bounded on the right by thin black lines showing the history of base-level change and the estimated rate of δA/δS as a function of time. Data courtesy the National Center for Earth-surface Dynamics Data Repository, http://www.nced.umn.edu/Data_Repository.html, [2019].

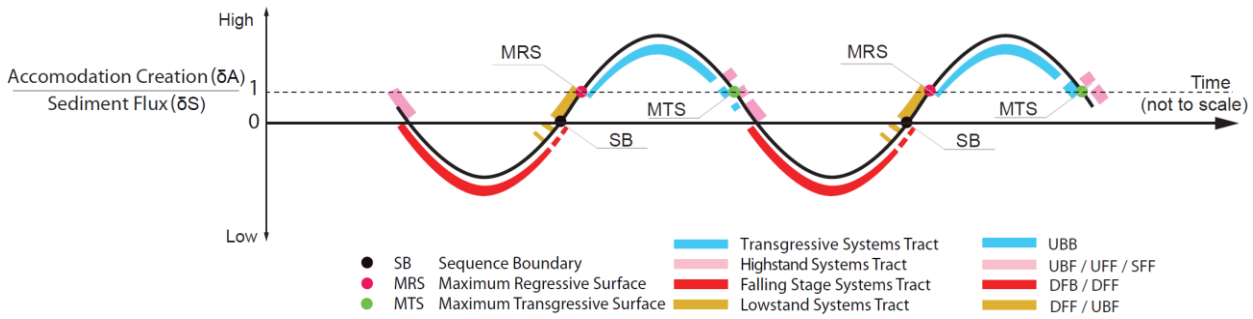

Figure 2.9: Timing of stratigraphic systems tracts formation and the associated surfaces in relation to the ratio of accommodation creation and sediment flux. The figure is made based on two core assumptions: 1) the coastal accommodation creation changes continuously and quasi-periodically at an inconsistent rate; 2) sediment potentially fills the space up to the base level and any surplus is transported farther seaward where excess accommodation is available (Helland-Hansen and Gjelberg, 1994; Neal et al., 2016).

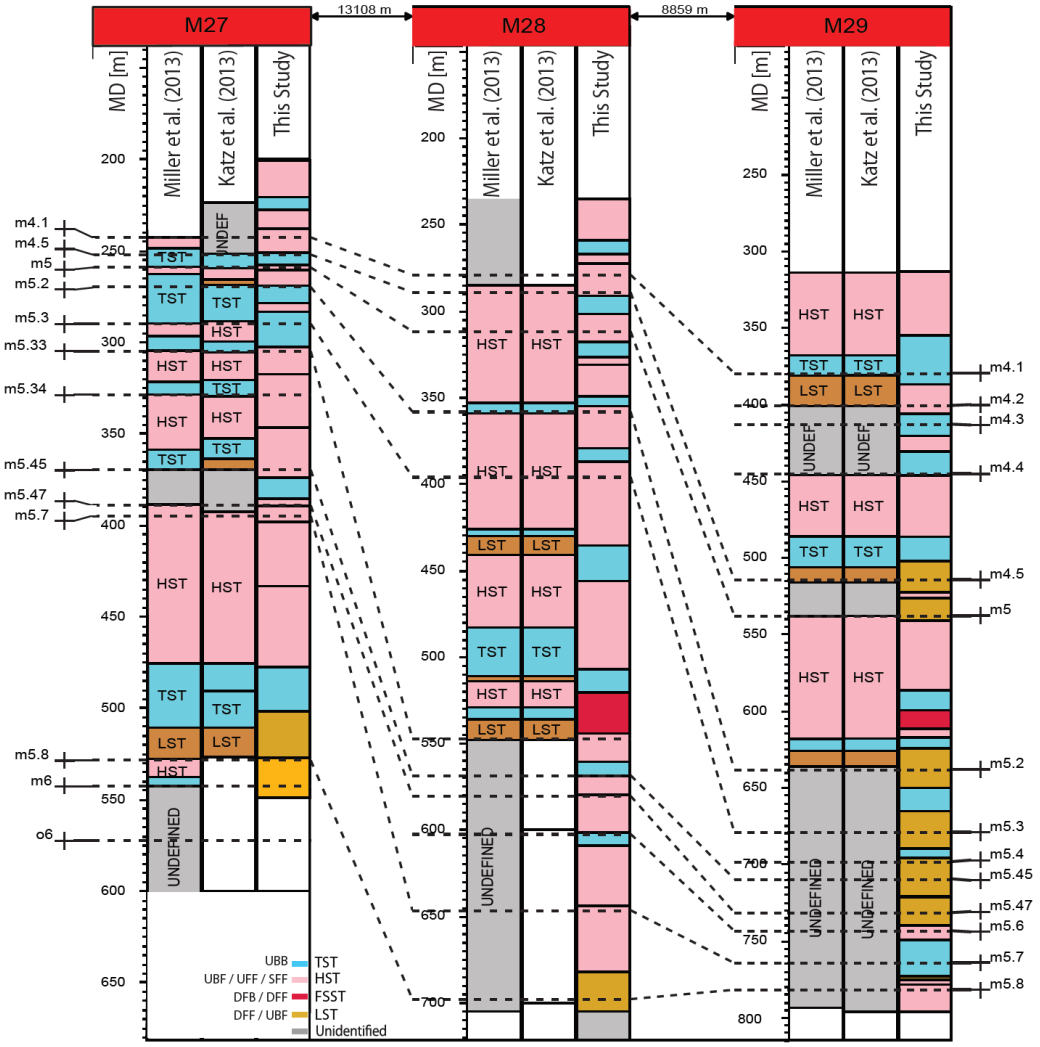

Figure 2.10: Sequence stratigraphic interpretation of the three wells M27, M28, and M29 in measured depth (MD). Figure 6 shows the position of the three wells in a map view. The first letter of each layer stands for the geological Epoch to which it belongs, with "o" standing for the Oligocene and "m" standing for the Miocene interval. Age data are from Browning et al. (2013). Site M27 was drilled at the topset of clinoforms where seismic data show signs of erosion and unconformity in the younger intervals. Site M28 had the worst coring recovery among three IODP wells (Mountain et al., 2010) due to the borehole instability and problems associated with drilling. Site M29 had an excellent core recovery (Mountain et al., 2010), and the majority of identified systems tracts have a thickness above the tuning thickness, which made them recognizable in both well and seismic data.

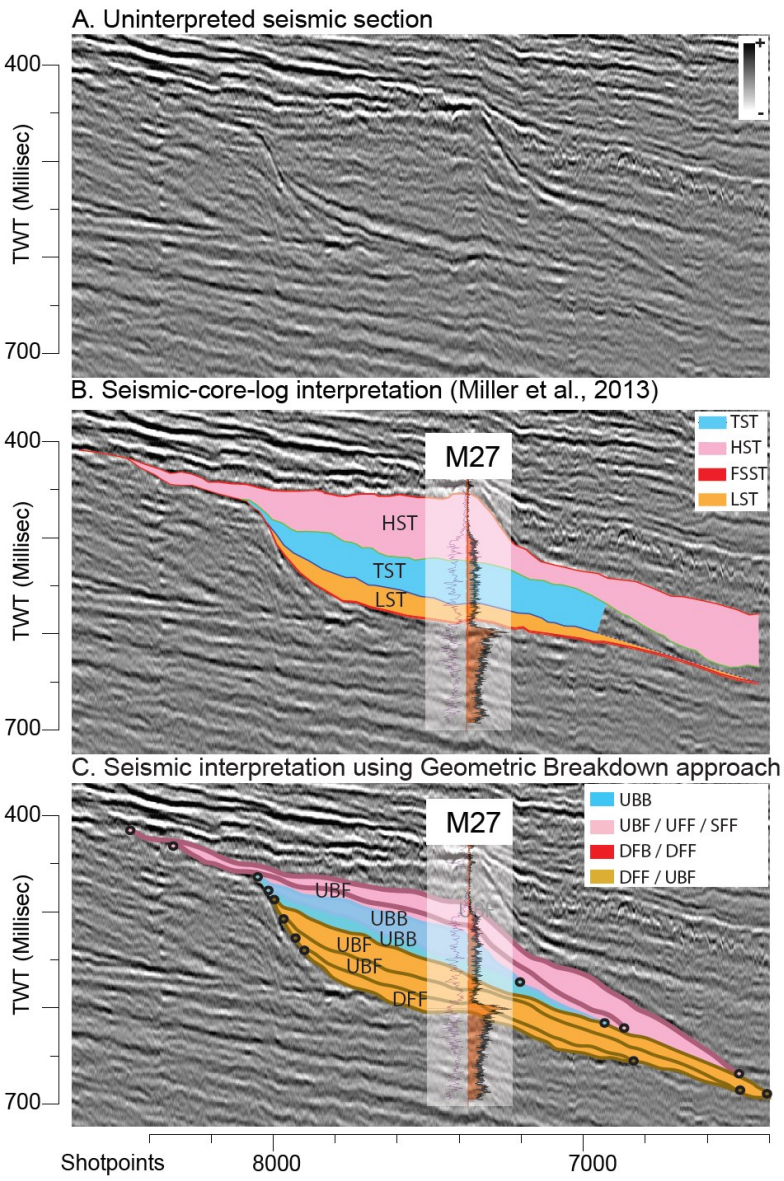

Figure 2.11: Comparison of seismic sequence stratigraphic interpretation in sequence m5.8. (A) Zoom on a part of the seismic section of the profile oc270 line 529 prior to interpretation; (B) Sequence stratigraphic interpretation of (A) from Miller et al. (2013) superimposed on log data. (C) Interpretation of the same sequence as in (B) but based on application of the GBA, which relies on the geometry of the reflection packages.

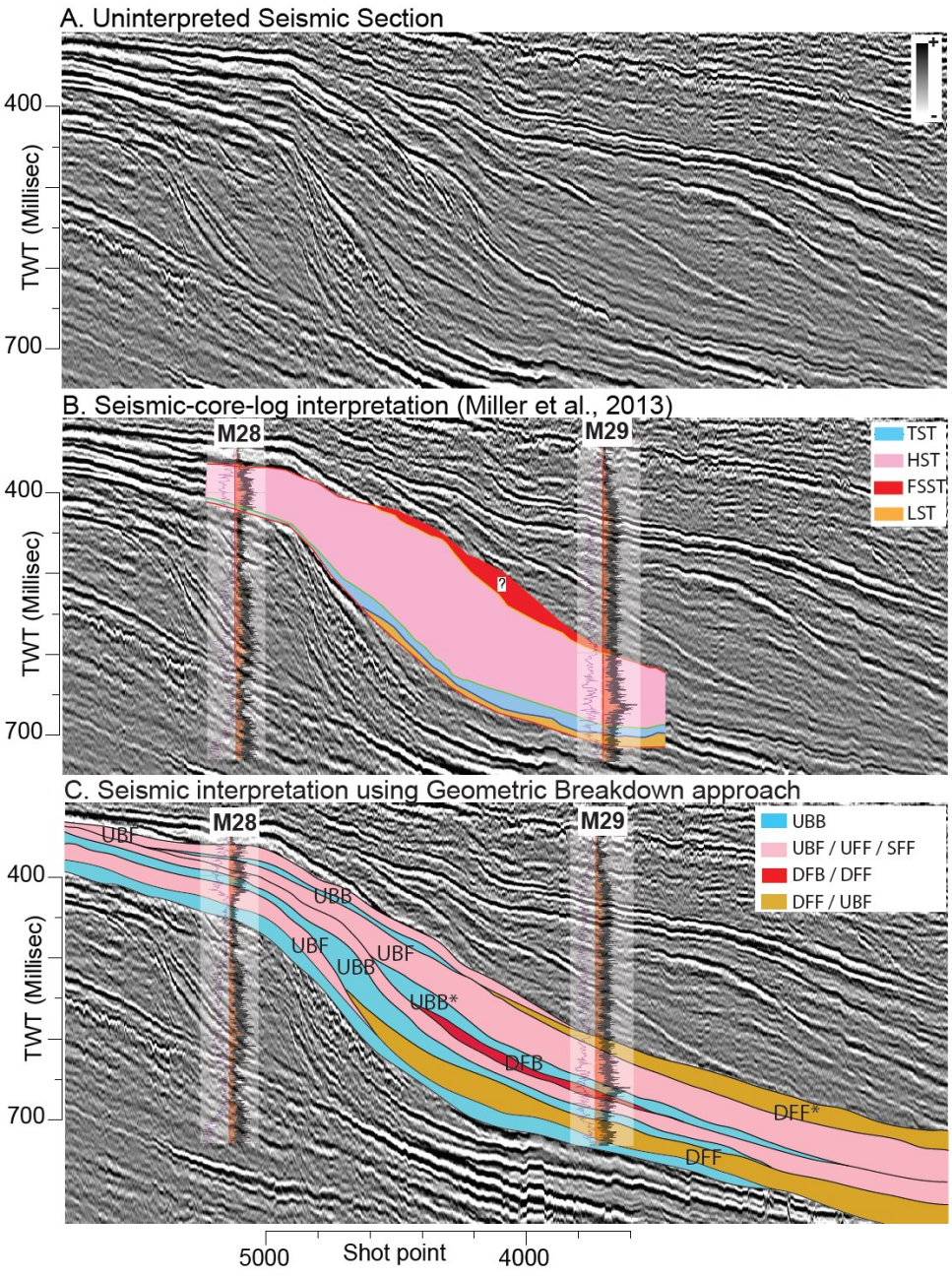

Figure 2.12: Comparison of seismic sequence stratigraphic interpretation in sequence m5.2. (A) Zoom on a part of the seismic section of the profile oc270 line 529 prior to interpretation; (B) Sequence stratigraphic interpretation of (A) from Miller et al. (2013) superimposed on log data. (C) Interpretation of the same sequence as in (B) but based on application of the GBA, which relies on the geometry of the reflection packages.

2.8 References

Bohacs, K.M., 1998, Contrasting expressions of depositional sequences in mudrocks from marine to non marine environs, *in* Basin studies, sedimentology, and paleontology, E. Schweizerbart, v. 1, p. 33–78.

Bosence, D.W.J., Holloway, R., Flint, S., and Howell, J., 2003, The sedimentary record of sea-level change: 2–4 p., doi:10.2277/0521831113.

Browning, J. V., Miller, K.G., Sugarman, P.J., Barron, J.A., McCarthy, F.M.G., Kulhanek, D.K., Katz, M.E., and Feigenson, M.D., 2013, Chronology of Eocene–Miocene sequences on the New Jersey shallow shelf: Implications for regional, interregional, and global correlations: Geosphere, v. 9, p. 1434–1456, doi:10.1130/GES00853.1.

Bullimore, S., Henriksen, S., Liestøl, F.M., and Helland-Hansen, W., 2005, Clinoform stacking patterns, shelf-edge trajectories and facies associations in Tertiary coastal deltas, offshore Norway: Implications for the prediction of lithology in prograding systems: Norsk Geologisk Tidsskrift, v. 85, p. 169–187.

Burgess, P.M., Allen, P.A., and Steel, R.J., 2016, Introduction to the future of sequence stratigraphy: Evolution or revolution? Journal of the Geological Society, v. 173, p. 801–802, doi:10.1144/jgs2016-078.

Catuneanu, O., 2002, Sequence stratigraphy of clastic systems: Concepts, merits, and pitfalls: Journal of African Earth Sciences, v. 35, p. 1–43, doi:10.1016/S0899-5362(02)00004-0.

Catuneanu, O. et al., 2009, Towards the standardization of sequence stratigraphy: Earth-Science Reviews, v. 92, p. 1–33, doi:10.1016/j.earscirev.2008.10.003.

Catuneanu, O., Bhattacharya, J.P., Blum, M.D., Dalrymple, R.W., Eriksson, P.G., and Fielding, C.R., 2010, Sequence stratigraphy : common ground after three decades of development: First Break, v. 28, p. 21–34.

Csato, I., Granjeon, D., Catuneanu, O., and Baum, G.R., 2013, A three-dimensional stratigraphic model for the Messinian crisis in the Pannonian Basin, eastern Hungary: Basin Research, v. 25, p. 121–148, doi:10.1111/j.1365-2117.2012.00553.x.

Embry, A., 2009, Practical Sequence Stratigraphy: Canadian Society of Petroleum Geologists, p. 1–79, doi:10.1017/CBO9781107415324.004.

Embry, A.F., and Johannessen, E.P., 1993, T–R sequence stratigraphy, facies analysis and reservoir distribution in the uppermost Triassic–Lower Jurassic succession, western Sverdrup Basin, Arctic Canada: Norwegian Petroleum Society Special Publications, v. 2, p. 121–146, doi:10.1016/B978-0-444-88943-0.50013-7.

Embry, A., and Johannessen, E.P., 2017, Two approaches to sequence stratigraphy: Elsevier Inc., v. 2, 85–118 p., doi:10.1016/bs.sats.2017.08.001.

Eriksson, P.G. et al., 2013, Secular changes in sedimentation systems and sequence stratigraphy: Gondwana Research, v. 24, p. 468–489, doi:10.1016/j.gr.2012.09.008.

Fulthorpe, C.S., Austin, J.A., and Mountain, G.S., 1999, Buried fluvial channels off New Jersey: Did sea-level lowstands expose the entire shelf during the Miocene? Geology, v. 27, p. 203–206, doi:10.1130/0091-7613(1999)027<0203:BFCONJ>2.3.CO;2.

Galloway, W.E., 1989, Genetic stratigraphic sequences in basin analysis II: application to northwest Gulf of Mexico Cenozoic basin: American Association of Petroleum Geologists Bulletin, v. 73, p. 143–154, doi:10.1306/703C9AFA-1707-11D7-8645000102C1865D.

Greenlee, S.M., Devlin, W.J., Miller, K.G., Mountain, G.S., and Flemings, P.B., 1992, Integrated sequence stratigraphy of Neogene deposits, New Jersey continental shelf and slope: comparison with the Exxon model: Geological Society of America Bulletin, v. 104, p.

1403–1411, doi:10.1130/0016-7606(1992)104<1403:ISSOND>2.3.CO;2.
Grow, J.A., and Sheridan, R.E., 1988, U.S. Atlantic Continental Margin; A typical Atlantic-type or passive continental margin, *in* Sheridan, R.E. and Grow, J.A. eds., The Atlantic Continental Margin, Geological Society of America, https://doi.org/10.1130/DNAG-GNA-I2.1.
Hallam, A., 1963, Major epeirogenic and eustatic changes since the Cretaceous, and their possible relationship to crustal structure: American Journal of Science, v. 261, p. 397–423, doi:10.2475/ajs.261.5.397.
Haq, B.U., Hardenbol, J., and Vail, P.R., 1987, Chronology of fluctuating sea levels since the Triassic: Science, v. 235, p. 1156–1167, doi:10.1126/science.235.4793.1156.
Helland-Hansen, W., and Gjelberg, J., 1994, Conceptual basis and variability in Sequence stratigraphy: a different perspective: v. 92, 31–52 p., doi:10.1016/0037-0738(94)90053-1.
Helland-Hansen, W., and Hampson, G.J., 2009, Trajectory analysis: Concepts and applications: Basin Research, v. 21, p. 454–483, doi:10.1111/j.1365-2117.2009.00425.x.
Helland-Hansen, W., and J. Martinsen, O., 1996, Shoreline trajectories and sequences: description of variable depositional-dip scenarios: v. 66.
Hunt, D., and Tucker, M.E., 1992, Stranded parasequences and the forced regressive wedge systems tract: deposition during base-level'fall: Sedimentary Geology, v. 81, p. 1–9, doi:10.1016/0037-0738(92)90052-S.
Jervey, M.T., 1988, Quantitative geological modeling of siliciclastic rock sequences and their seismic expression, *in* Wilgus, C.K., Hastings, B.S., Posamentier, H., Wagoner, J. Van, Ross, C.A., and Kendall, C.G.S.C. eds., Sea-Level Changes, SEPM (Society for Sedimentary Geology), p. 47–69, doi:10.2110/pec.88.01.0047.
Kallweit, R.S., and Wood, L.C., 1982, The limits of resolution of zero-phase wavelets.: Geophysics, v. 47, p. 1035–1046, doi:10.1190/1.1441367.
Katz, M.E., Browning, J. V., Miller, K.G., Monteverde, D.H., Mountain, G.S., and Williams, R.H., 2013, Paleobathymetry and sequence stratigraphic interpretations from benthic foraminifera: Insights on New Jersey shelf architecture, IODP Expedition 313: Geosphere, v. 9, p. 1488–1513, doi:10.1130/GES00872.1.
Kendall, C.G.S.C., Strobel, J., Cannon, R., Bezdek, J., and Biswas, G., 1991, The simulation of the sedimentary fill of basins: v. 96, p. 6911–6929.
Kim, W., Paola, C., Voller, V., and Swenson, J.B., 2014, Experimental measurement of the relative importance of controls on shoreline migration:, doi:10.2110/jsr.2006.019.
Kominz, M.A., van Sickel, W.A., Miller, K.G., and Browning, J. V., 2002, Sea-level estimates for the latest 100 million years : one- dimensional backstripping of onshore New Jersey boreholes: Gcssepm2002, p. 303–316, doi:10.1016/j.nrl.2009.12.006.
Loutit, T.S., Hardenbol, J., Vail, P.R., and Baum, G.R., 1988, Condensed sections: the key to age determination and correlation of continental margin sequences: Sea-Level Changes: An Integrated Approach, v. 42, p. 0, doi:10.2110/pec.88.01.0183.
Madof, A.S., Harris, A.D., and Connell, S.D., 2016, Nearshore along-strike variability: Is the concept of the systems tract unhinged? Geology, v. 44, p. 315–318, doi:10.1130/G37613.1.
Martin, J., Paola, C., Abreu, V., Neal, J., and Sheets, B., 2009, Sequence stratigraphy of experimental strata under known conditions of differential subsidence and variable base level: v. 4, p. 503–533, doi:10.1306/12110808057.
Matthews, R., and Al-Husseini, M., 2010, Orbital-forcing glacio-eustasy: A sequence-stratigraphic time scale: GeoArabia, v. 15, p. 155–167.

Matthews, R., and Frohlich, C., 1998, Forward modeling of sequence stratigraphy and diagenesis: Application to rapid, cost-effective carbonate reservoir characterization: v. 3, 359–384 p.
McCarthy, F.M.G. et al., 2013, Sea-level control of new jersey margin architecture: Palynological evidence from integrated ocean drilling program expedition 313: Geosphere, v. 9, p. 1457–1487, doi:10.1130/GES00853.1.
Miall, A., 2006, Reconstructing the architecture and sequence stratigraphy of the preserved fluvial record as a tool for reservoir development: A reality check: AAPG Bulletin, v. 90, p. 989–1002, doi:10.1306/02220605065.
Miller, K.G. et al., 2013, Testing sequence stratigraphic models by drilling Miocene foresets on the New Jersey shallow shelf: Geosphere, v. 9, p. 1236–1256, doi:10.1130/GES00884.1.
Miller, K.G., Browning, J. V., Mountain, G.S., Sheridan, R.E., Sugarman, P.J., Glenn, S., and Christensen, B.A., 2014, Chapter 3 History of continental shelf and slope sedimentation on the US middle Atlantic margin: Geological Society, London, Memoirs, v. 41, p. 21–34, doi:10.1144/M41.3.
Miller, K.G., Kominz, M.A., Browning, J. V., Wright, J.D., Mountain, G.S., Katz, M.E., Sugarman, P.J., Cramer, B.S., Christie-Blick, N., and Pekar, S.F., 2005, The phanerozoic record of global sea-level change: Science, v. 310, p. 1293–1298, doi:10.1126/science.1116412.
Miller, K.G., Lombardi, C.J., Browning, J. V., Schmelz, W.J., Gallegos, G., Mountain, G.S., and Baldwin, K.E., 2018, Back to basics of sequence stratigraphy: Early Miocene and Mid-Cretaceous examples from the New Jersey paleoshelf: Journal of Sedimentary Research, v. 88, p. 148–176, doi:10.2110/jsr.2017.73.
Miller, K.G., and Mountain, G.S., 1996, Drilling and dating New Jersey Oligocene-Miocene sequences: Ice Volume, Global Sea Level, and Exxon Records: Science, v. 271, p. 1092–1095, doi:10.1126/science.271.5252.1092.
Miller, K.G., and Mountain, G.S., 1994, Global Sea-Level Change and the New Jersey Margin: Proceedings of the Ocean Drilling Program, Initial Reports, v. 150, p. 11–20.
Miller, K.G., Mountain, G.S., Browning, J. V., Kominz, M.A., Sugarman, P.J., Christie-Blick, N., Katz, M.E., and Wright, J.D., 1998, Cenozoic global sea level, sequences, and the New Jersey transect: Results from coastal plain and continental slope drilling: Reviews of Geophysics, v. 36, p. 569–601, doi:10.1029/98RG01624.
Mitchum, R., and C. Van Wagoner, J., 1991, High-frequency sequences and their stacking patterns: sequence-stratigraphic evidence of high-frequency eustatic cycles: v. 70, 131–160 p., doi:10.1016/0037-0738(91)90139-5.
Mitchum, R., Vail, P.R., and Sangree, J.B., 1977a, Seismic stratigraphy and global changes of sea level, part 6: stratigraphic interpretation of seismic reflection patterns in depositional Sequences: Part 1: Seismic Stratigraphy — Applications to Hydrocarbon Exploration, v. 26, p. 0, doi:10.1306/M26490C8.
Mitchum, R., Vail, P.R., and Thompson, S., 1977b, Seismic stratigraphy and global changes of sea level: Part 2. The Depositional sequence as a basic unit for stratigraphic analysis: section 2. application of seismic reflection configuration to stratigraphic interpretation: Seismic Stratigraphy - Applications to Hydrocarbon Exploration., v. 165, p. 53–62, doi:10.1306/M26490.
Mitchum, R., Van Wagoner, J., Taylor, G., and Dockery, D.T., 1990, High-frequency sequences and eustatic cycles in the Gulf of Mexico Basin, *in* p. 257–267, doi:10.5724/gcs.90.11.0257.

Mountain, G.S. et al., 2007, The long-term stratigraphic record on continental margins: Continental Margin Sedimentation: From Sediment Transport to Sequence Stratigraphy, p. 381–458, doi:10.1002/9781444304398.ch8.
Mountain, G.S., Miller, K.G., Blum, P., Poag, C.W., Twichell, D.., and Aubry, M.-P., 1996, Data report: Eocene to upper Miocene calcareous nannofossil stratigraphy: Proc. ODP, Sci. Results, v. 150, p. 70–71.
Mountain, G.S., Miller, K.G., Christie-blick, N., Peter, J., and Fulthorpe, C.S., 2006, Shallow-Water Drilling of the New Jersey Continental Shelf: determining the links between sediment architecture and sea-level change: Research Proposal,.
Mountain, G.S., Proust, J.N., and Expedition 313 Science Party, 2010, The New Jersey margin scientific drilling project (IODP expedition 313): Untangling the record of global and local sea-level changes: Scientific Drilling, v. 10, p. 26–34, doi:10.2204/iodp.sd.10.03.2010.
Muto, T., Steel, R.J., and Swenson, J.B., 2007, Autostratigraphy: a framework norm for genetic stratigraphy: Journal of Sedimentary Research, v. 77, p. 2–12, doi:10.2110/jsr.2007.005.
National Center for Earth-surface Dynamics Data Repository, 2019, http://www.nced.umn.edu/Data_Repository.html.
Neal, J.E., and Abreu, V., 2009, Sequence stratigraphy hierarchy and the accommodation succession method: Geology, v. 37, p. 779–782, doi:10.1130/G25722A.1.
Neal, J.E., Abreu, V., Bohacs, K.M., Feldman, H.R., and Pederson, K.H., 2016, Accommodation succession ($\delta A / \delta S$) sequence stratigraphy: observational method, utility and insights into sequence boundary formation: Journal of the Geological Society, v. 173, p. 803–816, doi:10.1144/jgs2015-165.
Obaje, S.O., 2013, Sequence stratigraphy concepts and applications : a review: Journal of Environment and Earth Science, v. 3, p. 207–218.
Paola, C. et al., 2001, Experimental Stratigraphy: Gsa Today, v. 11, doi:10.1130/1052-5173(2001)011<0004:ES>2.0.CO;2.
Patruno, S., Hampson, G.J., Jackson, C.A.L., and Dreyer, T., 2015, Clinoform geometry, geomorphology, facies character and stratigraphic architecture of a sand-rich subaqueous delta: Jurassic Sognefjord Formation, offshore Norway: Sedimentology, v. 62, p. 350–388, doi:10.1111/sed.12153.
Perlmutter, M.A., Radovich, B.J., and Matthews, M.D., 1997, The impact of high-frequency sedimentation cycles on stratigraphic interpretation: University of South Carolina.
Plint, A.G., and Nummedal, D., 2000, The falling stage systems tract: recognition and importance in sequence stratigraphic analysis: Geological Society, London, Special Publications, v. 172, p. 1–17, doi:10.1144/GSL.SP.2000.172.01.01.
Poag, C.W., and Sevon, W.D., 1989, A record of Appalachian denudation in postrift Mesozoic and Cenozoic sedimentary deposits of the U.S. Middle Atlantic continental margin: Geomorphology, v. 2, p. 119–157, doi:10.1016/0169-555X(89)90009-3.
Posamentier, H.W., and Allen, G.P., 1993, Variability of the sequence stratigraphic model: effects of local basin factors: Sedimentary Geology, v. 86, p. 91–109, doi:10.1016/0037-0738(93)90135-R.
Posamentier, H.W., Jervey, M.T., and Vail, P.R., 1988, Eustatic controls on clastic deposition - conceptual framework: Sea-level changes: an integrated approach, p. 109–124, doi:10.2110/pec.88.01.0109.
Reynolds, D.J., Steckler, M.S., and Coakley, B.J., 1991, The role of the sediment load in sequence stratigraphy: The influence of flexural isostasy and compaction: Journal of

Geophysical Research: Solid Earth, v. 96, p. 6931–6949, doi:10.1029/90JB01914.
Schlager, W., 2004, Fractal nature of stratigraphic sequences: Geology, v. 32, p. 185–188, doi:10.1130/G20253.1.
Sheridan, R.E., 1987, Pulsation tectonics as the control of long-term stratigraphic cycles: Paleoceanography, v. 2, p. 97–118.
Sherriff, R.., 1977, Seismic stratigraphy: applications to hydrocarbon exploration: The American Association of Petroleum Geologists Bulletin, p. 3–14, doi:10.1306/m26490.
Sloss, L.L., Krumbein, W.C., and Dapples, E.C., 1949, Integrated facies analysis: v. 39, doi:10.1130/MEM39.
Steckler, M.S., Mountain, G.S., Miller, K.G., and Christie-Blick, N., 1999, Reconstruction of Tertiary progradation and clinoform development on the New Jersey passive margin by 2-D backstripping: Marine Geology, v. 154, p. 399–420, doi:10.1016/S0025-3227(98)00126-1.
Steckler, M.S., and Watts, A.B., 1978, Subsidence of the Atlantic-type continental margin off New York: Earth and Planetary Science Letters, v. 41, p. 1–13, doi:10.1016/0012-821X(78)90036-5.
Strasser, A., Hillgärtner, H., Hug, W., and Pittet, B., 2000, Third-order depositional sequences reflecting Milankovitch cyclicity: Terra Nova, v. 12, p. 303–311, doi:10.1046/j.1365-3121.2000.00315.x.
Strong, N., and Paola, C., 2006, Fluvial landscapes and stratigraphy in a flume: The Sedimentary Record, v. 4, p. 4–8, doi:10.2110/sedred.2006.2.4.
Vail, P.R., Mitchum, R., and Thompson, S., 1977, Seismic stratigraphy and global changes of sea level, part 4: global cycles of relative changes of sea level, *in* Payton, C.E. ed., Seismic Stratigraphy — Applications to Hydrocarbon Exploration, American Association of Petroleum Geologists, https://doi.org/10.1306/M26490C6.
Van Wagoner, J.C., Mitchum, R., Campion, K., and Rahmanian, V.D., 1990, Siliciclastic sequence stratigraphy for high resolution correlation of time and facies: AAPG Meth Explora Series, p. 7–55.
Van Wagoner, J., Posamentier, H.W., Mitchum, R., Vail, P.R., Sarg, J.F.F., Loutit, T.S., and Hardenbol, J., 1988, An overview of the fundamentals of sequence stratigraphy and key definitions: The Society of Economic Paleontologists and Mineralogists, p. 39–45, doi:10.2110/pec.88.01.0039.
Watts, A.B., and Steckler, M.S., 1979, Subsidence and eustasy at the continental margin of eastern North America, *in* p. 218–234, doi:10.1029/ME003p0218.
Weimer, P., and Posamentier, H.W., 1993, Siliciclastic sequence stratigraphy: recent developments and applications: American Association of Petroleum Geologists, doi:10.1306/M58581.
Wilgus, C.K., Hastings, B.S., Posamentier, H.W., Van Wagoner, J., Ross, C.A., and Kendall, ; Christopher G. St. C., 1988, SEPM SPECIAL PUBLICATION (42): Sea-Level Changes: SEPM SPECIAL PUBLICATION.
Williams, G.D., 1993, Tectonics and seismic sequence stratigraphy: an introduction: Geological Society, London, Special Publications, p. 1–13.
Wilson, R., 1998, Sequence stratigraphy : a revolution without a cause ? Geological Society, London, Special Publications, p. 303–314.
Zaitlin, B., Dalrymple, R.W., and Boyd, R., 1994, The stratigraphic organization of incised-valley systems associated with relative sea-level change.

CHAPTER 3: SEISMIC ANATOMY OF A SEQUENCE: A CASE STUDY ON THE MIOCENE FORESETS OF THE NEW JERSEY SHELF

3.1 Abstract

For four decades, the New Jersey continental margin has been a focal point for studying paleo sea-level changes. The stable tectonic history of this rifted margin and its smooth rate of thermal subsidence since the Triassic-Early Jurassic result in relative sea-level change being the leading driver of sedimentary processes and unconformity formation. The key objective of this study is to use the MGL1510 and Expedition 313 data to answer the following questions regarding margin evolution: 1) why are no shoreline features seen in the wells and 2D seismic data, even though the core samples from the topset strata show several hiatus and unconformities, and 2) what processes carried deposits seaward of Miocene clinoform rollovers. To address these questions, we collected 564 km^2 of ultra-high-resolution 3D seismic data to characterize shallow-marine sedimentological properties of the New Jersey margin at a significantly higher resolution (~5 m laterally) than previously achieved (~100s of m). The Geometrical Breakdown approach is used to interpret 22 sequences and 76 systems tracts spanning 8 million years of sediment deposition. These sequences provide a structural framework for geological and petrophysical analyses of the Miocene foresets. We incorporate a state-of-the- art quantitative seismic characterization techniques to study the repeating trends in rock-physics properties within these sequences. The estimated properties are further used as a proxy to interpret the energy level and depositional settings for four types of systems tracts.

3.2 Introduction

Clinoforms are the basic depositional morphology for sediment accumulation across a wide spectrum of scales, ranging from bars to continental margins (Helland-Hansen & Hampson, 2009; Pirmez et al., 1998). Clinoforms and clinothems – strata bounded by clinoforms (Rich, 1951) – occur at three different scales (Helland-Hansen & Hampson, 2009): 1) continental-scale clinoforms (also known as shelf-slope basin clinoforms), which record the advance of a shelf margin, are up to a few hundred meters high, and have their topset-foreset rollover at the the paleoshelf edge; 2) delta scale clinoforms (also known as shoreline clinoforms), which usually result from delta progradation, are up to tens of meters high, and have their topset-foreset rollover located near the shoreline; 3) subaqueous delta clinoforms, which are less than 100 m high and also result from delta progradation but form where the shoreline and topset-foreset rollover are separated.

Clinoformal sequence boundaries are characterized by acoustic impedance contrasts (Miller, Browning, et al., 2013). This is due to changes in depositional environment across the sequence boundary result in contrasting sediment petrophysical properties and therefore acoustic signatures. Subtle changes in the rates of accommodation creation and sediment supply influence the sequence geometries and stacking patterns (Catuneanu, 2017; Catuneanu et al., 2009; Neal & Abreu, 2009). The cyclic nature of stacking patterns (Wanless & Shepard, 1936; Wells, 1960) suggests that the variation of petrophysical properties across a stratigraphic sequence may follow a similar cyclic pattern.

Changes in a clinothem morphology and internal architecture record the interaction between a variety of geological mechanisms, such as eustasy, tectonic activity, rate of sediment influx, and oceanic currents (Boyd et al., 2008; Burgess et al., 2006; Cathro et al., 2003; Martinsen & Helland-Hansen, 1995; Swenson et al., 2005). Sediment influx, which can fluctuate considerably on tectonically active margins, is a source of uncertainty in stratigraphic interpretations (Burgess et al., 2006). The impacts of sediment loading and isostatic compensation add complexity to the history of deposition (Reynolds et al., 1991). However, at a particular geographic location, a single geological mechanism can dominantly contribute to formation of clinothems and their internal structure. For example, the unique geological setting of the New Jersey margin during

the Miocene resulted in eustasy being the controlling factor for the formation of continental-scale clinoforms.

The New Jersey margin is considered a classic example of a rifted margin (Mountain et al., 2007). Rifting started in the Late Triassic (Grow & Sheridan, 1988) followed by sea-floor spreading in the Middle Jurassic (Sheridan & Gradstein, 1983). The margin has since experienced a stable tectonic history, smooth thermal subsidence (Mountain et al., 2007) and continuous sediment loading (Reynolds et al., 1991; Watts & Steckler, 1979), making eustatic change the leading driver of near-shore sedimentary processes and unconformity formation (Miller et al., 2005) (Figure 3.1). The Miocene to Recent sedimentary record includes well-developed siliciclastic sequences in the form of prominent continental-scale clinoforms, which have become a primary target for investigating the effects of eustatic change (Fulthorpe et al., 1999; Monteverde et al., 2000; Mountain et al., 2007; Pellaton & Gorin, 2005). What we know about the of the New Jersey margin clinoforms has so far been mostly based on several sets of 2D seismic reflection profiles, and onshore and offshore drilling campaigns (Figure 3.2).

The New Jersey margin is particularly suited to addressing two major questions concerning the effects of eustatic change: 1) what are the spatial and temporal near-shore processes that formed the paleo shelf during eustatic cycles, and 2) how do the sedimentological parameters vary spatially within the eustatically driven sedimentary units formed since the mid-Oligocene? Improving our understanding of near-shore sedimentary processes and variations in depositional environment were among the main objectives of the International Ocean Drilling Program (IODP) Expedition 313 drilling in 2009, which drilled at three sites: M27, M28, and M29 in ~35 m of water, 45-65 km offshore New Jersey (Figure 3.2). The expedition provided valuable sediment samples and log data which have allowed 1) investigation of the amplitudes, rates and mechanisms of global sea-level (eustatic) changes since the Oligocene (Browning et al., 2013; Katz et al., 2013; Kotthoff et al., 2014; McCarthy et al., 2013; Mountain et al., 2006, 2010); and 2) evaluation of the sedimentary response of a rifted continental margin to eustatic changes (Ando et al., 2014; Degirmency, 2014; Gallegos, 2017; Hendra, 2010; Hodgson et al., 2017; Inwood et al., 2013; Lofi et al., 2013; McCarthy et al., 2013; Mountain et al., 2010).

The key objective of this study is to contribute to further our understanding of the margin evolution by answering the following subset of questions derived form the two major questions:

1) why are no shoreline features observed in the wells and 2D seismic data, even though the core samples from the topset strata show several hiatuses and unconformities, and 2) what processes carried deposits seaward of Miocene clinoform rollovers. To address these questions, we first carry out a sequence stratigraphic analysis by applying the Geometrical Breakdown Approach (Chapter 2) to the migrated 3D reflection volume formed by processing of 564 km^2 of ultra-high-resolution 3D multichannel seismic (MCS) data that we collected on R/V *Marcus G. Langseth* in 2015. This 3D MCS survey is centered on the three IODP Exp. 313 sites and encompasses several clinoform rollovers and paleo-shelves – one of the sedimentary features most sensitive to eustatic change (Mountain et al., 2009). Using the wire-line logs as control points, we invert the migrated 3D reflection volume in a step like fashion that culminated with a clay volume. The sequence stratigraphic model is then compared with the previous work (Miller, Browning, et al., 2013) obtained using 2D seismic data to extend the interpretation in 3D and, in combination with the clay volume, to deepen our understanding on the relationship between interpreted stratigraphic system tracks and predicted lithology.

3.3 Geology

The New Jersey margin has gone through several major events in its geological history that, combined, shaped it into a natural laboratory for studying eustatic change (Miller, Browning, et al., 2013). The separation of the North American and African plates began in the Late Triassic and was followed by a period of rifting of the margin in the Lower Jurassic. Seafloor spreading began off the coast of Georgia in the lower Jurassic and extended northward along the Atlantic margin during the Middle Jurassic (Withjack et al., 1998) to progressively unzip Pangea. The subsequent history of rifting and drifting in the US middle Atlantic region is recorded by almost 16 km of sediment deposited during the last 200 million years (Grow & Sheridan, 1988). The rifting process was associated with the formation of a diachronous post-rift unconformity that separated the active rifting stage of the margin from the drifting stage (Miller et al., 2014).

Since the beginning of the drifting stage, eustatic change, thermal subsidence, lithosphere flexure, mantle dynamics, and sediment compaction became the major processes shaping the margin's sedimentary structure until the Plio-Pleistocene (Miller & Mountain, 1994; Mountain et al., 2007; Reynolds et al., 1991b; Rowley et al., 2011; Watts & Steckler, 1981; Watts & Steckler,

1979). Eustatic change varied the depositional setting from terrestrial to shallow-marine depending on the position of the shoreline. Variations in sediment supply were also important. For example, periods of low sediment input resulted in starved pelagic sections with high sediment input from the Appalachian Mountains that formed thick fluvial-influenced shelf and slope deposits (Browning et al., 2008; Miller et al., 2014). Mantle dynamics influenced the post-rift history of the margin through a long period of subsidence (Liu, 2008). So far, the available mantle convection models have not predicted instability or uplift of the New Jersey margin since the Eocene, but these models have noted that the rate of subsidence has slowed significantly over time (Liu, 2008, 2015).

Over the past 100 Myr, the New Jersey margin sedimentary facies record eight depositional regimes (Browning et al., 2008): 1) Cretaceous riverine environment with warm climate, high sediment input, and high sea level; 2) Cenomanian to Early Turonian marine-dominated sediments deposited during high sea level with minor deltaic influence; 3) Late Turonian to Coniacian non-marine delta system during a long period of low sea level; 4) Santonian to Campanian wave-dominated marine environment with strong deltaic influence; 5) Maastrichtian to Middle Eocene starved marine ramp associated with high sea level, but low sediment input from the hinterland; 6) Eocene-Oligocene starved siliciclastic shelf environment; 7) Early-Middle Miocene prograding marine shelf with a strong wave-dominated deltaic influence, during which the New Jersey margin experienced multiple eustatic fluctuations; and 8) Late Miocene to recent eroded coastal system with a long period of low sea level and low sediment supply due to bypassing (Browning et al., 2008).(Browning et al., 2008)(Browning et al., 2008)

The first 2D seismic images from the New Jersey continental shelf revealed that the Miocene prograding marine shelf comprised several sedimentary packages with clinothem. In general, deposition occurred in two major contexts along the margin: 1) a river and storm-dominated shelf in an offshore to shoreface environment, with well-sorted silt and sand deposits and 2) intrashelf clinoform topset, clinoform rollover, clinoform front and toe-of-slope settings dominated by poorly-sorted, coarse-grained debrites and turbidites with interbedded silt and silty clays (Expedition 313 summary). The Miocene shallow-marine to shelfal depositional environment had a proximal paleo-water depth of 50-80 m to 70-120 m in the distal shelf (Katz et al., 2013). The Miocene sediments are 100% siliciclastics with grain size varying from silty clay to coarse-grain sand (Mountain et al., 2010). The Expedition 313 core samples show several

intervals with rapid changes in grain size (Figure 3.3). The strong seismic reflections in the Miocene section are often results of one of two transitions: 1) abrupt upward change from coarse to fine-grained sediments (e.g., a shaley layer overlying sandy clinoform topsets), typically occurring at a flooding or transgressive surface, or 2) abrupt upward change from fine- to coarse-grained sediments (e.g., a distal shale overlain by fluvio-deltaic coarse sand), which can be also a sequence boundary. The second case is an example of a basinward shift in facies with a sharp angular contact at the base – the classic criteria for an erosional unconformity as a sequence boundary. Moreover, several hiatuses and periods of erosion are also present in the Miocene sedimentary record. These gaps in sedimentation formed: 1) angular unconformity surfaces close to clinoform rollovers and toes, which are difficult to track along the topsets; and 2) strong acoustic impedance contrasts associated with rapid changes in grain size. The core and log data from Expedition 313 do not show any intervals of pure clay-size sediments in the Miocene section.

3.4 Data

Two complementary data sets used for this study include an ultra-high resolution 3D MCS migrated reflection volume formed using the data we collected during the R/V *Marcus G. Langseth* cruise MGL1510 in 2015, and core and wireline log data from the three IODP Expedition 313 sites drilled in 2009 (Figure 3.2). The 3D MCS survey involved an innovative hybrid design comprised of 24 short-offset P-cable streamers and one 2D long-offset streamer (Figure 3.4). The P-cable streamers were 50 m long and towed from the cross cable at a water depth of ~4.5 m with 12.5 m lateral distance between the streamers. Each P-cable had 8 hydrophone groups spread over 6.25 m interval. Recording time window was 4 s with a sampling rate of 0.5 ms. However, the top 1.5 s of the data was used for seismic data processing at a sampling rate of 1 ms. The minimum source-receiver offset was 55 m. The source was a linear airgun array shot every 12.5 m and composed of four guns with a total volume of 700 cu. in. (11.47 L). The 3D survey covers an area of about 11 by 54 km (564 km^2) centered on the three IODP 313 drill sites. In total, the 3D MCS volume comprises 1803 inlines (156 to 1959) spaced 6.25 m and 17417 crosslines (1691 to 19108) spaced 12.5 m, which together yield a nominal bin size of 3.125 m X 6.25 m and a fold range of 2 to 4.

The process of seismic data collection and analysis aimed to maximize the spatial resolution of the image from structures of interest in the top 1.5 s of seismic data. The hybrid survey design resulted in a better velocity control for processing the 3D volume. The wide-offset data coverage, achieved with a 3-km 2D streamer helped determine the velocity for complex geological structures that may produce nonhyperbolic reflection patterns (Colombo, 2005). RadExPro was contracted to process the seismic data and apply the necessary data corrections. A 3D F-Kx-Ky regularization step was done to minimize the gaps in common offset volumes and binning grids. The 3D MCS data were migrated using pre-stack Kirchhoff migration in the time domain to move seismic features to their proper positions in space, laterally as well as vertically. Further, wavelet signature deconvolution was applied to attenuate residual ghost effects in seismic data, resulting in zero-phase wavelet shape. Finally, a time-variant bandpass filter, with corner frequencies 5-10-250-350 Hz from 0 ms to 1000 ms, and 5-10-75-150 Hz from 1000 ms to 1500 ms and with a tapering width of 100 ms, was applied to the 3D seismic data to remove noise outside of the signal frequency spectrum.

We used measurements from Sites M27 - M29 including spectral gamma-ray (thorium, uranium, and potassium radiation), both through pipe and in open hole, sonic (open hole), caliper, resistivity (open hole); magnetic susceptibility (open hole), acoustic image (open hole), and vertical seismic profile (through pipe and in open hole). We applied de-spiking and a high-cut-filter (100 Hz high pass, 120 Hz high cut) to eliminate questionable measurements (extremely low or high values) in the sonic log as well as P-wave velocity measurements made on cores using the shipboard multisensory track. Downhole sonic logging at Site M27 was conducted in two intervals: from 192 to 342 m wireline log depth below seafloor (WSF) and from 418 to 623 m WSF. Due to the formation of a bridge and infilling uphole from 342 m WSF, the base of the log measurements from the 192 to 342 m WSF interval becomes shallower with each run. The missing sonic measurements in the 342-418 m WSF interval were reconstructed by using V_p measured in the shipboard laboratory on core samples, after adjusting for the effect of sediment decompaction. Because V_p is a function of bulk pressure and pore fluid saturation, such laboratory measurements may not match those from *in situ* wireline measurements. Therefore, the measurements from the core samples were normalized with respect to the sonic log. The conditioned V_p log and laboratory measurements for density were used to generate a zero-offset synthetic seismogram for each site using a convolutional model. The synthetic seismogram was

used to tie the 3D MCS data to the logs at the three sites using a refined time-depth function generated from both wireline P-wave logs and VSP travel time (Table 3.1-3.3).

3.5 Methods

3.5.1 Sequence stratigraphy using Geometrical Breakdown Approach

The GBA (Aali et al., 2020) was used to interpret the stratigraphic sequences within the 564 km^2 area covered MGL1510 3D reflection volume from the New Jersey continental margin. This approach focuses on geometric criteria to break down sequences into reflection packages and systems tracts using the following steps: 1) identify packages of sediment between prominent seismic surfaces and locate their rollover point; 2) mark the landward and seaward terminations of each package; 3) identify the direction of horizontal shift of the landward and seaward terminations, and the direction of vertical shift in their rollover point respect to the underlying package, and assign a three-letter acronym accordingly; 4) identify systems tracts and associated surfaces that comprise individual sequences based on the pattern of three-letter-acronyms; and 5) apply steps 1-4 to multiple sequences to define sequence sets and composite sequences.

This study is the first extension of the GBA approach for 3D for stratigraphic interpretation. We considered the stacking pattern of reflection packages in NW-SE direction to identify their three-letter-acronyms. The sequence boundaries were interpreted in the seismic volume by loop-tying, without auto-tracking, which was compromised because of the spatial variability in the seismic signature of sedimentary packages. The information from core samples and log data at three IODP site was then used to identify the age of the sequence boundaries.

3.5.2 Seismic-guided estimation of petrophysical properties

Integration of seismic amplitudes in time and well data in depth permits characterization of sedimentary properties away from the IODP sites. We used the wireline sonic logs and V_p and density measurements, made on core by using Multi-Sensor Core Logger (MSCL), to generate a synthetic seismic trace and to perform seismic/borehole ties. Incorporating the well data in the 3D stratigraphic model yielded reliable measurements of variations in sedimentary properties, paleo-water depth (Katz et al., 2013), sediment composition (Hendra, 2010; Mountain et al., 2010) and age (Browning et al., 2013) along the key surfaces in both dip and strike directions across the 3D reflection volume. The IODP sites M27-M29, drilled in ~ 35m of water depth,

provided detailed core samples and log data from each sequences at three locations: 1) the shallowest topset sediment most susceptible to relative sea-level change, 2) the bottomset sediments at the clinoform toe, and 3) basinward of the clinoform toe, where the sediments are less disturbed and microfossil abundances are maximized for optimal age control (Fulthorpe et al., 2008). The log data were upscaled to the resolution of seismic data for further well-to-seismic data integration.

We applied a model-based post-stack seismic inversion (Appendix A.3) to estimate acoustic properties from the seismic amplitude within the 3D seismic volume. The inversion process iterates between forward modelling and inverted impedance values at the borehole locations to drive a deterministic relationship that minimizes the error in seismic inversion. The inversion process then uses the determined relationship to compute acoustic impedance from the seismic amplitudes away from the boreholes. Figure 3.6 shows the correlation between inverted and measured acoustic impedance at Sites M27 and M29 after six inversion iterations. A section from the final inverted volume crossing the Expedition 313 sites is shown in Figure 3.7. At shallow depths, the limited compaction and minor changes in lithology and acoustic properties produce minor reflectivity contrasts. At greater depths (>300 m), the impedance contrasts intensify (Figure 3.7) as sediments experience a longer period of diagenesis and greater overburden pressure.

The estimated acoustic impedance along with the original seismic amplitude and more than 30 seismic attributes were fed into a Multi-Attribute Linear Regression (MALR) process (Appendix A.2) to predict V_p (Figures 3.Figure 3.8-3.9), density (Figures 3.10-3.11), and ultimately, the volume of clay (Figure 3.12). We implemented stepwise regression to identify the attributes that yield better prediction in the MALR process based on the average validation error (between the real measurements and predicted values) at three well locations.

In the target interval of the Early to Mid Miocene, V_p showed an acceptable overall correlation coefficient (CC) in both training (CC=0.91) and validation (CC=0.85) phases. The average validation error for the predicted V_p was 82 m/s at Site M29 and 104 m/s at Site M27. At Site M28, with no borehole wireline sonic log, the Faust model was used to estimate the V_p from the available open-hole resistivity measurements (Werthmüller et al., 2013). The synthesized V_p log was then normalized in respect to the measured velocity from Sites M27 and M29. The final

synthetic V_p log was used as a blind well to validate the MALR process. The predicted V_p had the validation error of 80.5 m/s at Site M28.

We applied the MALR to also estimate density from the seismic data. In the target interval of the Early to Mid Miocene, Density showed a good correlation coefficient (CC) in both training (CC=0.85) and validation (CC=0.72) phases between the predicted values using the MALR process and MSCL measurement on core samples. The validation error for estimating density was 0.128 g/cc at Site M27, 0.09 g/cc at Site M28, and 0.09 g/cc at Site M29.

Density, V_p, acoustic impedance, and seismic amplitude volumes were fed into a MALR process to maximize the correlation between the predicted and measured clay volume from the core analysis. Even though these sediments comprised almost 100% siliciclastic deposits, wide variations in consolidation make it challenging for MALR to define a single relationship for predicting clay volume. We performed two separate MALR analyses for shallow less-unconsolidated (with an approximate burial depth < 300m) and deeper, more-consolidated sediments (with an approximate burial depth > 300 m). The correlation coefficient function shows CC=0.81 between the core measurements and the predicted values for more consolidated sediments, and CC=0.68 for the shallow unconsolidated to poorly consolidated sediments. The predicted clay volume in 3D yields determine the extension of sedimentary facies that were previously identified only in three IODP sites.

3.6 Results

The resulting 3D stratigraphic model provided an unprecedented ability to dissect the Miocene sedimentary record in detail using the MGL1510 seismic volume. Spanning 8 million years of sediment deposition in the Miocene, we identified 22 sequences and 76 systems tracts (Figure 3.5), of which only 19 sequences and 53 systems tracts were previously identified in earlier work using 2D reflection sections and well data. Implementing GBA to the 3D MCS data has resulted in identification of ~40% more structure within the Miocene sequences than previously determined (Miller, Browning, et al., 2013) for further geological and petrophysical analyses of the Miocene foresets.

The identified reflection packages also show a significant along-strike variability. In the topset area close to the well M27, the relatively conformable sedimentary packages, are unconformable

in strike direction and form interbedded reflection packages. In the foreset area, the rollover points of the reflection packages vary significantly from the Early Miocene to the Mid Miocene (Figure 3.5). The foreset of clinoforms in the Early Miocene backsteps landward from NE to SW. However, the clinoforms deposited in the Mid Miocene show over 30 degrees rotation and foresteps seaward from NE to SW.

Seismic attribute analyses in the topset of Miocene clinoforms show several persistent paleo-ocean streams that could contribute to the long period of nondeposition in this area (Figure 3.18). These features are imaged by extracting with a dip azimuth value of 220-225 degrees. The dip azimuth attribute calculates the direction of dip for the seismic reflections within 3D data. Even though the width of the seismic volume is quite narrow, the observed features have two distinct characteristics: 1) the morphology elongated in NW-SW direction; 2) the seismic reflection within these features is dipping toward SW. The age of these features can be traced back from the Early Miocene to the Late Tortonian. Similar features (Figure 3.18 B) are present in the lower Burdigalian and creep southward, out of the 3D volume, by the Langhian.

The 3D seismic images reveal a polygonal fault system (Cartwright & Dewhurst, 1998) as an array of extensional faults within the fine-grained stratigraphic intervals in the clinoform toe. Gravity sliding (Clausen et al., 1999; Higgs & McClay, 1993), dewatering, differential compaction between the layers (Henriet et al., 1989; Watterson et al., 2000), and low frictional strength of compacting sediments cause poorly consolidated sedimentary structures to fail under the directional overburden stress from the new deposits (Goulty, 2001). The seismic velocity gradually increases downdip basinward of the clinoform toe (Figure 3.12) attributing to consolidation and dewatering of the most deeply buried part of the sequence. These normal faults have modest throws of up to 15 meters and form polygonal patterns in map view (Figure 3.12). The predicted clay content shows a succession of clay-rich and sandy sediments with the age of the Mid-Miocene that covers the entire area basinward of the clinoform toe (Figure 3.13).

The detailed analyses of predicted elastic properties demonstrate cyclic patterns within the 76 systems tracts and 22 sequences spanning 8 Myr. The established sequence stratigraphic framework was subdivided into nine regions, based on proximity to land, to capture the regional trend in the petrophysical properties. The predicted elastic properties were averaged within each region to determine the general trend for each property and their distribution across each type of

systems tract. The trends of elastic properties within the systems tracts are simplified in geometrical breakdown models of the slug diagram for the estimated acoustic impedance (Figure 3.14), V_p (Figure 3.15), density (Figure 3.16), and clay content (Figure 3.17).

Unlike seismic amplitude, which is an interface property, the inverted acoustic impedance represents an inherent property of strata that makes it a more direct means of characterizing reflection packages. The acoustic impedance profile also resolves thin layers below the tuning thickness (Chopra et al., 2009) to enable better determination of the extent of reflection packages within the 3D volume (Figure 3.6). A statistical analysis of acoustic impedance changes across the systems tracts revealed contrasting trends (Figure 3.14); while LST and FSST show a reduction in acoustic impedance basinward, TST and HST display a basinward increase in their impedance values. Because acoustic impedance is a product of V_p and density, interpreting variations in the sedimentary environment requires independent knowledge about these two physical properties.

Diagenesis and compaction both increase V_p by consolidating sediment and reducing pore volume (Avseth et al., 2010). The predicted V_p section (Figure 3.15) shows how these two processes result in a continuous basinward, downslope increase in V_p in the Miocene interval of the profile, which comprises almost 100% siliciclastic sediments. The along strike changes of V_p within reflection packages are subtle, especially in the shallow intervals. All four systems tracts show a continuous increase in the V_p in dip direction (Figure 3.15), which are attributed to the higher overburden pressure as the reflection packages are deepening basinward.

Lithofacies change imposes a stronger influence on density than on velocity. In other words, in the Miocene section, downdip changes in lithofacies are more pronounced than those in the V_p profile. The shallow topset area, dominated by Quaternary coarse-grained, unconsolidated sediments, is predicted to have high density. Figure 3.16 shows the trends of density for each type of systems tract in the dip direction. The transgressive systems tract shows a 3%-5% density increase basinward from topset to bottomset. However, HST, FSST, and LST all show density reduction basinward. HST (~8%) has a higher drop in density than LST (5%). Although few FSST samples were available from the New Jersey margin, they nevertheless show a continuous decrease in predicted density basinward.

The Miocene section comprises siliciclastic sediments, ranging from clay to gravel-size grains, with no significant carbonate deposits. The distribution of clay within the systems tracts, and from one systems tract to another, follows a systematic trend. HST, LST, and FSST show a fining trend basinward. However, the TST shows a coarsening trend basinward (Figure 3.17). The model does not reflect vertical changes in the elastic properties, caused by post-depositional processes such as overburden pressure and compaction. Such processes may influence the spatial trends observed within individual systems tracts, especially in unconsolidated and poorly consolidated sediments.

3.6 Discussion

3.6.1 Rock physics interpretation

Water motion predominantly drives sediment transport processes (Nittrouer & Wright, 1994) on the continental shelf in both dip and strike directions. The ratio of accommodation creation to sediment flux influences the efficiency of along- and cross-shelf sediment transport (Driscoll & Hogg, 1995). During the formation of LSTs, the down-dip component of sediment transport was likely more efficient than along-strike processes, resulting in a gradual decrease in grain size in the onshore-offshore direction within the systems tract (Figure 3.17). During the formation of the TSTs, along-strike transport processes likely overpowered down-dip transport processes (Driscoll & Karner, 1999), which can disrupt the usual basinward fining trend in sediment deposition (Figure 3.17).

The predicted clay content of the Miocene sediments is a proxy for energy level and depositional setting for the four types of systems tracts. The energy level of the environment directly controls the percentage of clay in the siliciclastic sediments (Reineck & Singh, 1973); the fraction of small-size particles increases as the energy of the environment decreases. In a low-energy near-shore environment, along-strike sediment transport is mainly controlled by diffusive processes, resulting in a fining trend in basinward direction. In contrast, in a high energy environment, wave energy and shore-parallel currents predominantly influence shelf sediment transport along strike by both advection and diffusion processes (Driscoll & Karner, 1999) (Figure 3.18). These along-strike processes on high-energy continental shelves are usually the stronger component of sediment transportation than down-dip shelf processes (Butman et al., 1979; Cacchione et al.,

1990; Wiberg et al., 1996). The trend observed in transgressive systems tracts can be attributed to the presence of a strong along-shore advective processes that carried away fine-grain material in the deeper part of the shelf.

The last 25 years of global ocean current simulations for the Miocene interval consistently show a strong Gulf Stream offshore the New Jersey margin (von der Heydt & Dijkstra, 2006). The presence of strong currents was not limited to deep water, but also persisted on the shelf. Ocean currents influencing the New Jersey shelf have annual, seasonal, storm, tidal, and wave components (Beardsley & Boicourt, 1981). While the annual along-shore current on the modern New Jersey shelf has an average velocity of less than 20 cm/s, it can exceed 60 cm/s during winter storms, strong enough to transport unconsolidated sediment along the shelf (Beardsley & Boicourt, 1981; Gong et al., 2008; Lyne et al., 1990). These strong along-shore current can explain the presence of coarse-grain material further basinward in TSTs in the Miocene interval.

Australia's Northwest Shelf (Sanchez et al., 2012a, 2012b; Tagliaro et al., 2018) and the Canterbury Basin in New Zealand (Carter et al., 2004; Lu et al., 2003, 2005) are analogues to the New Jersey margin that underwent similar processes during the Miocene. On the Northwest Shelf, changes in ocean circulation in the Indian Ocean caused along-strike sediment transport superimposed on deltaic progradation (Tagliaro et al., 2018). Measurements of the along-strike (migration) and down-dip (progradation) movement of these deltas are well documented by Sanchez et al. (2012a, 2012b). In the Miocene shelf depositional setting of the Canterbury Basin, along-strike currents were strong enough to control sequence thickness, and cause development of elongate sediment drifts within the shelf/slope system (Carter et al., 2004) — similar features to what we observe in the Miocene sediments of the New Jersey shelf. The small size and relative scarcity of mid-late Miocene shelf canyons on the New Jersey margin suggest that waves and currents on the paleo shelf diffused the fluvial point sources to produce a linear system for sediment delivery to clinoform fronts (Fulthorpe et al., 2008). As a result, individual point sources failed to overcome along-strike forces to form lobate depocenters seaward of clinoform rollovers.

3.6.2 Change of the slope azimuth on the New Jersey margin

Analysis of dip azimuth (the direction of maximum dip) within the seismic data shows that the direction of sediment flux has changed since the late Miocene (Figure 3.19). While the general

dip direction for the Oligocene and early Miocene deposits was S14E, it had shifted 13° to S1E by the late Miocene-Pliocene. Seismic attribute analysis in the topset of Miocene clinoforms also reveals persistent channelized streams with a NE-SW strike that could transport and diffuse sediments basinward and cause a long period of nondeposition on the clinoform topsets. They present in reflection packages from the early Miocene to the end of Tortonian (Figure 3.18). Similar features with a NE-SW trend are observed on clinoform bottomsets within the seismic volume, beginning in the Lower Burdigalian and migrating southward by the Langhian.

Miocene systems tracts also show a significant along-strike variability. The relatively conformable sedimentary packages are laterally unconformable in the topset area close to the well M27. These packages with limited continuity are interbedded and show lower volume of clay (Figure 3.11). In the foreset area, the rollover points of the reflection packages vary significantly from the Early Miocene to the Mid Miocene. The foreset of clinoforms in the Early Miocene retrograde landward from NE to SW (Appendix A6). However, the clinoforms deposited in the Mid Miocene prograde seaward from NE to SW which show close to a 45-degree rotation in 8 Myr.

The NE-SW strike of the polygonal faults (Figure 3.13) forms an acute angle with the general onshore-offshore direction. The southward excessive stress load of deposits, imaged by 3D seismic data (Appendix A6), accelerated gravity sliding of sediments and exerted a significant influence on the organization of the fault arrays and their strike. Rather than consolidation without any shear failure that could happen in a passively subsiding basin, the presence of the directional stress caused grains to slip across the boundaries. Moreover, gentle slopes at the toe of clinoforms induced a gravity force and resulted in the detachment of isolated sediments from their base and slid them into the deeper depth (Cartwright & Dewhurst, 1998; Higgs & McClay, 2008). The downslope gravitational stress provided the necessary conditions for sliding and formation of intraformational faults that broke these sediments into smaller blocks and provided a modifying influence on the type and orientation of the observed polygonal faults in the margin.

Change of the slope azimuth on the New Jersey margin, rotation of clinoforms strike due to higher sedimentation on one side, and the orientation of polygonal faults are supporting evidence for the presence of strong advective coastal currents flowing parallel to clinform strike in the Early to Mid Miocene. Miocene clinoform topsets were probably never subaerially exposed in

the Miocene, and the advective along-shore current was responsible for topset erosional surfaces. These strong coastal currents along with the mechanical failure of unconsolidated deposits were most likely the source of turbidite deposits found in the Expedition 313 cores near clinoform toes.

Mantle dynamics and local tectonic activities are other processes that could have a similar impact on the sedimentary record and result in differential subsidence on the Southwest side. To date, the available mantle convection models have not concluded instability or uplift of the New Jersey margin since the Eocene (Liu, 2008, 2015). We also did not encounter any major vertical displacement (Burbank & Anderson, 2011) associated with tectonic activities within the 3D seismic data. However, the MGL1510 volume only covers a narrow part of the shelf and acquiring additional seismic data is required to image the sedimentary structure on the Southwest side of the study area.

3.7 Conclusions

This study presented a detailed sequence stratigraphic model for the Miocene sediments offshore the New Jersey margin that integrated three interpretation approaches in a 3D subsurface model: quantitative seismic interpretation (estimating acoustic impedance, V_p, density, and clay volume within the seismic volume); attribute analysis (identifying surface, interval and volume attributes); and seismic stratigraphy (depositional sequences interpreted using objective geometric criteria). We identified 76 systems tracts within the 3D seismic volume to interpret the variations in sedimentary structures and their petrophysical properties in the New Jersey margin. With a vertical resolution of less than 5 m and a lateral resolution of 3 m by 6 m in an area of ~564 km^2, this study enhanced the previous frameworks for the New Jersey margin that were mainly based on 1D and 2D datasets. Furthermore, the analysis of the sequences and systems tracts and their petrophysical properties resulted in modeling the rock physics of clinothems in shallow marine siliciclastic clinoforms. We defined rock physics trends of four main petrophysical properties (acoustic impedance, density, V_p, and clay content) that can be used as guidelines for characterizing shallow marine clinothems. The defined trends allow incorporating clinoforms in statistical characterization of subsurface properties that rely only on limited and sparse measurements.

The predicted clay content of the siliciclastic sediments was further used as a proxy to interpret the energy level and depositional settings for four types of systems tracts found within the Miocene section of the New Jersey margin. The results accentuate the role of alongshore currents in the formation of the sedimentary architecture and facies. This study also provided supporting evidence that the topset of clinoforms in the margin has never been subaerially exposed in the Miocene. The along-strike flow identified in the topsets and bottomsets of clinoforms, and caused by along-strike currents, were responsible for several intervals of erosion in the topset area and for the presence of turbidite deposits in the clinoform toe.

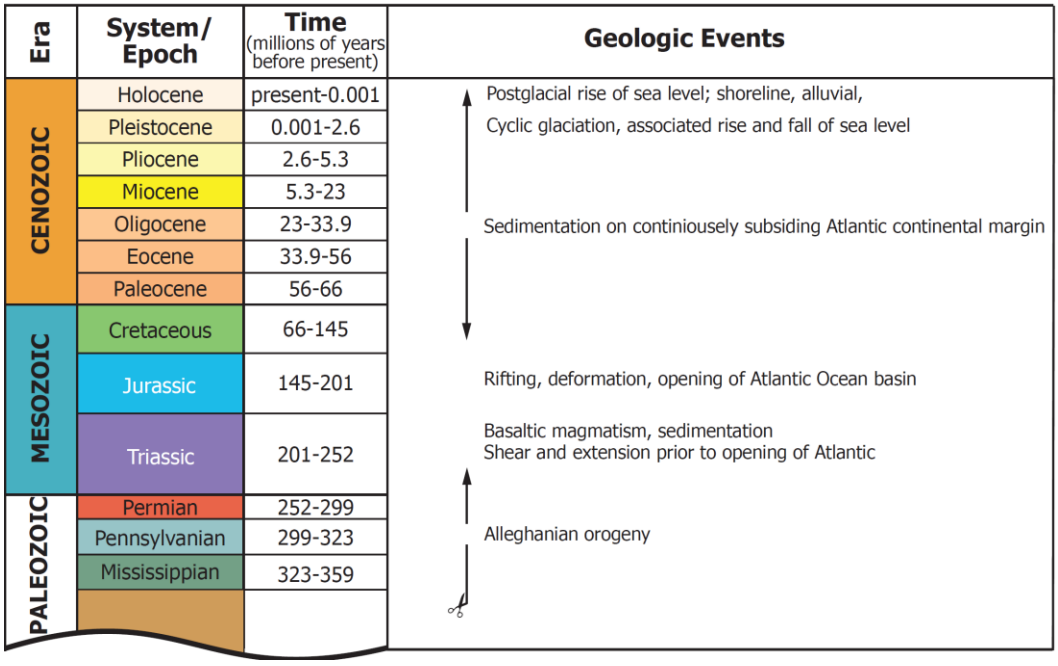

Figure 3.1: An overview of major geological events on the New Jersey continental margin.

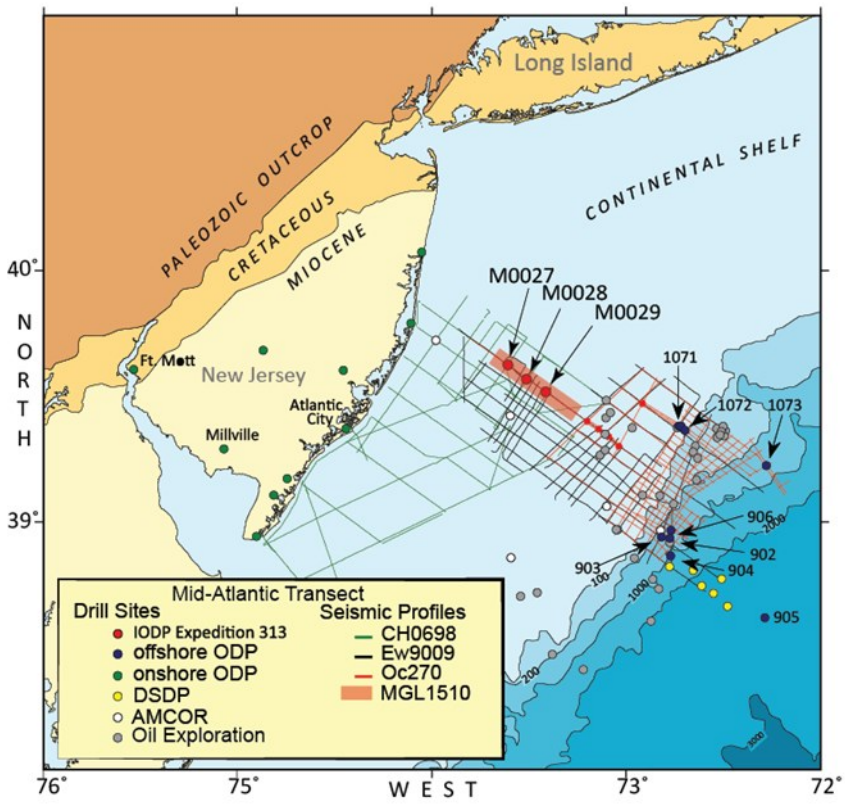

Figure 3.2: Map of the New Jersey continental margin showing the location of the MGL1510 3D MCS survey carried out in 2015 together with the earlier 2D MCS profiles and drill holes, including the most recent IODP Sites M27, M28, and M29 that were drilled during Expedition in 2009.

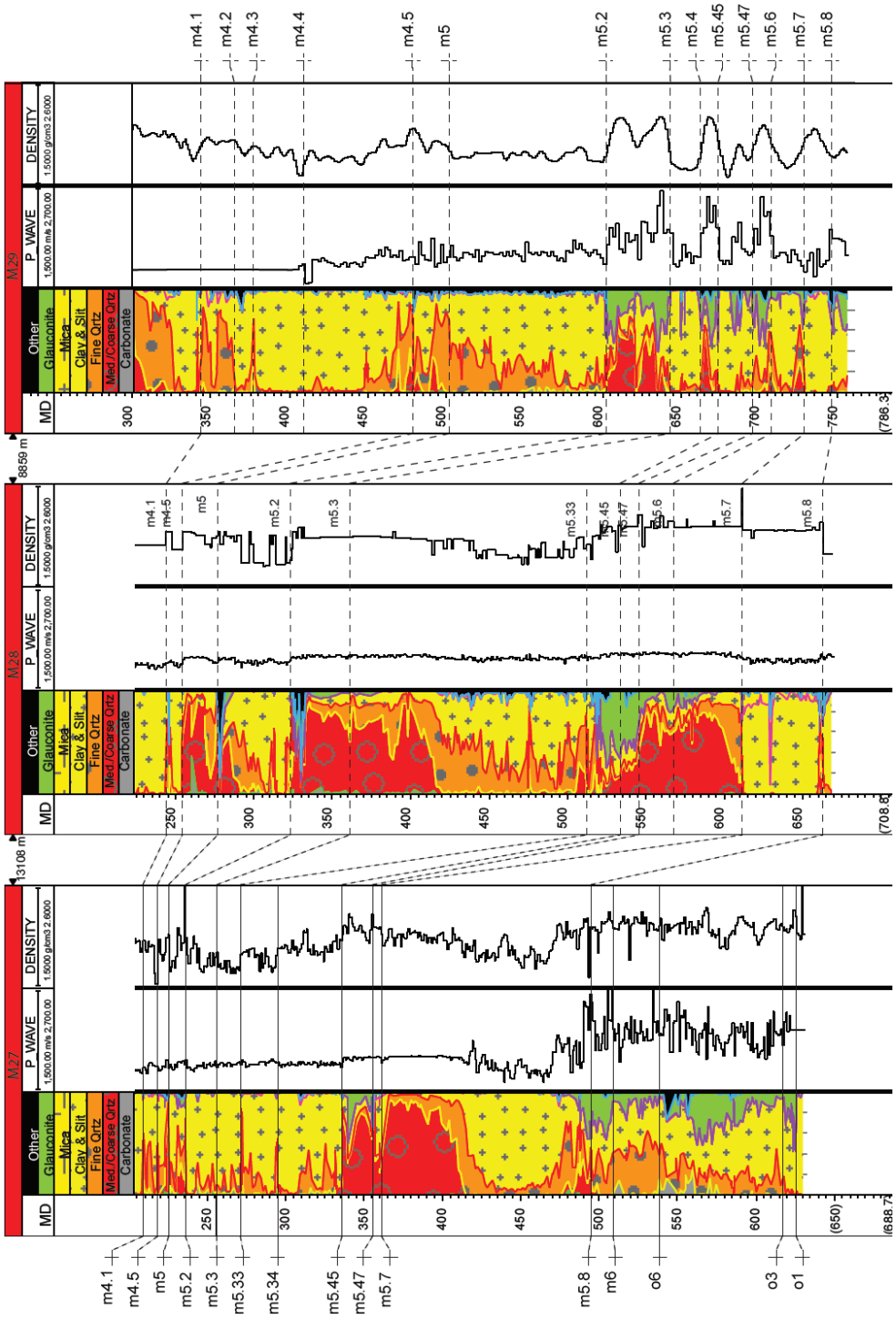

Figure 3.3: Litho-stratigraphy, P-wave velocity, and density logs for IODP Sites M27-M29. The lithostratigraphic description of the sediments and their compositions were defined by analyzing the core samples from bottom to top in the wells M27- M29 (Mountain et al., 2010).The missing middle part for the sonic measurements in M27 was reconstructed by using the measured P-wave velocity from the core samples after adjusting for the effect of sediment decompaction. At Site M28, with no borehole wireline sonic log, the Faust model was used to estimate the P-wave velocity from the available open-hole resistivity measurements (Werthmüller et al., 2013).

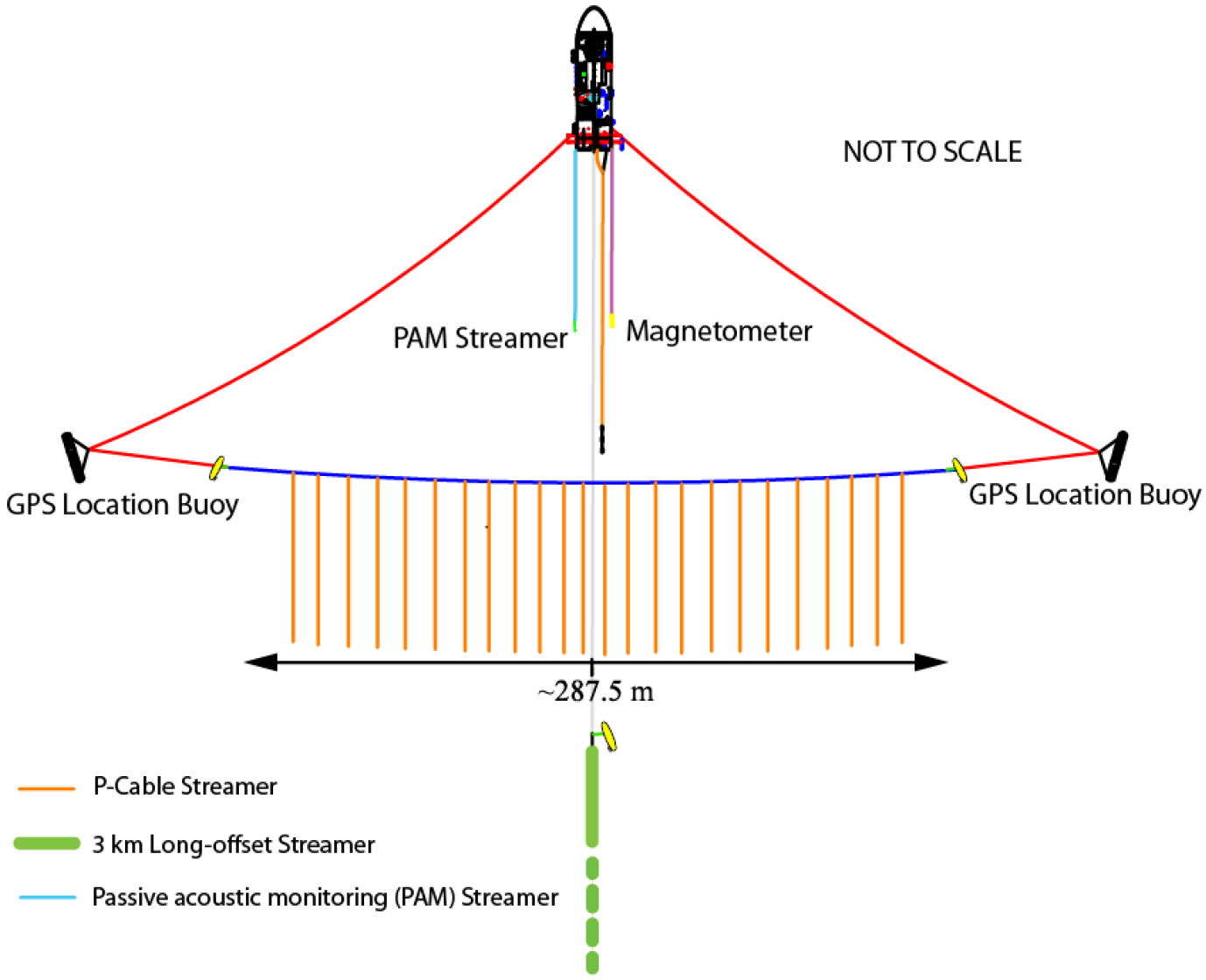

Figure 3.4: MGL1510 survey design. The 3D survey hybrid design comprises 24 short-offset P-cable streamers, used to achieve the ultra-high spatial resolution with small bin size of 3.125 m X 6.25 m, and one 2D long-offset streamer, used to provide velocity control for seismic data processing.

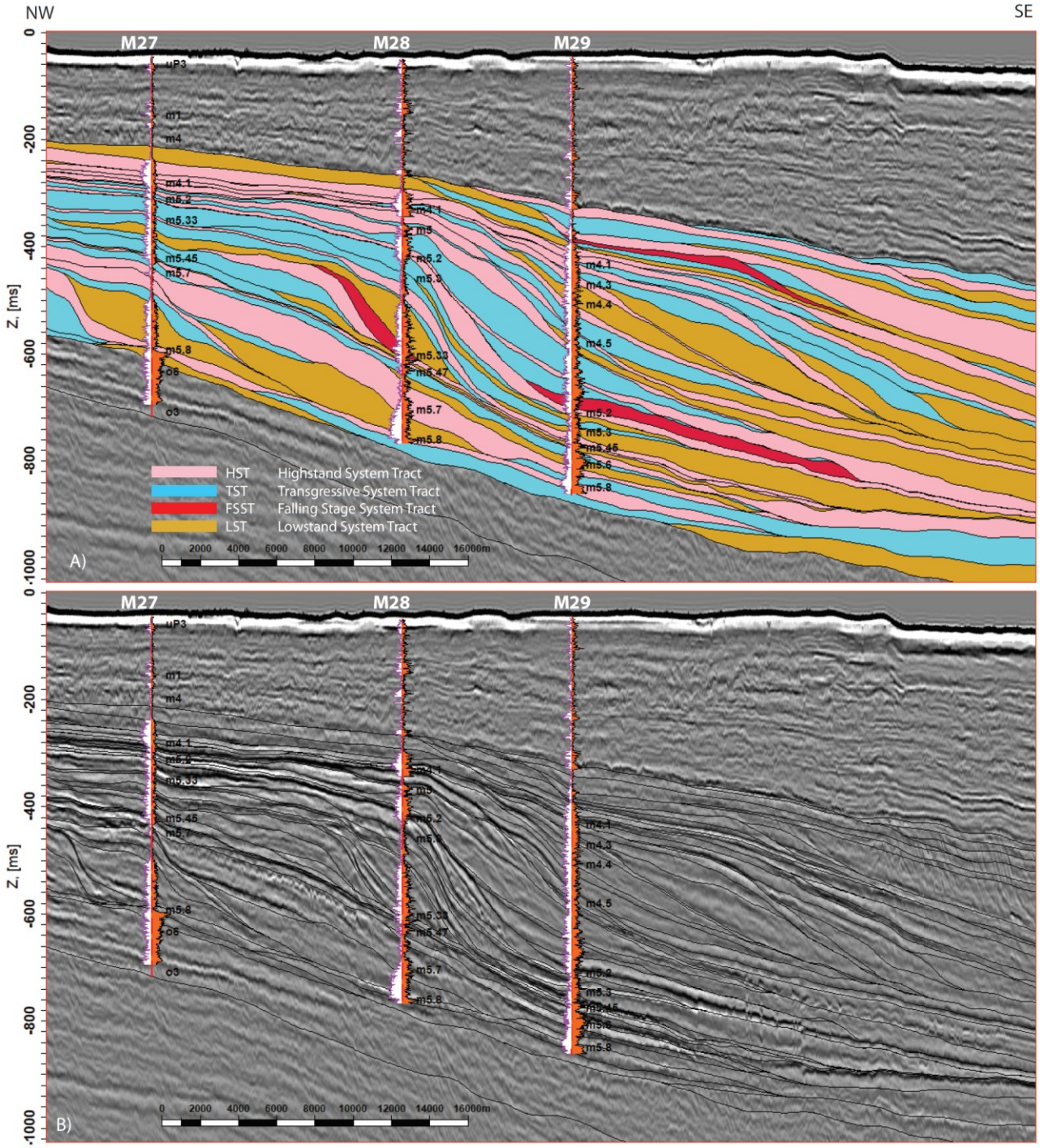

Figure 3.5: Interpreted (upper) and uninterpreted (lower) seismic section (inline 960) crossing the Expedition 313 drill sites. The resulting model, which included 22 sequences and 76 systems tracts spanning 8 million years of sediment deposition.

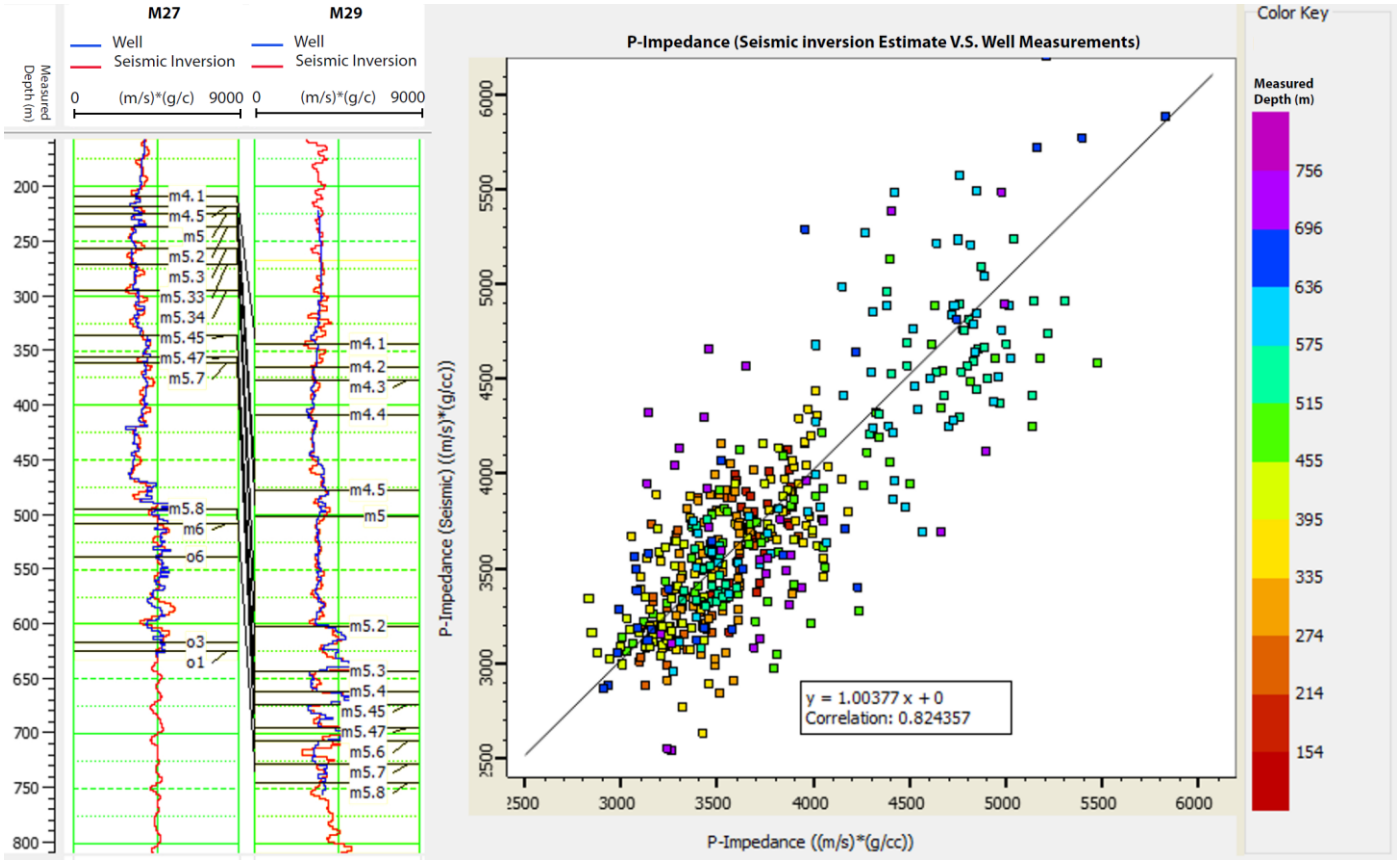

Figure 3.6: Seismic inversion analysis for Sites M27 and M29. The blue lines represent the computed acoustic impedance logs, and the red lines are the inverted impedance values using the seismic trace at the borehole location. (right) The cross plot shows good correlation between the inverted and measured acoustic impedance.

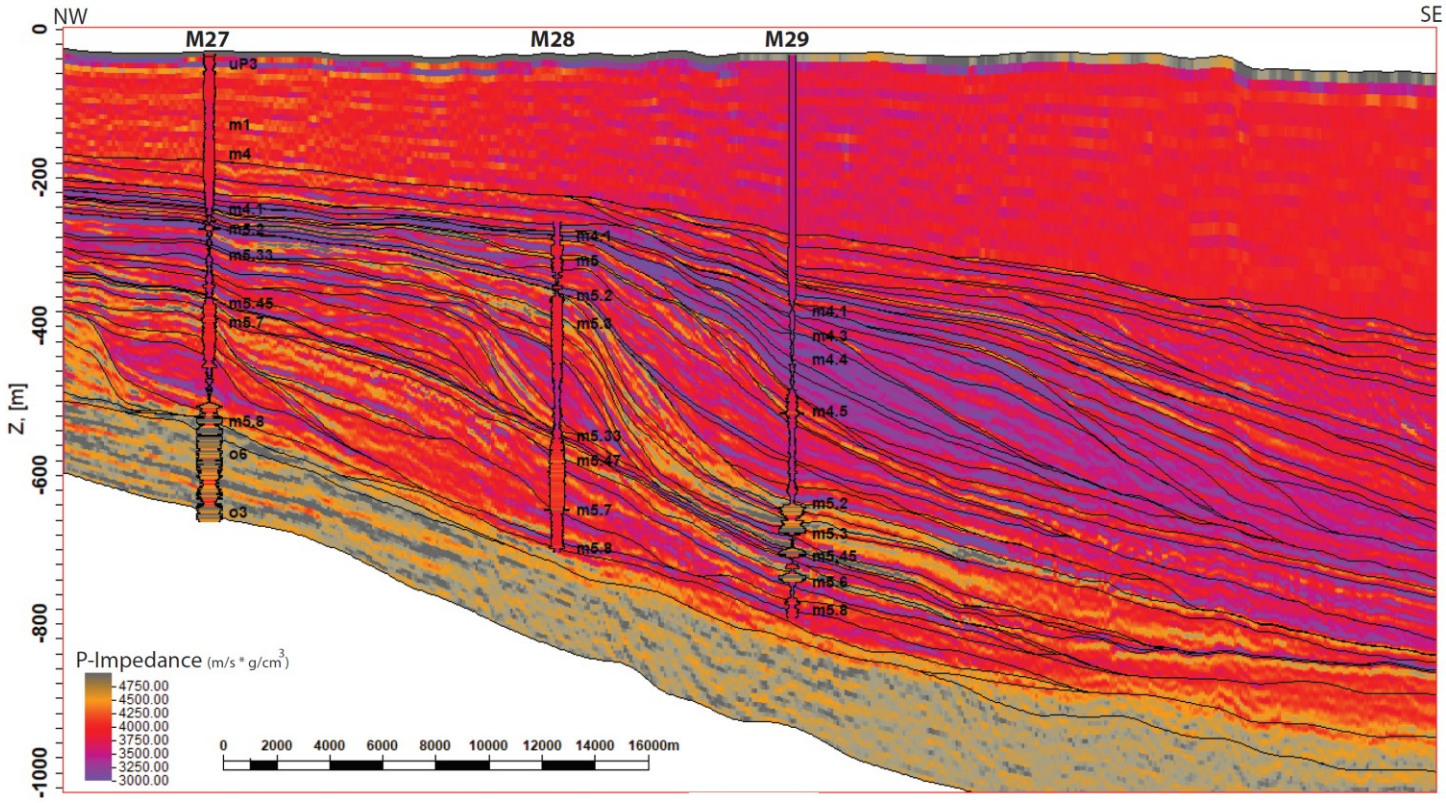

Figure 3.7: Inline 960 crossing the IODP wells showing inverted acoustic impedance obtained by post-stack model-based seismic inversion. The acoustic impedance calculated from density and Vp logs are displayed at the IODP site locations.

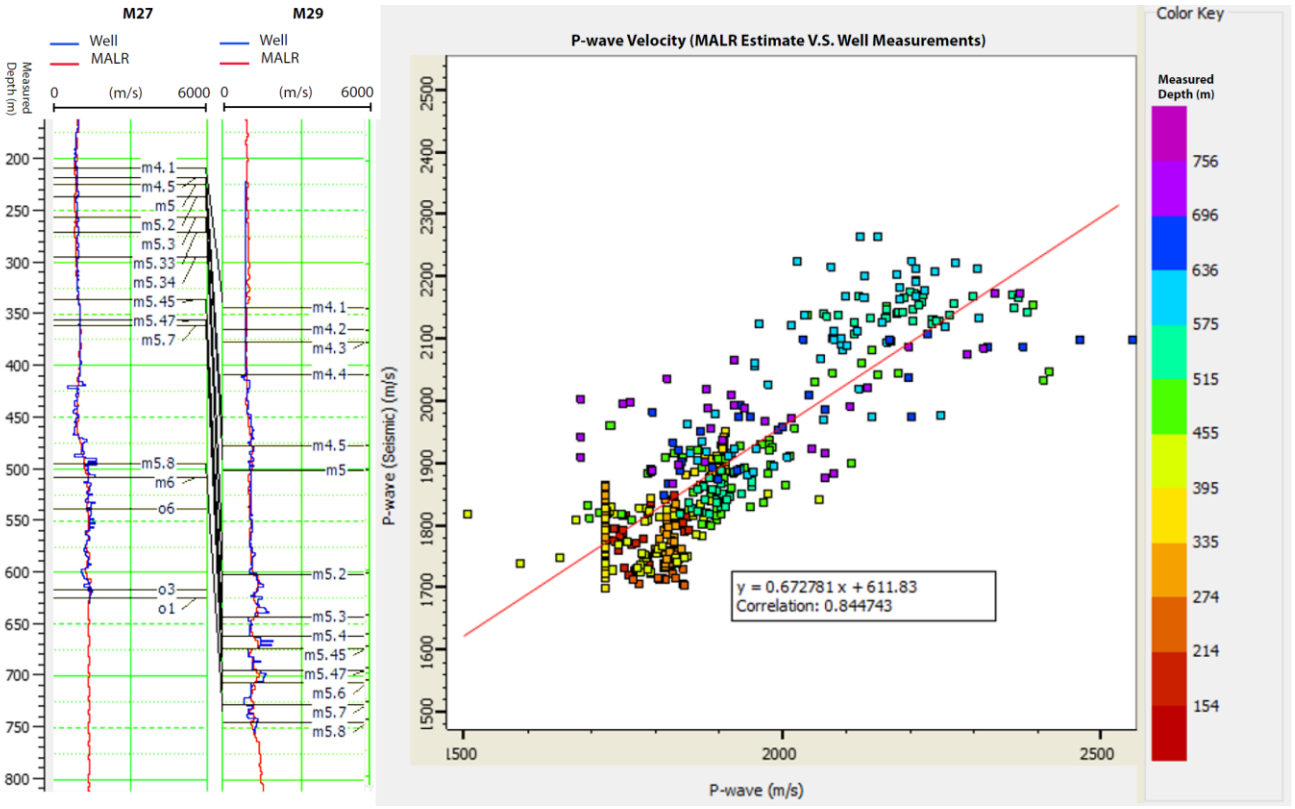

Figure 3.8: MALR for Vp at sites M27 and M29. The blue lines represent Vp from the well data, and the red lines are the predicted Vp values using the acoustic impedance volume and a group of seismic attributes as inputs to a MALR process. (right) The cross plot shows good correlation between the predicted and measured Vp.

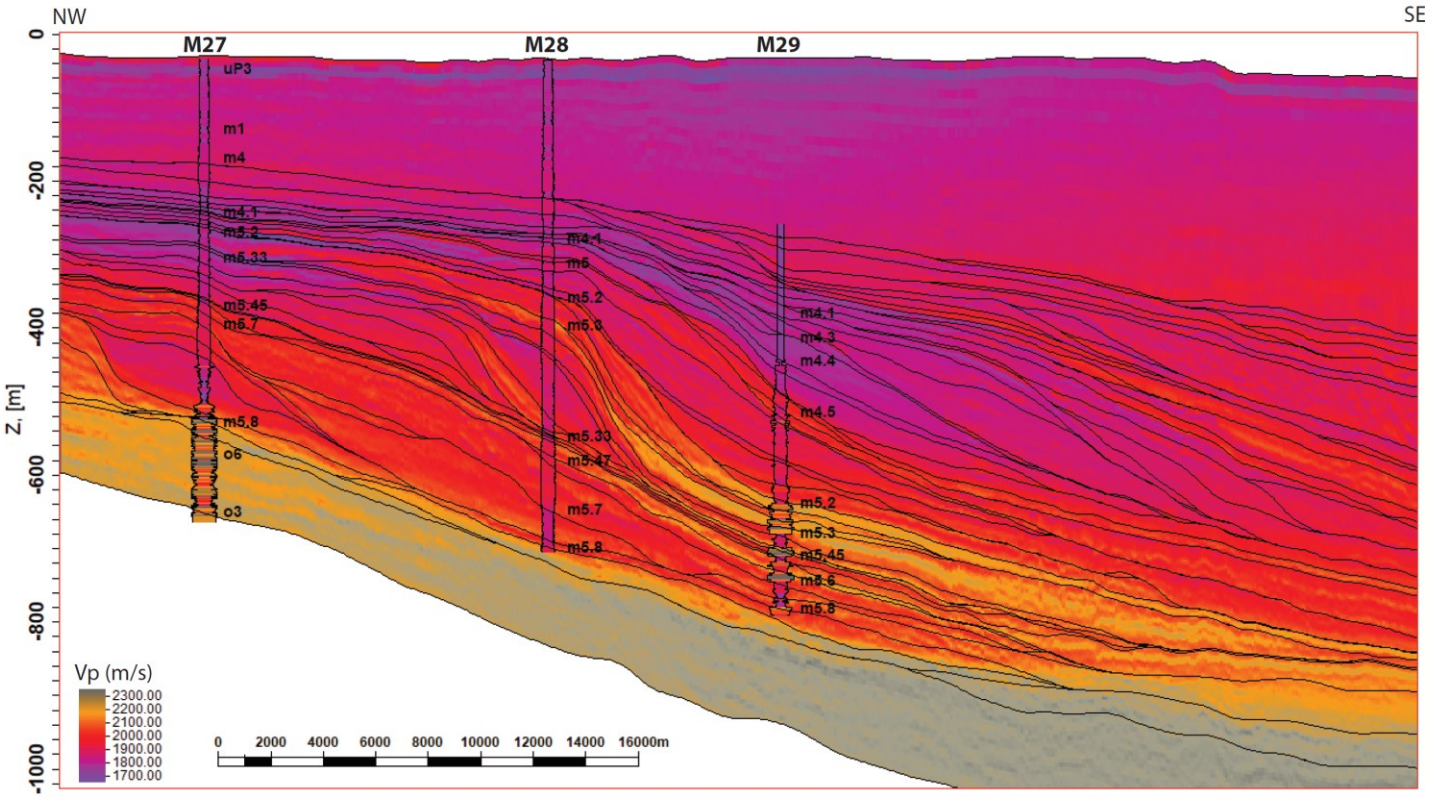

Figure 3.9: Inline 960 crossing the IODP wells showing the predicted Vp section obtained by MALR. The Vp logs are displayed at the well locations.

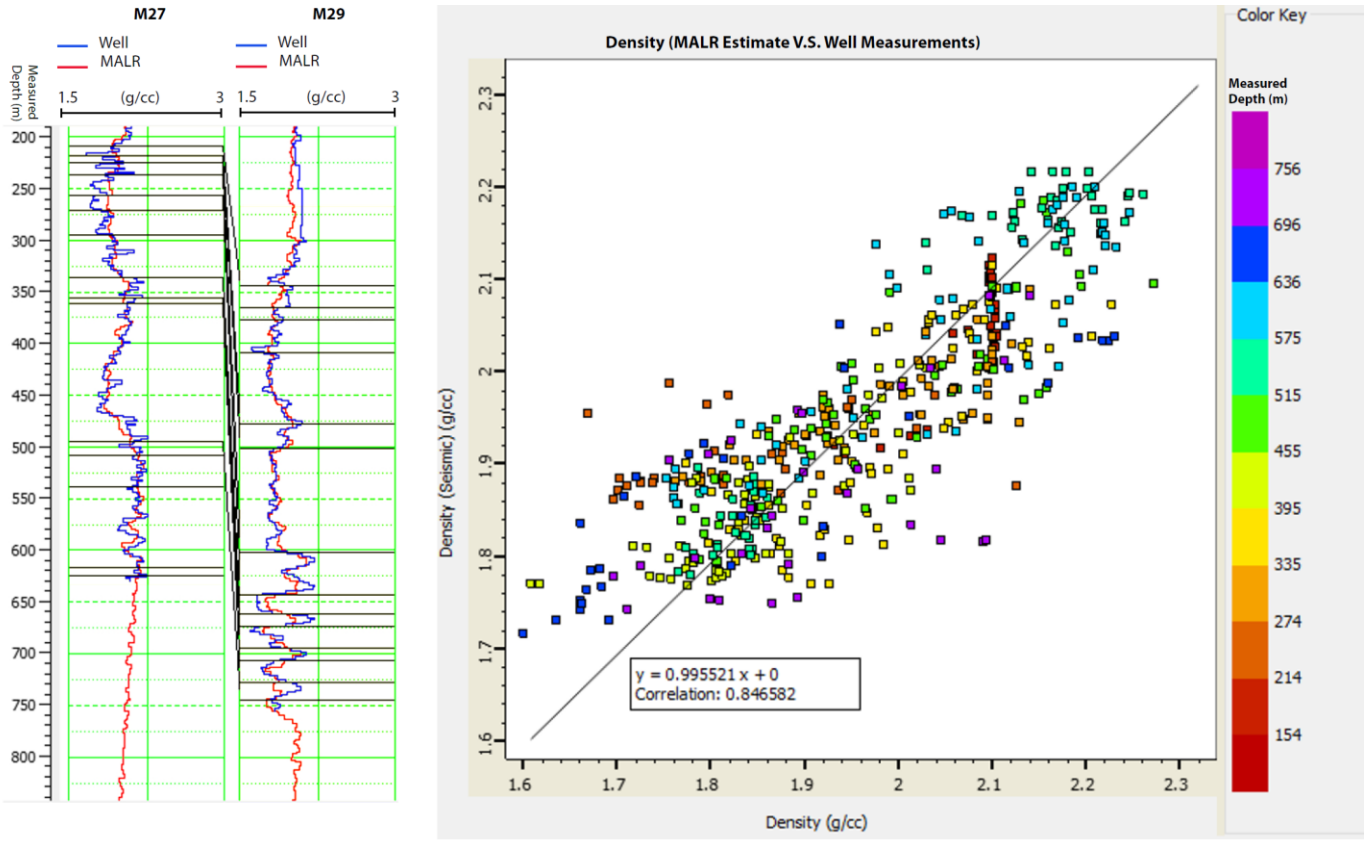

Figure 3.10: MALR for density at sites M27 and M29. (left) The blue lines represent the density measured on cores using the Multi-Sensor Core Logger (MSCL) and the red lines represents the predicted density values using the acoustic impedance volume, Vp and a group of seismic attributes as inputs to a MALR process. (right) The cross plot shows good correlation between the predicted and measured density.

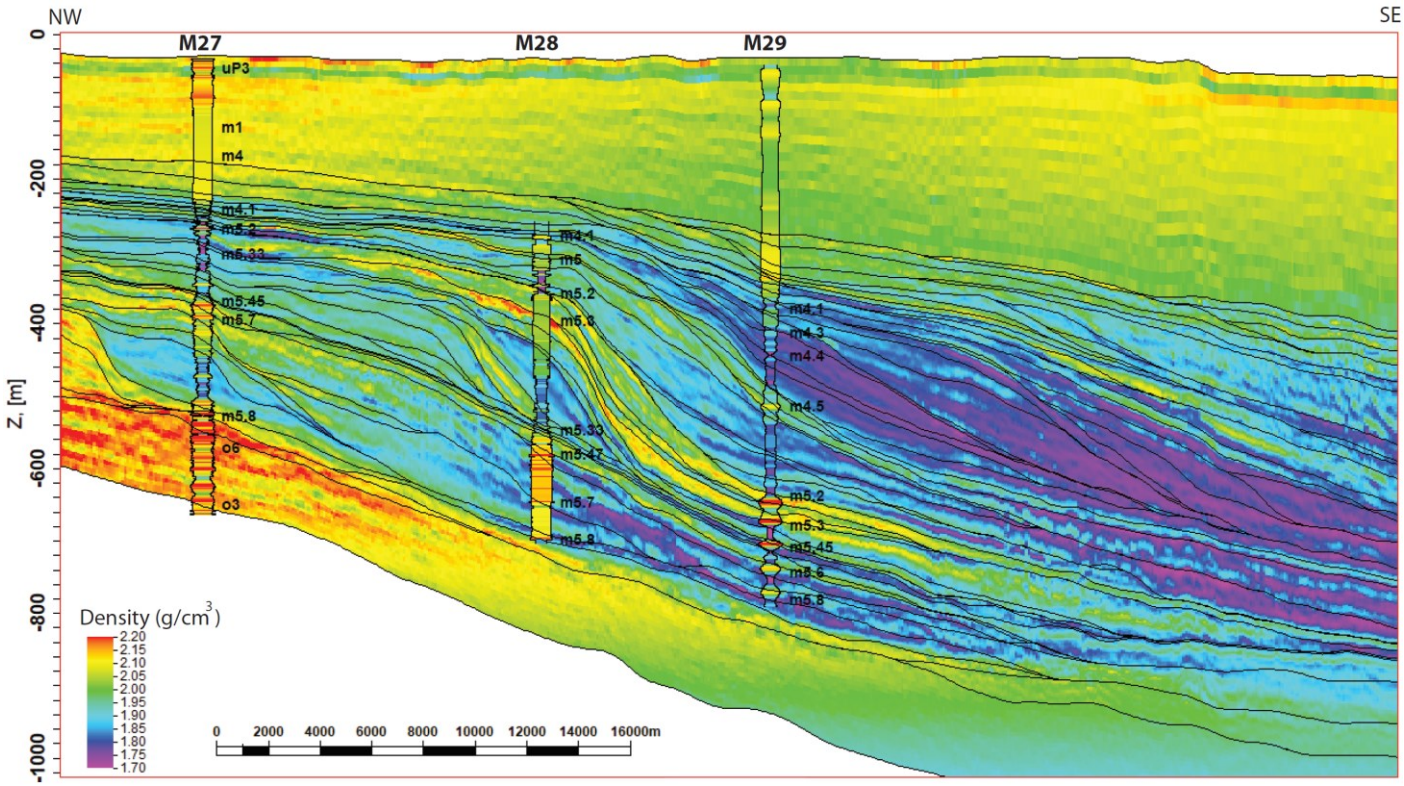

Figure 3.11: Inline 960 crossing the IODP wells showing the predicted density section obtained by MALR. The measured densities are displayed at the well locations.

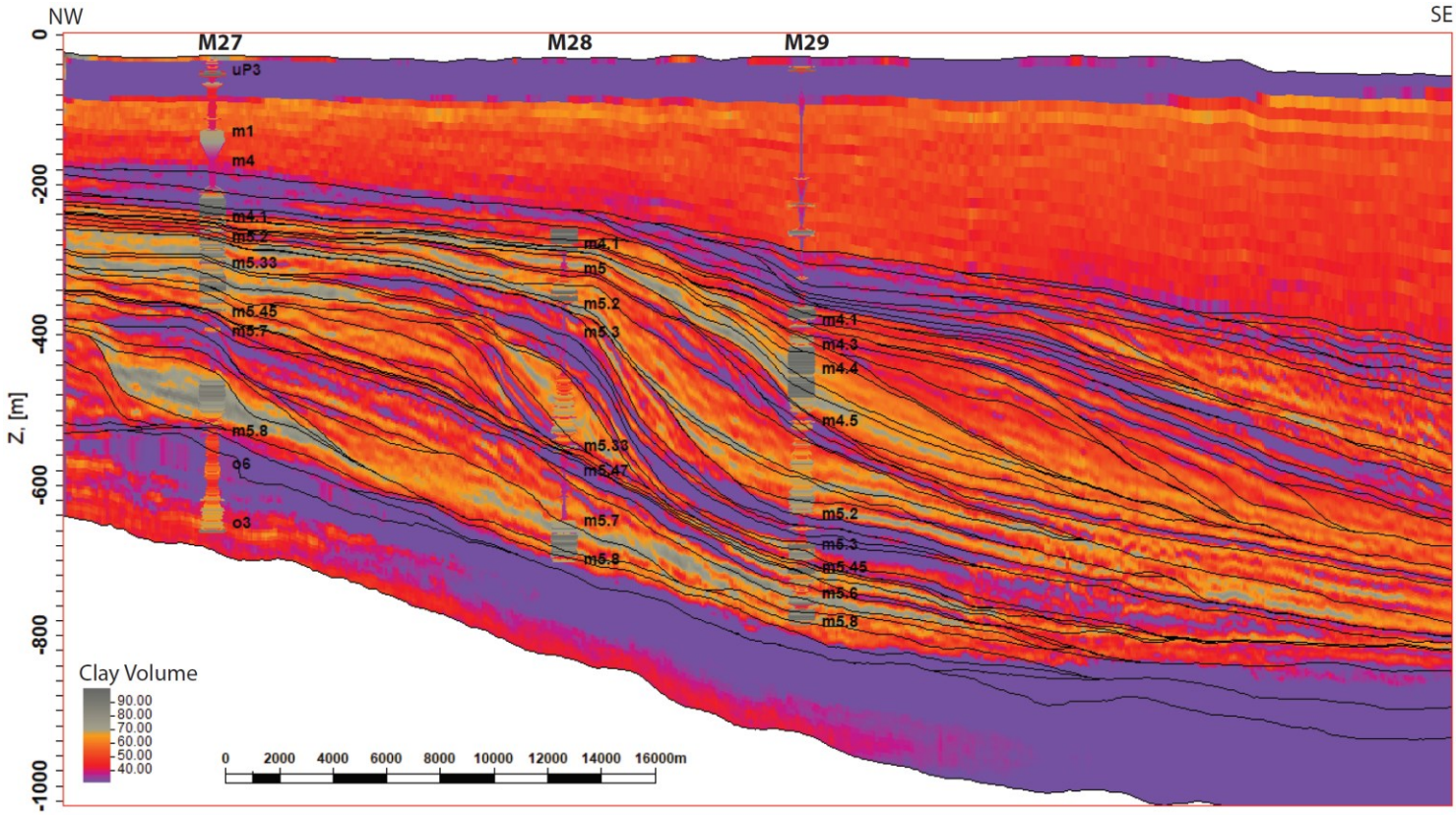

Figure 3.12: Inline 960 crossing the IODP wells showing the predicted clay volume (in percent) obtained by MALR. The clay volumes extracted from core measurements are displayed at the IODP site locations.

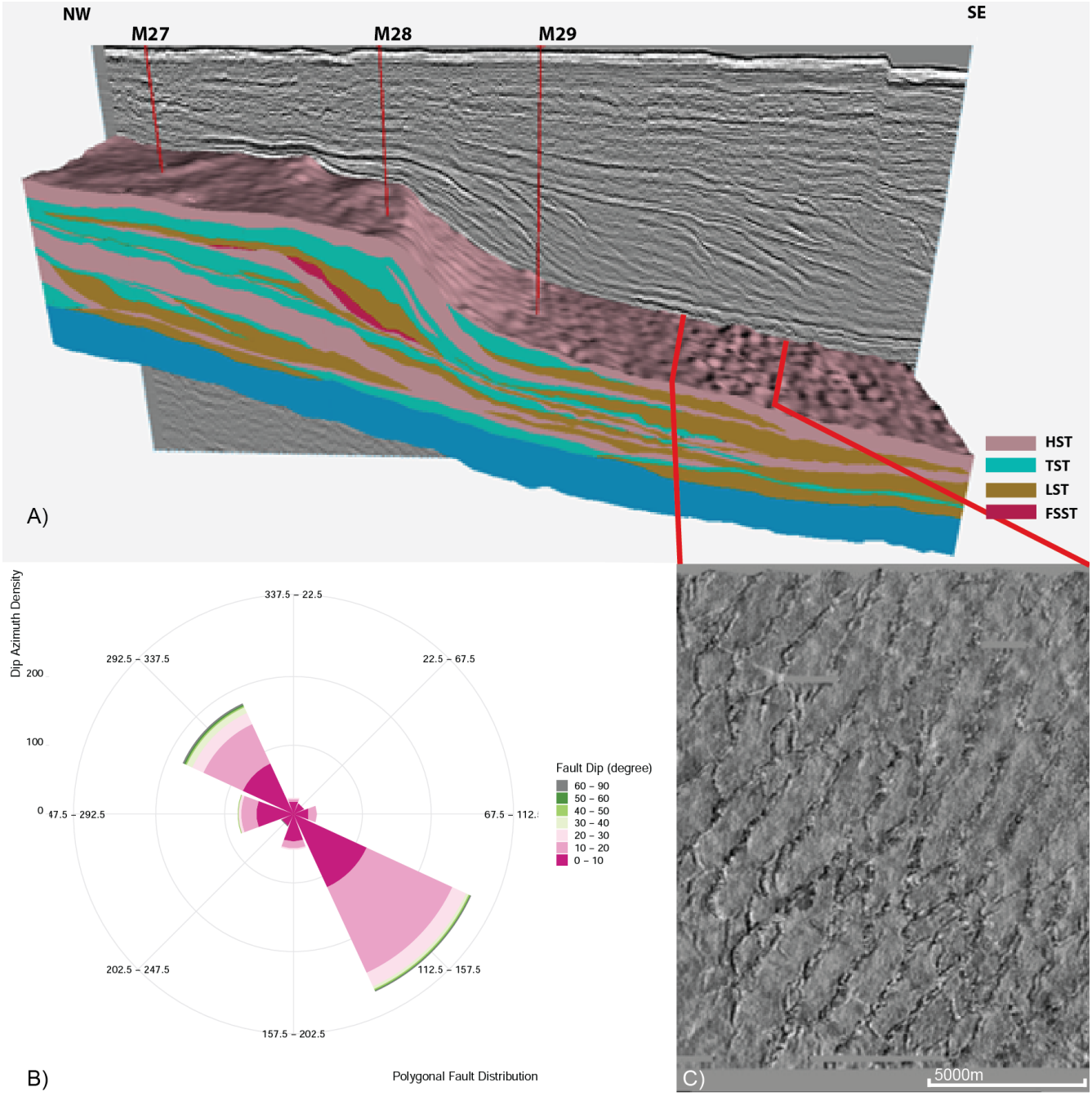

Figure 3.13: The 3D stratigraphic model of sequences from the Late-Oligocene to Mid-Miocene (Figure A), the slope and direction of fault dips for the identified polygonal faults in the clinoforms toe (Figure B), and plan-view of the polygonal faults imaged in a time slice through the 3D seismic attribute "inline dip illumination" (Figure C). The slice lies basinward of the clinoform toe. The predicted clay-volume profile shows a succession of clay-rich and sandy sediments basinward of the clinoform toe (Figure 3.12).

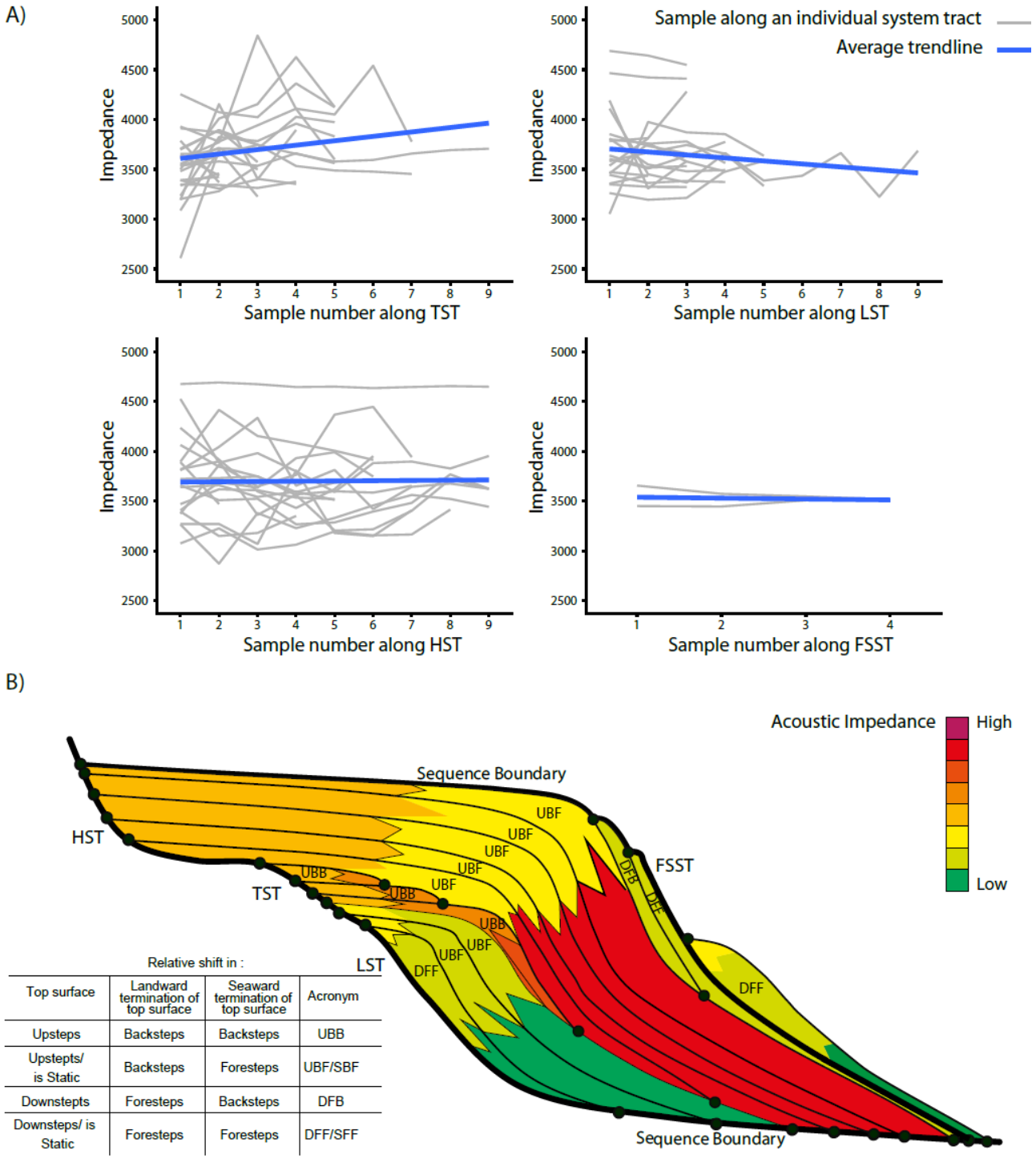

Top surface	Landward termination of top surface	Seaward termination of top surface	Acronym
Upsteps	Backsteps	Backsteps	UBB
Upstepts/ is Static	Backsteps	Foresteps	UBF/SBF
Downstepts	Foresteps	Backsteps	DFB
Downsteps/ is Static	Foresteps	Foresteps	DFF/SFF

Figure 3.14: Variation of acoustic Impedance in the dip direction (A). Generalized model of acoustic impedance distribution in a Geometrical breakdown model of the slug diagram (B). The inverted acoustic impedance was averaged within each of nine intervals to determine its general trend along each systems tract and from one systems tract to another. The gray lines in (A) represents the change in this property along each individual systems tracts. The blue line represents the overall trend in impedance. While LST and FSST show a reduction in acoustic impedance basinward, TST and HST have an increase in their impedance value.

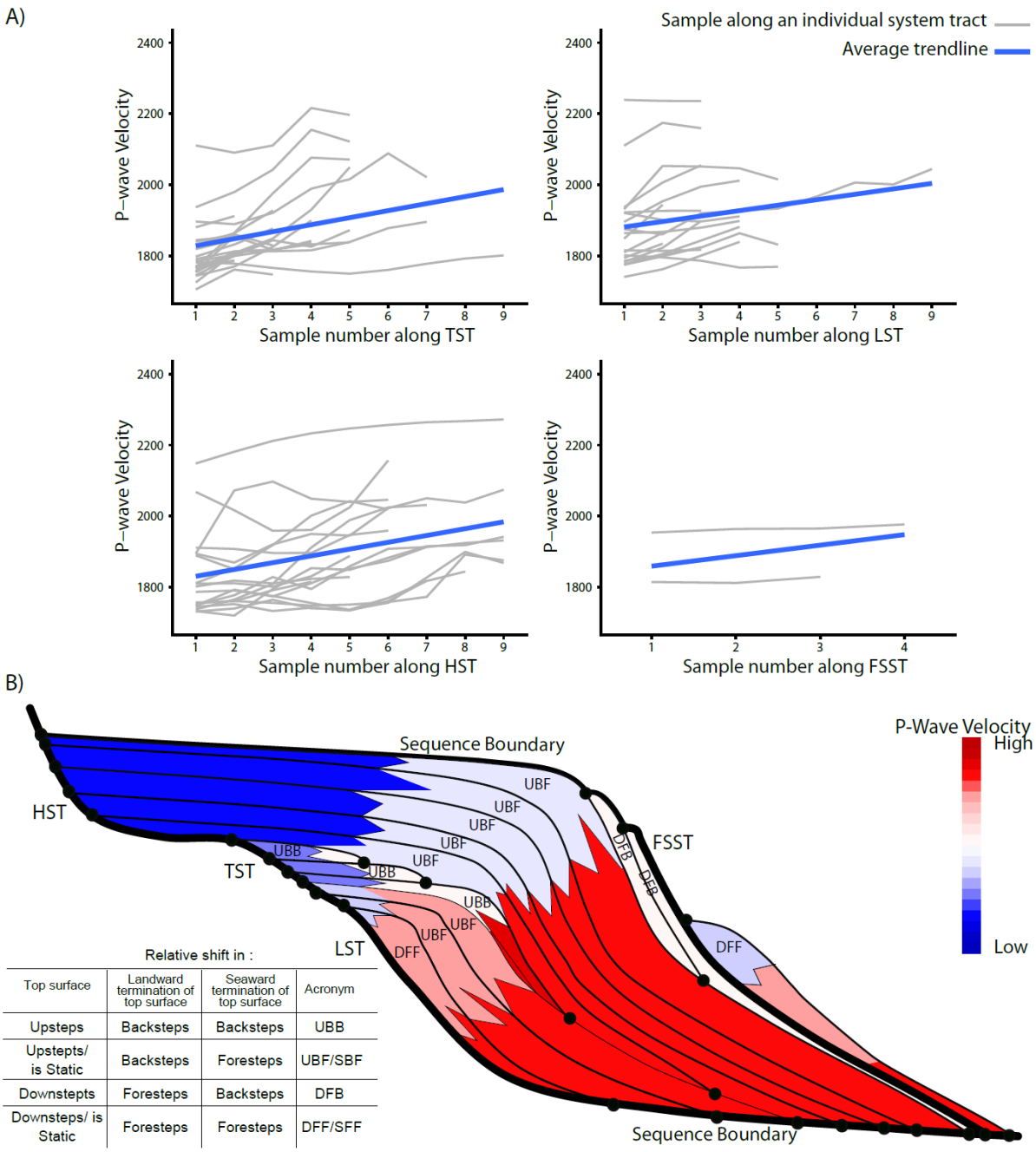

Figure 3.15: Variation of Vp in the dip direction (A). Generalized model of Vp distribution in a Geometrical breakdown model of the slug diagram (B). The predicted Vp was averaged within each of nine intervals to determine its general trend along each systems tract and from one systems tract to another. The gray lines in (A) represent the change in this property along each individual systems tracts. The blue line represents the overall trend in Vp, which shows a continuous basinward increase for all four systems tracts.

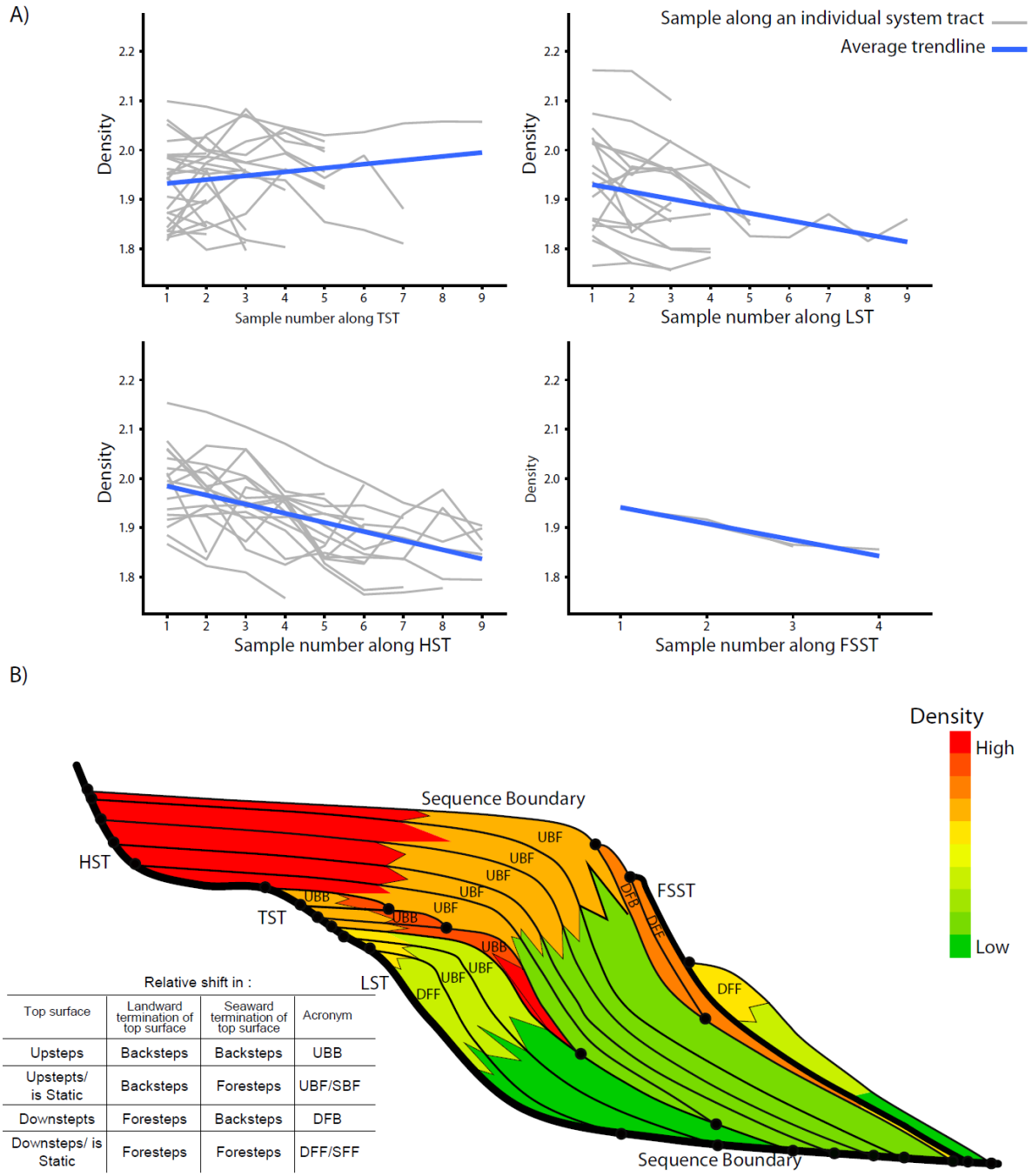

Figure 3.16: Variation of density in the dip direction (A). Generalized model of density distribution in a Geometrical breakdown model of the slug diagram (B). The predicted density was averaged within each of nine intervals to determine its general trend along each systems tract and from one systems tract to another. The gray lines in (A) represent the change in this property along each individual systems tracts. The blue line represents the overall trend in density. TST shows an increase in density basinward from topset to bottomset. However, HST, FSST, and LST all show reduction of density basinward. FSST shows a continuous decrease in the predicted density.

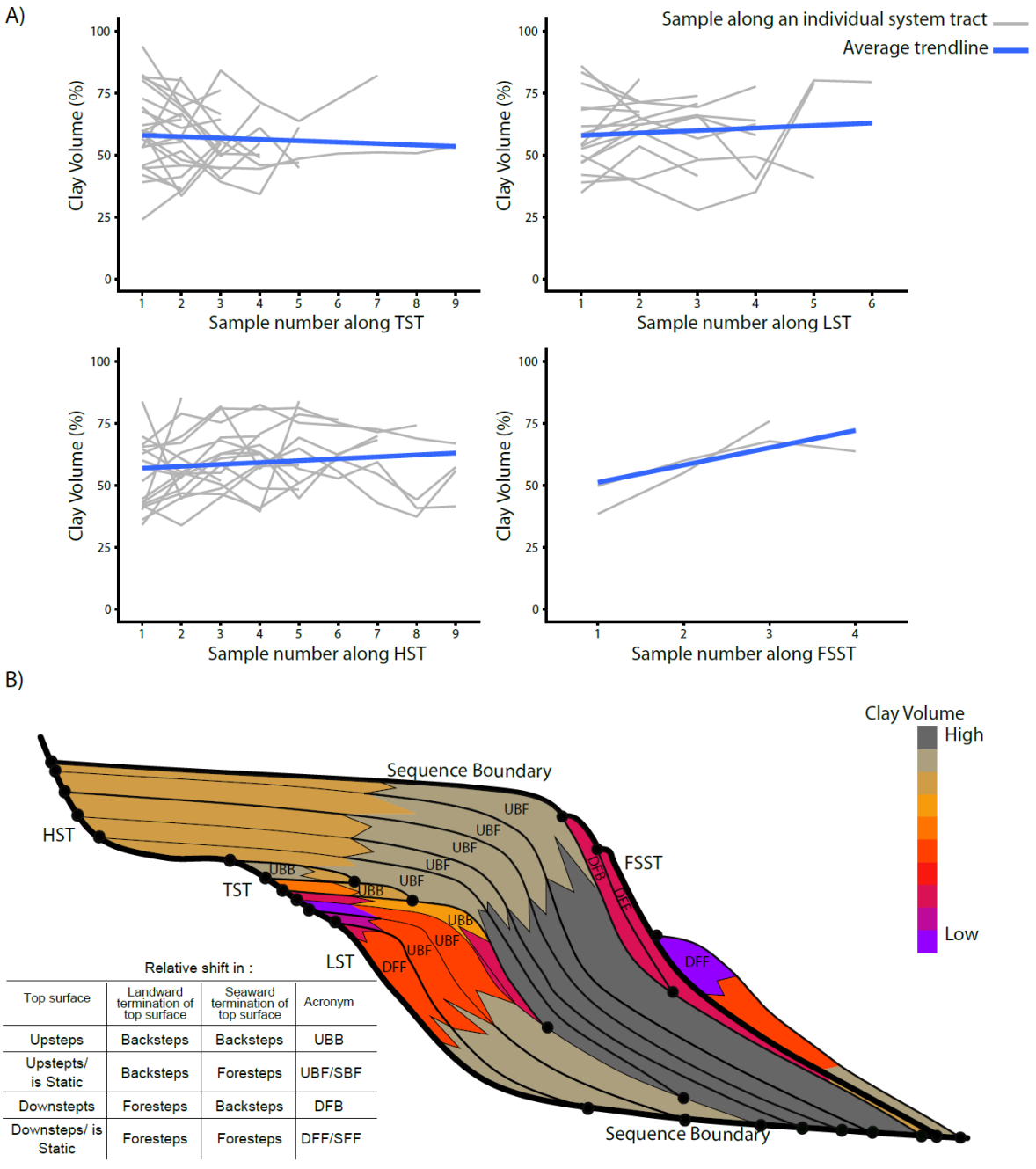

Figure 3.17: Variation of clay content in the dip direction (A). Generalized model of clay content distribution in a Geometrical breakdown model of the slug diagram (B). The predicted clay content was averaged within each of nine intervals to determine its general trend along each systems tract and from one systems tract to another. The gray lines in (A) represent the change in this property along each individual systems tracts. The blue line represents the overall trend in clay content. Of the four types of systems tracts, HST, LST, and FSST show a fining trend basinward. However, the TST shows a coarsening trend basinward.

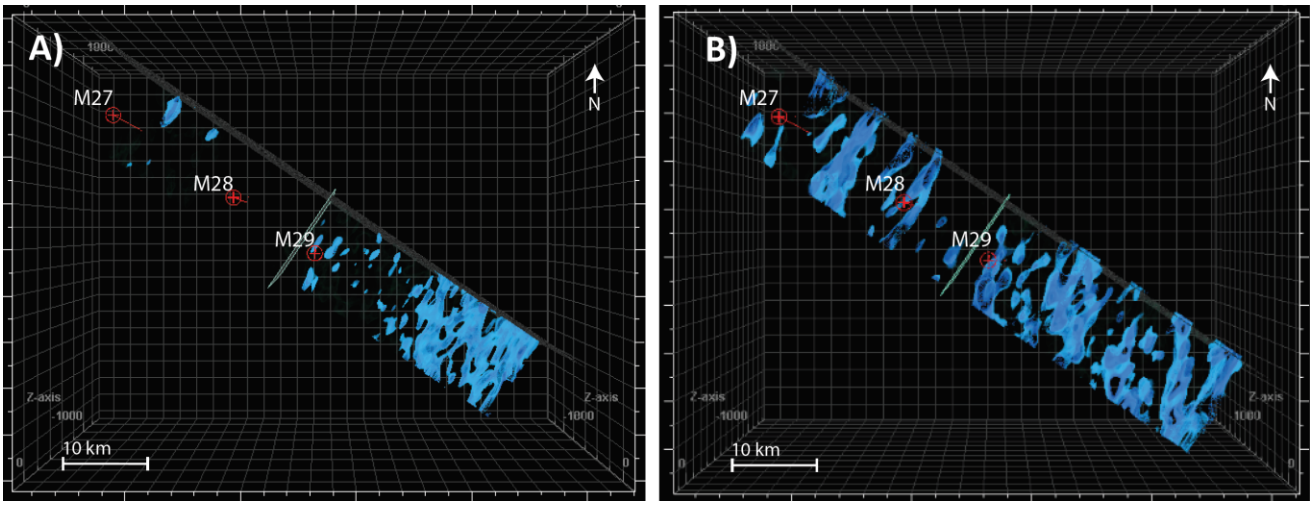

Figure 3.18: Evidence of along-strike flow identified in the seismic volume from 300 msec to 500 msec (A), and from 800 msec to 1000 msec (B) using the dip azimuth seismic attribute. These images were generated by extracting features with dip azimuth value of 220-225 degrees. Besides being elongated in the NE-SW direction, the features also dip toward the SW.

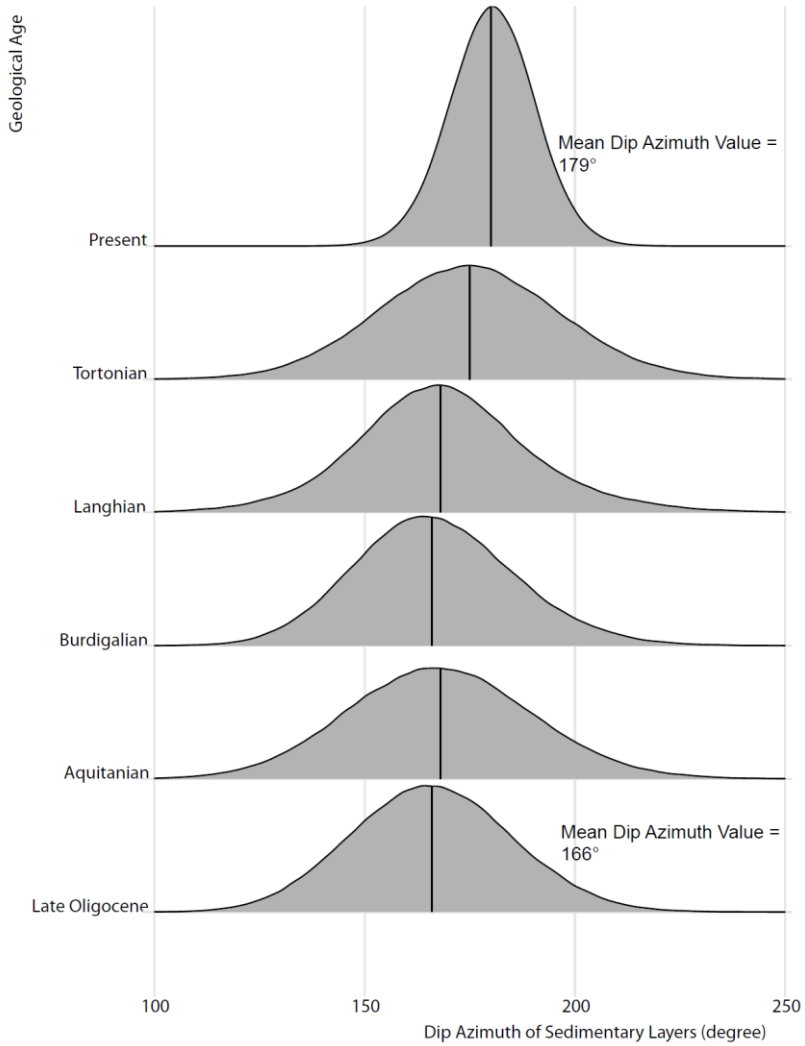

Figure 3.19: Dip azimuth distribution of the sediments deposited in Oligocene, Miocene, and Late Miocene to Pliocene. General dip azimuth for Oligocene and early Miocene deposits is 166°. By late Miocene-Pliocene, the mean dip azimuth rotates southward to 179°.

Site M27					
Sequence	**Depth (mcd)**	**TWT (ms below sea floor)**	**Int. Vel (m/s)**	**TWT-Modified (ms)**	**Int. Vel -Modified (m/s)**
uP3	13.57	15		61.1	1505
uP1	21.42	31	981.3	70.1	1744.44
m1	96	161	1147.4	155.59	1744.77
m3	111	182	1428.6	172.78	1745.20
m4	135	211	1655.2	200.29	1744.82
m4.1	209	288	1922.1	285.32	1740.56
m4.5	218.39	296	2347.5	296.16	1732.47
m5	225.45	298	7060.0	303.34	1966.57
m5.2	236.15	320	972.7	315.28	1792.29
m5.3	256.19	336	2505.0	336.96	1848.71
m5.33	271.23	382	653.9	353.53	1815.33
m5.45	336.06	432	2593.2	428.48	1729.95
m5.47	355.53	446	2781.4	445.35	2308.24
m5.7	361.28	458	958.3	450.38	2286.28
m5.8	494.87	591	2008.9	596.09	1833.64
m6	509	607	1766.3	610.4	1974.84
o6	538.68			637.06	2226.56
o3	617			706.29	2262.60
o1	625.83			714.08	2267.01

Table 3.1: Seismic well tie analysis at the site M27. From left to right, the columns are the stratigraphic sequence name, the measured depth for the sequence(based on core and log observations) the two-way-time from Miller et al., 2013 (Miller, Browning, et al., 2013), the interval velocity between two adjacent sequence based on the previous two-way-time measurements, the modified two-way-time based the quantitative seismic well tie using the wireline sonic log, the predicted interval velocity for two adjacent sequences using the new seismic well tie. The interval velocity values below the speed of sound in seawater (~1500 m/s) are most likely erroneous.

Site M28					
Sequence	**Depth (mcd)**	**TWT (ms below sea floor)**	**Int. Vel (m/s)**	**TWT-Modified (ms)**	**Int. Vel -Modified (m/s)**
m4.1	244.16	333	1701.5	330.1	1718.8
m4.5	254.23	344	1830.9	342.75	1592.1
m5	276.81	366	2052.7	370.5	1627.4
m5.2	323.23	423	1628.8	419.68	1887.8
m5.3	361	458	2158.3	456.89	2030.1
m5.34	479	612	1532.5	571.72	2055.2
m5.45	533.59	633	5199.0	622.69	2142.0
m5.47	545.5	646	1832.3	633.52	2199.4
m5.6	567.5	666	2200.0	655.24	2025.8
m5.7	611.6	710	2004.5	698.71	2029.0
m5.8	662.98	772	1657.4	750.37	1989.2

Table 3.2: Seismic well tie analysis at the site M27. From left to right, the columns are the stratigraphic sequence name, the measured depth for the sequence(based on core and log observations) the two-way-time from Miller et al., 2013 (Miller, Browning, et al., 2013), the interval velocity between two adjacent sequence based on the previous two-way-time measurements, the modified two-way-time based the quantitative seismic well tie using the synthetic sonic log, the predicted interval velocity for two adjacent sequences using the new seismic well tie.

Site M29					
Sequence	**Depth (mcd)**	**TWT (ms below sea floor)**	**Int. Vel (m/s)**	**TWT-Modified (ms)**	**Int. Vel -Modified (m/s)**
m4.1	343.81	437		432.57	1774.2
m4.2	364.86	460	1830.4	453.71	1991.5
m4.3	377.15	471	2234.5	466.84	1872.0
m4.4	409.27	510	1647.2	505.97	1641.7
m4.5	478.61	568	2391.0	591.43	1622.7
m5	502.01	597	1613.8	618.01	1760.7
m5.2	602.25	710	1774.2	712.14	2129.8
m5.3	643.19	754	1860.9	746.21	2403.3
m5.4	662.37	769	2557.3	764.69	2075.8
m5.45	673.71	768	NaN	773.43	2595.0
m5.47	695	798	1419.3	797.11	1853.0
m5.6	707.56	825	930.4	806.83	2450.6
m5.7	728.56	849	1750.0	827.75	2007.6
m5.8	746	860	3170.9	846.32	1878.3

Table 3.3: Seismic well tie analysis at the site M27. From left to right, the columns are the stratigraphic sequence name, the measured depth for the sequence(based on core and log observations) the two-way-time from miller et al (Miller, Browning, et al., 2013), the interval velocity between two adjacent sequence based on the previous two-way-time measurements, the modified two-way-time based the quantitative seismic well tie using the wireline sonic log, the predicted interval velocity for two adjacent sequences using the new seismic well tie.

3.8 References:

Ando, H., Oyama, M., & Nanayama, F. (2014). Data report: grain size distribution of Miocene successions, IODP Expedition 313 Sites M0027, M0028, and M0029, New Jersey shallow shelf. *Proceedings of the Integrated Ocean Drilling Program*, *313*. https://doi.org/10.2204/iodp.proc.313.201.2014

Avseth, P., Mukerji, T., Mavko, G., & Dvorkin, J. (2010). Rock-physics diagnostics of depositional texture, diagenetic alterations, and reservoir heterogeneity in high-porosity siliciclastic sediments and rocks - A review of selected models and suggested work flows. *Geophysics*, *75*(5). https://doi.org/10.1190/1.3483770

Beardsley, R. C., & Boicourt, W. C. (1981). On Estuarine and Atlantic Bight. *Evolution of Physical Oceanography*, 198–233. https://ocw.mit.edu/resources/res-12-000-evolution-of-physical-oceanography-spring-2007/part-1/wunsch_chapter7.pdf%5Cnhttp://ocw.mit.edu/resources/res-12-000-evolution-of-physical-oceanography-spring-2007/index.htm

Boyd, R., Ruming, K., Goodwin, I., Sandstrom, M., & Schröder-Adams, C. (2008). Highstand transport of coastal sand to the deep ocean: A case study from Fraser Island, southeast Australia. *Geology*, *36*(1), 15–18. https://doi.org/10.1130/G24211A.1

Browning, J. V., Miller, K. G., Sugarman, P. J., Barron, J. A., McCarthy, F. M. G. G., Kulhanek, D. K., Katz, M. E., & Feigenson, M. D. (2013). Chronology of Eocene–Miocene sequences on the New Jersey shallow shelf: Implications for regional, interregional, and global correlations. *Geosphere*, *9*(6), 1434–1456. https://doi.org/10.1130/GES00853.1

Browning, J. V., Miller, K. G., Sugarman, P. J., Kominz, M. A., Mclaughlin, P. P., Kulpecz, A. A., & Feigenson, M. D. (2008). 100 Myr record of sequences, sedimentary facies and sea level change from Ocean Drilling Program onshore coreholes, US Mid-Atlantic coastal plain. *Basin Research*, *20*(2), 227–248. https://doi.org/10.1111/j.1365-2117.2008.00360.x

Burbank, D., & Anderson, R. (2011). *Tectonic Geomorphology*. wiley.

Burgess, P. M., Lammers, H., van Oosterhout, C., & Granjeon, D. (2006). Multivariate sequence stratigraphy: Tackling complexity and uncertainty with stratigraphic forward modeling, multiple scenarios, and conditional frequency maps. *AAPG Bulletin*, *90*(12), 1883–1901. https://doi.org/10.1306/06260605081

Butman, B., Noble, M., & Folger, D. W. (1979). Long-term observations of bottom current and bottom sediment movement on the mid-Atlantic continental shelf. *Journal of Geophysical Research: Oceans*, *84*(C3), 1187–1205. https://doi.org/10.1029/JC084iC03p01187

Cacchione, D. A., Drake, D. E., Losada, M. A., & Medina, R. (1990). Bottom-boundary-layer measurements on the continental shelf off the Ebro River, Spain. *Marine Geology*, *95*(3–4), 179–192. https://doi.org/10.1016/0025-3227(90)90115-Z

Carter, R. M., Fulthorpe, C. S., & Lu, H. (2004). Canterbury drifts at Ocean Drilling Program site 1119, New Zealand: Climatic modulation of southwest Pacific intermediate water flows since 3.9 Ma. *Geology*, *32*(11), 1005–1008. https://doi.org/10.1130/G20783.1

Cathro, D. L., Austin, J. A., & Moss, G. D. (2003). Progradation along a deeply submerged Oligocene-Miocene heterozoan carbonate shelf: How sensitive are clinoforms to sea level variations? *American Association of Petroleum Geologists Bulletin*, *87*(10), 1547–1574. https://doi.org/10.1306/05210300177

Catuneanu, O. (2017). Sequence Stratigraphy: Guidelines for a Standard Methodology. In *Advances in Sequence Stratigraphy* (1st ed., Vol. 2, Issue September). Elsevier Inc.

https://doi.org/10.1016/bs.sats.2017.07.003
Catuneanu, O., Abreu, V., Bhattacharya, J. P., Blum, M. D., Dalrymple, R. W., Eriksson, P. G., Fielding, C. R., Fisher, W. L., Galloway, W. E., Gibling, M., Giles, K. A., Holbrook, J. M., Jordan, R., Kendall, ; Christopher G. St. C., Macurda, B., Martinsen, O. J., Miall, A., Neal, J. E., Nummedal, D., … Winker, C. (2009). Towards the standardization of sequence stratigraphy. *Earth-Science Reviews*, *92*(1–2), 1–33. https://doi.org/10.1016/j.earscirev.2008.10.003
Chopra, S., Castagna, J. P., & Xu, Y. (2009). When Thin Is In – Relative Acoustic Impedance Helps. *Frontiers + Innovation – CSPG CSEG CWLS Convention*, 705–708.
Colombo, D. (2005). Benefits of wide-offset seismic for commercial exploration targets. *Leading Edge*.
Degirmency, T. (2014). Upper Middle to Upper Miocene Seismic Sequences, New Jersey Middle to Outer Continental Shelf. *MSc Dissertation*.
Driscoll, N. W., & Hogg, J. R. (1995). Stratigraphic response to basin formation: Jeanne d'Arc Basin, offshore Newfoundland. *Geological Society Special Publication*, *80*(80), 145–163. https://doi.org/10.1144/GSL.SP.1995.080.01.07
Driscoll, N. W., & Karner, G. D. (1999). Three-dimensional quantitative modeling of clinoform development. *Marine Geology*, *154*(1–4), 383–398. https://doi.org/10.1016/S0025-3227(98)00125-X
Fulthorpe, C. S., Austin, J. A., & Mountain, G. S. (1999). Buried fluvial channels off New Jersey: Did sea-level lowstands expose the entire shelf during the Miocene? *Geology*, *27*(3), 203–206. https://doi.org/10.1130/0091-7613(1999)027<0203:BFCONJ>2.3.CO;2
Gallegos, G. (2017). Lower Miocene (ca . 20-18 Ma) New Jersey Sequence Stratigraphy : Architecture and Onshore-Offshore Correlations. *MSc Dissertation*.
Gong, D., Kohut, J., & Glenn, S. (2008). Seasonal Climatology of Wind-Driven Circulation on the NJ Shelf. *AGU Fall Meeting Abstracts*.
Grow, J. A., & Sheridan, R. E. (1988). U.S. Atlantic Continental Margin; A typical Atlantic-type or passive continental margin. In Robert E Sheridan & J. A. Grow (Eds.), *The Atlantic Continental Margin*. Geological Society of America. https://doi.org/10.1130/DNAG-GNA-I2.1
Helland-Hansen, W., & Hampson, G. J. (2009). Trajectory analysis: Concepts and applications. *Basin Research*, *21*(5), 454–483. https://doi.org/10.1111/j.1365-2117.2009.00425.x
Hendra, W. (2010). Lithofacies and Depositional Environment Spanning the Cretaceous-Paleogene Boundary on the New Jersey Coastal Plain. *MSc Dissertation*, *5*(1976), 265–288.
Hodgson, D. M., Browning, J. V., Miller, K. G., Hesselbo, S. P., Poyatos-Moré, M., Mountain, G. S., & Proust, J. N. (2017). Sedimentology, stratigraphic context, and implications of Miocene intrashelf bottomset deposits, offshore New Jersey. *Geosphere*, *14*(1), 95–114. https://doi.org/10.1130/GES01530.1
Inwood, J., Lofi, J., Davies, S., Basile, C., Bjerum, C., Mountain, G. S., Proust, J. N., Otsuka, H., & Valppu, H. (2013). Statistical classifi cation of log response as an indicator of facies variation during changes in sea level: Integrated Ocean Drilling Program Expedition 313. *Geosphere*, *9*(4), 1025–1043. https://doi.org/10.1130/GES00913.1
Katz, M. E., Browning, J. V., Miller, K. G., Monteverde, D. H., Mountain, G. S., & Williams, R. H. (2013). Paleobathymetry and sequence stratigraphic interpretations from benthic foraminifera: Insights on New Jersey shelf architecture, IODP Expedition 313. *Geosphere*, *9*(6), 1488–1513. https://doi.org/10.1130/GES00872.1

Kotthoff, U., Greenwood, D. R., McCarthy, F. M. G. G., Müller-Navarra, K., Prader, S., & Hesselbo, S. P. (2014). Late Eocene to middle Miocene (33 to 13 million years ago) vegetation and climate development on the North American Atlantic Coastal Plain (IODP Expedition 313, Site M0027). *Climate of the Past*, *10*(4), 1523–1539. https://doi.org/10.5194/cp-10-1523-2014

Liu, L. (2008). The case for dynamic subsidence of the U.S. east coast since the Eocene. *Geophysical Research Letters*, *35*(8), 1–6. https://doi.org/10.1029/2008GL033511

Liu, L. (2015). The ups and downs of North America: Evaluating the role of mantle dynamic topography since the Mesozoic. *Review of Geophysics*, *45*(2), 1–24. https://doi.org/10.1029/2006RG000197.1.INTRODUCTION

Lofi, J., Inwood, J., Proust, J. N., Monteverde, D. H., Loggia, D., Basile, C., Otsuka, H., Hayashi, T., Stadler, S., Mottl, M. J., Fehr, A., & Pezard, P. A. (2013). Fresh-water and salt-water distribution in passive margin sediments: Insights from integrated ocean drilling program expedition 313 on the New Jersey Margin. *Geosphere*, *9*(4), 1009–1024. https://doi.org/10.1130/GES00855.1

Lu, H., Fulthorpe, C. S., & Mann, P. (2003). Three-dimensional architecture of shelf-building sediment drifts in the offshore Canterbury Basin, New Zealand. *Marine Geology*, *193*(1–2), 19–47. https://doi.org/10.1016/S0025-3227(02)00612-6

Lu, H., Fulthorpe, C. S., Mann, P., & Kominz, M. A. (2005). Miocene-recent tectonic and climatic controls on sediment supply and sequence stratigraphy: Canterbury basin, New Zealand. *Basin Research*, *17*(2), 311–328. https://doi.org/10.1111/j.1365-2117.2005.00266.x

Lyne, V. D., Butman, B., & Grant, W. D. (1990). Sediment movement along the U.S. east coast continental shelf-I. Estimates of bottom stress using the Grant-Madsen model and near-bottom wave and current measurements. *Continental Shelf Research*, *10*(5), 397–428. http://pubs.er.usgs.gov/publication/70016373

Martinsen, O. J., & Helland-Hansen, W. (1995). Strike variability of clastic depositional systems: does it matter for sequence-stratigraphic analysis? *Geology*, *23*(5), 439–442. https://doi.org/10.1130/0091-7613(1995)023<0439:SVOCDS>2.3.CO;2

McCarthy, F. M. G. G., Katz, M. E., Kotthoff, U., Browning, J. V., Miller, K. G., Zanatta, R., Williams, R. H., Drljepan, M., Hesselbo, S. P., Bjerum, C., & Mountain, G. S. (2013). Sea-level control of new jersey margin architecture: Palynological evidence from integrated ocean drilling program expedition 313. *Geosphere*, *9*(6), 1457–1487. https://doi.org/10.1130/GES00853.1

Miller, K. G., Browning, J. V., Mountain, G. S., Bassetti, M. A., Monteverde, D. H., Katz, M. E., Inwood, J., Lofi, J., & Proust, J. N. (2013). Sequence boundaries are impedance contrasts: Core-seismic-log integration of Oligocene-Miocene sequences, New Jersey shallow shelf. *Geosphere*, *9*(5), 1257–1285. https://doi.org/10.1130/GES00858.1

Miller, K. G., Browning, J. V., Mountain, G. S., Sheridan, R. E., Sugarman, P. J., Glenn, S., & Christensen, B. A. (2014). Chapter 3 History of continental shelf and slope sedimentation on the US middle Atlantic margin. *Geological Society, London, Memoirs*, *41*(1), 21–34. https://doi.org/10.1144/M41.3

Miller, K. G., Kominz, M. A., Browning, J. V., Wright, J. D., Mountain, G. S., Katz, M. E., Sugarman, P. J., Cramer, B. S., Christie-Blick, N., & Pekar, S. F. (2005). The phanerozoic record of global sea-level change. *Science*, *310*(5752), 1293–1298. https://doi.org/10.1126/science.1116412

Miller, K. G., & Mountain, G. S. (1994). Global Sea-Level Change and the New Jersey Margin. *Proceedings of the Ocean Drilling Program, Initial Reports*, *150*, 11–20.

Monteverde, D. H., Miller, K. G., & Mountain, G. S. (2000). Correlation of offshore seismic profiles with onshore New Jersey Miocene sediments. *Sedimentary Geology*, *134*(1–2), 111–127. https://doi.org/10.1016/S0037-0738(00)00016-6

Mountain, G. S., Burger, R. L., Delius, H., Fulthorpe, C. S., Austin, J. A., Goldberg, D. S., Steckler, M. S., Mchugh, C. M., Miller, K. G., Monteverde, D. H., Orange, D. L., & Pratson, L. F. (2007). The long-term stratigraphic record on continental margins. *Continental Margin Sedimentation: From Sediment Transport to Sequence Stratigraphy*, 381–458. https://doi.org/10.1002/9781444304398.ch8

Mountain, G. S., Miller, K. G., Christie-blick, N., Peter, J., & Fulthorpe, C. S. (2006). Shallow-Water Drilling of the New Jersey Continental Shelf: Determining the Links Between Sediment Architecture and Sea-Level Change. *Research Proposal*.

Mountain, G. S., Proust, J.-N., & McInroy, D. (2009). *Shallow-water drilling of the New Jersey continental shelf: global sea level and architecture of passive margin sediments*. *313*. https://doi.org/10.2204/iodp.sp.313.2009

Mountain, G. S., Proust, J. N. J.-N., & Expedition 313 Science Party. (2010). The New Jersey margin scientific drilling project (IODP expedition 313): Untangling the record of global and local sea-level changes. *Scientific Drilling*, *10*(10), 26–34. https://doi.org/10.2204/iodp.sd.10.03.2010

Neal, J. E., & Abreu, V. (2009). Sequence stratigraphy hierarchy and the accommodation succession method. *Geology*, *37*(9), 779–782. https://doi.org/10.1130/G25722A.1

Nittrouer, C. A., & Wright, L. D. (1994). Transport of particles across continental shelves. *Reviews of Geophysics*, *32*(1), 85–113. https://doi.org/10.1029/93RG02603

Pellaton, C., & Gorin, G. E. (2005). The Miocene New Jersey Passive Margin as a Model for the Distribution of Sedimentary Organic Matter in Siliciclastic Deposits. *Journal of Sedimentary Research*, *75*(6), 1011–1027. https://doi.org/10.2110/jsr.2005.076

Pirmez, C., Pratson, L. F., & Steckler, M. S. (1998). Clinoform development by advection-diffusion of suspended sediment: Modeling and comparison to natural systems. *Journal of Geophysical Research*, *103*(B10), 24141. https://doi.org/10.1029/98JB01516

Reineck, H.-E., & Singh, I. B. (1973). *Depositional Sedimentary Environments*. Springer Berlin Heidelberg. https://doi.org/10.1007/978-3-642-96291-2

Reynolds, D. J., Steckler, M. S., & Coakley, B. J. (1991). The role of the sediment load in sequence stratigraphy: The influence of flexural isostasy and compaction. *Journal of Geophysical Research: Solid Earth*, *96*(B4), 6931–6949. https://doi.org/10.1029/90JB01914

Rich, J. L. (1951). THREE CRITICAL ENVIRONMENTS OF DEPOSITION, AND CRITERIA FOR RECOGNITION OF ROCKS DEPOSITED IN EACH OF THEM. *Bulletin of the Geological Society of America*, *62*(October), 1–20.

Rowley, D. B., Forte, A. M., Moucha, R., Mitrovica, J. X., Simmons, N. A., & Grand, S. P. (2011). *Dynamic Topography Change of the Eastern US since 4 Ma: Implications for Sea Level and Stratigraphic Architecture of Passive Margins*.

Sanchez, C. M., Fulthorpe, C. S., & Steel, R. J. (2012a). Middle Miocene-Pliocene siliciclastic influx across a carbonate shelf and influence of deltaic sedimentation on shelf construction, Northern Carnarvon Basin, Northwest Shelf of Australia. *Basin Research*, *24*(6), 664–682. https://doi.org/10.1111/j.1365-2117.2012.00546.x

Sanchez, C. M., Fulthorpe, C. S., & Steel, R. J. (2012b). Miocene shelf-edge deltas and their

impact on deepwater slope progradation and morphology, Northwest Shelf of Australia. *Basin Research*, *24*(6), 683–698. https://doi.org/10.1111/j.1365-2117.2012.00545.x
Sheridan, R.E., & Gradstein, F. M. (1983). *Initial Reports of the Deep Sea Drilling Project, 76* (Vol. 76). U.S. Government Printing Office. https://doi.org/10.2973/dsdp.proc.76.1983
Suess, E. (1905). The Face of the Earth (Das Antlitz der Erde). *Nature*, *72*(1861), 193–194. https://doi.org/10.1038/072193a0
Swenson, J. B., Paola, C., Pratson, L., Voller, V. R., & Murray, A. B. (2005). Fluvial and marine controls on combined subaerial and subaqueous delta progradation: Morphodynamic modeling of compound-clinoform development. *Journal of Geophysical Research: Earth Surface*, *110*(2), 1–16. https://doi.org/10.1029/2004JF000265
Tagliaro, G., Fulthorpe, C. S., Gallagher, S. J., McHugh, C. M., Kominz, M. A., & Lavier, L. L. (2018). Neogene siliciclastic deposition and climate variability on a carbonate margin: Australian Northwest Shelf. *Marine Geology*, *403*(June), 285–300. https://doi.org/10.1016/j.margeo.2018.06.007
von der Heydt, A., & Dijkstra, H. A. (2006). Effect of ocean gateways on the global ocean circulation in the late Oligocene and early Miocene. *Paleoceanography*, *21*(1), 1–18. https://doi.org/10.1029/2005PA001149
Wanless, H. R., & Shepard, F. P. (1936). Sea level and climate changes related to late Paleozoic cyclothems. *Bulletin of the American Geographical Society*, *47*(2), 143–145. https://doi.org/10.2307/201801
Watts, A. B., & Steckler, M. S. (1981). Subsidence and tectonics of Atlantic-type continental margins. *Oceanologica ACTA*, 143–154.
Watts, A. B., & Steckler, M. S. (1979). *Subsidence and eustasy at the continental margin of eastern North America* (pp. 218–234). https://doi.org/10.1029/ME003p0218
Wells, A. J. (1960). Cyclic sedimentation: a review. *Geological Magazine*, *97*(5), 389–403.
Werthmüller, D., Ziolkowski, A., & Wright, D. (2013). Background resistivity model from seismic velocities. *Geophysics*, *78*(4), E213–E233. https://doi.org/10.1190/GEO2012-0445.1
Wiberg, P. L., Cacchione, D. A., Sternberg, R. W., Donelson Wright, L., & Wright, D. (1996). Linking sediment transport and stratigraphy on the continental shelf. *Oceanography*, *9*(SPL.ISS. 3), 153–157. https://doi.org/10.5670/oceanog.1996.02
Withjack, M. O., Schlische, R. W., & Olsen, P. E. (1998). Diachronous rifting, drifting, and inversion on the passive margin of central eastern North America: an analog for other passive margins. *AAPG Bulletin*, *82*(5 A), 817–835. https://doi.org/10.1306/1D9BC60B-172D-11D7-8645000102C1865D

CHAPTER4. EVIDENCE FOR MILANKOVIĆ CYCLICITY IN 8 MYR OF MARINE STRATIGRAPHIC RECORD FROM THE NEW JERSEY MARGIN

4.1 Abstract

The link between cyclicity of shallow marine stratigraphic sequences and orbitally-forced eustacy is a longstanding observation that has mostly been described qualitatively and resolved with coarse time resolution (>1 Myr) for pre-Pleistocene sequences. This is because the presence of other controlling factors at rifted margins in general, such as tectonics and sediment supply, which have similar impacts on the sedimentary record, challenge any attempt to quantify the impact of eustasy. At the New Jersey rifted continental margin, however, this is not the case. Since the Oligocene, this margin has experienced a relatively stable tectonic history and rate of sediment supply, leaving eustatic changes as the dominant controlling factor in shaping the sedimentary architectures. These characteristics make the New Jersey shelf a prime location to investigate the effect of short-term eustatic changes on the marine sedimentary record. To study the impact of eustatic changes on sedimentary geometries, we use data from three IODP boreholes and a high-resolution 3D seismic volume that encompasses them. We show that the margin's Miocene clinoforms have recorded 22 cycles and 76 phases of eustatic changes over 8 Myr. While previous studies suggest a correspondence between 1.2 Myr obliquity modulation cycles and third-order sequences, our spectral analysis of the cyclicity of the Miocene sedimentary record yields local spectral peaks at 25 Kyr and 40 Kyr in high-frequency spectra, and 2.5 Myr cycles in the low-frequency spectra. These spectral peaks correspond to the cyclicity observed in insolation due to changes in the axial tilt and precession of the Earth's orbit. Further, we track the Miocene onshore-offshore movements of stratigraphic sequences, which show a 42% correlation with the mathematically driven insolation log within the studied period. These findings suggest that even short-period, orbitally-driven eustatic changes had a direct impact on the Miocene sedimentary record of the New Jersey continental margin.

4.2 Introduction

Studying the influence of the Earth's orbital parameters on climate goes back to the nineteenth century with an initial focus on the astronomical theory of the Ice Age (Adhémar, 1842; Croll, 1864). These early studies used discontinuous records from river terraces and moraine deposits, with no independent age control, to find the link between ice ages and orbitally-driven variations in insolation (Hays et al., 1976; Imbrie et al., 1984). In a series of theoretical work in the early 20th century, Milutin Milanković (1920, 1941) hypothesized that variation in the kinematics of Earth is a strong driver of Earth's long-term climate by imposing cyclicity in the solar radiation (insolation) reaching the Earth. Milanković described the cyclical variation in the Earth's eccentricity, axial tilt, and precession – now known as Milanković cycles – as parameters that are caused by the gravitational interactions between bodies in the Solar System. The variation in insolation has been influential for triggering the beginning and end of glaciation periods over the geological time (Muller & MacDonald, 1997).

The deep-sea Swedish Expedition Albatross in 1947 recovered piston cores of deep marine sediments for the first time (Kullenberg, 1947; Pettersson, 1951), providing the scientific community with a continuous record of Ice Age history from the deep-sea (Emiliani, 1955), as well as the first seismic reflection measurements of sediment thickness in deep ocean. This expedition was a breakthrough in constructing the astronomical time scale and supported the astronomical theory of the Ice Age (Hays et al., 1976; Imbrie et al., 1984). Ever since, a large body of studies have focused on understanding the physics of Milanković cycles (Berger et al., 2006; Girkin, 2005), modeling oscillations in the insolation (Laskar et al., 2004; 2011), and estimating their impact as controlling mechanisms on climate and eustasy on a global scale (Aitken & Flint, 1995; Busch & Rollins, 1984; Greb et al., 2008; Heckel, 1987).

Despite the volume of work on defining the relationship between paleo-eustatic change and astronomical parameters, skepticism remained because of 1) the presence of several superimposing mechanisms, variable rate of sediment influx and deposition (Algeo & Wilkinson, 1988; Hinnov, 2013), and interference of cycles (de Boer et al., 2013) impose uncertainty to isolate and quantify the impact of one controlling mechanism; 2) the poor resolution and precision of dating techniques make it challenging to demonstrate the link between the observed

cyclicities and a natural phenomenon with a cyclicity of tens of thousands years (Klein 1990); 3) erosion and periods of non-deposition, result in incomplete sedimentary records (Hinnov, 2013).

Previous studies suggest that bundling patterns of clinoforms show periodicity and the average clinothem periods are estimated in the Milanković range (McCarthy et al., 2013; Miller et al., 1998, 2004). However, the impact of orbital control has not been measured and lacks quantitative support (Algeo & Wilkinson, 1988; Meyers, 2008). Difficulties in correlating deep-sea stratigraphy with depositional units in continental shelves and limitations of analyzing Oxygen-18 isotope records in shallow marine environments have made it challenging to unravel how the composite Milanković cyclicity impacted the shelf deposits. These limitations call for an integrated stratigraphic approach, supported by independent age control, to investigate the stratigraphic cyclicity and correlate it with Milanković cycles (Hilgen et al., 2015).

We present a case from the New Jersey continental margin, where the development of stratigraphic sequences is mainly dominated by eustasy (Miller et al., 2005), a fundamental notion incorporated in the majority of models of sequence stratigraphy (Mitchum et al., 1977; Van Wagoner et al., 1988a). At this rifted margin, due to the small rate of subsidence by lithospheric cooling (Mountain et al., 2007), limited tectonic activity, and continuous sediment supply (Reynolds et al., 1991; Watts & Steckler, 1979), eustatic changes have been the main mechanism controlling sedimentation in the shallow marine environment (Fulthorpe et al., 1999; Monteverde et al., 2000; Mountain et al., 2007; Pellaton & Gorin, 2005). Further, four decades of research have provided a wealthy repository of data available along the shelf of this margin (Figure 4.1).

This study focuses on the footprints of the Miocene glacio-eustasy in the stratigraphic record. We use the current 3D stratigraphic model of the shelf (Aali et al, in preparation) to test whether the onshore-offshore oscillation of these seismically identified systems tracts can be explained in terms of Milanković cycles. Further, we analyze the synchronicity between cyclic variation in insolation and gamma measurements from the drill sites in time and frequency domains. These results provide an independent but complementary measure for estimating the impact of orbitally-driven eustatic changes on the Miocene sedimentary record.

4.3 Data and Methodology

We collected 564 km^2 of ultra-high-resolution 3D multichannel seismic (MCS) data on R/V *Marcus G. Langseth* in 2015 that encompasses three IODP drill sites from the Expedition 313 (Figure 4.1). Spanning 8 Myr, the early- to mid-Miocene sedimentary record shows 22 clinoforms and 76 systems tracts (Figure 4.2) (Aali et al, in preparation) that are attributed to different phases of eustatic oscillation (Figure 4.3). The Expedition 313 drill sites provide core samples and wireline log data from the topset, forest, and bottomset of the Miocene shallow marine clinoforms, stratigraphic features with sigmoidal (sloped) geometry that are formed during a cyclic change of accommodation and sediment influx (Mountain et al., 2010).

Correlating the sedimentary record with its contemporary astronomical parameters requires tying depth to geological time. The age estimates from three IODP drill sites (Browning et al., 2013; Kominz et al., 2016) with a resolution of +/- 0.25 Myr (Browning et al., 2013) were used as the initial age models (Figure 4.4). These age data are based on strontium isotopic dating of calcium carbonate material, and biostratigraphic analysis of calcareous nannofossil, dinoflagellate cyst, and diatom biostratigraphy. Paleomagnetic and mineral magnetic analyses were carried out on Miocene sediment samples from the Expedition 313 (Nilsson et al., 2013). Even though the initial paleomagnetic results from this interval showed several paleomagnetic reversal boundaries, these techniques were not used to improve the precision obtained from strontium isotope and biostratigraphy. Further studies showed that the Miocene sediments have been chemically re-magnetized by diagenetic processes and dissolution of the primary magnetic mineral (Urbat, 1996) in several intervals.

We selected 20 out of 35 dated surfaces from Kominz et al (2016) to make coeval age surfaces along the three IODP drill sites for further age calibration. In an iterative process, the initial age model was used as the mean value to generate a series of random age models with a normal distribution and standard deviation of 30 Kyr. In this procedure, 99.7% of the randomly generated ages fall within +/- 90 Kyr from the input age model. Each of the generated age models were used to transfer the gamma-ray logs from the depth domain to the geological age domain.

Stepwise regression workflow was used to calibrate the age models by maximizing the correlation of gamma measurements at three IODP sites in geological time domain. In a stepwise regression process, the randomly generated age models were used to find the ages that maximize correlation between three gamma logs. Starting from top to bottom surfaces, we correlated the gamma-ray logs from the sea bed to the top of dated surfaces and iteratively changed the age of the oldest surface to find an age that gave the most statistically significant improvement of the correlation between the wells. This process was repeated by extending the studied interval to the next dated surface in the initial model.

The calibrated age/depth model, which produced the highest correlation between the three wells, was used to transfer the spectra gamma-ray logs from depth to age domain (Figure 4.5). The total gamma radiation log records the intensity of radioactive sources (clay minerals as a major component) presented in the mineralogical composition of sediment (Nazeer et al., 2016). The gamma measurements from three IODP sites were stacked in the geological age domain to enhance the signal from the more regional changes in the paleo-environment, and to fill the local gaps due to periods of nondeposition or erosion in the sediment record. We de-trended the composite gamma log by subtracting a moving average, with a 3 Myr window, from the original log. Detrending the composite log amplified the short-term (< 3 Myr) changes in the composite gamma log (Figure 4.6).

We defined a time series for onshore-offshore movements of the depocenter of the Miocene systems tracts within the seismic volume. The 3D stratigraphic model of the New Jersey shelf (Aali et al., in preparation) was used to categorize the Miocene systems tract based on the relative shift in the positions of their landward termination, rollover point, and sea-ward termination. The stratigraphic surfaces were then dated using the calibrated model to study their position respect to their contemporary insolation on the earth in the Miocene.

The long-term numerical solution for the orbital parameters (Laskar et al., 2011) was used to estimate insolation for the Miocene New Jersey margin on the spring equinox spanning from 23 to 12 Mya. The estimated insolation is further filtered with Nyquist periods of 200 Kyr, 20 Kyr, and 2 Kyr (Figure 4.6) to upscale the resolution of insolation log to the resolution of gamma log and the stratigraphic time series.

4.4 Results

Stacking gamma measurements along the three wells reduced the gaps in the gamma measurements from 29 to 5 hiatuses which were persistent in three IODP drill sites. This increase in the data coverage for the sedimentary record improved our ability to identify and characterize the cyclic events in the gamma-ray measurements. Figure 4.7 shows the periodogram of the composite gamma-ray log in high-frequency spectra.

The calibrated age model improved the correlation coefficient between insolation and composite gamma log from 0.17 to 0.52. In high-frequency spectra, the ~20 Kyr, ~40 Kyr, and ~100 Kyr peaks are distinctable from others by their high amplitude in the periodogram (Figure 4.7). In low-frequency spectra, the de-trended composite gamma-ray log also shows a cyclic pattern with an average period of approximately 2.5 Myr (Figure 4.8). The short length of studied time interval and presence of several periods of nondeposition make it challenging to extract a meaningful signal from the lower frequency spectra.

The age of stratigraphic surfaces, mapped in seismic data, vary unevenly between consecutive surfaces. This fluctuation in age forms a nonuniformly-sampled time series between facies' depocenter and their age. We used the Lomb-Scargle algorithm (Lomb, 1976; Scargle, 1982) to compute the periodogram for the along-dip movement of facies' depocenter and to characterize the periodic signals in its time series (Figure 4.9). The periodogram distinguishable local spectral peaks at proximity to the period of 20 Kyr, 40 Kyr, and 100 Kyr.

4.5 Discussion

Cyclic imprints of astronomically induced climate change in stratigraphic records have played a key role in understanding past sedimentation and climate change (Hilgen et al., 2015). Due to their high precision, astronomical target curves, generated by mathematical modelling of the Solar System, are used to calibrate the age of sedimentary records for most of the Cenozoic Era (Hilgen et al., 2015; Hinnov & Hilgen, 2012; Vandenberghe, 2013) in deep marine environments. The complexity and fragmentary nature of the stratigraphic records in the shallow marine environment have made it challenging to register orbitally-driven climate changes with high resolution. However, data from these environments are inherently more accessible and have better spatial coverage to integrate and provide a more continuous sedimentary record in

geological time scale (tens of thousands to a few million years). The evidence given in this study comes from applying an integrated stratigraphic approach, using seismic sequence stratigraphy, biostratigraphy, and geochronology.

4.5.1 Cyclicity in gamma measurements

The composite gamma log (Figure 4.6) provides a relatively continuous time series for spectral analysis of cyclic events in the depositional environment. 83% of the hiatuses found in the IODP Expedition 313 records are not traceable in all three wells and were formed by local processes. Stacking the gamma logs, helped to reconstruct the lithological change in an interval that experienced local erosion or non-deposition and provided a more continuous record of the deposition on the shelf.

In low-frequency spectra, the detrended composite gamma log shows a cyclic pattern with a period of 2.5 million years (Figure 4.8). These cycles generally start with a rapid increase in the gamma measurements followed by a gradual decrease in the gamma log. High gamma measurements are attributed to a decrease in the energy level in the environment of deposition and can be the result of an increase in the relative sea level. The timing of the mid-Miocene cycles is contemporaneous with the beginning of the global climatic optimum, when the earth experienced a rapid increase in global temperature. Figure 4.8 shows the detrended global oxygen isotope values (Mudelsee et al., 2014) in comparison with the corresponding detrended gamma measurements. These measurements suggest a strong correlation between the changes in the global oxygen isotope values and the gamma radiation of the sedimentary record.

The finely sampled (with a sampling rate of 1 Kyr) gamma-ray measurements were used for spectral analysis in high-frequency spectra. The intensity of gamma-radiation, which is a proxy for the fraction of clay presented in the sediments, is directly proportionate to the energy level in the environment as well as the rate of sediment flux to accommodation creation. As insolation influences climate, it also affects the rate of sediment flux in the hinterland and the rate of accommodation by controlling the eustatic changes on a global scale.

A strong correlation between the composite gamma values and the insolation is in favor of our hypothesis that the presence of local spectral peaks at 25 Kyr and 40 Kyr in high-frequency spectra corresponds to the cyclicity observed in insolation due to changes in the axial tilt and precession of the Earth's orbit (Figure 4.7) . Previous studies (e.g Hilgen et al., 2015) on

footprints of orbital parameters in Miocene-Pleistocene sedimentary records suggest that obliquity and precession dominated the insolation and acquired a spectral peak in analyses of sedimentary records using Oxygen-18 isotopes. Eccentricity also influences the insolation by modulating the precession amplitude (Hilgen et al., 2015; Huybers & Wunsch, 2003; Weedon, 2003).

4.5.2 Cyclicity in the stratigraphic record

The high correlation value of +0.42 (Figure 4.10) indicates that insolation had a significant impact on the onshore-offshore migration of sedimentary facies over geological time. The corresponding periodogram for movements of the depocenter (Figure 4.9) shows distinguishable local spectral peaks at proximity to the period of ~ 20 Kyr, ~ 40 Kyr, and 95 Kyr which are close to 23 Kyr, 40 Kyr and 100 Kyr Milankovitch cycles in the Miocene. As low insolation on Earth resulted in periods glaciation and low global sea-level, the corresponding systems tracts also have depocenters further offshore. An increase in the insolation is associated with migration of facies depocenters onshore (Figure 4.10).

Analyzing the onshore-offshore movement of stratigraphic record has several advantages, respect to the thickness of deposited strata and the average cycle length, for correlating the high-resolution estimates of insolation with changes in the depositional environment. For instance, it may take tens of thousands of years of sea-level rise before depositing a considerable amount of marine shale on top of pre-existing sediments (van den Belt et al., 2015), resulting in a significant time lag between the varying insolation and its corresponding change in marine sedimentary record in one dimension. Further, the cycle length estimated by dividing the succession duration by the number of cycles observed in the geological data could result in overestimating the cycle length in areas with periods of non-deposition and erosion. The presence of allocyclic or autocyclic processes (Cecil, 2003), such as isostatic rebounding and delta-lobe switching (e.g. Fielding, 1984), might widen the spectra observed in the sedimentary record.

The impact of cyclic insolation fluctuations on paleoclimate and therefore on the Earth's sedimentary record has been questioned by scholars in the field (e.g Bailey, 1998; Robin John Bailey, 2009; Rubincam, 1994; Wunsch, 2004). Bailey (1998) argues that the complex and chaotic systems that control the stratigraphic records have extremely repetitive outputs and the

recorded cyclicity does not necessarily reflect the cyclic forcing of a systematic system. Algeo & Wilkinson (1988) argue that the periodic alteration of sedimentary records in the Milanković frequency band is fortuitous and related to internal autogenic processes causing cyclic sedimentary processes. They use the migration of fluvial channels and repetitive delta-lobe switching as instances that sedimentary processes are controlled by internal autogenic processes and form repetitive geological records. However, these hypotheses have been refuted by numerous other studies (Abels, 2008; Abels et al., 2012) that use independent time control to show that in some cases the astronomically-forced climate changes may even dictate river avulsion. For instance, paleo-climate studies based on the high-resolution ocean-atmosphere general circulation model show that an approximately 5% increase in Northern Hemisphere summer insolation in the Mid-Holocene caused up to a 46% increase in precipitation during the summer monsoon in North Africa (Bosmans et al., 2011).

4.5.3 Calibration of age model in 2D

The traditional dating techniques use 1D data samples and do not incorporate petrophysical properties of sedimentary records to estimate the absolute age of each sample. The Steno's law of facies continuity in dip direction governs that, despite the presence of erosional surfaces, the vertical depositional pattern should match in all three well locations. In other words, the ideal age models should result in the maximum correlation between the stratigraphic columns in the three wells. We used this assumption as the key criterion to calibrate the published age model.

The 2D age model calibration improved the precision of the age estimates from +/- 250 Kyr to less than 100 Kyr. The filtered the insolation log sampled every 100 Kyr shows a strong correlation with the studied properties in the time domain, insolation logs sampled every 1 Kyr and 10 Kyr show little to no correlation (Figure 4.6). However, the periodogram of the composite gamma values shows local spectral peaks at ~23 Kyr, 40 Kyr and 100 Kyr, corresponding to the Milankovic cyclicity observed in insolation due to changes in the axial tilt, precession, and obliquity of Earth. These observations suggest that the 2D age calibration approach improved the precision of the age data points but not their accuracy in an absolute term.

The major challenge in spectral analysis of chronostratigraphic events in the Miocene is the poor resolution of dating techniques, specifically in shallow marine environments. Difficulties in

estimating the ages of the sediment with a desirable accuracy remains as the key challenge for tying the geological time with the depth of sediments.

4.6 Conclusion

This study aimed to provide unambiguous quantitative support for the widely held view that the Miocene eustatic oscillations formed in response to Milanković-controlled global climate changes. We showed that the internal structure of the Miocene shallow-marine clinothems contains a strong record of orbitally-driven eustatic oscillations offshore the New Jersey rifted margin. We used fluctuation in gamma-radiation of sedimentary records as well as the onshore-offshore movement of sedimentary facies to study the short-period cyclicity in the Miocene depositional environment. Our findings suggest that even short-period orbitally-driven eustatic changes had a direct impact on the Miocene sedimentary record of the New Jersey continental margin.

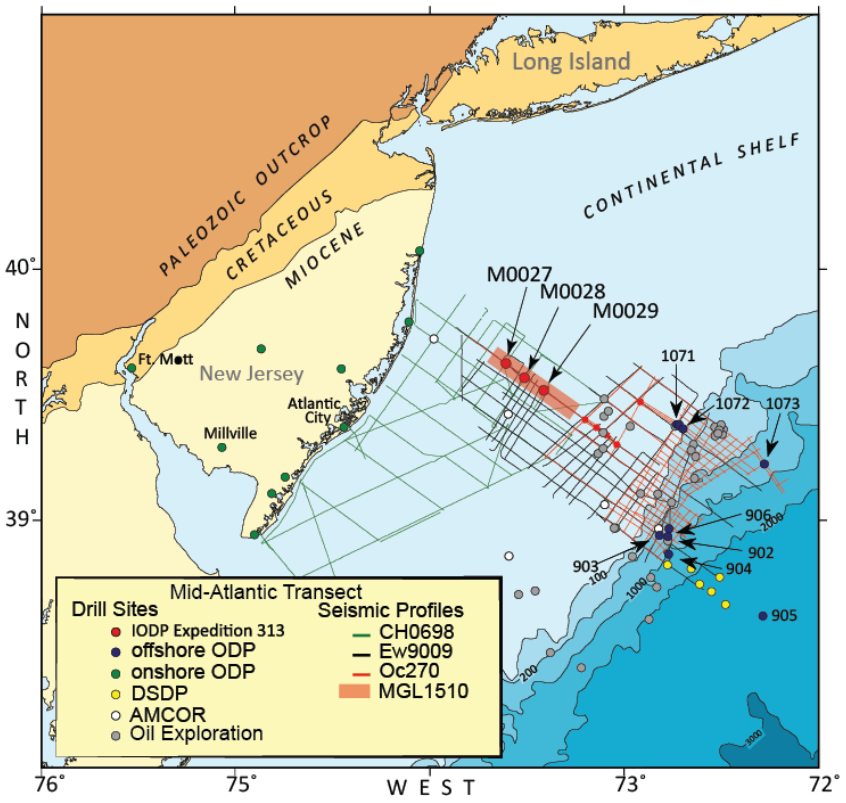

Figure 4.1: Seismic and well data collected across the New Jersey continental margin. This study used M27, M28 and M29 core and log data collected in 2009 by the IODP Expedition 313 (red dots) and the ultra high-resolution 3D seismic data from the MGL1510 survey conducted in 2015 (red rectangle).

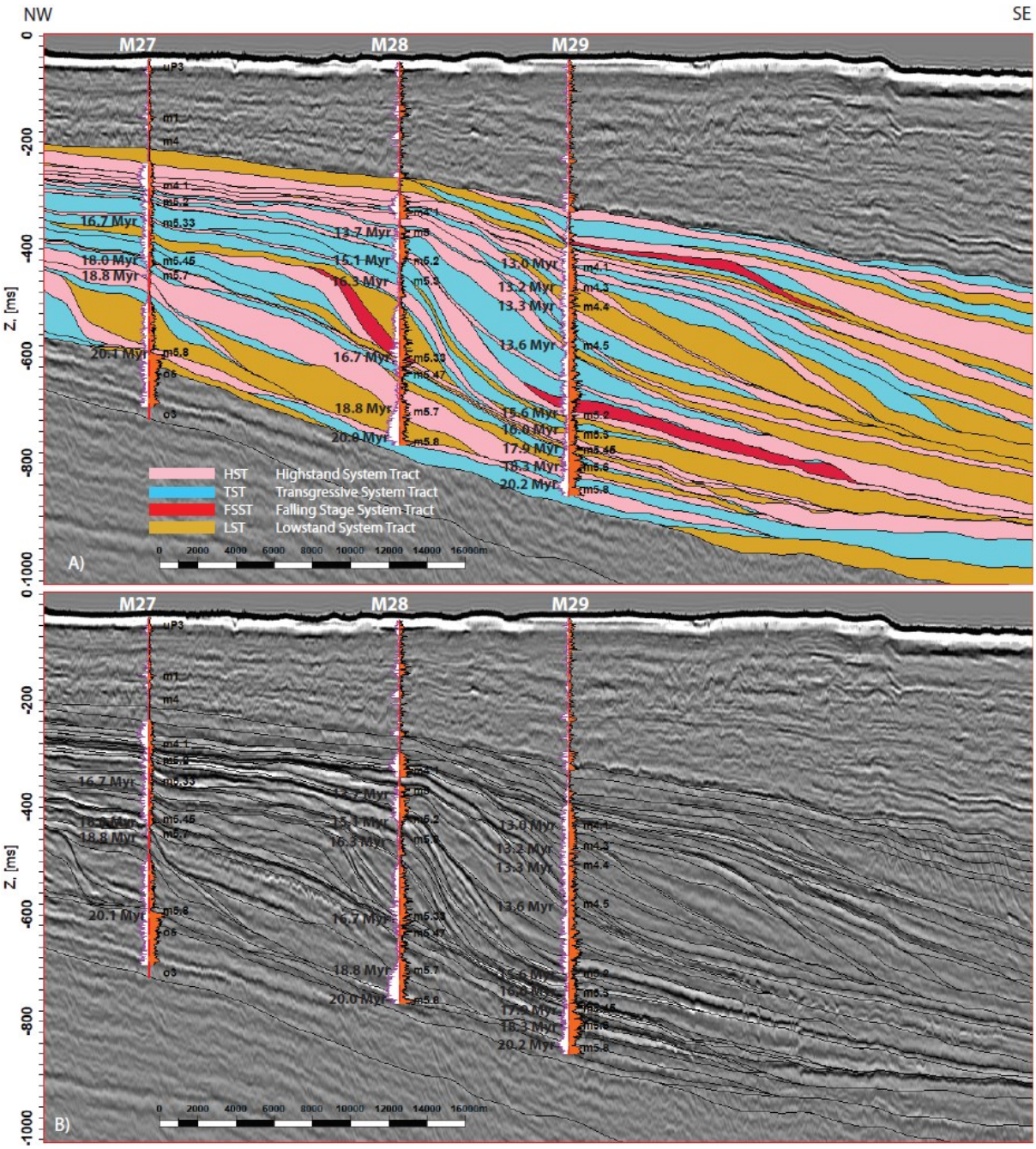

Figure 4.2: The faintly interpreted (lower image) and fully interpreted (upper) seismic sections crossing the Expedition 313 drill sites. 22 sequences and 75 systems tracts were interpreted spanning 8 million years of sediment deposition in Miocene foresets. The age of surfaces (Browning et al., 2013) are shown on the right side of the wells.

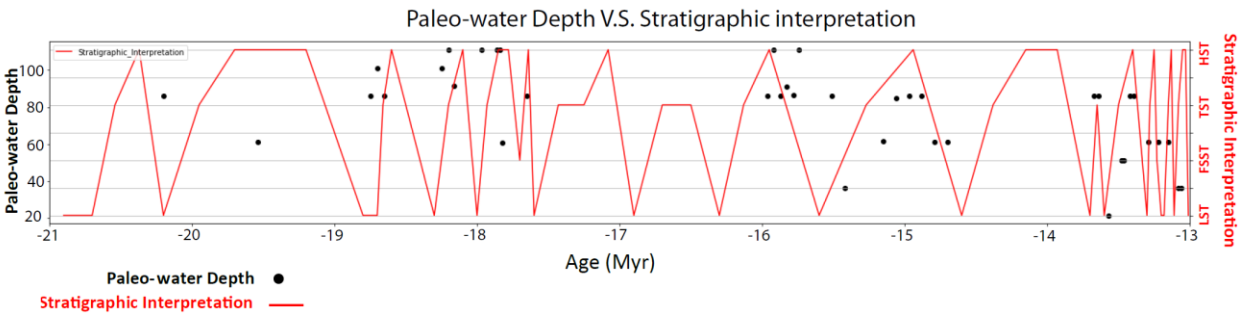

Figure 4.3: The interpreted seismic sequence stratigraphic cycles versus fluctuations of the paleo-water depth, estimated from the core samples at IODP Expedition 313 sites (Katz et al., 2013) in the New Jersey continental rifted margin.

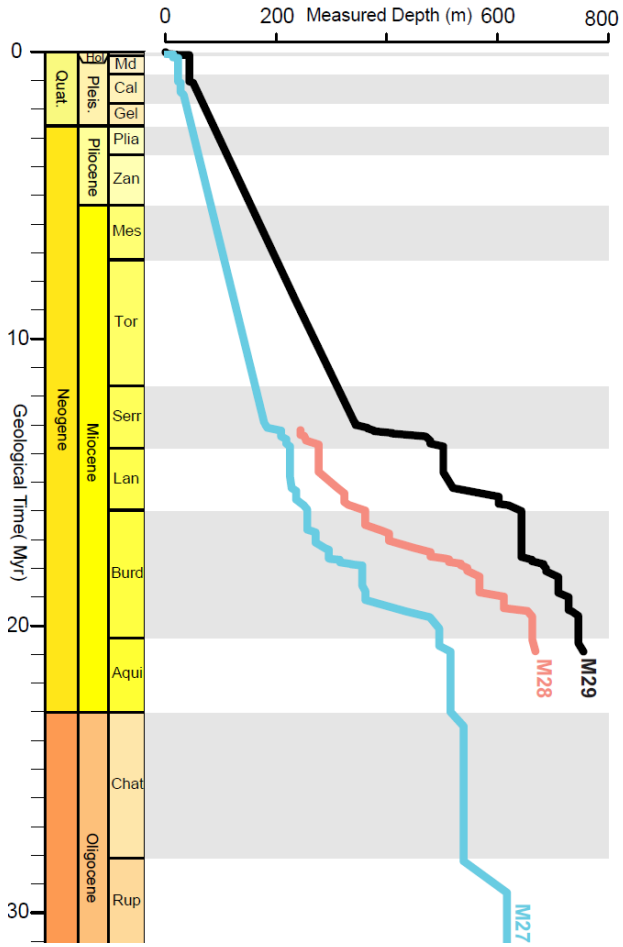

Figure 4.4: The geological age (Browning et al., 2013; Kominz et al., 2016) versus depth for three IODP wells M27-M29. The vertical portion of the logs represents periods of nondeposition or erosion within the sedimentary record. Sedimentary processes in the continental shelf such as ocean currents, slumping of sediments, and basin starvation make the depositional environment susceptible to hiatus (Aubry, 1991; Keller & Barron, 1983). However, only 17% of the identified discontinuities in the sedimentary record are common between three drill sites.

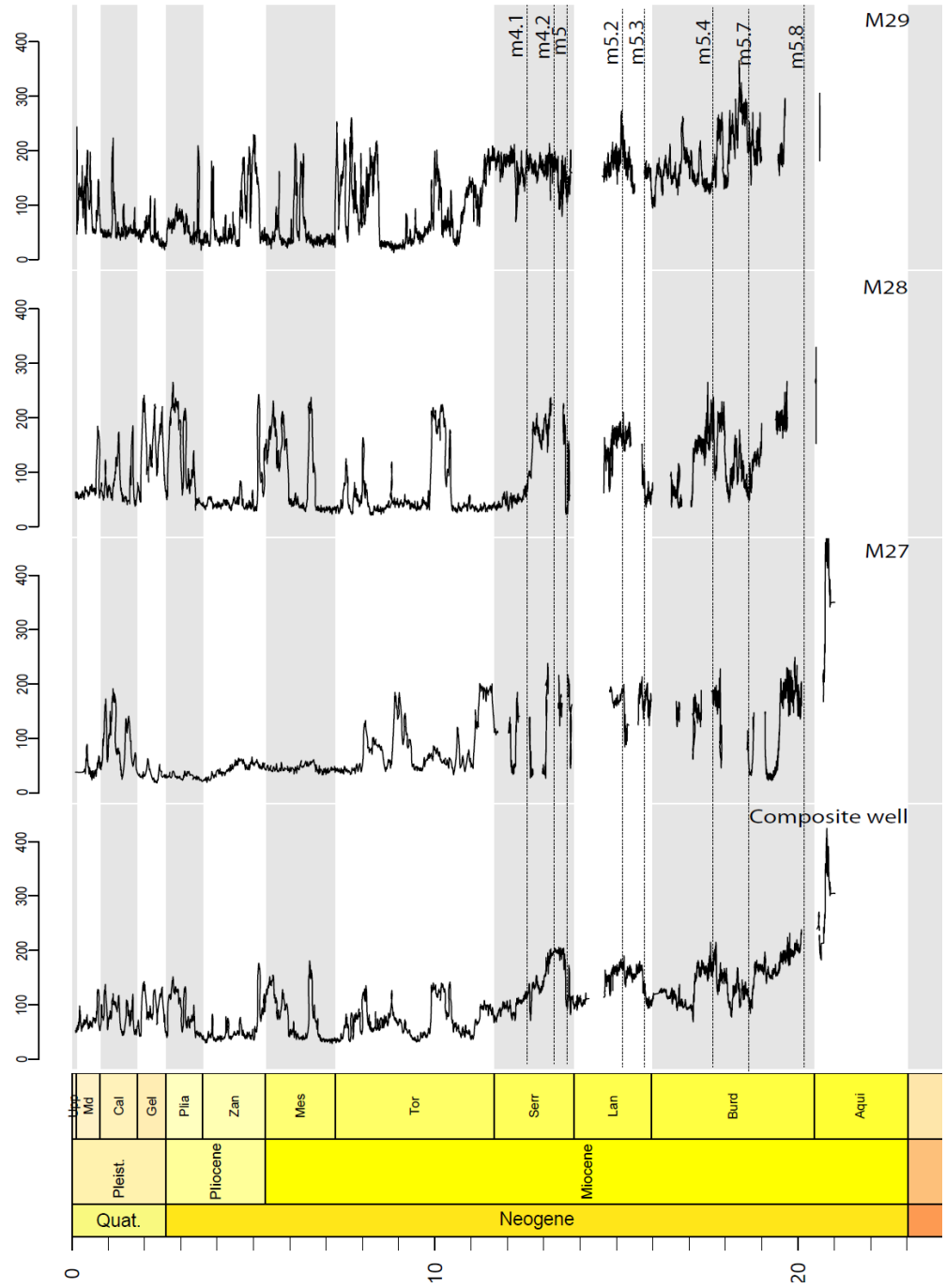

Figure 4.5: The gamma-ray logs in three IODP wells M27-M29 in geological time. Stacking the gamma measurements in the geological time domain also increases the signal to noise ratio by diminishing the gamma readings due to local heterogeneities and not changes in the depositional environment.

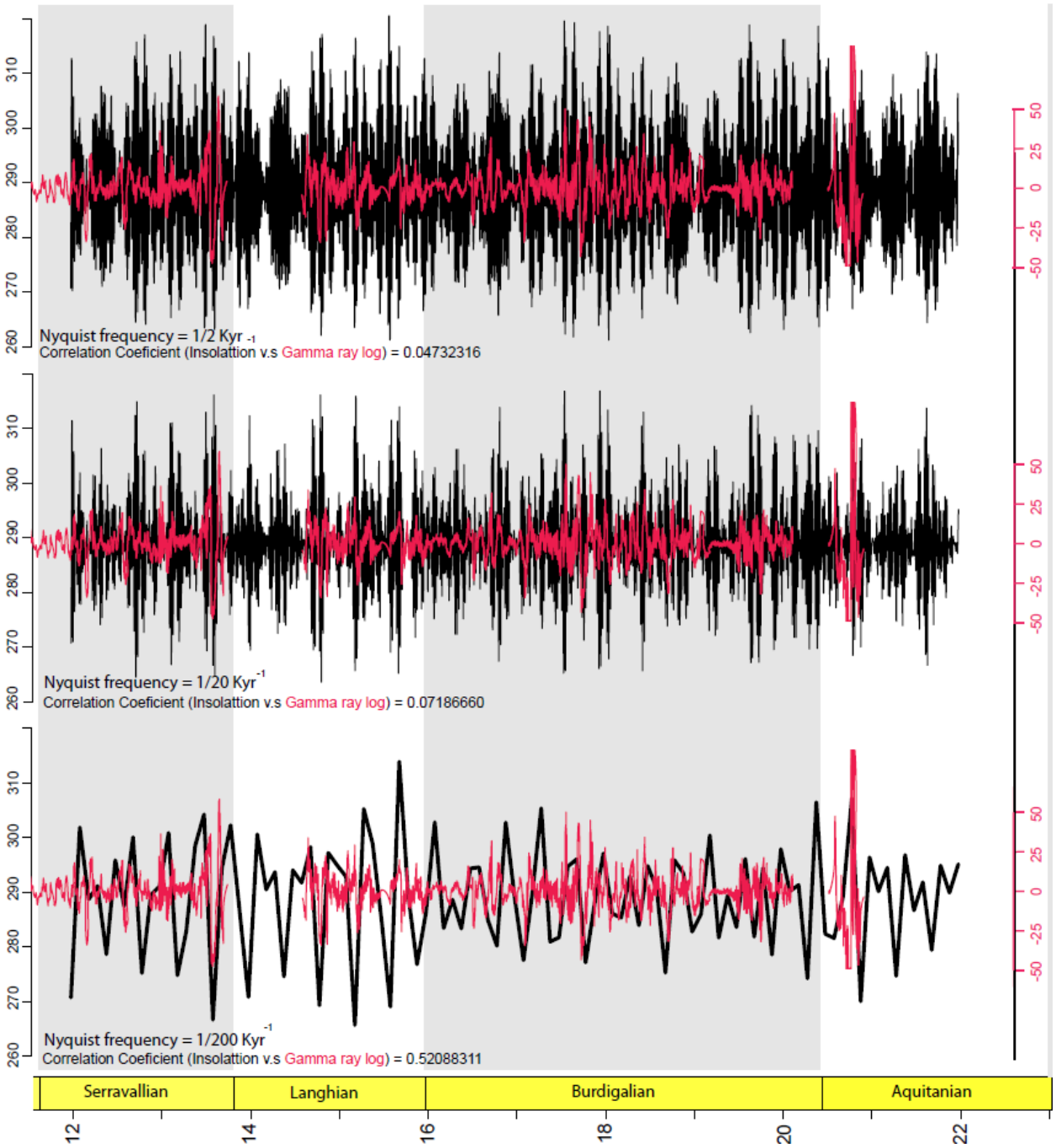

Figure 4.6: The detrended composite gamma-ray log overlapped on the insolation (Laskar et al., 2004) with sampling rates of 1 Kyr, 10 Kyr, and 100 Kyr (Nyquist period of 2 Kyr, 20Kyr, and 200 Kyr, respectively). While the correlation coefficient is close to zero for the 1 Kyr and 10 Kyr sampled insolation, this value increases to 0.52 for 100 Kyr-sampled insolation.

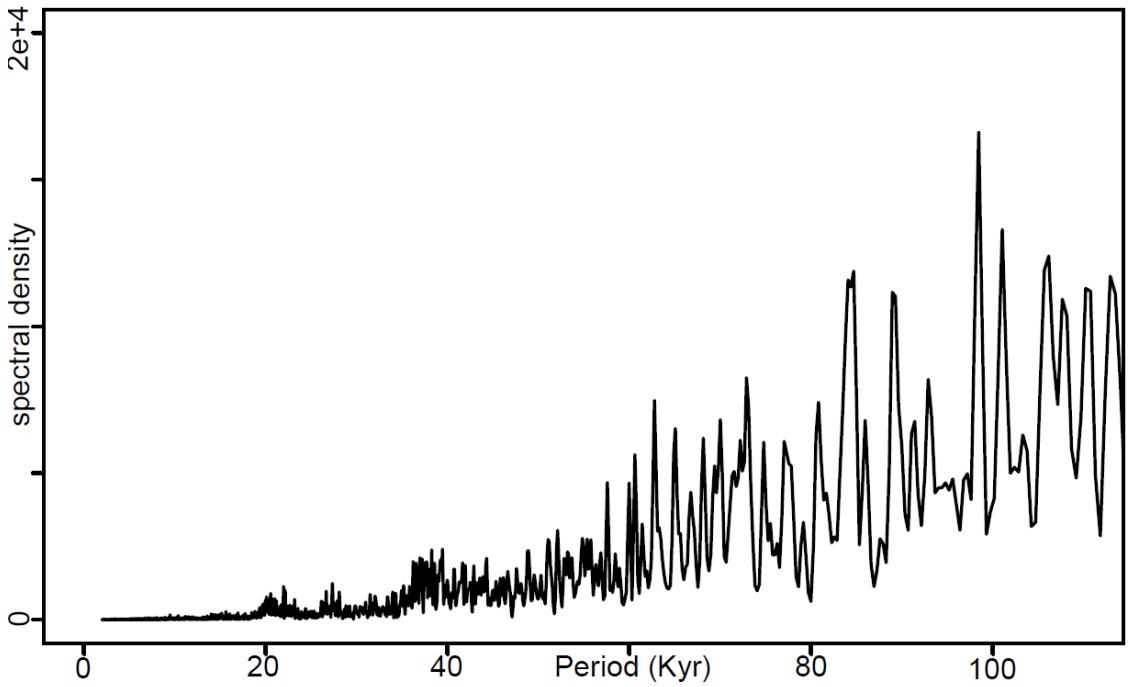

Figure 4.7: The periodogram of the detrended composite log in higher spectra. The periodogram shows local spectral peaks at around 23 Kyr, 40 Kyr, and 100 Kyr. These spectral peaks may correspond to the cyclicity observed in insolation due to changes in the axial tilt, precession, and eccentricity of the Earth's orbit.

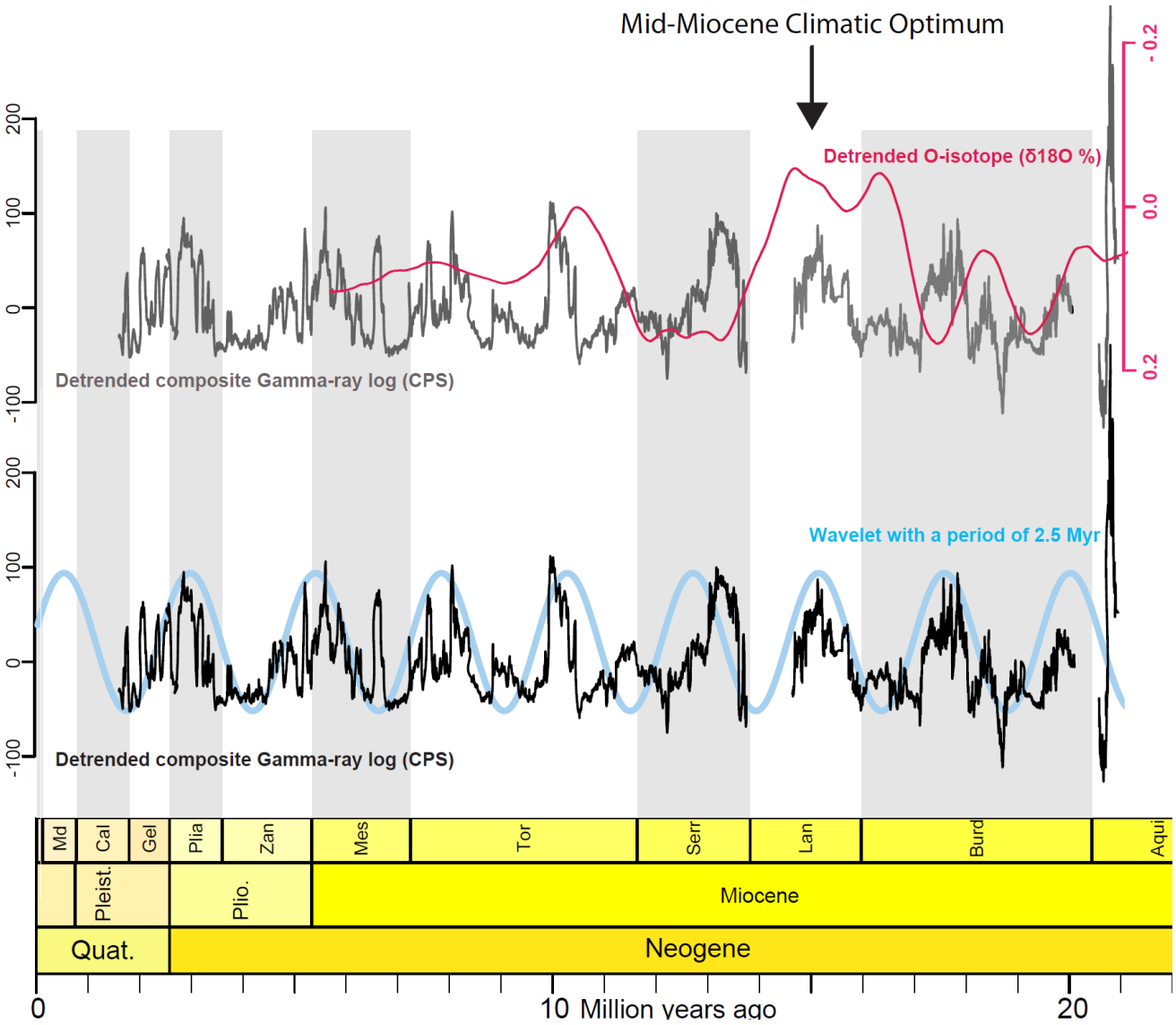

Figure 4.8: The detrended global O18 isotope (in red), composite gamma measurements from the Expedition 313 wells (in black), and a sinusoid with the period of 2.5 Myr (in blue).

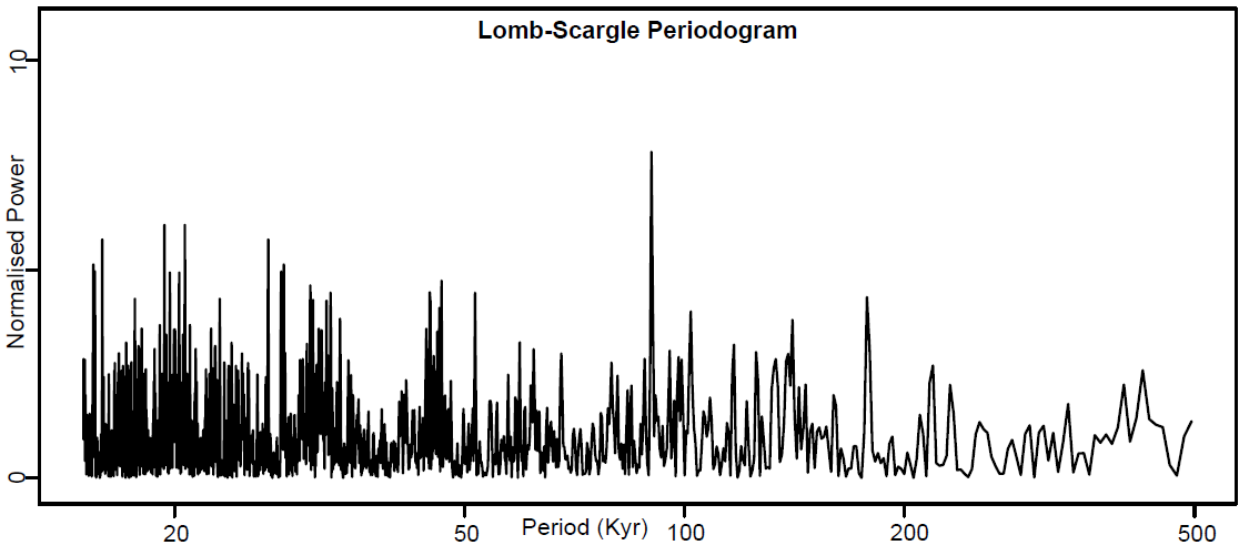

Figure 4.9: The Lomb-Scargle periodogram for the onshore-offshore cyclic movement of sedimentary facies in the Miocene interval. The periodogram shows local spectral peaks at around 20 Kyr, 40 Kyr and 100 Kyr.

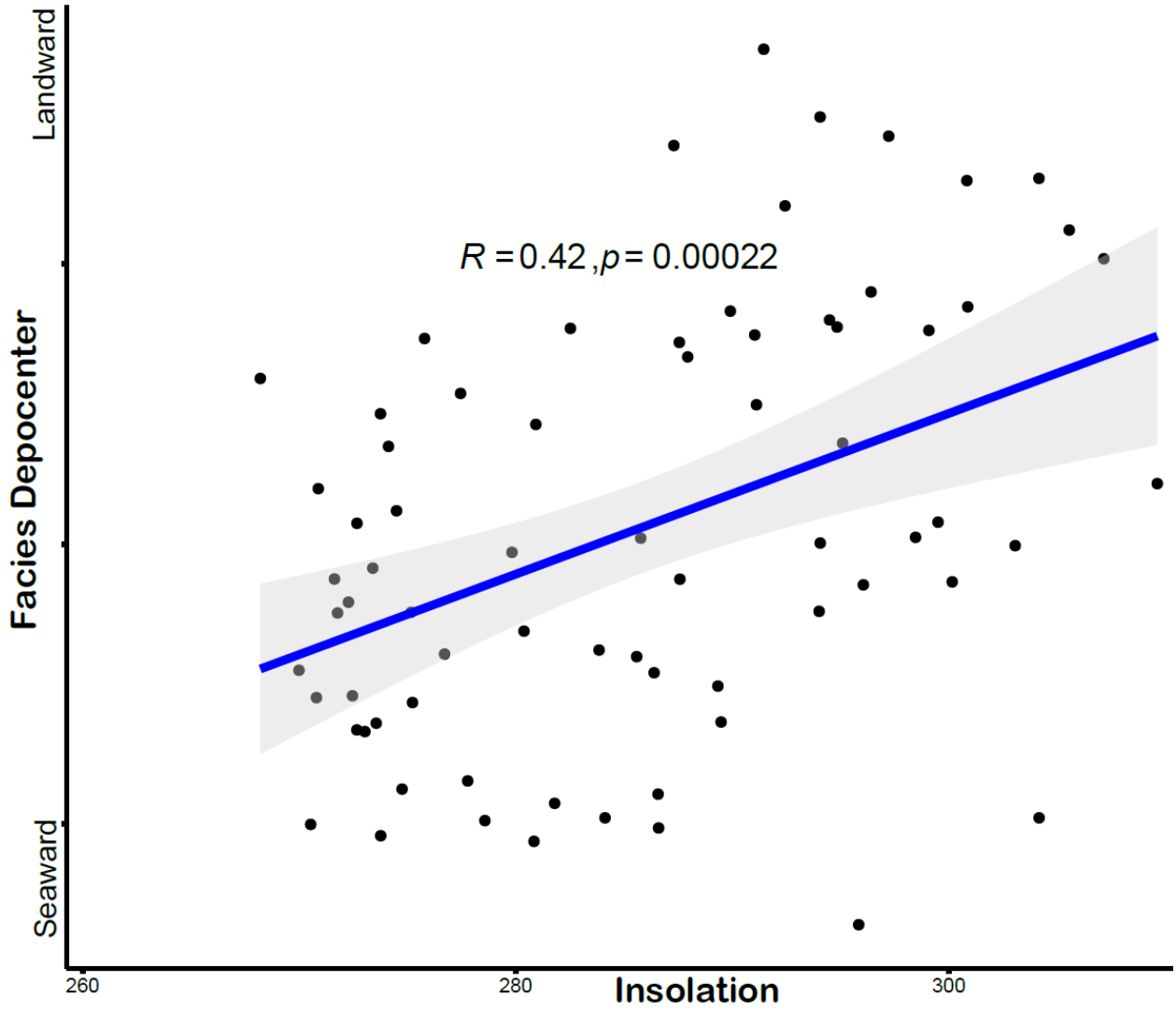

Figure 4.10: A cross plot correlating the onshore-offshore movement of facies' depocenters with the corresponding insolation for the Miocene interval. Pearson correlation (R) measures the linear dependency or correlation between insolation and landward-seaward movement of facies' depocenters. Positive correlation shows an increase in the insolation on the Earth's surface has a direct impact on seaward migration of sedimentary facies and depocenter over geological time.

4.7 References:

Abels, H. A. (2008). *Long-period orbital climate forcing [PhD Thesis]* (Issue 297). Utrecht University.

Abels, H. A., Clyde, W. C., Gingerich, P. D., Hilgen, F. J., Fricke, H. C., Bowen, G. J., & Lourens, L. J. (2012). Terrestrial carbon isotope excursions and biotic change during Palaeogene hyperthermals. *Nature Geoscience*, *5*(5), 326–329. https://doi.org/10.1038/ngeo1427

Adhémar, J. A. (1842). *Revolutions of the Sea*.

Aitken, J. F., & Flint, S. S. (1995). The application of high-resolution sequence stratigraphy to fluvial systems: a case study from the Upper Carboniferous Breathitt Group, eastern Kentucky, USA. *Sedimentology*, *42*(1), 3–30. https://doi.org/10.1111/j.1365-3091.1995.tb01268.x

Algeo, thomas, & Wilkinson, B. (1988). Periodicity of Mesoscale Phanerozoic Sedimentary Cycles and the Role of Milankovitch Orbital Modulation. *Journal of Geology - J GEOL*, *96*, 313–322. https://doi.org/10.1086/629222

Bailey, R. J. (1998). *Review : Stratigraphy , meta-stratigraphy and chaos*.

Bailey, R. J. (2009). Cyclostratigraphic reasoning and orbital time calibration. *Terra Nova*, *21*(5), 340–351. https://doi.org/10.1111/j.1365-3121.2009.00890.x

Berger, A., Loutre, M. F., & Mélice, J. L. (2006). Climate of the Past Equatorial insolation: from precession harmonics to eccentricity frequencies *. *Clim. Past*, *2*, 131–136.

Bosmans, J., Drijfhout, S., Tuenter, E., Lourens, L., Hilgen, F., & Weber, S. L. (2011). Monsoonal response to mid-holocene orbital forcing in a high resolution GCM. *Climate of the Past Discussions*, *7*. https://doi.org/10.5194/cpd-7-3609-2011

Browning, J. V., Miller, K. G., Sugarman, P. J., Barron, J. A., McCarthy, F. M. G. G., Kulhanek, D. K., Katz, M. E., & Feigenson, M. D. (2013). Chronology of Eocene–Miocene sequences on the New Jersey shallow shelf: Implications for regional, interregional, and global correlations. *Geosphere*, *9*(6), 1434–1456. https://doi.org/10.1130/GES00853.1

Busch, R. M., & Rollins, H. B. (1984). Correlation of Carboniferous strata using a hierarchy of transgressive- regressive units. *Geology*, *12*(8), 471–474. https://doi.org/10.1130/0091-7613(1984)12<471:COCSUA>2.0.CO;2

Cecil, C. (2003). The concept of autocyclic and allocyclic controls on sedimentation and stratigraphy, emphasizing the climatic variable. *Journal of Sedimentary Research*, *Special Pu*, 13–20.

Croll, J. (1864). XIII. On the physical cause of the change of climate during geological epochs. *The London, Edinburgh, and Dublin Philosophical Magazine and Journal of Science*, *28*(187), 121–137. https://doi.org/10.1080/14786446408643733

de Boer, B., van de Wal, R. S. W., Lourens, L. J., Bintanja, R., & Reerink, T. J. (2013). A continuous simulation of global ice volume over the past 1 million years with 3-D ice-sheet models. *Climate Dynamics*, *41*(5), 1365–1384. https://doi.org/10.1007/s00382-012-1562-2

Emiliani, C. (1955). Pleistocene Temperatures. *The Journal of Geology*, *63*(6), 538–578. https://doi.org/10.1086/626295

Fielding, C. R. (1984). Upper delta plain lacustrine and fluviolacustrine facies from the Westphalian of the Durham coalfield, NE England. *Sedimentology*, *31*(4), 547–567. https://doi.org/10.1111/j.1365-3091.1984.tb01819.x

Fulthorpe, C. S., Austin, J. A., & Mountain, G. S. (1999). Buried fluvial channels off New Jersey: Did sea-level lowstands expose the entire shelf during the Miocene? *Geology*, *27*(3), 203–206. https://doi.org/10.1130/0091-7613(1999)027<0203:BFCONJ>2.3.CO;2

Girkin, A. N. (2005). *A COMPUTATIONAL STUDY ON THE EVOLUTION OF THE DYNAMICS OF THE OBLIQUITY OF THE EARTH*. Miami University.

Greb, S. F., Pashin, J. C., Martino, R. L., & Eble, C. F. (2008). Appalachian sedimentary cycles during the Pennsylvanian: Changing influences of sea level, climate, and tectonics. In *Special Paper 441: Resolving the Late Paleozoic Ice Age in Time and Space* (pp. 235–248). Geological Society of America. https://doi.org/10.1130/2008.2441(16)

Hays, J. D., Imbrie, J., & Shackleton, N. J. J. (1976). Variations in the Earth ' s Orbit : Pacemaker of the Ice Ages. *Science*, *194*(4270). https://doi.org/10.1126/science.194.4270.1121

Heckel, P. H. (1987). Reply on "Sea-level curve for Pennsylvanian eustatic marine transgressive-regressive depositional cycles along midcontinent outcrop belt, North America." *Geology*, *15*(3), 276–278. https://doi.org/10.1130/0091-7613(1987)15<276b:CAROSC>2.0.CO;2

Hilgen, F. J., Hinnov, L. A., Abdul Aziz, H., Abels, H. A., Batenburg, S., Bosmans, J., de Boer, B., Hüsing, S. K., Kuiper, K. F., Lourens, L. J., Rivera, T., Tuenter, E., Van de Wal, R. S. W., Wotzlaw, J. F., & Zeeden, C. (2015). Stratigraphic continuity and fragmentary sedimentation: The success of cyclostratigraphy as part of integrated stratigraphy. *Geological Society Special Publication*, *404*, 157–197. https://doi.org/10.1144/SP404.12

Hinnov, L. A. (2013). Cyclostratigraphy and its revolutionizing applications in the earth and planetary sciences. *Bulletin of the Geological Society of America*, *125*(11–12), 1703–1734. https://doi.org/10.1130/B30934.1

Hinnov, L. A., & Hilgen, F. (2012). Cyclostratigraphy and Astrochronology. In *The Geological Time Scale* (Vol. 2012, pp. 63–83). https://doi.org/10.1016/B978-0-444-59425-9.00004-4

Huybers, P., & Wunsch, C. (2003). Rectification and precession signals in the climate system. *Geophysical Research Letters*, *30*(19). https://doi.org/10.1029/2003GL017875

Imbrie, J., Hays, J. D., Martinson, D. G., McIntyre, A., Mix, A. C., Morley, J. J., Pisias, N. G., Prell, W. L., & Shackleton, N. J. (1984). The orbital theory of Pleistocene climate: Support from a revised chronology of the marine d18O record. *Milankovitch and Climate: Understanding the Response to Astronomical Forcing*, *1*(January), 269–305. https://doi.org/-

Kominz, M. A., Miller, K. G., Browning, J. V., Katz, M. E., & Mountain, G. S. (2016). Miocene relative sea level on the New Jersey shallow continental shelf and coastal plain derived from one-dimensional backstripping: A case for both eustasy and epeirogeny. *Geosphere*, *12*(5), 1437–1456. https://doi.org/10.1130/GES01241.1

Kullenberg, B. (1947). *The piston core sampler*.

Laskar, J., Fienga, A., Gastineau, M., & Manche, H. (2011). *La2010: A new orbital solution for the long term motion of the Earth*. *March 2011*. https://doi.org/10.1051/0004-6361/201116836

Laskar, J., Roboutel, P., Joutel, F., Gastineau, M., Correia, A. C. M., & Levrard, B. (2004). Long-term solution for the insolation quantities of the Earth. *Proceedings of the International Astronomical Union*, *2*(14), 465. https://doi.org/10.1017/S1743921307011404

Lomb, N. R. (1976). Least-squares frequency analysis of unequally spaced data. *Astrophysics and Space Science*, *39*(2), 447–462. https://doi.org/10.1007/BF00648343

McCarthy, F. M. G. G., Katz, M. E., Kotthoff, U., Browning, J. V., Miller, K. G., Zanatta, R.,

Williams, R. H., Drljepan, M., Hesselbo, S. P., Bjerum, C., & Mountain, G. S. (2013). Sea-level control of new jersey margin architecture: Palynological evidence from integrated ocean drilling program expedition 313. *Geosphere*, *9*(6), 1457–1487. https://doi.org/10.1130/GES00853.1

Meyers, S. R. (2008). Resolving milankovitchian controversies: The Triassic Latemar limestone and the Eocene Green River Formation. *Geology*, *36*(4), 319–322. https://doi.org/10.1130/G24423A.1

Milanković, M. (1920). *Théorie Mathématique des Phénomènes Thermiques Produits par la Radiation Solaire*. Gauthier-Villars et Cie.

Miller, K. G., Kominz, M. A., Browning, J. V., Wright, J. D., Mountain, G. S., Katz, M. E., Sugarman, P. J., Cramer, B. S., Christie-Blick, N., & Pekar, S. F. (2005). The phanerozoic record of global sea-level change. *Science*, *310*(5752), 1293–1298. https://doi.org/10.1126/science.1116412

Miller, K. G., Mountain, G. S., Browning, J. V., Kominz, M. A., Sugarman, P. J., Christie-Blick, N., Katz, M. E., & Wright, J. D. (1998). Cenozoic global sea level, sequences, and the New Jersey transect: Results from coastal plain and continental slope drilling. *Reviews of Geophysics*, *36*(4), 569–601. https://doi.org/10.1029/98RG01624

Miller, K. G., Sugarman, P. J., Browning, J. V., Kominz, M. A., Olsson, R. K., Feigenson, M. D., & Hernández, J. C. (2004). Upper Cretaceous sequences and sea-level history, New Jersey Coastal Plain. *Bulletin of the Geological Society of America*, *116*(3–4), 368–393. https://doi.org/10.1130/B25279.1

Mitchum, R., Vail, P. R., & Thompson, S. (1977). Seismic Stratigraphy and Global Changes of Sea Level: Part 2. The Depositional Sequence as a Basic Unit for Stratigraphic Analysis: Section 2. Application of Seismic Reflection Configuration to Stratigraphic Interpretation. *Seismic Stratigraphy - Applications to Hydrocarbon Exploration.*, *165*, 53–62. https://doi.org/10.1306/M26490

Monteverde, D. H., Miller, K. G., & Mountain, G. S. (2000). Correlation of offshore seismic profiles with onshore New Jersey Miocene sediments. *Sedimentary Geology*, *134*(1–2), 111–127. https://doi.org/10.1016/S0037-0738(00)00016-6

Mountain, G. S., Burger, R. L., Delius, H., Fulthorpe, C. S., Austin, J. A., Goldberg, D. S., Steckler, M. S., Mchugh, C. M., Miller, K. G., Monteverde, D. H., Orange, D. L., & Pratson, L. F. (2007). The long-term stratigraphic record on continental margins. *Continental Margin Sedimentation: From Sediment Transport to Sequence Stratigraphy*, 381–458. https://doi.org/10.1002/9781444304398.ch8

Mudelsee, M., Bickertl, T., Lear, C., & Lohmann, G. (2014). Cenozoic climate changes: A review based on time series analysis of marine benthic δ18O records. *Reviews of Geophysics*, *52*(3), 333–374. https://doi.org/10.1002/2013RG000440PANGAEASupplementaryData

Muller, R. A., & MacDonald, G. J. (1997). Glacial cycles and astronomical forcing. *Science*, *277*(5323), 215–218. https://doi.org/10.1126/science.277.5323.215

Nilsson, A., Lee, Y. S., Snowball, I., & Hill, M. (2013). Magnetostratigraphic importance of secondary chemical remanent magnetizations carried by greigite (Fe3S4) in Miocene sediments, New Jersey shelf (IODP Expedition 313). *Geosphere*, *9*(3), 510–520. https://doi.org/10.1130/GES00854.1

Pellaton, C., & Gorin, G. E. (2005). The Miocene New Jersey Passive Margin as a Model for the Distribution of Sedimentary Organic Matter in Siliciclastic Deposits. *Journal of*

Sedimentary Research, *75*(6), 1011–1027. https://doi.org/10.2110/jsr.2005.076
Pettersson, H. (1951). Radium and Deep-Sea Chronology. *Nature*, *167*(4258), 942–942. https://doi.org/10.1038/167942a0
Reynolds, D. J., Steckler, M. S., & Coakley, B. J. (1991). The role of the sediment load in sequence stratigraphy: The influence of flexural isostasy and compaction. *Journal of Geophysical Research: Solid Earth*, *96*(B4), 6931–6949. https://doi.org/10.1029/90JB01914
Rubincam, D. P. (1994). Insolation in terms of Earth's orbital parameters. *Theoretical and Applied Climatology*, *48*(4), 195–202. https://doi.org/10.1007/BF00867049
Scargle, J. D. (1982). Studies in astronomical time series analysis. II. Statistical aspects of spectral analysis of unevenly spaced data. *\apj*, *263*, 835–853. https://doi.org/10.1086/160554
Urbat, M. (1996). Rock-Magnetic Properties of Pleistocene Passive Margin sediments: Environmental Change and Diagenesis offshore New Jersey. *Proc. ODP Sci. Res.*, *150*. https://doi.org/10.2973/odp.proc.sr.150.025.1996
van den Belt, F. J. G., van Hoof, T. B., & Pagnier, H. J. M. (2015). Revealing the hidden Milankovitch record from Pennsylvanian cyclothem successions and implications regarding late Paleozoic chronology and terrestrial-carbon (coal) storage. *Geosphere*, *11*(4), 1062–1076. https://doi.org/10.1130/GES01177.1
Van Wagoner, J., Posamentier, H. W., Mitchum, R., Vail, P. R., Sarg, J. F. F., Loutit, T. S., & Hardenbol, J. (1988). An overview of the fundamentals of sequence stratigraphy and key definitions. *The Society of Economic Paleontologists and Mineralogists*, *42*, 39–45. https://doi.org/10.2110/pec.88.01.0039
Vandenberghe, J. (2013). Grain size of fine-grained windblown sediment: A powerful proxy for process identification. *Earth-Science Reviews*, *121*, 18–30. https://doi.org/10.1016/j.earscirev.2013.03.001
Watts, A. B., & Steckler, M. S. (1979). *Subsidence and eustasy at the continental margin of eastern North America* (pp. 218–234). https://doi.org/10.1029/ME003p0218
Weedon, G. P. (2003). *Time-Series Analysis and Cyclostratigraphy: Examining Stratigraphic Records of Environmental Cycles*. Cambridge University Press. https://doi.org/DOI: 10.1017/CBO9780511535482
Wunsch, C. (2004). Quantitative estimate of the Milankovitch-forced contribution to observed Quaternary climate change. *Quaternary Science Reviews*, *23*(9–10), 1001–1012. https://doi.org/10.1016/j.quascirev.2004.02.014

CHAPTER 5 CONCLUSION AND FUTURE WORK

With the recent acceleration in global warming and ice-cover melting, sea-level rise and its effect on these low-lying areas have become a potential socio-economic hazard on a global scale. The New Jersey margin, with well-developed siliciclastic sequences of prominent clinoforms, has been a focus area for investigating the effects of eustatic changes on sedimentary systems. Large (>100m) sea-level changes have been occurring since the mid-Oligocene and have greatly affected sedimentation processes on this rifted margin (Mountain et al. 2007).

This research was the first to benefit from the MGL1510 3D seismic dataset to map and characterize paleo-sedimentological processes on the shelf. The 3D seismic imaging was used to map and characterize the nearshore sedimentary structure. Characterizing the sedimentological properties of these features and associated facies, that developed during periods of known eustatic variations, is essential to understanding the evolution of shorelines and quantifying timing and amplitude of the eustatic changes in each geological period.

5.1 The Geometrical Breakdown Approach to interpretation of stratigraphic sequences

Determining the trend of sedimentary properties within 76 systems tracts required a systematic approach for their identification. To address this problem, I developed the Geometrical Breakdown Approach that uses the geometry of depositional units and their spatial relationships as the basic criteria to determine the type of systems tracts, regardless of their deriving geological mechanisms. The approach is centred on the data-driven interpretation of seismic data that resulted in consistent and replicative identification of systems tracts.

5.2 Rock physics characteristics of sequences in a shallow-marine environment

These identified sequences provided a structural framework for geological and petrophysical analyses of the Miocene foresets. The elastic properties of shallow-marine unconsolidated sediments were characterized to determine their sedimentological parameters and spatial distributions within each stratigraphic sequence. The study conducted in the third chapter of this thesis suggests that the variation of sedimentary properties follows a spatially repeating

pattern within a clinothem. The petrophysical models introduced in this study allow incorporation of the deposits in a clinothem in more advanced well and seismic reservoir characterization techniques; understanding the variation of petrophysical properties in stratigraphic units is crucial for further quantitative interpretations.

5.3 Milancovitch cycles in the shallow-marine sedimentary records

A relatively stable tectonic history and rate of sediment supply in the Miocene left eustatic changes as the dominant controlling factor for imposing cyclicity in the sedimentary architectures along the margin. While previous studies suggest a correspondence between 1.2 Myr obliquity modulation cycles and third-order sequences, analyses of the seismic and well data from the Miocene sedimentary record yielded local spectral peaks at 25 Kyr and 40 Kyr in high-frequency, and 2.5 Myr in low-frequency spectra. These high- frequency spectral peaks correspond to the cyclicity observed in insolation due to changes in the axial tilt and precession of the Earth's orbit. This evidence showed the cyclic imprints of astronomically induced climate change in stratigraphic records in wide spectra, from 2.5 Myr to 25 Kyr. Despite the complexity and fragmentary nature of the stratigraphic records, the internal structure of the Miocene shallow-marine clinothems contains a strong record of orbitally-driven eustatic oscillations.

5.4 Future work

Four decades of research offshore New Jersey has created more scientific questions than concluding answers. The research work presented in this thesis is based on the MGL1510 3D seismic survey and the results from the IODP Expedition 313. The high resolution of seismic data integrated with more than 80% core recovery from the wells provided unprecedented data coverage within the study area. However, these data cover only a small portion of the Miocene sedimentary record.

The global ocean current simulations for the Miocene interval consistently show a strong Gulf Stream on the New Jersey shelf (von der Heydt & Dijkstra, 2006). The evidence of along-strike flow identified in the seismic volume, generated by extracting features with dipping seaward, are elongated in the NE-SW direction. These observed features suggest that

clinoform topsets were not subaerially exposed during the Miocene and the identified channel system caused the erosion of the topset strata. These channels are evidence of along-strike processes on high-energy continental shelves. Acquiring additional 3D seismic data on the shelf can yield understand the scale and extension of these along-strike features as well as the driving mechanisms causing 13° change in the direction of sediment flux in the past 30 Myr.

The Geometrical Breakdown Approach (GBA) can define a framework for automated interpretation of sequences and systems tracts, independent of their scale and the mechanisms underlying their formation. The results from two case studies presented in this dissertation suggest that the GBA can become a standard tool in interpreting the seismic stratigraphic features with a higher resolution than previously achieved. Coding a computer algorithm, based on the methodology defined in the second chapter, can reduce the time and work effort for applying the GBA to high-resolution seismic data with greater detail.

The introduced schematic models for sedimentary properties of the clinothem internal structure are based on the Miocene sedimentary record of the New Jersey margin, where eustasy has been considered the dominant driver for shaping the sedimentary record. In other places, a variety of controlling mechanisms such as tectonics, active sediment transport processes, and pre-existing structures can make similar impacts on a comparable scale to the sedimentary structure. Further work is required to assess the impact of other controlling mechanisms on the distribution of sedimentary properties in scenarios where they become the dominant controlling mechanism. Moreover, this study used a statistical approach to predict the volume of clay from acoustic impedance and other elastic properties driven from post-stack seismic data. Incorporating the prestack data and the variation of Vp/Vs ratio may enhance the accuracy of the predicted clay volume, and consequently, the schematic model for clay-volume distribution within clinothems.

Analysis of dip azimuth for the reflection packages shows that the direction of sediment flux has shifted from S14E in the early Miocene to S1E by the late Miocene-Pliocene. The poor age constraint and low signal to noise ratio of the seismic data for the pre-Miocene deposits made it challenging to analyze the change in the dip azimuth for these sediments. As such, driving mechanism for the rotation of the basin dipping direction is not clear. Mantle dynamics and isostatic rebounding can contribute to this shift in the basin dipping direction.

However, further work is needed to shed light on its underlying mechanisms and their impact on sedimentation within the continental shelf.

Spectral analyses of the onshore-offshore movements of systems tracts incorporated only those that were found within the MGL1510 3D seismic volume. The more regional 2D seismic lines have revealed numerous clinoforms both landward and seaward of the studied area. Expanding the geological time interval and study area to include more sequences and cycles of systems tracts would make it possible to better understand the impact of orbitally-driven insolation on sedimentary structures.

REFERENCES

Abels, H. A. (2008). *Long-period orbital climate forcing [PhD Thesis]* (Issue 297). Utrecht University.

Abels, H. A., Clyde, W. C., Gingerich, P. D., Hilgen, F. J., Fricke, H. C., Bowen, G. J., & Lourens, L. J. (2012). Terrestrial carbon isotope excursions and biotic change during Palaeogene hyperthermals. *Nature Geoscience*, *5*(5), 326–329. https://doi.org/10.1038/ngeo1427

Adhémar, J. A. (1842). *Revolutions of the Sea*.

Aitken, J. F., & Flint, S. S. (1995). The application of high-resolution sequence stratigraphy to fluvial systems: a case study from the Upper Carboniferous Breathitt Group, eastern Kentucky, USA. *Sedimentology*, *42*(1), 3–30. https://doi.org/10.1111/j.1365-3091.1995.tb01268.x

Algeo, thomas, & Wilkinson, B. (1988). Periodicity of Mesoscale Phanerozoic Sedimentary Cycles and the Role of Milankovitch Orbital Modulation. *Journal of Geology - J GEOL*, *96*, 313–322. https://doi.org/10.1086/629222

Ando, H., Oyama, M., & Nanayama, F. (2014). Data report: grain size distribution of Miocene successions, IODP Expedition 313 Sites M0027, M0028, and M0029, New Jersey shallow shelf. *Proceedings of the Integrated Ocean Drilling Program*, *313*. https://doi.org/10.2204/iodp.proc.313.201.2014

Angevine, C. L. (1989). Relationship of Eustatic Oscillations to Regressions and Transgressions on Passive Continental Margins. In *Origin and Evolution of Sedimentary Basins and Their Energy and Mineral Resources* (pp. 29–35). American Geophysical Union (AGU). https://doi.org/10.1029/GM048p0029

Arvidsson, R. (1996). Fennoscandian Earthquakes : Whole Crustal Rupturing Related to Postglacial Rebound. *Science*, *274*(5288), 744–746. http://www.jstor.org/stable/2891742

Aubry, M.-P. (1991). Sequence stratigraphy: Eustasy or tectonic imprint? *Journal of Geophysical Research: Solid Earth*, *96*(B4), 6641–6679. https://doi.org/10.1029/90JB01204

Avseth, P., Mukerji, T., Mavko, G., & Dvorkin, J. (2010). Rock-physics diagnostics of

depositional texture, diagenetic alterations, and reservoir heterogeneity in high-porosity siliciclastic sediments and rocks - A review of selected models and suggested work flows. *Geophysics*, *75*(5). https://doi.org/10.1190/1.3483770

Bailey, R. J. (1998). *Review : Stratigraphy , meta-stratigraphy and chaos*.

Bailey, R. J. (2009). Cyclostratigraphic reasoning and orbital time calibration. *Terra Nova*, *21*(5), 340–351. https://doi.org/10.1111/j.1365-3121.2009.00890.x

Barclay, F., Bruun, A., Rasmussen, K. B., Alfaro, J. C., Cooke, A., Cooke, D. A., Salter, D., Godfrey, R., Lowden, D., Steve, M., Ozdemir, H., Pickering, S., Pineda, F. G., Herwanger, J., Volterrani, S., Murineddu, Andrea Rasmussen, A., & Roberts, R. (2007). Seismic Inversion : Reading Between the Lines. *Oilfield Review*, 42–63.

Beardsley, R. C., & Boicourt, W. C. (1981). On Estuarine and Atlantic Bight. *Evolution of Physical Oceanography*, 198–233. https://ocw.mit.edu/resources/res-12-000-evolution-of-physical-oceanography-spring-2007/part-1/wunsch_chapter7.pdf%5Cnhttp://ocw.mit.edu/resources/res-12-000-evolution-of-physical-oceanography-spring-2007/index.htm

Beaumont, C. (2007). The evolution of sedimentary basins on a viscoelastic lithosphere: Theory and examples. In *Geophysical Journal of the Royal Astronomical Society* (Vol. 55). https://doi.org/10.1111/j.1365-246X.1978.tb04283.x

Behrmann, S. K. J., Völker, D., Stipp, M., Berndt, C., Urgeles, R., Chaytor, J. D., & Huhn, K. (2003). *Submarine Mass Movements and Their Consequences* (Vol. 19). https://doi.org/10.1007/978-94-010-0093-2

Berger, A., Loutre, M. F., & Mélice, J. L. (2006). Climate of the Past Equatorial insolation: from precession harmonics to eccentricity frequencies *. *Clim. Past*, *2*, 131–136.

Bohacs, K. M. (1998). Contrasting expressions of depositional sequences in mudrocks from marine to non marine environs. *Basin Studies, Sedimentology, and Paleontology*, *1*, 33–78.

Bosence, D. W. J., Holloway, R., Flint, S., & Howell, J. (2003). *The Sedimentary Record of Sea-Level Change* (Issue June). https://doi.org/10.2277/0521831113

Bosmans, J., Drijfhout, S., Tuenter, E., Lourens, L., Hilgen, F., & Weber, S. L. (2011).

Monsoonal response to mid-holocene orbital forcing in a high resolution GCM. *Climate of the Past Discussions*, *7*. https://doi.org/10.5194/cpd-7-3609-2011

Boulila, S., Galbrun, B., Miller, K. G., Pekar, S. F., Browning, J. V., Laskar, J., & Wright, J. D. (2011). On the origin of Cenozoic and Mesozoic "third-order" eustatic sequences. *Earth-Science Reviews*, *109*(3–4), 94–112. https://doi.org/10.1016/j.earscirev.2011.09.003

Boyd, R., Ruming, K., Goodwin, I., Sandstrom, M., & Schröder-Adams, C. (2008). Highstand transport of coastal sand to the deep ocean: A case study from Fraser Island, southeast Australia. *Geology*, *36*(1), 15–18. https://doi.org/10.1130/G24211A.1

Bradley, D. C. (2008). Passive margins through earth history. *Earth-Science Reviews*, *91*(1–4), 1–26. https://doi.org/10.1016/j.earscirev.2008.08.001

Browning, J. V., Miller, K. G., McLaughlin, P. P., Kominz, M. A., Sugarman, P. J., Monteverde, D., Feigenson, M. D., & Hernández, J. C. (2006). Quantification of the effects of eustasy, subsidence, and sediment supply on Miocene sequences, mid-Atlantic margin of the United States. *Bulletin of the Geological Society of America*, *118*(5–6), 567–588. https://doi.org/10.1130/B25551.1

Browning, J. V., Miller, K. G., Sugarman, P. J., Barron, J. A., McCarthy, F. M. G. G., Kulhanek, D. K., Katz, M. E., & Feigenson, M. D. (2013). Chronology of Eocene–Miocene sequences on the New Jersey shallow shelf: Implications for regional, interregional, and global correlations. *Geosphere*, *9*(6), 1434–1456. https://doi.org/10.1130/GES00853.1

Browning, J. V., Miller, K. G., Sugarman, P. J., Kominz, M. A., Mclaughlin, P. P., Kulpecz, A. A., & Feigenson, M. D. (2008). 100 Myr record of sequences, sedimentary facies and sea level change from Ocean Drilling Program onshore coreholes, US Mid-Atlantic coastal plain. *Basin Research*, *20*(2), 227–248. https://doi.org/10.1111/j.1365-2117.2008.00360.x

Brune, S. (2016). Rifts and Rifted Margins: A Review of Geodynamic Processes and Natural Hazards. *Plate Boundaries and Natural Hazards*, 11–37. https://doi.org/10.1002/9781119054146.ch2

Brune, S., Babeyko, A. Y., Ladage, S., & Sobolev, S. V. (2010). Landslide tsunami hazard in the Indonesian Sunda Arc. *Natural Hazards and Earth System Science*, *10*(3), 589–604. https://doi.org/10.5194/nhess-10-589-2010

Burbank, D., & Anderson, R. (2011). *Tectonic Geomorphology*. wiley.

Burgess, P. M., Allen, P. A., & Steel, R. J. (2016). Introduction to the future of sequence stratigraphy: Evolution or revolution? *Journal of the Geological Society*, *173*(5), 801–802. https://doi.org/10.1144/jgs2016-078

Burgess, P. M., Lammers, H., van Oosterhout, C., & Granjeon, D. (2006). Multivariate sequence stratigraphy: Tackling complexity and uncertainty with stratigraphic forward modeling, multiple scenarios, and conditional frequency maps. *AAPG Bulletin*, *90*(12), 1883–1901. https://doi.org/10.1306/06260605081

Busch, R. M., & Rollins, H. B. (1984). Correlation of Carboniferous strata using a hierarchy of transgressive- regressive units. *Geology*, *12*(8), 471–474. https://doi.org/10.1130/0091-7613(1984)12<471:COCSUA>2.0.CO;2

Butman, B., Noble, M., & Folger, D. W. (1979). Long-term observations of bottom current and bottom sediment movement on the mid-Atlantic continental shelf. *Journal of Geophysical Research: Oceans*, *84*(C3), 1187–1205. https://doi.org/10.1029/JC084iC03p01187

Cacchione, D. A., Drake, D. E., Losada, M. A., & Medina, R. (1990). Bottom-boundary-layer measurements on the continental shelf off the Ebro River, Spain. *Marine Geology*, *95*(3–4), 179–192. https://doi.org/10.1016/0025-3227(90)90115-Z

Camargo, J. M. R., Silva, M. V. B., Júnior, A. V. F., & Araújo, T. C. M. (2019). Marine geohazards: A bibliometric-based review. *Geosciences (Switzerland)*, *9*(2). https://doi.org/10.3390/geosciences9020100

Carlson, A. (2011). Ice sheets and sea level in Earth's past. *Nature Education Knowledge*, *3*.

Carter, R. M., Fulthorpe, C. S., & Lu, H. (2004). Canterbury drifts at Ocean Drilling Program site 1119, New Zealand: Climatic modulation of southwest Pacific intermediate water flows since 3.9 Ma. *Geology*, *32*(11), 1005–1008. https://doi.org/10.1130/G20783.1

Cartwright, J. J., & Dewhurst, D. N. (1998). Layer-bound compaction faults in fine-grained sediments. *Bulletin of the Geological Society of America*, *110*(10), 1242–1257. https://doi.org/10.1130/0016-7606(1998)110<1242:LBCFIF>2.3.CO;2

Cartwright, Joe, James, D., & Bolton, A. (2003). The genesis of polygonal fault systems: a

review. *Geological Society, London, Special Publications*, *216*(1), 223–243. https://doi.org/10.1144/GSL.SP.2003.216.01.15

Cartwright, Joseph. (1994a). Cartwright, 1994 - Episodic basin-wide fluid expulsion from geopressured sahle sequences in the North sea basin. *Geology*, *22*(5), 447–450.

Cartwright, Joseph. (1994b). Episodic basin-wide hydrofracturing of overpressured Early Cenozoic mudrock sequences in the North Sea Basin. *Marine and Petroleum Geology*, *11*(5), 587–607. https://doi.org/https://doi.org/10.1016/0264-8172(94)90070-1

Cathro, D. L., Austin, J. A., & Moss, G. D. (2003). Progradation along a deeply submerged Oligocene-Miocene heterozoan carbonate shelf: How sensitive are clinoforms to sea level variations? *American Association of Petroleum Geologists Bulletin*, *87*(10), 1547–1574. https://doi.org/10.1306/05210300177

Catuneanu, O. (2017). Sequence Stratigraphy: Guidelines for a Standard Methodology. In *Advances in Sequence Stratigraphy* (1st ed., Vol. 2, Issue September). Elsevier Inc. https://doi.org/10.1016/bs.sats.2017.07.003

Catuneanu, O., Abreu, V., Bhattacharya, J. P., Blum, M. D., Dalrymple, R. W., Eriksson, P. G., Fielding, C. R., Fisher, W. L., Galloway, W. E., Gibling, M., Giles, K. A., Holbrook, J. M., Jordan, R., Kendall, ; Christopher G. St. C., Macurda, B., Martinsen, O. J., Miall, A., Neal, J. E., Nummedal, D., … Winker, C. (2009). Towards the standardization of sequence stratigraphy. *Earth-Science Reviews*, *92*(1–2), 1–33. https://doi.org/10.1016/j.earscirev.2008.10.003

Catuneanu, O., Bhattacharya, J. P., Blum, M. D., Dalrymple, R. W., Eriksson, P. G., & Fielding, C. R. (2010). Sequence stratigraphy : common ground after three decades of development. *First Break*, *28*(January), 21–34.

Cecil, C. (2003). The concept of autocyclic and allocyclic controls on sedimentation and stratigraphy, emphasizing the climatic variable. *Journal of Sedimentary Research*, *Special Pu*, 13–20.

Chopra, S., Castagna, J. P., & Xu, Y. (2009). When Thin Is In – Relative Acoustic Impedance Helps. *Frontiers + Innovation – CSPG CSEG CWLS Convention*, 705–708.

Christie-Blick, N., Mountain, G. S., & Miller, K. G. (1990). Seismic Stratigraphic Record of Sea-Level Change. *Sea-Level Change*, *JANUARY 1990*, 116–140.

Clarke, S., Hubble, T., Airey, D., Yu, P., Boyd, R., Keene, J., Exon, N., Gardner, J., & Ward, S. (2014). Morphology of Australia's eastern continental slope and related tsunami hazard. *Advances in Natural and Technological Hazards Research*, *37*(July), 529–538. https://doi.org/10.1007/978-3-319-00972-8_47

Clausen, J. A., Gabrielsen, R. H., Reksnes, P. A., & Nysæther, E. (1999). Development of intraformational (Oligocene-Miocene) faults in the northern North Sea: Influence of remote stresses and doming of Fennoscandia. *Journal of Structural Geology*, *21*(10), 1457–1475. https://doi.org/10.1016/S0191-8141(99)00083-8

Colombo, D. (2005). Benefits of wide-offset seismic for commercial exploration targets. *Leading Edge*.

Cooke, D. A. (1983). Generalized linear inversion of reflection seismic data. In *Geophysics* (Vol. 48, Issue 6, p. 665). https://doi.org/10.1190/1.1441497

Croll, J. (1864). XIII. On the physical cause of the change of climate during geological epochs. *The London, Edinburgh, and Dublin Philosophical Magazine and Journal of Science*, *28*(187), 121–137. https://doi.org/10.1080/14786446408643733

Csato, I., Granjeon, D., Catuneanu, O., & Baum, G. R. (2013). A three-dimensional stratigraphic model for the Messinian crisis in the Pannonian Basin, eastern Hungary. *Basin Research*, *25*(2), 121–148. https://doi.org/10.1111/j.1365-2117.2012.00553.x

de Boer, B., van de Wal, R. S. W., Lourens, L. J., Bintanja, R., & Reerink, T. J. (2013). A continuous simulation of global ice volume over the past 1 million years with 3-D ice-sheet models. *Climate Dynamics*, *41*(5), 1365–1384. https://doi.org/10.1007/s00382-012-1562-2

Degirmency, T. (2014). Upper Middle to Upper Miocene Seismic Sequences, New Jersey Middle to Outer Continental Shelf. *MSc Dissertation*.

Draper, N., & Smith, H. (1966). Applied regression analysis. In *John Wiley & Sons*. https://doi.org/10.1002/bimj.19690110613

Driscoll, N. W., & Hogg, J. R. (1995). Stratigraphic response to basin formation: Jeanne d'Arc

Basin, offshore Newfoundland. *Geological Society Special Publication*, *80*(80), 145–163. https://doi.org/10.1144/GSL.SP.1995.080.01.07

Driscoll, N. W., & Karner, G. D. (1999). Three-dimensional quantitative modeling of clinoform development. *Marine Geology*, *154*(1–4), 383–398. https://doi.org/10.1016/S0025-3227(98)00125-X

Einsele, G., Chough, S. K., & Shiki, T. (1996). Depositional events and their records - an introduction. *Sedimentary Geology*, *104*(1–4), 1–9. https://doi.org/10.1016/0037-0738(95)00117-4

Einsele, G., Ricken, W., & Seilacher, A. (1991). *Cycles and Events in Stratigraphy*.

Embry, A. (2009). Practical Sequence Stratigraphy. *Canadian Society of Petroleum Geologists*, 1–79. https://doi.org/10.1017/CBO9781107415324.004

Embry, A., & Johannessen, E. P. (2017). Two Approaches to Sequence Stratigraphy. In *Advances in Sequence Stratigraphy* (1st ed., Vol. 2). Elsevier Inc. https://doi.org/10.1016/bs.sats.2017.08.001

Emery, K. O. (1968). *Positions of empty pelecypod valves on the continental shelf*. *38*(4), 1264–1269.

Emiliani, C. (1955). Pleistocene Temperatures. *The Journal of Geology*, *63*(6), 538–578. https://doi.org/10.1086/626295

Eriksson, P. G., Banerjee, S., Catuneanu, O., Corcoran, P. L., Eriksson, K. A., Hiatt, E. E., Laflamme, M., Lenhardt, N., Long, D. G. F. F., Miall, A., Mints, M. V., Pufahl, P. K., Sarkar, S., Simpson, E. L., & Williams, G. E. (2013). Secular changes in sedimentation systems and sequence stratigraphy. *Gondwana Research*, *24*(2), 468–489. https://doi.org/10.1016/j.gr.2012.09.008

Fielding, C. R. (1984). Upper delta plain lacustrine and fluviolacustrine facies from the Westphalian of the Durham coalfield, NE England. *Sedimentology*, *31*(4), 547–567. https://doi.org/10.1111/j.1365-3091.1984.tb01819.x

Fine, I. V., Rabinovich, A. B., Bornhold, B. D., Thomson, R. E., & Kulikov, E. A. (2005). The Grand Banks landslide-generated tsunami of November 18, 1929: Preliminary analysis and

numerical modeling. *Marine Geology*, *215*(1-2 SPEC. ISS.), 45–57. https://doi.org/10.1016/j.margeo.2004.11.007

Frigola, A., Prange, M., & Schulz, M. (2018). Boundary conditions for the Middle Miocene Climate Transition (MMCT v1.0). *Geoscientific Model Development*, *11*(4), 1607–1626. https://doi.org/10.5194/gmd-11-1607-2018

Fulthorpe, C. S. (1991). Geological controls on seismic sequence resolution. *Geology*, *19*(1), 61–65. https://doi.org/10.1130/0091-7613(1991)019<0061:GCOSSR>2.3.CO;2

Fulthorpe, C. S., & Austin, J. A. (2008). Assessing the significance of along-strike variations of middle to late Miocene prograding clinoformal sequence geometries beneath the New Jersey continental shelf. *Basin Research*, *20*(2), 269–283. https://doi.org/10.1111/j.1365-2117.2008.00350.x

Fulthorpe, C. S., Austin, J. A., & Mountain, G. S. (1999). Buried fluvial channels off New Jersey: Did sea-level lowstands expose the entire shelf during the Miocene? *Geology*, *27*(3), 203–206. https://doi.org/10.1130/0091-7613(1999)027<0203:BFCONJ>2.3.CO;2

Fulthorpe, C. S., Austin, J. A., & Mountain, G. S. (2000). Morphology and distribution of Miocene slope incisions of New Jersey: Are they diagnostic of sequence boundaries? *Bulletin of the Geological Society of America*, *112*(6), 817–828. https://doi.org/10.1130/0016-7606(2000)112<817:MADOMS>2.0.CO;2

Fulthorpe, C. S., Miller, K. G., Droxler, A. W., Hesselbo, S. P., Camoin, G. F., & Kominz, M. A. (2008). Drilling to decipher long-term sea-level changes and effects - A joint consortium for ocean leadership, ICDP, IODP, DOSECC, and Chevron Workshop. *Scientific Drilling*, *6*, 19–28. https://doi.org/10.2204/lodp.sd.6.02.2008

Gallegos, G. (2017). Lower Miocene (ca . 20-18 Ma) New Jersey Sequence Stratigraphy : Architecture and Onshore-Offshore Correlations. *MSc Dissertation*.

Galloway, W. E. (1989). Genetic stratigraphic sequences in basin analysis II: application to northwest Gulf of Mexico Cenozoic basin. *American Association of Petroleum Geologists Bulletin*, *73*(2), 143–154. https://doi.org/10.1306/703C9AFA-1707-11D7-8645000102C1865D

Galloway, W. E. (2008). Chapter 15 Depositional Evolution of the Gulf of Mexico Sedimentary Basin. In *Sedimentary Basins of the World* (Vol. 5, Issue C). Elsevier. https://doi.org/10.1016/S1874-5997(08)00015-4

Galloway, W. E., Ganey-Curry, P. E., Li, X., & Buffler, R. T. (2000). Cenozoic depositional history of the Gulf of Mexico basin. *AAPG Bulletin*, *11*(11), 1743–1774. https://doi.org/10.1306/8626C37F-173B-11D7-8645000102C1865D

Girkin, A. N. (2005). *A computational study on the evolution of the dynamics of the obliquity of the earth*. Miami University.

Goff, J. A., Swift, D. J. P. P., Duncan, C. S., Mayer, L. A., & Hughes-Clarke, J. (1999). High-resolution swath sonar investigation of sand ridge, dune and ribbon morphology in the offshore environment of the New Jersey margin. *Marine Geology*, *161*(2–4), 307–337. https://doi.org/10.1016/S0025-3227(99)00073-0

Goldner, A., Ramstein, G., Favre, E., Utescher, T., Hamon, N., Munhoven, G., Erdei, B., Krapp, M., Dury, M., Henrot, A.-J., François, L., & Herold, N. (2016). Middle Miocene climate and vegetation models and their validation with proxy data. *Palaeogeography, Palaeoclimatology, Palaeoecology*, *467*, 95–119. https://doi.org/10.1016/j.palaeo.2016.05.026

Gong, D., Kohut, J., & Glenn, S. (2008). Seasonal Climatology of Wind-Driven Circulation on the NJ Shelf. *AGU Fall Meeting Abstracts*.

Goodwin, P. W., Anderson, E. J., Goodman, W. M., & Saraka, L. J. (1986). Punctuated aggradational cycles: Implications for stratigraphic analysis. *Paleoceanography*, *1*(4), 417–429. https://doi.org/10.1029/PA001i004p00417

Goulty, N. (2001). Polygonal fault networks in fine-grained sediments - An alternative to the syneresis mechanism. In *First Break* (Vol. 19). https://doi.org/10.1046/j.1365-2397.2001.00137.x

Greb, S. F., Pashin, J. C., Martino, R. L., & Eble, C. F. (2008). Appalachian sedimentary cycles during the Pennsylvanian: Changing influences of sea level, climate, and tectonics. In *Special Paper 441: Resolving the Late Paleozoic Ice Age in Time and Space* (pp. 235–248). Geological Society of America. https://doi.org/10.1130/2008.2441(16)

Greenlee, S. M., Devlin, W. J., Miller, K. G., Mountain, G. S., & Flemings, P. B. (1992). Integrated sequence stratigraphy of Neogene deposits, New Jersey continental shelf and slope: comparison with the Exxon model. *Geological Society of America Bulletin*, *104*(11), 1403–1411. https://doi.org/10.1130/0016-7606(1992)104<1403:ISSOND>2.3.CO;2

Grow, J. A., & Sheridan, R. E. (1988). U.S. Atlantic Continental Margin; A typical Atlantic-type or passive continental margin. In Robert E Sheridan & J. A. Grow (Eds.), *The Atlantic Continental Margin*. Geological Society of America. https://doi.org/10.1130/DNAG-GNA-I2.1

Guillaume, B., Pochat, S., Monteux, J., Husson, L., & Choblet, G. (2016). Can eustatic charts go beyond first order? Insights from the Permian-Triassic. *Lithosphere*, *8*(5), 505–518. https://doi.org/10.1130/L523.1

Hampson, D. P., Schuelke, J. S., & Quirein, J. A. (2001). Use of multiattribute transforms to predict log properties from seismic data. *Geophysics*, *66*(1), 220–236. https://doi.org/10.1190/1.1444899

Hampton, M. A., Lee, H. J., & Locat, J. (1996). Submarine landslides. *Reviews of Geophysics*, *34*(1), 33–59. https://doi.org/10.1029/95RG03287

Haq, B. U., Hardenbol, J., & Vail, P. R. (1987). Chronology of Fluctuating Sea Levels Since the Triassic. *Science*, *235*(4793), 1156–1167. https://doi.org/10.1126/science.235.4793.1156

Harbitz, C. B., Løvholt, F., & Bungum, H. (2014). Submarine landslide tsunamis: How extreme and how likely? *Natural Hazards*, *72*(3), 1341–1374. https://doi.org/10.1007/s11069-013-0681-3

Hays, J. D., Imbrie, J., & Shackleton, N. J. J. (1976). Variations in the Earth ' s Orbit : Pacemaker of the Ice Ages. *Science*, *194*(4270). https://doi.org/10.1126/science.194.4270.1121

Heckel, P. H. (1987). Reply on "Sea-level curve for Pennsylvanian eustatic marine transgressive-regressive depositional cycles along midcontinent outcrop belt, North America." *Geology*, *15*(3), 276–278. https://doi.org/10.1130/0091-7613(1987)15<276b:CAROSC>2.0.CO;2

Heezen, B. C., Tharp, M., & Ewing, M. (Eds.). (1959). *The Floors of the Oceans: I. The North*

Atlantic. https://doi.org/10.1130/SPE65

Heidbach, O., Tingay, M., Barth, A., Reinecker, J., Kurfeß, D., & Müller, B. (2010). Global crustal stress pattern based on the World Stress Map database release 2008. *Tectonophysics*, *482*(1–4), 3–15. https://doi.org/10.1016/j.tecto.2009.07.023

Helland-Hansen, W., & G. Gjelberg, J. (1994). Conceptual basis and variability in Sequence stratigraphy: a different perspective. In *Sedimentary Geology* (Vol. 92). https://doi.org/10.1016/0037-0738(94)90053-1

Helland-Hansen, W., & Hampson, G. J. (2009). Trajectory analysis: Concepts and applications. *Basin Research*, *21*(5), 454–483. https://doi.org/10.1111/j.1365-2117.2009.00425.x

Helland-Hansen, W., & J. Martinsen, O. (1996). Shoreline Trajectories and Sequences: description of Variable Depositional-Dip Scenarios. In *Journal of Sedimentary Research* (Vol. 66).

Hendra, W. (2010). Lithofacies and Depositional Environment Spanning the Cretaceous-Paleogene Boundary on the New Jersey Coastal Plain. *MSc Dissertation*, *5*(1976), 265–288.

Henriet, J. P., De Batist, M., Van Vaerenbergh, W., & Verschuren, M. (1989). Seismic facies and clay tectonic features in the southern North Sea. *Bulletin of the Belgian Geological Society*, *97*, 457–472.

Henriksen, S., Hampson, G. J., Helland-Hansen, W., Johannessen, E. P., & Steel, R. J. (2009). Shelf edge and shoreline trajectories, a dynamic approach to stratigraphic analysis. *Basin Research*, *21*(5), 445–453. https://doi.org/10.1111/j.1365-2117.2009.00432.x

Henry, H., & Ran, E. (1994). Late Pliocene-Pleistocene high resolution pollen sequence of Colombia: An overview of climatic change. In *Quaternary International* (Vol. 21). https://doi.org/10.1016/1040-6182(94)90021-3

Herold, N., Huber, M., & Müller, R. D. (2011). Modeling the Miocene Climatic Optimum. Part I: Land and Atmosphere*. *Journal of Climate*, *24*(24), 6353–6372. https://doi.org/10.1175/2011jcli4035.1

Higgs, W. G., & McClay, K. R. (2008). Analogue sandbox modelling of Miocene extensional faulting in the Outer Moray Firth. *Geological Society, London, Special Publications*, *71*(1),

141–162. https://doi.org/10.1144/gsl.sp.1993.071.01.07

Hilgen, F. J., Hinnov, L. A., Abdul Aziz, H., Abels, H. A., Batenburg, S., Bosmans, J., de Boer, B., Hüsing, S. K., Kuiper, K. F., Lourens, L. J., Rivera, T., Tuenter, E., Van de Wal, R. S. W., Wotzlaw, J. F., & Zeeden, C. (2015). Stratigraphic continuity and fragmentary sedimentation: The success of cyclostratigraphy as part of integrated stratigraphy. *Geological Society Special Publication*, *404*, 157–197. https://doi.org/10.1144/SP404.12

Hinnov, L. A. (2000). *New perspectives on orbitally forced stratigraphy*. *12*(8), 727–732. https://doi.org/10.1177/0741713604268894

Hinnov, L. A. (2013). Cyclostratigraphy and its revolutionizing applications in the earth and planetary sciences. *Bulletin of the Geological Society of America*, *125*(11–12), 1703–1734. https://doi.org/10.1130/B30934.1

Hinnov, L. A., & Hilgen, F. (2012). Cyclostratigraphy and Astrochronology. In *The Geological Time Scale* (Vol. 2012, pp. 63–83). https://doi.org/10.1016/B978-0-444-59425-9.00004-4

Hinnov, L. A., & Ogg, J. G. G. (2007). Cylostratigraphy and the Astronomical Time Scale. *Beyond the GSSP: New Developments in Chronostratigraphy*, 239–251.

Hodgson, D. M., Browning, J. V., Miller, K. G., Hesselbo, S. P., Poyatos-Moré, M., Mountain, G. S., & Proust, J. N. (2017). Sedimentology, stratigraphic context, and implications of Miocene intrashelf bottomset deposits, offshore New Jersey. *Geosphere*, *14*(1), 95–114. https://doi.org/10.1130/GES01530.1

Holbrook, J. M., Kuhnt, W., Schulz, M., Flores, J. A., & Andersen, N. (2007). Orbitally-paced climate evolution during the middle Miocene "Monterey" carbon-isotope excursion. *Earth and Planetary Science Letters*, *261*(3–4), 534–550. https://doi.org/10.1016/j.epsl.2007.07.026

Hossain, Z., Mukerji, T., Dvorkin, J., & Fabricius, I. L. (2011). Rock physics model of glauconitic greensand from the North Sea. *Geophysics*, *76*(6), E199--E209. https://doi.org/10.1190/geo2010-0366.1

Houghton, J. T., L.G. Meira Filho, B.A. Callander, N. H., Maskell, A. K. and K., & K. (1996). *The science of climate change. contribution of working group 1 to the second assessment*

report of the intergovernmental panel. 588. https://doi.org/10.1017/CBO9781107415324.004

Hoyal, D. C. J. D., & Sheets, B. A. (2009). Morphodynamic evolution of experimental cohesive deltas. *JOURNAL OF GEOPHYSICAL RESEARCH*, *114*(January), 1–18. https://doi.org/10.1029/2007JF000882

Hunt, D., & Tucker, M. E. (1992). Stranded parasequences and the forced regressive wedge systems tract: deposition during base-level'fall. *Sedimentary Geology*, *81*(1–2), 1–9. https://doi.org/10.1016/0037-0738(92)90052-S

Huybers, P., & Wunsch, C. (2003). Rectification and precession signals in the climate system. *Geophysical Research Letters*, *30*(19). https://doi.org/10.1029/2003GL017875

Imbrie, J., Hays, J. D., Martinson, D. G., McIntyre, A., Mix, A. C., Morley, J. J., Pisias, N. G., Prell, W. L., & Shackleton, N. J. (1984). The orbital theory of Pleistocene climate: Support from a revised chronology of the marine d18O record. *Milankovitch and Climate: Understanding the Response to Astronomical Forcing*, *1*(January), 269–305. https://doi.org/-

Intergovernmental panel on climate change. (2018). *Intergovernmental panel on climate change (IPCC) report*. *June*.

Inwood, J., Lofi, J., Davies, S., Basile, C., Bjerum, C., Mountain, G. S., Proust, J. N., Otsuka, H., & Valppu, H. (2013). Statistical classifi cation of log response as an indicator of facies variation during changes in sea level: Integrated Ocean Drilling Program Expedition 313. *Geosphere*, *9*(4), 1025–1043. https://doi.org/10.1130/GES00913.1

JERVEY, M. T. (1988). Quantitative Geological Modeling of Siliciclastic Rock Sequences and Their Seismic Expression. In C. K. Wilgus, B. S. Hastings, H. Posamentier, J. Van Wagoner, C. A. Ross, & C. G. S. C. Kendall (Eds.), *Sea-Level Changes* (pp. 47–69). SEPM (Society for Sedimentary Geology). https://doi.org/10.2110/pec.88.01.0047

John, C. M., Mutti, M., & Adatte, T. (2003). Mixed carbonate-siliciclastic record on the North African margin (Malta) - Coupling of weathering processes and mid Miocene climate. *Bulletin of the Geological Society of America*, *115*(2), 217–229. https://doi.org/10.1130/0016-7606(2003)115<0217:MCSROT>2.0.CO;2

Kallweit, R. S., & Wood, L. C. (1982). The limits of resolution of zero-phase wavelets. *Geophysics*, *47*(7), 1035–1046. https://doi.org/10.1190/1.1441367

Karner, G. D., & Driscoll, N. W. (1997). Three-dimensional interplay of advective and diffusive processes in the generation of sequence boundaries. *Journal of the Geological Society*, *154*(3), 443–449. https://doi.org/10.1144/gsjgs.154.3.0443

Karner, G. D., & Watts, A. B. (1982). On isostasy at Atlantic type margins. *Journal of Geophysical Research*, *87*, 2923–2984.

Katz, M. E., Browning, J. V., Miller, K. G., Monteverde, D. H., Mountain, G. S., & Williams, R. H. (2013). Paleobathymetry and sequence stratigraphic interpretations from benthic foraminifera: Insights on New Jersey shelf architecture, IODP Expedition 313. *Geosphere*, *9*(6), 1488–1513. https://doi.org/10.1130/GES00872.1

Keen, C. E., & Beaumont, C. (1990). Geodynamics of Rifted Continental Margins. In M. J. Keen & G. L. Williams (Eds.), *Geology of the Continental Margin of Eastern Canada*. Geological Society of America. https://doi.org/10.1130/DNAG-GNA-I1.391

Keller, G., & Barron, J. A. (1983). *Occurrence of hiatuses PH and NH 1 through NH 7 in DSDP holes*. PANGAEA. https://doi.org/10.1594/PANGAEA.719185

Kendall, C. G. S. C., Strobel, J., Cannon, R., Bezdek, J., & Biswas, G. (1991). *The simulation of the sedimentary fill of basins*. *96*(90), 6911–6929.

Kim, W., Paola, C., Voller, V., & Swenson, J. B. (2014). *Experimental Measurement of the Relative Importance of Controls on Shoreline Migration*. *July*. https://doi.org/10.2110/jsr.2006.019

Knorr, G., & Lohmann, G. (2014). Climate warming during Antarctic ice sheet expansion at the Middle Miocene transition. *Nature Geoscience*, *7*(5), 376–381. https://doi.org/10.1038/ngeo2119

Kominz, M. A., Miller, K. G., & Browning, J. V. (1998). Long-term and short-term global Cenozoic sea-level estimates. *Geology*, *7613*(4), 311–314. https://doi.org/10.1130/0091-7613(1998)026<0311

Kominz, M. A., Miller, K. G., Browning, J. V., Katz, M. E., & Mountain, G. S. (2016). Miocene

relative sea level on the New Jersey shallow continental shelf and coastal plain derived from one-dimensional backstripping: A case for both eustasy and epeirogeny. *Geosphere*, *12*(5), 1437–1456. https://doi.org/10.1130/GES01241.1

Kominz, M. A., & Pekar, S. F. (2001). Oligocene eustasy from two-dimensional sequence stratigraphic backstripping. *Bulletin of the Geological Society of America*, *113*(3), 291–304. https://doi.org/10.1130/0016-7606(2001)113<0291:OEFTDS>2.0.CO;2

Kominz, M. A., van Sickel, W. A., Miller, K. G., & Browning, J. V. (2002). Sea-Level Estimates for the Latest 100 Million Years : One- Dimensional Backstripping of Onshore New Jersey Boreholes. *Gcssepm2002*, 303–316. https://doi.org/10.1016/j.nrl.2009.12.006

Kopp, R. E., Horton, R. M., Little, C. M., Mitrovica, J. X., Oppenheimer, M., Rasmussen, D. J., Strauss, B. H., & Tebaldi, C. (2014). Probabilistic 21st and 22nd century sea-level projections at a global network of tide-gauge sites. *Earth's Future*, *2*(8), 383–406. https://doi.org/10.1002/2014EF000239

Korup, O. (2012). Earth's portfolio of extreme sediment transport events. *Earth-Science Reviews*, *112*(3–4), 115–125. https://doi.org/10.1016/j.earscirev.2012.02.006

Kotthoff, U., Greenwood, D. R., McCarthy, F. M. G. G., Müller-Navarra, K., Prader, S., & Hesselbo, S. P. (2014). Late Eocene to middle Miocene (33 to 13 million years ago) vegetation and climate development on the North American Atlantic Coastal Plain (IODP Expedition 313, Site M0027). *Climate of the Past*, *10*(4), 1523–1539. https://doi.org/10.5194/cp-10-1523-2014

Kullenberg, B. (1947). *The piston core sampler*.

Kulp, S., & Strauss, B. H. (2016). Global DEM Errors Underpredict Coastal Vulnerability to Sea Level Rise and Flooding. *Frontiers in Earth Science*, *4*(April), 1–8. https://doi.org/10.3389/feart.2016.00036

Kutterolf, S., Jegen, M., Mitrovica, J. X., Kwasnitschka, T., Freundt, A., & Huybers, P. J. (2013). A detection of Milankovitch frequencies in global volcanic activity. *Geology*, *41*(2), 227–230. https://doi.org/10.1130/G33419.1

Kutterolfa, S., Schindlbeckb, J. C. C., Jegena, M., Freundta, A., & Straubc, S. M. M. (2018).

Milankovitch frequencies in tephra records at volcanic arcs: The relation of kyr-scale cyclic variations in volcanism to global climate changes. *Quaternary Science Reviews*. https://doi.org/10.1080/09654313.2014.916254

Laskar, J., Fienga, A., Gastineau, M., & Manche, H. (2011). *La2010: A new orbital solution for the long term motion of the Earth*. *March 2011*. https://doi.org/10.1051/0004-6361/201116836

Laskar, J., Roboutel, P., Joutel, F., Gastineau, M., Correia, A. C. M., & Levrard, B. (2004). Long-term solution for the insolation quantities of the Earth. *Proceedings of the International Astronomical Union*, *2*(14), 465. https://doi.org/10.1017/S1743921307011404

Lavier, L. L., Steckler, M. S., & Brigaud, F. (2001). Climatic and tectonic control on the Cenozoic evolution of the West African margin. *Marine Geology*, *178*(1–4), 63–80. https://doi.org/10.1016/S0025-3227(01)00175-X

Leynaud, D., Mienert, J., & Vanneste, M. (2009). Submarine mass movements on glaciated and non-glaciated European continental margins: A review of triggering mechanisms and preconditions to failure. *Marine and Petroleum Geology*, *26*(5), 618–632. https://doi.org/10.1016/j.marpetgeo.2008.02.008

Lindseth, R. O. (1979). Synthetic sonic logs—a process for stratigraphic interpretation. *Geophysics*, *44*(1), 3. https://doi.org/10.1190/1.1440922

Liu, L. (2008). The case for dynamic subsidence of the U.S. east coast since the Eocene. *Geophysical Research Letters*, *35*(8), 1–6. https://doi.org/10.1029/2008GL033511

Liu, L. (2015). The ups and downs of North America: Evaluating the role of mantle dynamic topography since the Mesozoic. *Review of Geophysics*, *45*(2), 1–24. https://doi.org/10.1029/2006RG000197.1.INTRODUCTION

Lofi, J., Inwood, J., Proust, J. N., Monteverde, D. H., Loggia, D., Basile, C., Otsuka, H., Hayashi, T., Stadler, S., Mottl, M. J., Fehr, A., & Pezard, P. A. (2013). Fresh-water and salt-water distribution in passive margin sediments: Insights from integrated ocean drilling program expedition 313 on the New Jersey Margin. *Geosphere*, *9*(4), 1009–1024. https://doi.org/10.1130/GES00855.1

Lomb, N. R. (1976). Least-squares frequency analysis of unequally spaced data. *Astrophysics and Space Science*, *39*(2), 447–462. https://doi.org/10.1007/BF00648343

Lourens, L., & Tuenter, E. (2009). The Role of Variations of the Earth's Orbital Characteristics in Climate Change. *Climate Change*. https://doi.org/10.1016/B978-0-444-53301-2.00005-1

Loutit, T. S., Hardenbol, J., Vail, P. R., & Baum, G. R. (1988). Condensed Sections: The Key to Age Determination and Correlation of Continental Margin Sequences. In C. K. Wilgus, B. S. Hastings, H. Posamentier, J. Van Wagoner, C. A. Ross, & C. G. S. C. Kendall (Eds.), *Sea-Level Changes: An Integrated Approach* (Vol. 42, p. 0). SEPM Society for Sedimentary Geology. https://doi.org/10.2110/pec.88.01.0183

Løvholt, F., Kühn, D., Bungum, H., Harbitz, C. B., & Glimsdal, S. (2012). Historical tsunamis and present tsunami hazard in eastern Indonesia and the southern Philippines. *Journal of Geophysical Research: Solid Earth*, *117*(9), 1–19. https://doi.org/10.1029/2012JB009425

Lu, H., Fulthorpe, C. S., & Mann, P. (2003). Three-dimensional architecture of shelf-building sediment drifts in the offshore Canterbury Basin, New Zealand. *Marine Geology*, *193*(1–2), 19–47. https://doi.org/10.1016/S0025-3227(02)00612-6

Lu, H., Fulthorpe, C. S., Mann, P., & Kominz, M. A. (2005). Miocene-recent tectonic and climatic controls on sediment supply and sequence stratigraphy: Canterbury basin, New Zealand. *Basin Research*, *17*(2), 311–328. https://doi.org/10.1111/j.1365-2117.2005.00266.x

Lyne, V. D., Butman, B., & Grant, W. D. (1990). Sediment movement along the U.S. east coast continental shelf-I. Estimates of bottom stress using the Grant-Madsen model and near-bottom wave and current measurements. *Continental Shelf Research*, *10*(5), 397–428. http://pubs.er.usgs.gov/publication/70016373

Mann, P. (2015). Passive Plate Margin. *Encyclopedia of Marine Geosciences*. https://doi.org/10.1007/978-94-007-6644-0_100-1

Martin, J., Paola, C., Abreu, V., Neal, J., & Sheets, B. (2009). *Sequence stratigraphy of experimental strata under known conditions of differential subsidence and variable base level*. *4*(4), 503–533. https://doi.org/10.1306/12110808057

Martinsen, O. J., & Helland-Hansen, W. (1995). Strike variability of clastic depositional systems: does it matter for sequence-stratigraphic analysis? *Geology*, *23*(5), 439–442. https://doi.org/10.1130/0091-7613(1995)023<0439:SVOCDS>2.3.CO;2

Matthews, M. D., & Perlmutter, M. A. (2009). Global Cyclostratigraphy: An Application to the Eocene Green River Basin. In *Orbital Forcing and Cyclic Sequences* (pp. 459–481). Blackwell Publishing Ltd. https://doi.org/10.1002/9781444304039.ch28

Matthews, R., & Al-Husseini, M. (2010). Orbital-forcing glacio-eustasy: A sequence-stratigraphic time scale. *GeoArabia*, *15*(3), 155–167.

Matthews, R., & Frohlich, C. (1998). *Forward modeling of sequence stratigraphy and diagenesis: Application to rapid, cost-effective carbonate reservoir characterization* (Vol. 3).

McCarthy, F. M. G. G., Katz, M. E., Kotthoff, U., Browning, J. V., Miller, K. G., Zanatta, R., Williams, R. H., Drljepan, M., Hesselbo, S. P., Bjerum, C., & Mountain, G. S. (2013). Sea-level control of new jersey margin architecture: Palynological evidence from integrated ocean drilling program expedition 313. *Geosphere*, *9*(6), 1457–1487. https://doi.org/10.1130/GES00853.1

Meyers, S. R. (2008). Resolving milankovitchian controversies: The Triassic Latemar limestone and the Eocene Green River Formation. *Geology*, *36*(4), 319–322. https://doi.org/10.1130/G24423A.1

MGL1510 expedition Proposal. (2011). *MGL1510 Proposal-Collaborative Research : Community-Based 3D Imaging that Ties Clinoform Geometry to Facies Successions and Neogene Sea-Level Change*. *fall*.

Miall, A. (2006). Reconstructing the architecture and sequence stratigraphy of the preserved fluvial record as a tool for reservoir development: A reality check. *AAPG Bulletin*, *90*(7), 989–1002. https://doi.org/10.1306/02220605065

Miall, A., & Miall, C. (2001). *Sequence Stratigraphy as a Scientific Enterprise: The Evolution and Persistence of Conflicting Paradigms* (Vol. 54). https://doi.org/10.1016/S0012-8252(00)00041-6

Micheal, O., Glavovic, B., Hinkel, J., Roderik, van, Magnan, A., Abd-Elgawad, A., Rongshu, C., Miguel, C.-J., Robert, D., Ghosh, T., Hay, J., Ben, M., Meyssignac, B., Sebesvari, Z., A.J., S., Dangendorf, S., & Frederikse, T. (2019). *Sea Level Rise and Implications for Low Lying Islands, Coasts and Communities*.

Micheels, A., Bruch, A., & Mosbrugger, V. (2009). Miocene climate modelling sensitivity experiments for different co 2 concentrations Arne Micheels , Angela Bruch , and Volker Mosbrugger. *Palaeontologia Electronica*, *12*(2), 5A. http://palaeo-electronica.org/2009_2/172/index.html

Middleton, G. V. (1973). Johannes Walther's Law of the Correlation of Facies. *GSA Bulletin*, *84*(3), 979–988. http://dx.doi.org/10.1130/0016-7606(1973)84%3C979:JWLOTC%3E2.0.CO

Milanković, M. (1920). *Théorie Mathématique des Phénomènes Thermiques Produits par la Radiation Solaire*. Gauthier-Villars et Cie.

Miller, K. G., Browning, J. V., John Schmelz, W., Kopp, R. E., Mountain, G. S., & Wright, J. D. (2020). Cenozoic sea-level and cryospheric evolution from deep-sea geochemical and continental margin records. *Science Advances*, *6*(20). https://doi.org/10.1126/sciadv.aaz1346

Miller, K. G., Browning, J. V., Mountain, G. S., Bassetti, M. A., Monteverde, D. H., Katz, M. E., Inwood, J., Lofi, J., & Proust, J. N. (2013). Sequence boundaries are impedance contrasts: Core-seismic-log integration of Oligocene-Miocene sequences, New Jersey shallow shelf. *Geosphere*, *9*(5), 1257–1285. https://doi.org/10.1130/GES00858.1

Miller, K. G., Browning, J. V., Mountain, G. S., Sheridan, R. E., Sugarman, P. J., Glenn, S., & Christensen, B. A. (2014). Chapter 3 History of continental shelf and slope sedimentation on the US middle Atlantic margin. *Geological Society, London, Memoirs*, *41*(1), 21–34. https://doi.org/10.1144/M41.3

Miller, K. G., & Fairbanks, R. G. (1983). Evidence for Oligocene–Middle Miocene abyssal circulation changes in the western North Atlantic. *Nature*, *306*, 250. https://doi.org/10.1038/306250a0

Miller, K. G., Kominz, M. A., Browning, J. V., Wright, J. D., Mountain, G. S., Katz, M. E.,

Sugarman, P. J., Cramer, B. S., Christie-Blick, N., & Pekar, S. F. (2005). The phanerozoic record of global sea-level change. *Science*, *310*(5752), 1293–1298. https://doi.org/10.1126/science.1116412

Miller, K. G., Lombardi, C. J., Browning, J. V., Schmelz, W. J., Gallegos, G., Mountain, G. S., & Baldwin, K. E. (2018). Back To Basics of Sequence Stratigraphy: Early Miocene and Mid-cretaceous Examples from the New Jersey Paleoshelf. *Journal of Sedimentary Research*, *88*(1), 148–176. https://doi.org/10.2110/jsr.2017.73

Miller, K. G., & Mountain, G. S. (1994). Global Sea-Level Change and the New Jersey Margin. *Proceedings of the Ocean Drilling Program, Initial Reports*, *150*, 11–20.

Miller, K. G., & Mountain, G. S. (1996). Drilling and Dating New Jersey Oligocene-Miocene Sequences: Ice Volume, Global Sea Level, and Exxon Records. *Science*, *271*(5252), 1092–1095. https://doi.org/10.1126/science.271.5252.1092

Miller, K. G., Mountain, G. S., Browning, J. V., Katz, M. E., Monteverde, D. H., Sugarman, P. J., Ando, H., Bassetti, M. A., Bjerum, C., Hodgson, D. M., Hesselbo, S. P., Karakaya, S., Proust, J. N., & Rabineau, M. (2013). Testing sequence stratigraphic models by drilling Miocene foresets on the New Jersey shallow shelf. *Geosphere*, *9*(5), 1236–1256. https://doi.org/10.1130/GES00884.1

Miller, K. G., Mountain, G. S., Browning, J. V., Kominz, M. A., Sugarman, P. J., Christie-Blick, N., Katz, M. E., & Wright, J. D. (1998). Cenozoic global sea level, sequences, and the New Jersey transect: Results from coastal plain and continental slope drilling. *Reviews of Geophysics*, *36*(4), 569–601. https://doi.org/10.1029/98RG01624

Miller, K. G., Sugarman, P. J., Browning, J. V., Kominz, M. A., Olsson, R. K., Feigenson, M. D., & Hernández, J. C. (2004). Upper Cretaceous sequences and sea-level history, New Jersey Coastal Plain. *Bulletin of the Geological Society of America*, *116*(3–4), 368–393. https://doi.org/10.1130/B25279.1

Miller, K. G., Sugarman, P. J., Browning, J. V., Sheridan, R. E., Kulhanek, D. K., Monteverde, D. H., Wehmiller, J. F., Lombardi, C., & Feigenson, M. D. (2013). Pleistocene sequence stratigraphy of the shallow continental shelf, offshore New Jersey: Constraints of integrated ocean drilling program Leg 313 core holes. *Geosphere*, *9*(1), 74–95.

https://doi.org/10.1130/GES00795.1

Mitchum, R., & C. Van Wagoner, J. (1991). High-frequency sequences and their stacking patterns: sequence-stratigraphic evidence of high-frequency eustatic cycles. In *Sedimentary Geology* (Vol. 70). https://doi.org/10.1016/0037-0738(91)90139-5

Mitchum, R., Vail, P. R., & Sangree, J. B. (1977). Seismic Stratigraphy and Global Changes of Sea Level, Part 6: Stratigraphic Interpretation of Seismic Reflection Patterns in Depositional Sequences1. In C. E. Payton (Ed.), *Seismic Stratigraphy — Applications to Hydrocarbon Exploration* (Vol. 26, p. 0). American Association of Petroleum Geologists. https://doi.org/10.1306/M26490C8

Mitchum, R., Vail, P. R., & Thompson, S. (1977). Seismic Stratigraphy and Global Changes of Sea Level: Part 2. The Depositional Sequence as a Basic Unit for Stratigraphic Analysis: Section 2. Application of Seismic Reflection Configuration to Stratigraphic Interpretation. *Seismic Stratigraphy - Applications to Hydrocarbon Exploration.*, *165*, 53–62. https://doi.org/10.1306/M26490

Mitchum, R., Van Wagoner, J., Taylor, G., & Dockery, D. T. (1990). *High-Frequency Sequences and Eustatic Cycles in the Gulf of Mexico Basin* (pp. 257–267). https://doi.org/10.5724/gcs.90.11.0257

Molnar, P. (2001). Climate change, flooding in arid environments, and erosion rates. *Geology*, *29*(12), 1071–1074. https://doi.org/10.1130/0091-7613(2001)029<1071:CCFIAE>2.0.CO

Molnar, P. (2004). late cenozoic increase in accumulation rates of terrestrial sediment: How Might Climate Change Have Affected Erosion Rates? *Annual Review of Earth and Planetary Sciences*, *32*(1), 67–89. https://doi.org/10.1016/j.matcom.2017.10.010

Monteverde, D. H., Miller, K. G., & Mountain, G. S. (2000). Correlation of offshore seismic profiles with onshore New Jersey Miocene sediments. *Sedimentary Geology*, *134*(1–2), 111–127. https://doi.org/10.1016/S0037-0738(00)00016-6

Monteverde, D. H., Mountain, G. S., & Miller, K. G. (2008). Early Miocene sequence development across the New Jersey margin. *Basin Research*, *20*(2), 249–267. https://doi.org/10.1111/j.1365-2117.2008.00351.x

Moore, J. G., & Normark, W. R. (1994). Giant hawaiian landslides. *Annual Review of Earth and Planetary Science*, *22*.

Mountain, G. S., Burger, R. L., Delius, H., Fulthorpe, C. S., Austin, J. A., Goldberg, D. S., Steckler, M. S., Mchugh, C. M., Miller, K. G., Monteverde, D. H., Orange, D. L., & Pratson, L. F. (2007). The long-term stratigraphic record on continental margins. *Continental Margin Sedimentation: From Sediment Transport to Sequence Stratigraphy*, 381–458. https://doi.org/10.1002/9781444304398.ch8

Mountain, G. S., Miller, K. G., Blum, P., Poag, C. W., Twichell, D. ., & Aubry, M.-P. (1996). Data report: Eocene to upper Miocene calcareous nannofossil stratigraphy. *Proc. ODP, Sci. Results, 150*, 70–71.

Mountain, G. S., Miller, K. G., Christie-blick, N., Peter, J., & Fulthorpe, C. S. (2006). Shallow-Water Drilling of the New Jersey Continental Shelf: Determining the Links Between Sediment Architecture and Sea-Level Change. *Research Proposal*.

Mountain, G. S., Proust, J.-N., & McInroy, D. (2009). *Shallow-water drilling of the New Jersey continental shelf: global sea level and architecture of passive margin sediments*. *313*. https://doi.org/10.2204/iodp.sp.313.2009

Mountain, G. S., Proust, J. N. J.-N., & Expedition 313 Science Party. (2010). The New Jersey margin scientific drilling project (IODP expedition 313): Untangling the record of global and local sea-level changes. *Scientific Drilling*, *10*(10), 26–34. https://doi.org/10.2204/iodp.sd.10.03.2010

Mountjoy, J. J., Mckean, J., Barnes, P. M., & Pettinga, J. R. (2009). Terrestrial-style slow-moving earth fl ow kinematics in a submarine landslide complex. *Marine Geology*, *267*(3–4), 114–127. https://doi.org/10.1016/j.margeo.2009.09.007

Mudelsee, M., Bickertl, T., Lear, C., & Lohmann, G. (2014). Cenozoic climate changes: A review based on time series analysis of marine benthic δ18O records. *Reviews of Geophysics*, *52*(3), 333–374. https://doi.org/10.1002/2013RG000440PANGAEASupplementaryData

Muller, R. A., & MacDonald, G. J. (1997). Glacial cycles and astronomical forcing. *Science*, *277*(5323), 215–218. https://doi.org/10.1126/science.277.5323.215

Müller, R. D., Sdrolias, M., Gaina, C., & Roest, W. R. (2008). Age, spreading rates, and spreading asymmetry of the world's ocean crust. *Geochemistry, Geophysics, Geosystems*, *9*(4), 1–19. https://doi.org/10.1029/2007GC001743

Murray-Wallace, C. V, & Woodroffe, C. D. (2014). *Quaternary Sea-Level Changes: A Global Perspective*. Cambridge University Press. https://doi.org/10.1017/CBO9781139024440

Naish, T., Powell, R., Levy, R., Wilson, G., Scherer, R., Talarico, F., Krissek, L., Niessen, F., Pompilio, M., Wilson, T., Carter, L., DeConto, R., Huybers, P., McKay, R., Pollard, D., Ross, J., Winter, D., Barrett, P., Browne, G., … Williams, T. (2009). Obliquity-paced Pliocene West Antarctic ice sheet oscillations. *Nature*, *458*(7236), 322–328. https://doi.org/10.1038/nature07867

National Center for Earth-surface Dynamics Data Repository. (2019). http://www.nced.umn.edu/Data_Repository.html.

Neal, J. E., & Abreu, V. (2009). Sequence stratigraphy hierarchy and the accommodation succession method. *Geology*, *37*(9), 779–782. https://doi.org/10.1130/G25722A.1

Neal, J. E., Abreu, V., Bohacs, K. M., Feldman, H. R., & Pederson, K. H. (2016). Accommodation succession ($\delta A / \delta S$) sequence stratigraphy: observational method, utility and insights into sequence boundary formation. *Journal of the Geological Society*, *173*(5), 803–816. https://doi.org/10.1144/jgs2015-165

Nilsson, A., Lee, Y. S., Snowball, I., & Hill, M. (2013). Magnetostratigraphic importance of secondary chemical remanent magnetizations carried by greigite (Fe3S4) in Miocene sediments, New Jersey shelf (IODP Expedition 313). *Geosphere*, *9*(3), 510–520. https://doi.org/10.1130/GES00854.1

Nittrouer, C. A., & Wright, L. D. (1994). Transport of particles across continental shelves. *Reviews of Geophysics*, *32*(1), 85–113. https://doi.org/10.1029/93RG02603

Obaje, S. O. O. (2013). Sequence Stratigraphy Concepts and Applications : A Review. *Journal of Environment and Earth Science*, *3*(12), 207–218.

Olsen, P. E. (1997). Stratigraphic Record of the Early Mesozoic Breakup of Pangea in the Laurasia-Gondwana Rift System. *Annual Review of Earth and Planetary Sciences*, *25*(1),

337–401. https://doi.org/10.1146/annurev.earth.25.1.337

Oppenheimer, M., O'Neil, B. C., Webster, M., & Agrawala, S. (2007). The Limits of Consensus The Limits of Consensus. *Science*, *Spetember*.

Pälike, H., Laskar, J., & Shackleton, N. J. (2004). Geologic constraints on the chaotic diffusion of the solar system. *Geology*, *32*(11), 929–932. https://doi.org/10.1130/G20750.1

Paola, C., Mullin, J., Ellis, C., Mohrig, D., Swenson, J., Parker, G., Hickson, T., Heller, P. L., Pratson, L., Syvitski, J., Sheets, B., & Strong, N. (2001). Experimental Stratigraphy. *Gsa Today*, *11*. https://doi.org/10.1130/1052-5173(2001)011<0004:ES>2.0.CO;2

Patruno, S., Hampson, G. J., & Jackson, C. A. L. (2015). Quantitative characterisation of deltaic and subaqueous clinoforms. *Earth-Science Reviews*, *142*, 79–119. https://doi.org/10.1016/j.earscirev.2015.01.004

Pazzaglia, F. J., & Brandon, M. T. (1996). Macrogeomorphic evolution of the post-TriassicAppalachian mountains determined by deconvolutionof the offshore basin sedimentary record. *Basin Research*, *8*(1996), 1–24. file:///Users/lstevens/Papers2/Articles/1996/Unknown/Unknown/1996_.pdf%5Cnpapers2://publication/uuid/7EBAB4BB-024D-4383-B73C-43E20BCCD91C

Pazzaglia, F. J., & Gardner, W. (1994). Late Cenozoic flexural deformation of the middle U.S. Atlantic passive margin. *Atlantic*, *99*.

Pekar, S., & M. DeConto, R. (2006). Pekar, S. F. & DeConto, R. M. High-resolution ice-volume estimates for the early Miocene: evidence for a dynamic ice sheet in Antarctica. Palaeogeog. Palaeoclimatol. Palaeoecol. 231, 101-109. *Palaeogeography, Palaeoclimatology, Palaeoecology*, *231*, 101–109. https://doi.org/10.1016/j.palaeo.2005.07.027

Pellaton, C., & Gorin, G. E. (2005). The Miocene New Jersey Passive Margin as a Model for the Distribution of Sedimentary Organic Matter in Siliciclastic Deposits. *Journal of Sedimentary Research*, *75*(6), 1011–1027. https://doi.org/10.2110/jsr.2005.076

Perlmutter, M. A., Brennan, P. A., Hook, S. C., Dempster, K., & Pasta, D. (1995). Global cyclostratigraphic analysis of the Seychelles Southern Shelf for potential reservoir, seal and

source rocks. *Sedimentary Geology*, *96*(1–2), 93–118. https://doi.org/10.1016/0037-0738(94)00128-H

Perlmutter, M. A., Radovich, B. J., & Matthews, M. D. (1997). *The Impact of High-Frequency Sedimentation Cycles on Stratigraphic Interpretation*. University of South Carolina.

Pettersson, H. (1951). Radium and Deep-Sea Chronology. *Nature*, *167*(4258), 942–942. https://doi.org/10.1038/167942a0

Pfeffer, W. T., Harper, J. T., & O'Neel, S. (2008). Kinematic Constraints on Glacier Contributions to 21st-Century Sea-Level Rise. *Science*, *311*(January), 212–216.

Pirmez, C., Pratson, L. F., & Steckler, M. S. (1998). Clinoform development by advection-diffusion of suspended sediment: Modeling and comparison to natural systems. *Journal of Geophysical Research*, *103*(B10), 24141. https://doi.org/10.1029/98JB01516

Pisias, N. G., & Shackleton, N. J. (1984). Modelling the global climate response to orbital forcing and atmospheric carbon dioxide changes. *Nature*, *310*, 757. https://doi.org/10.1038/310757a0

Pitman, W. I. I. I., & Golovchenk, X. (1983). The effect of sea-level change on the shelf edge and slope of passive margins. *SEPM Special Publication*, *33*, 41–58.

Plint, A. G., & Nummedal, D. (2000). The falling stage systems tract: recognition and importance in sequence stratigraphic analysis. *Geological Society, London, Special Publications*, *172*(1), 1–17. https://doi.org/10.1144/GSL.SP.2000.172.01.01

Poag, C. W., & Sevon, W. D. (1989). A record of Appalachian denudation in postrift Mesozoic and Cenozoic sedimentary deposits of the U.S. Middle Atlantic continental margin. *Geomorphology*, *2*(1–3), 119–157. https://doi.org/10.1016/0169-555X(89)90009-3

Posamentier, H. W., Jervey, M. T., & Vail, P. R. (1988). Eustatic controls on clastic deposition - conceptual framework. *Sea-Level Changes: An Integrated Approach*, *October*, 109–124. https://doi.org/10.2110/pec.88.01.0109

Potter, P. E., & Szatmari, P. (2009). Global Miocene tectonics and the modern world. *Earth-Science Reviews*, *96*(4), 279–295. https://doi.org/10.1016/j.earscirev.2009.07.003

Poulsen, C. J., Flemings, P. B., Robinson, R. A. J. J., & Metzger, J. M. (1998). Three-

dimensional stratigraphic evolution of the Miocene Baltimore Canyon region: Implications for eustatic interpretations and the systems tract model. *Bulletin of the Geological Society of America*, *110*(9), 1105–1122. https://doi.org/10.1130/0016-7606(1998)110<1105:TDSEOT>2.3.CO;2

Prokopenko, A. A., Hinnov, L. A., Williams, D. F., & Kuzmin, M. I. (2006). Orbital forcing of continental climate during the Pleistocene: a complete astronomically tuned climatic record from Lake Baikal, SE Siberia. *Quaternary Science Reviews*, *25*(23–24), 3431–3457. https://doi.org/10.1016/j.quascirev.2006.10.002

Proust, J. N., Pouderoux, H., Ando, H., Hesselbo, S. P., Hodgson, D. M., Lofi, J., Rabineau, M., & Sugarman, P. J. (2018). Facies architecture of Miocene subaqueous clinothems of the New Jersey passive margin: Results from IODP-ICDP Expedition 313. *Geosphere*, *14*(4), 1564–1591. https://doi.org/10.1130/GES01545.1

Reineck, H.-E., & Singh, I. B. (1973). *Depositional Sedimentary Environments*. Springer Berlin Heidelberg. https://doi.org/10.1007/978-3-642-96291-2

Reynolds, D. J., Steckler, M. S., & Coakley, B. J. (1991). The role of the sediment load in sequence stratigraphy: The influence of flexural isostasy and compaction. *Journal of Geophysical Research: Solid Earth*, *96*(B4), 6931–6949. https://doi.org/10.1029/90JB01914

Rich, J. L. (1951). Three critical environments of deposition, and criteria for recognition of rocks deposited in each of them. *Bulletin of the Geological Society of America*, *62*(October), 1–20.

Rieke, H. H., & Chilingarian, G. V. (1974). Chapter 4 Effect of Compaction on Some Properties of Argillaceous Sediments. *Developments in Sedimentology*, *16*(C), 123–217. https://doi.org/10.1016/S0070-4571(08)70774-X

Rohling, E. J., Haigh, I. D., Foster, G. L., Roberts, A. P., & Grant, K. M. (2013). A geological perspective on potential future sea-level rise. *Scientific Reports*, *3*. https://doi.org/10.1038/srep03461

Rowley, D. B., Forte, A. M., Moucha, R., Mitrovica, J. X., Simmons, N. A., & Grand, S. P. (2011). *Dynamic Topography Change of the Eastern US since 4 Ma: Implications for Sea Level and Stratigraphic Architecture of Passive Margins*.

Rubincam, D. P. (1994). Insolation in terms of Earth's orbital parameters. *Theoretical and Applied Climatology*, *48*(4), 195–202. https://doi.org/10.1007/BF00867049

Ruddiman, W. F. (2003). Orbital insolation, ice volume, and greenhouse gases. *Quaternary Science Reviews*, *22*, 1597–1629. https://doi.org/10.1016/S0277-3791(03)00087-8

Ruffman, A., & Hann, V. (2006). The Newfoundland Tsunami of November 18 , 1929 : An Examination of the Twenty-eight Deaths of the " South Coast Disaster ." *Newfoundland and Labrador Studies*, *21*(1), 1719–1726.

Sanchez, C. M., Fulthorpe, C. S., & Steel, R. J. (2012a). Middle Miocene-Pliocene siliciclastic influx across a carbonate shelf and influence of deltaic sedimentation on shelf construction, Northern Carnarvon Basin, Northwest Shelf of Australia. *Basin Research*, *24*(6), 664–682. https://doi.org/10.1111/j.1365-2117.2012.00546.x

Sanchez, C. M., Fulthorpe, C. S., & Steel, R. J. (2012b). Miocene shelf-edge deltas and their impact on deepwater slope progradation and morphology, Northwest Shelf of Australia. *Basin Research*, *24*(6), 683–698. https://doi.org/10.1111/j.1365-2117.2012.00545.x

Scargle, J. D. (1982). Studies in astronomical time series analysis. II. Statistical aspects of spectral analysis of unevenly spaced data. *\apj*, *263*, 835–853. https://doi.org/10.1086/160554

Schlager, W. (2004). Fractal nature of stratigraphic sequences. *Geology*, *32*(3), 185–188. https://doi.org/10.1130/G20253.1

Scholle, P. A. (1980). Geological studies of the COST No. B-3 Well, United States Mid-Atlantic continental slope area. In *Circular*. https://doi.org/10.3133/cir833

Schulten, I., Mosher, D. C., Krastel, S., Piper, D. J. W., Kienast, M., By, N. S., & Kiel, C. (2018). Surficial sediment failures due to the 1929 Grand Banks Earthquake , St Pierre Slope Natural Resources Canada , Bedford Institute of Oceanography , 1 Challenger. *The Geological Society of London*.

Shackleton, N. J., Hall, M. A., Raffi, I., Tauxe, L., & Zachos, J. (2000). Astronomical calibration age for the Oligocene-Miocene boundary. *Geology*, *28*(5), 447–450. https://doi.org/10.1130/0091-7613(2000)028<0447:ACAFTO>2.3.CO;2

Shepherd, A., Ivins, E., Rignot, E., Smith, B., van den Broeke, M., Velicogna, I., Whitehouse, P., Briggs, K., Joughin, I., Krinner, G., Nowicki, S., Payne, T., Scambos, T., Schlegel, N., A, G., Agosta, C., Ahlstrøm, A., Babonis, G., Barletta, V. R., … Team, T. I. (2020). Mass balance of the Greenland Ice Sheet from 1992 to 2018. *Nature*, *579*(7798), 233–239. https://doi.org/10.1038/s41586-019-1855-2

Sheridan, R.E., & Gradstein, F. M. (1983). *Initial Reports of the Deep Sea Drilling Project, 76* (Vol. 76). U.S. Government Printing Office. https://doi.org/10.2973/dsdp.proc.76.1983

Sheridan, Robert E. (1987). Pulsation Tectonics As the Control of Long-Term Stratigraphic Cycles. *Paleoceanography*, *2*(2), 97–118.

Sherriff, R. . (1977). Seismic Stratigraphy: Applications to Hydrocarbon Exploration. *The American Association of Petroleum Geologists Bulletin*, 3–14. https://doi.org/10.1306/m26490

Sloss, L. L., Krumbein, W. C., & Dapples, E. C. (1949). *Integrated facies analysis*. *39*. https://doi.org/10.1130/MEM39

Solomon, S., Alley, R., Gregory, J., Lemke, P., & Manning, M. (2008). A Closer Look at the IPCC Report. *Science*, *319*(5862), 409 LP – 410. https://doi.org/10.1126/science.319.5862.409c

Steckler, M. S., Mountain, G. S., Miller, K. G., & Christie-Blick, N. (1999). Reconstruction of Tertiary progradation and clinoform development on the New Jersey passive margin by 2-D backstripping. *Marine Geology*, *154*(1–4), 399–420. https://doi.org/10.1016/S0025-3227(98)00126-1

Steckler, M. S., Reynolds, D. J., Coakley, B. J., Swift, B. A., & Jarrard, R. (1993). Modelling Passive Margin Sequence Stratigraphy. In *Sequence Stratigraphy and Facies Associations*. https://doi.org/10.1002/9781444303810

Steckler, M. S., & Watts, A. B. (1978). Subsidence of the Atlantic-type continental margin off New York. *Earth and Planetary Science Letters*, *41*(1), 1–13. https://doi.org/10.1016/0012-821X(78)90036-5

Steffen, H., & Kaufmann, G. (2005). Glacial isostatic adjustment of Scandinavia and

northwestern Europe and the radial viscosity structure of the Earth's mantle. *Geophysical Journal International*, *163*(2), 801–812. https://doi.org/10.1111/j.1365-246X.2005.02740.x

Stein, S., Sleep, N. H., Geller, R. J., Wang, S.-C., & Kroeger, G. C. (1979). EARTHQUAKES ALONG THE PASSIVE MARGIN OF EASTERN CANADA Seth. *Geophysical Research Letters*, *6*(7).

Stern, N., & Herbert, N. (2015). Stern Review: The Economics of Climate Change. *Cambridge University Press*. https://doi.org/10.1257/aer.98.2.1

Strasser, A., Hilgen, F. J., & Heckel, P. H. (2006). Cyclostratigraphy – concepts, definitions, and applications. *Newsletters on Stratigraphy*, *42*(2), 75–114. https://doi.org/10.1127/0078-0421/2006/0042-0075

Strasser, A., Hillgärtner, H., Hug, W., & Pittet, B. (2000). Third-order depositional sequences reflecting Milankovitch cyclicity. *Terra Nova*, *12*(6), 303–311. https://doi.org/10.1046/j.1365-3121.2000.00315.x

Strong, N., & Paola, C. (2006). Fluvial Landscapes and Stratigraphy in a Flume. *The Sedimentary Record*, *4*(2), 4–8. https://doi.org/10.2110/sedred.2006.2.4

Suess, E. (1905). The Face of the Earth (Das Antlitz der Erde). *Nature*, *72*(1861), 193–194. https://doi.org/10.1038/072193a0

Swarbrick, R., Osborne, M., & Yardley, G. (2002). Comparison of overpressure magnitude resulting from the main generating mechanisms. In *AAPG Memoir* (pp. 1–12).

Swenson, J. B., Paola, C., Pratson, L., Voller, V. R., & Murray, A. B. (2005). Fluvial and marine controls on combined subaerial and subaqueous delta progradation: Morphodynamic modeling of compound-clinoform development. *Journal of Geophysical Research: Earth Surface*, *110*(2), 1–16. https://doi.org/10.1029/2004JF000265

Swift, D. J. P., & Thorne, J. A. (2009). Sedimentation on Continental Margins, I: A General Model for Shelf Sedimentation. In *Shelf Sand and Sandstone Bodies* (pp. 1–31). John Wiley & Sons, Ltd. https://doi.org/10.1002/9781444303933.ch1

Tagliaro, G., Fulthorpe, C. S., Gallagher, S. J., McHugh, C. M., Kominz, M. A., & Lavier, L. L. (2018). Neogene siliciclastic deposition and climate variability on a carbonate margin:

Australian Northwest Shelf. *Marine Geology*, *403*(June), 285–300. https://doi.org/10.1016/j.margeo.2018.06.007

Tesson, M., Gensous, B., Allen, G. P., & Ravenne, C. (1990). Late Quaternary deltaic lowstand wedges on the Rhône continental shelf, France. *Marine Geology*, *91*(4), 325–332. https://doi.org/https://doi.org/10.1016/0025-3227(90)90053-M

Tinti, S., Maramai, A., & Graziani, L. (2004). The New Catalogue of Italian Tsunamis. *Natural Hazards*, *33*, 439–465. https://www.fool.com/investing/2016/06/04/3-reasons-comcast-bought-dreamworks.aspx?source=iedfolrf0000001

Tosi, L., Teatini, P., & Strozzi, T. (2013). Natural versus anthropogenic subsidence of Venice. *Scientific Reports*, *3*(1), 2710. https://doi.org/10.1038/srep02710

Urbat, M. (1996). Rock-Magnetic Properties of Pleistocene Passive Margin sediments: Environmental Change and Diagenesis offshore New Jersey. *Proc. ODP Sci. Res.*, *150*. https://doi.org/10.2973/odp.proc.sr.150.025.1996

Vail, P. R., Mitchum, R., & Thompson, S. (1977). Seismic Stratigraphy and Global Changes of Sea Level, Part 4: Global Cycles of Relative Changes of Sea Level. In C. E. Payton (Ed.), *Seismic Stratigraphy — Applications to Hydrocarbon Exploration*. American Association of Petroleum Geologists. https://doi.org/10.1306/M26490C6

van den Belt, F. J. G., van Hoof, T. B., & Pagnier, H. J. M. (2015). Revealing the hidden Milankovitch record from Pennsylvanian cyclothem successions and implications regarding late Paleozoic chronology and terrestrial-carbon (coal) storage. *Geosphere*, *11*(4), 1062–1076. https://doi.org/10.1130/GES01177.1

Van Wagoner, J. C., Mitchum, R., Campion, K., & Rahmanian, V. D. (1990). Siliciclastic sequence stratigraphy for high resolution correlation of time and facies. *AAPG Meth Explora Series*, 7–55.

Van Wagoner, J., Posamentier, H. W., Mitchum, R., Vail, P. R., Sarg, J. F. F., Loutit, T. S., & Hardenbol, J. (1988). An overview of the fundamentals of sequence stratigraphy and key definitions. *The Society of Economic Paleontologists and Mineralogists*, *42*, 39–45. https://doi.org/10.2110/pec.88.01.0039

Vandenberghe, J. (2013). Grain size of fine-grained windblown sediment: A powerful proxy for process identification. *Earth-Science Reviews*, *121*, 18–30. https://doi.org/10.1016/j.earscirev.2013.03.001

von der Heydt, A., & Dijkstra, H. A. (2006). Effect of ocean gateways on the global ocean circulation in the late Oligocene and early Miocene. *Paleoceanography*, *21*(1), 1–18. https://doi.org/10.1029/2005PA001149

Wade, B. S., & Pälike, H. (2004). Oligocene climate dynamics. *Paleoceanography*, *19*(4), 1–16. https://doi.org/10.1029/2004PA001042

Wanless, H. R., & Shepard, F. P. (1936). Sea level and climate changes related to late Paleozoic cyclothems. *Bulletin of the American Geographical Society*, *47*(2), 143–145. https://doi.org/10.2307/201801

Watkins, J. S., & Mountain, G. S. (1988). *The Role of ODP Drilling in the Inverstigation of Global Changes in Sea Level*.

Watterson, J., Walsh, J., Nicol, A., Nell, P. A. R., & Bretan, P. G. (2000). Geometry and origin of a polygonal fault system. *Journal of the Geological Society, London*, *157*(1), 151–162. http://jgs.lyellcollection.org/cgi/content/abstract/157/1/151

Watts, A. B., & Steckler, M. S. (1981). Subsidence and tectonics of Atlantic-type continental margins. *Oceanologica ACTA*, 143–154.

Watts, A. B., & Steckler, M. S. (1979). *Subsidence and eustasy at the continental margin of eastern North America* (pp. 218–234). https://doi.org/10.1029/ME003p0218

Watts, A. B., & Thorne, J. A. (1984). Tectonic global changes in sea-level and their relationship to stratigraphic sequences at the U.S. Atlantic continental margin. *Mar. Petrol Geol.*, *1(4)*(1977), 319–339. https://doi.org/10.1016/0264-8172(84)90134-X

Weedon, G. P. (2003). *Time-Series Analysis and Cyclostratigraphy: Examining Stratigraphic Records of Environmental Cycles*. Cambridge University Press. https://doi.org/DOI: 10.1017/CBO9780511535482

Weimer, P., & Posamentier, H. W. (1993). *Siliciclastic Sequence Stratigraphy: Recent Developments and Applications*. American Association of Petroleum Geologists.

https://doi.org/10.1306/M58581

Wells, A. J. (1960). Cyclic sedimentation: a review. *Geological Magazine*, *97*(5), 389–403.

Werthmüller, D., Ziolkowski, A., & Wright, D. (2013). Background resistivity model from seismic velocities. *Geophysics*, *78*(4), E213–E233. https://doi.org/10.1190/GEO2012-0445.1

Wiberg, P. L., Cacchione, D. A., Sternberg, R. W., Donelson Wright, L., & Wright, D. (1996). Linking sediment transport and stratigraphy on the continental shelf. *Oceanography*, *9*(SPL.ISS. 3), 153–157. https://doi.org/10.5670/oceanog.1996.02

Wilgus, C. K., Hastings, B. S., Posamentier, H. W., Van Wagoner, J., Ross, C. A., & Kendall, ; Christopher G. St. C. (1988). *SEPM SPECIAL PUBLICATION (42): Sea-Level Changes* (42nd ed.). SEPM SPECIAL PUBLICATION.

Williams, D. F., Peck, J., Karabanov, E. B., A. A. Prokopenko, V. Kravchinsky, King, J., & Kuzmin, M. I. (2010). *Lake Baikal Record of Continental Climate Response to Orbital Insolation During the Past 5 Million Years Lake Baikal Record of Continental Climate Response to Orbital Insolation During the Past 5 Million Years*. *1114*(1997), 1114–1117. https://doi.org/10.1126/science.278.5340.1114

Williams, G. D. (1993). Tectonics and seismic sequence stratigraphy: an introduction. *Geological Society, London, Special Publications*, *71*, 1–13.

Wilson, R. (1998). Sequence stratigraphy : a revolution without a cause ? *Geological Society, London, Special Publications*, *143*, 303–314.

Withjack, M. O., Schlische, R. W., & Olsen, P. E. (1998). Diachronous rifting, drifting, and inversion on the passive margin of central eastern North America: an analog for other passive margins. *AAPG Bulletin*, *82*(5 A), 817–835. https://doi.org/10.1306/1D9BC60B-172D-11D7-8645000102C1865D

Wu, P. (1998). Intraplate earthquakes and Postglacial Rebound in Eastern Canada and Northern Europe. *Dynamics of the Ice Age Earth: A Modern Perspective*, 603–628.

Wunsch, C. (2004). Quantitative estimate of the Milankovitch-forced contribution to observed Quaternary climate change. *Quaternary Science Reviews*, *23*(9–10), 1001–1012.

https://doi.org/10.1016/j.quascirev.2004.02.014

Zachos, J. C., Shackleton, N. J., Revenaugh, J. S., Palike, H., & Flower, B. P. (2001). Climate Response to Orbital ForcingAcross the Oligocene-Miocene Boundary. *Science*, *292*(5515), 274–278. http://www.sciencemag.org/cgi/content/abstract/292/5515/274

APPENDIX

A.1 Inversion of seismic amplitude

The amplitude of a reflected seismic wave is a function of the contrast in acoustic impedance (product of seismic wave velocity and density) of two layers forming the interface. Inverting the seismic reflection amplitude in a sedimentary environment yields the relative impedances of the deposits on both sides of each interface. Like any other inversion technique, seismic inversion is a mathematical way to estimate an answer (in this case seismic Impedance), check it against observation (well log data), and modify it with an objective of minimizing the error between the estimated values and their corresponding observations. Seismic amplitude inversion uses the amplitude of reflected seismic wave and its arrival time to estimate the relative impedance of layers forming the reflecting interfaces.

A model-based seismic inversion process begins with the observed geophysical properties along a borehole. The product of measured density and Vp is first converted to the reflection coefficient log along the well. The reflection coefficient log is then convolved with a seismic wavelet (representing the seismic source signature wavelet used during the seismic survey) to model a synthetic seismic trace at the well location. The inversion process takes an actual recorded seismic trace at that location, removes the seismic pulse, and computes the impedance value adjacent to the well. The inversion process is then iterated between forward modelling and inverted values to define a deterministic relationship that minimizes the error in predicted values. Because of its simplicity and reliability, the model-based seismic inversion was used to derive acoustic impedance from the post-stack 3D seismic data. Figure 3. shows the correlation between inverted acoustic impedance along the well M27 and M29 after six inversion iteration. A section of the final inverted volume crossing the Expedition 313 wells is shown in Figure 3.

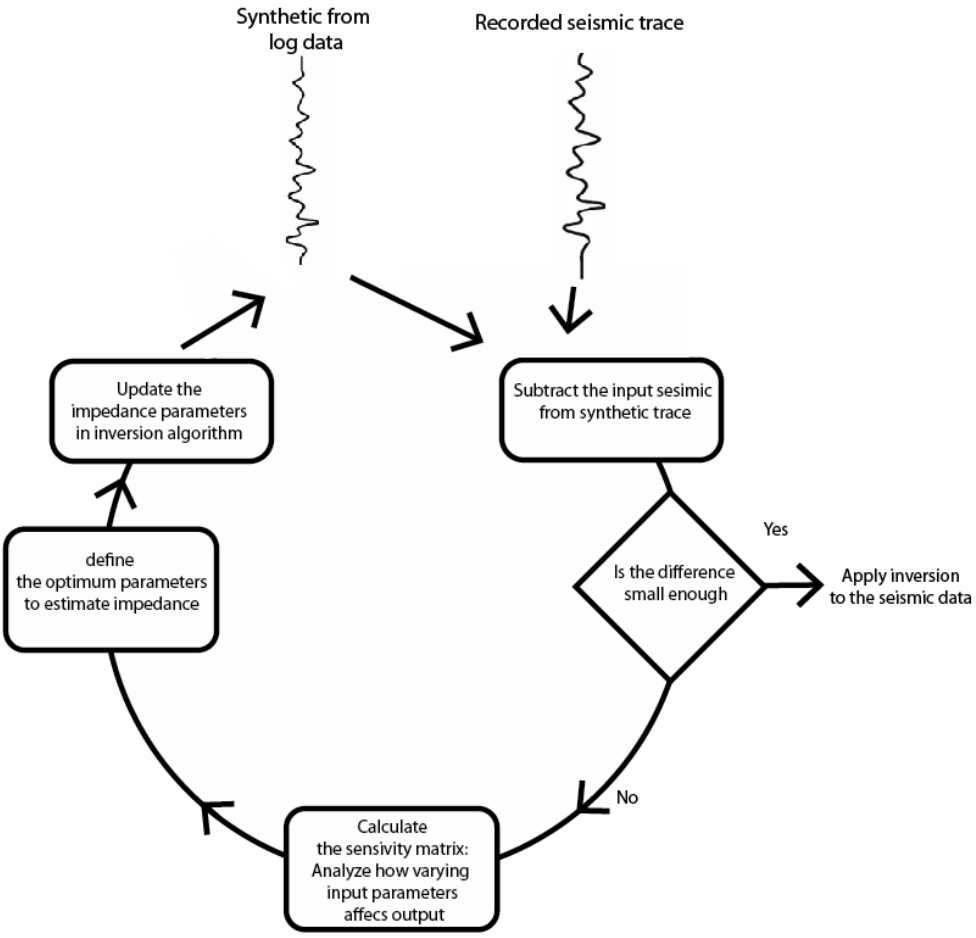

Figure A1: Iterative loop of model-based inversion process to find the optimum parameters for inversion.

A.2 Multi-attribute linear regression

Integrating seismic and well-log data is a crucial step to characterize subsurface structures to characterize the subsurface away from the drilled wells. Forward modeling of synthetic seismic data from well logs and inversion of seismic amplitude to estimate the acoustic impedance are two traditional integrating approaches that have been practiced extensively by the petroleum industry (Barclay et al., 2007; Cooke, 1983; Lindseth, 1979). To estimate the log properties other than acoustic impedance, multi-attribute linear regression defines a direct statistical relationship between the input and target datasets at the well location, and then, expands it to the entire seismic volume.

The aim of this methodology is to find an operator using seismic attributes that predicts a target property along the well from neighbouring seismic data. The benefit of using seismic attributes along with raw seismic is that many attributes represent nonlinear characteristics of seismic data and they break down the reflected seismic wave into its components. Consequently, seismic attributes reduce the dimensionality of raw data that eases recognizing patterns in the training data and increase the predictive power of the technique (Hampson et al., 2001).

Determining the right attributes to feed into a multi-attribute linear regression process happens through step-wise regression (Draper & Smith, 1966), an eliminating procedure to shortlist a limited number of attributes that are most beneficial to predict a target property. The main assumption of the stepwise regression process is that if the optimal combination of X attributes is already known, then the optimal combination of X+1 attributes includes all the previous X attributes.

$$L(t) = w_0 + w_1 * A_1(t) + w_2 * A_2(t) + W_3 * A_3(t)$$

$$E^2 = \frac{1}{N} \sum_{i=0}^{N} (\mathrm{L_i} - \mathrm{w_0} - \mathrm{w_1} * \mathrm{A_{1i}} - \mathrm{w_2} * \mathrm{A_{2i}} - \mathrm{w_3} * \mathrm{A_{3i}})^2$$

Where w_i is the derived weight for each attribute; A_i is the selected attribute; * represents convolution operator; N is the number of desired attributes; L_i represents the value of target property; L(t) represents the linear regression for the modelled target property; E is the calculated prediction error between the regression line and the target property.

In practice, stepwise regression starts with finding the single best attribute (A_1) that correlates best with the target property and has the lowest prediction error. In order to find the optimal combination of two attributes to predict the target property, stepwise regression assumes that A_1 is one of them, and looks for a second attribute (A_2) that in combination with A_1 produces the lowest prediction error. In order to find the optimal combination of three attributes to predict the target property, stepwise regression assumes that A_1 and A_2 are two of three optimal attributes, and looks for a third attribute (A_3) that in combination with A_1 and A_2 produces the lowest prediction error. This procedure is carried on depending on the number of attributes that we desire to feed into a multi-attribute linear regression process. Even though stepwise regression does not guarantee to find the best combination of X+1 attributes with the lowest prediction error

for a target property; each attribute that is found by this procedure to the shortlist should lower the overall prediction error.

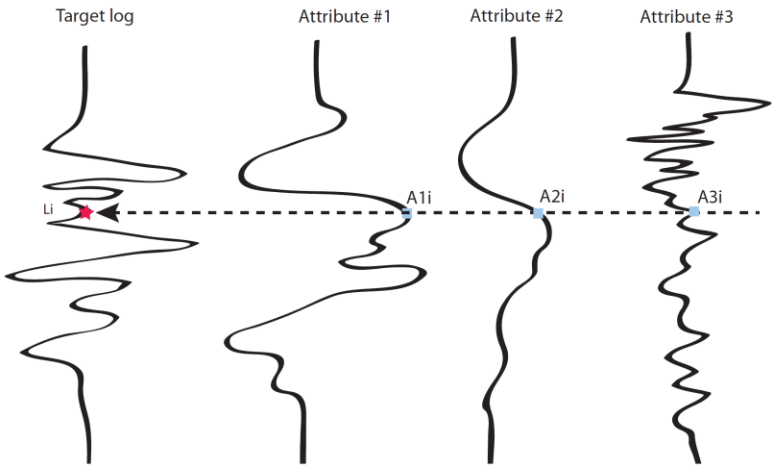

Figure A2: Multi-attribute linear regression is designed to find a linear relationship between input attributes (A) and the corresponding value for the target log (L) at each depth.

A.3 Polygonal faults

Polygonal faults were first recognized by Henriet et al. (1989) in the Southern North sea, as a "clay tectonic" feature resulting from the deformation of soft sediments. Their size and strain characteristics distinguish them from tectonic normal faults. Length of tectonic normal faults and their vertical extension ranges from 100 m to a few kilometres and across a variety of layers, respectively. On the other hand, polygonal faults are delimited in dip direction by the extension of fine-grained facies and have a significantly shorter vertical length that is controlled by the number of layers (Cartwright et al., 2003).

Gravity sliding (Clausen et al., 1999; Higgs & McClay, 2008), dewatering, differential compaction between the layers (Henriet et al., 1989; Watterson et al., 2000), and low frictional strength of the compacting sediments are some of the genetic mechanisms involved in creation of the polygonal faults.The normal gravitational load and low frictional strength of compacting sediments can cause poorly-consolidated sedimentary structures to fail under the directional overburden stress from the new deposits (Goulty, 2001). Rather than consolidation without any shear failure that could happen in a passively subsiding basin, the presence of the directional stress can cause grains to slip across the boundaries. Moreover, gentle slopes at the toe of

clinoforms can induce a gravity force that may results in the detachment of isolated sediments from their base and slid them into the deeper depth (J. J. Cartwright & Dewhurst, 1998; Higgs & McClay, 2008). The downslope gravitational stress provides the necessary conditions for sliding and formation of intraformational faults that break these sediments into smaller blocks .

A.4 Lithologic descriptions and interpreted depositional environments

The lithostratigraphic descriptions and sediment compositions were defined by analyzing the core samples and measuring their petrophysical properties at Sites M27- M29 (Mountain et al., 2010). Core analysis shows that two main lithologies and depositional environments existed at the time of sedimentation: 1) well-sorted sand and silt deposited in a mixed storm- and river-dominated shelf from near shoreface to offshore environments; and 2) poorly sorted coarse-grained debrites and turbidites with interbedded silt and silty clays deposited in intrashelf clinoform rollover, clinoform slope, and toe-of-slope settings (Mountain et al., 2010).

Late Eocene core samples were only cored at Site M27. Clay size sediments deposited in a deep marine environment form the dominant lithology (Katz et al., 2013).

o1-m6 (Oligocene to lowermost Miocene) displays large-scale upward coarsening from silt to very fine sand at the base to glauconite-rich, coarse-grained sand debrites and turbidites. This unit of sediments was cored at Site M27 and is the oldest stratigraphic unit at Site M28; these sediments comprise dark brown siltstone with thin-articulated shells deposited in a low-energy, deep-marine environment. A similar lithology was observed in the part of the unit penetrated at Site M29.

m6-m5.8 (upper Aquitanian to lower Burdigalian) records progradation of a storm-dominated and river-influenced delta over the toe-of-slope apron (Mountain et al., 2010). This unit of sediments comprises pale brown clayey silt with intercalated fine sand beds that represent a river-dominated prodelta environment (McCarthy et al., 2013; Miller, Mountain, et al., 2013).

m5.8-m5.4 (lower to mid-Burdigalian) was deposited on top of a falling stage systems tract and has a sharp stratigraphic boundary at its base. From bottom to top, the lithofacies change from poorly-sorted glauconitic sand to fine-grained silt and then to medium/coarse-grained sand. The environment of deposition is poorly constrained for this unit. The contact between this unit and the overlain unit at Site M28 is abrupt and bioturbated, consisting of poorly-sorted, coarse-

grained gravity-flow sediments. Farther basinward at Site M29, this unit comprises granuliferous quartz and coarse-grained glauconitic sands separated by bioturbated silt.

m5.4-m5.3 (mid to upper Burdigalian) shows a transition from a transgressive deepening-upward shoreface to an offshore succession without any regressive facies. At the top, an erosional surface separates this unit from the overlying unit. From Site M27 to Site M29, the lithofacies change basinward to gravity-flow sediments deposited by river flood events in an offshore environment.

m5.3-m5.2 (upper Burdigalian to lower Langhian) deposits at Site M27 represent a silty offshore and onshore-offshore transitional environment that shows both deepening- and shallowing-upward trends that are highly influenced by storm disturbances. This unit at Site M28 comprises four shallowing-upward subunits formed in a storm-dominated, river-influenced delta (Miller, Mountain, et al., 2013). The lowest subunit mainly comprises coarse-grained sand and gravel in a toe-of-clinoform apron setting. The second and third subunits comprise interbedded storm flow deposits of silt and sand representing a shoreface-offshore transitional setting. The upper subunit is made of clean quartz sandstone deposited in a shoreface environment.

m5.2-m4.1 (Langhian to upper Miocene) comprises a series of incomplete fining- and deepening-upward sedimentary cycles at Site M27. The depositional environment is considered to be a transgressive shoreface evolving to a shoreface-offshore transition with a clay-rich offshore succession at the top of the unit. This unit at Site M28 is formed by a series of offshore to shoreface cycles that are divided into several subunits. The lowest subunit is a mix of poorly-sorted sediments from mud to gravel that becomes finer uphole and was deposited at a clinoform rollover. The next subunit has a sharp contact with the underlying subunit and consists of shoreface-offshore transition deposits that are initially fine-grained and gradually coarsen uphole. In the uppermost subunit, a basal erosional surface is overlain by coarse- to fine-grained sand with glauconite grains indicating condensed deposition (hiatus), which is in turn overlain by clay deposited in an offshore environment (Mountain et al., 2010). The unit at Site M29 comprises a basal succession of silt and very fine-grained sandy silt that was deposited in a relatively deep offshore environment, overlain by a coarsening upward trend from medium-grained sand to silt. The unit is topped by poorly-sorted shelly silt with gravel. Sediment gravity-flow deposition on the clinoform slope may have occurred either within a submarine channel or

in a slope apron environment. The uppermost part of this unit II at Site M29 comprises silts and very fine sandy silts, which represent a river-influenced offshore environment.

m4.1-UP3 (upper Miocene-upper Pleistocene) is the shallowest unit sampled at the three sites. It comprises sand and gravels at Site M27, deposited in shoreface, coastal plain, estuarine, and incised valley environments. This unit was not cored at Site M28. However, at Site M29, it still comprises deposits from shallow marine shoreface to coastal plain and estuarine environments.

A.5 Petrophysical characteristics of the Miocene sedimentary record

Eocene-Oligocene sequences

Only site M27 reached Eocene-Oligocene sediments. Bio-stratigraphic analysis yields a paleo-water depth of 75 to 100 m at the time of deposition (Katz et al., 2013). Due to age and long-lasting over-burden pressure, these sediments are well consolidated and have high density and V_p relative to the younger sediments. The presence of Glauconite, with a density of up to 2.9 g/cm^3 and V_p of ~3 km/s (Hossain et al., 2011), further increases these properties of contaminated sediments. However, Eocene-Oligocene sequence boundaries are poorly resolved in the seismic and borehole data.

Sequence o1 contains the oldest seismic facies identified from both borehole and seismic data. The lower sequence boundary has a negative impedance contrast that separates glauconitic silty sand above from underlying fine-grained silt and clay, with significantly lower density and V_p values. The o1 sequence boundary is not well resolved in the seismic amplitude section (Figure 3.8), but it can be mapped by following the contrast in the inverted V_p and density sections (Figures 3.10 and 3.12). Overall, the predicted clay volume shows an upward increase in grain size within the sequence (Figure 3.13). From bottom to top, the strata within the sequence upstep and forestep, representing a period of normal regression. The o1 sequence boundary represents a distinct erosional surface at Site M27 (Miller, Mountain, et al., 2013).

The sediments deposited in the late Oligocene are mainly glauconitic clay and silt, with a positive impedance contrast at the boundary with the underlying sediments. From bottom to top, an increase in the concentration of glauconite boosts the predicted density and V_p values. This high-density and high-velocity layer gradually disappears at the clinoform toe, as a result of a decrease in glauconite content and increase in clay content.

Late Oligocene- Middle Miocene

Sequence m6

Sequence boundary m6 is associated with a negative impedance contrast caused by higher glauconite concentration in the overlying sediments. The forced regression observed in the stratal stacking pattern corresponds to the forestepping and downstepping of these sediments. The thickness of sequence m6 is not constant and decreases basinward toward the clinoform toe. The predicted V_p and density are high within the sequence and gradually increase from bottom to top and from proximal to distal areas (Figures 3.10 and 3.12). V_p decreases from foreset to bottomset, possibly because the sandy foreset dewatered faster than the fine-grained bottom sets; finer grain size and lower glauconite content in the bottomset can also amplify this drop in V_p. Sequence m6 was penetrated only at Site M27.

Sequence m5.8

The lower boundary of sequence m5.8 separates underlying interbedded glauconite sand and clay from quartzose glauconite sandstone above with a resultant downward increase in acoustic impedance. As the depositional environment progressively changes to offshore prodelta during deposition of sequence m5.8, the clay volume consistently increases from the foreset toward the bottomset (Miller, Mountain, et al., 2013). With respect to underlying sequence m6, sequence m5.8 shows normal regression with progradation and aggradation. At the base of this sequence, the predicted images of petrophysical properties show a thin layer with locally high velocity and density, characterized by larger grain size and interpreted as a lowstand systems tract (Figures 3.10 and 3.12) (Miller, Browning, et al., 2013). In NE-SW direction, the onlapping strata backstep and upstep and progradational stratal pattern that spread out to the toe and lower part of clinoform rollover. The overlying strata show upstepping and backstepping (aggradation and progradation) simultaneously and represent a highstand systems tract (HST).

Sequence m5.7

In the transition from sequence 5.8 to 5.7, V_p and density values show a jump to higher values and continuously increase through sequence 5.7 from bottom to top. Velocity and density both decline from the topset toward the clinoform toe (Figures 3.10 and 3.12). The cored sediments at Sites M27- M29 show a similar trend in sediment grain size, which becomes finer from M27 to M29. The coarsening upward trend in sequence m5.7 and the normal regressive stacking patterns reflect a HST. In a higher hierarchical order, strata within the sequence show progradation and a

down stepping stacking pattern. A drop in accommodation, or higher sediment supply during the time of sedimentation are among the factors that could result in a such a stacking pattern. However, the overall stacking pattern for the sequence shows normal regression.

Sequence m5.6

The m5.6 sequence boundary, cored only at Sites M28 and M29, is associated with a major negative acoustic impedance contrast. From the bottomset to topset, core samples from both sites show a rapid increase in glauconite deposition in fine- to coarse-grained sands.

Sequence m5.4

An erosional surface represents the sequence boundary separating the overlying glauconite sands of sequence m5.4 from underlying sediments (Mountain et al., 2010). the boundary can be traced as a positive reflector with a high seismic amplitude. The inverted elastic properties (Figure 3.10-3.13) sequence comprises several internal layers. The predicted V_p and density vary periodically from medium to high within the internal layers; however, they are uniform across the dip profiles (Figure 3.10 and 3.12). The grain size coarsens upward within the sequence. The stacked sediments from the top of sequence boundary m5.7 to the bottom of m5.2 show progradation and aggradation and the rate of progradation increases over time. The upper part of the sequence has an aggradational trend with consistent thickness from SW to NE.

Sequence m5.2

Sequence m5.2 features an overall upward coarsening trend iso observed at all three IODP sites. Elastic properties are inverted, with an increase in density toward the top of the sequence, reaching a maximum at the upper sequence boundary (Figure 3.12). The 3D seismic images revealed an array of extensional faults within the fine-grained stratigraphic intervals in the clinoform toe, where the seismic velocity gradually increases downdip ; this increase in V_p and presence of a polygonal fault system basinward of the clinoform toe (Figure 3.14) are attributed to consolidation and dewatering of the most deeply buried part of the sequence. These normal faults have modest throws of up to 15 meters and form polygonal patterns in map view (Figure 3.14). The predicted clay content reveals a succession of clay-rich and sandy sediments within m5.2 that covers the entire area basinward of the clinoform toe (3.13). Differential compaction of these layers might have resulted in pressure build-up and consequent hydraulic fracturing of these layers (Cartwright, 1994b, 1994a).

Sequence m4

Sequence m4 is subdivided into several subsequences of higher hierarchical order (Browning et al., 2013; Mountain et al., 2010). The sequence boundary for subsequence m4.5 is characterized by a strong reflection at Site M27, which gradually weakens basinward. The boundary defines a lithologic contact of silty clay overlying a layer of coarse sand. Basinward at Sites M28 and M29, the average grain size of the underlain sand decreases. Similar trends are observed in the predicted density and V_p that decrease the impedance contrast across subsequence boundary m4.5. Subsequence m4.5 foresteps and downsteps basinward, representing a period of forced regression. The highly truncational boundary of subsequence m4.3 is located where shelly sand at the base of subsequence m4.3 overlies silty clay. from the subsequence boundaries m4.3 to m4.2, the depositional trend changes to progradation. The m4.2 subsequence boundary separates silty clay from overlaying fine-grained sands and has been identified only at Site M29. The erosion associated with subsequence boundary m4.2 suggests that subsequence m4.2 may be a lowstand systems tract (LST) (Miller, Browning, et al., 2013). Even though the estimated paleo-water depth from analyzing benthic foraminiferal in subsequent m4.2 shows stable water-depth over the geological time (Katz et al., 2013), the presence of several erosional surfaces at the clinoform topset and absence of subsequence m4.2 at Sites M27 and M28 suggest that a high rate of sediment supply suppressed the available accommodation and eroded the clinoform top. The transition from subsequence m4.2 to subsequence m4.1 is associated with a rapid increase in paleo-water depth (from ~50m to ~100m) (Katz et al., 2013), represented by deposition of silty clays above the subsequence boundary overlying fine-grained sands below, which resulted in a strong and continuous reflection from the sequence boundary. Poor core recovery within subsequence m4.1 and younger sediments increases the uncertainty in sequence stratigraphic analysis of core samples. However, the 3D seismic data distinguish eight units within subsequence m4.1. We traced facies package m4.18 only in the northern part of the 3D volume, where it downlaps onto the clinoform topset of subsequence boundary m4.1. While no cores are available from this interval, the predicted V_p and density values increase upsection, which can be attributed to higher grain size. Within the facies package m4.17, the stratal stacking patterns show downstepping and forestepping during a period of forced regression that decelerates over time and transforms to aggradation in subsequence m4.16. The stratal stacking patterns above m4.16 reveal a second cycle of forced regression that gradually decelerates and converts to

normal regression at the top of m4.1. The sediments above subsequence m4.1 are of upper-middle Miocene and younger ages. There is limited facies information available about these sediments; however, other studies consider them to be mainly fluvial and partially associated with paleosols (Browning et al., 2013; Miller, Mountain, et al., 2013).

A.6 Perspective view of seismically defined systems tracts on the New Jersey shelf

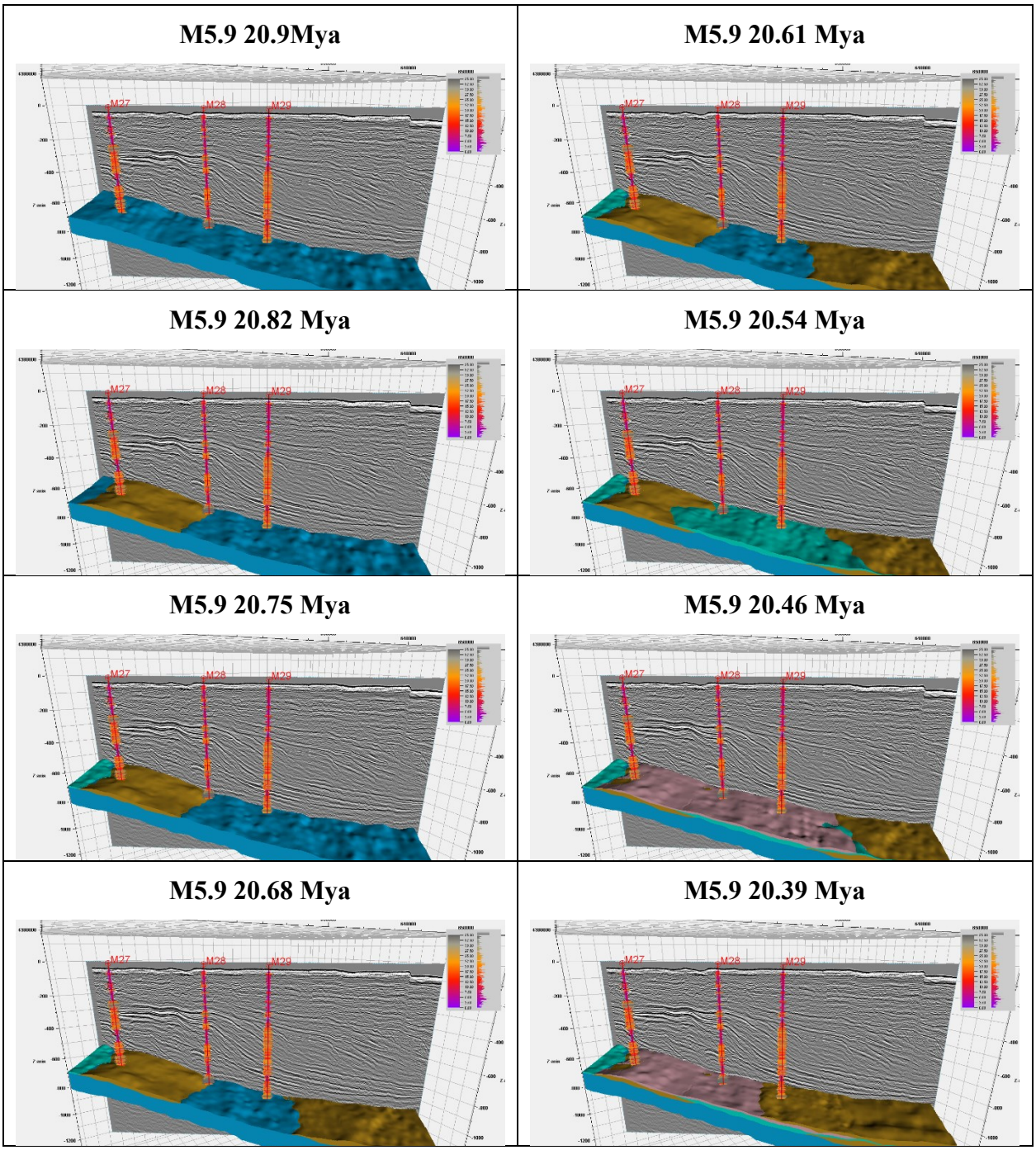
M5.9 20.9Mya
M5.9 20.61 Mya
M5.9 20.82 Mya
M5.9 20.54 Mya
M5.9 20.75 Mya
M5.9 20.46 Mya
M5.9 20.68 Mya
M5.9 20.39 Mya
M27
M28
M29
Falling Stage Systems Tract
Highstand Systems Tract
Transgressive Systems Tract
Lowstand Systems Tract
Clay
Sand

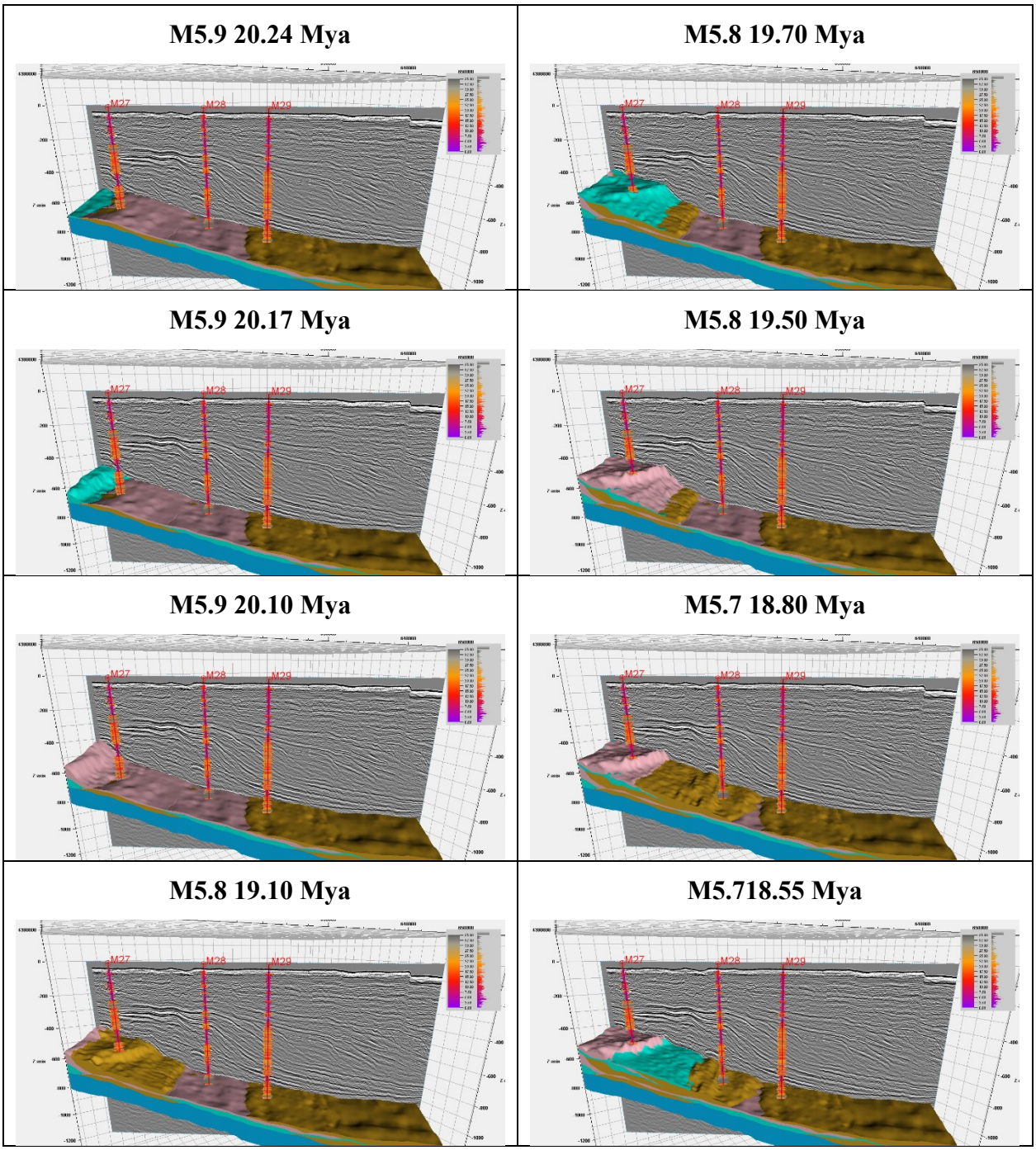
M5.9 20.24 Mya
M5.8 19.70 Mya
M5.9 20.17 Mya
M5.8 19.50 Mya
M5.9 20.10 Mya
M5.7 18.80 Mya
M5.8 19.10 Mya
M5.718.55 Mya
M27
M28
M29
Falling Stage Systems Tract
Highstand Systems Tract
Transgressive Systems Tract
Lowstand Systems Tract
Clay
Sand

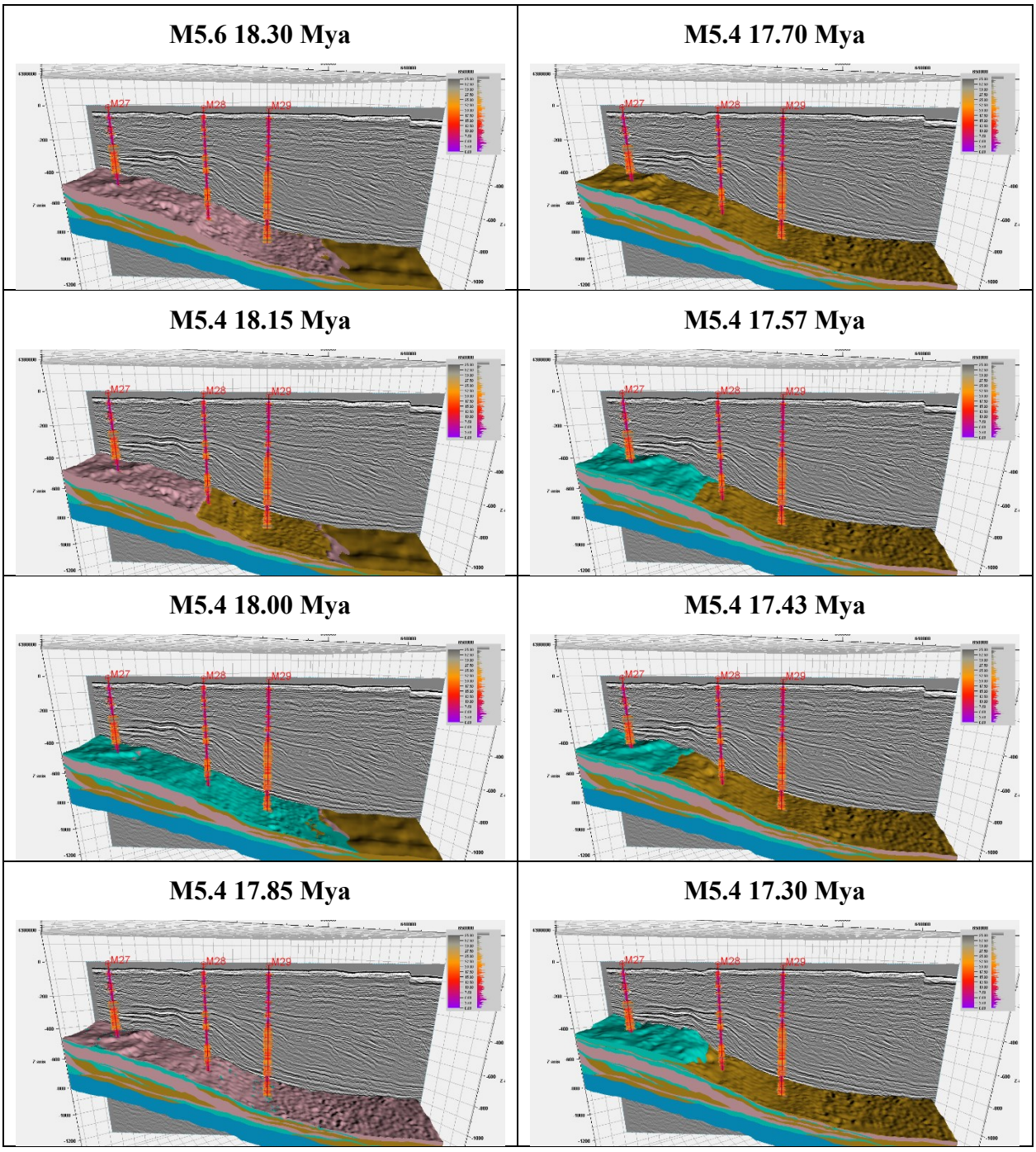
M5.6 18.30 Mya
M5.4 17.70 Mya
M5.4 18.15 Mya
M5.4 17.57 Mya
M5.4 18.00 Mya
M5.4 17.43 Mya
M5.4 17.85 Mya
M5.4 17.30 Mya
M27
M28
M29
Falling Stage Systems Tract
Highstand Systems Tract
Transgressive Systems Tract
Lowstand Systems Tract
Clay
Sand

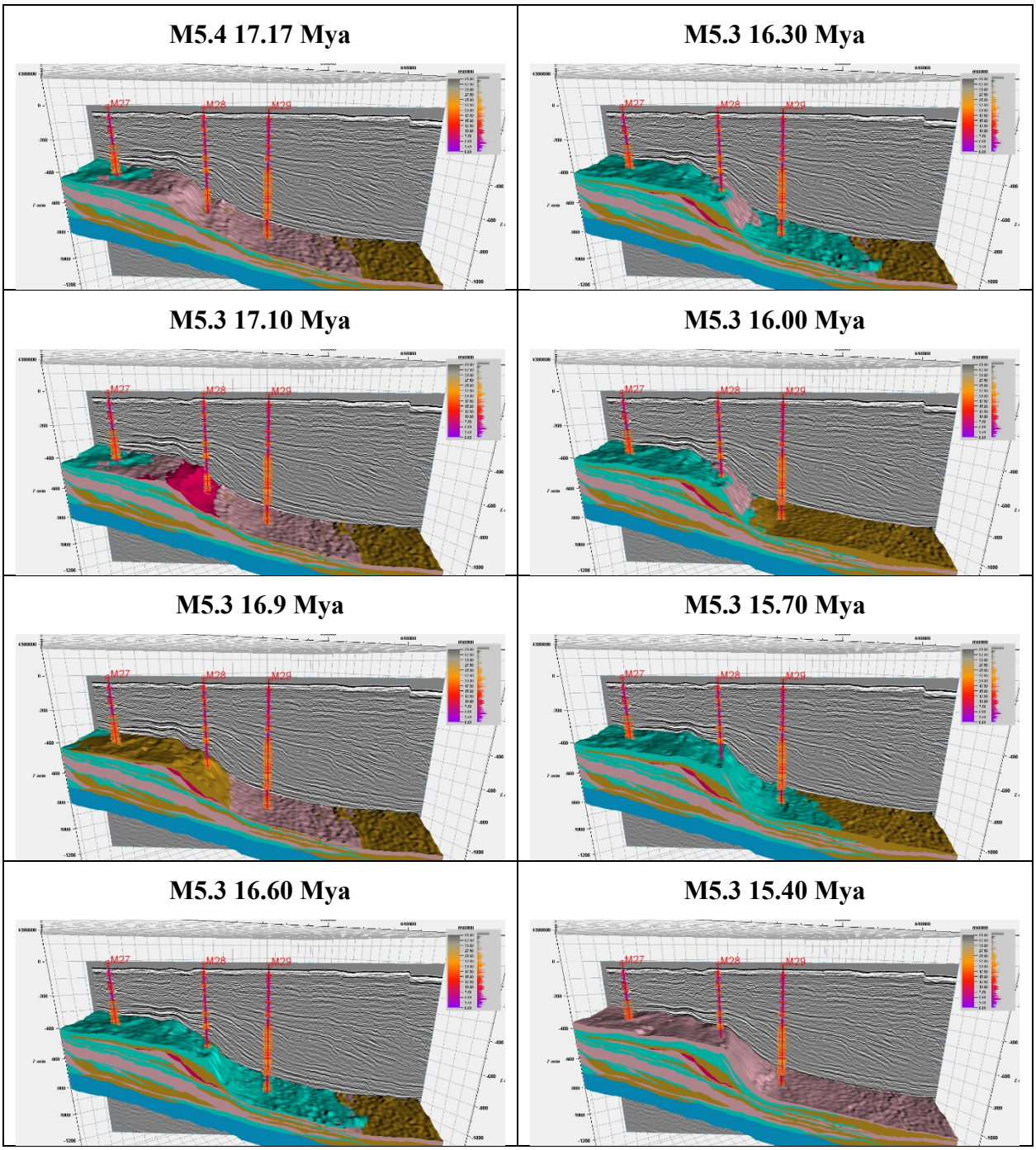
M5.4 17.17 Mya
M5.3 16.30 Mya
M5.3 17.10 Mya
M5.3 16.00 Mya
M5.3 16.9 Mya
M5.3 15.70 Mya
M5.3 16.60 Mya
M5.3 15.40 Mya
M27
M28
M29
Falling Stage Systems Tract
Highstand Systems Tract
Transgressive Systems Tract
Lowstand Systems Tract
Clay
Sand

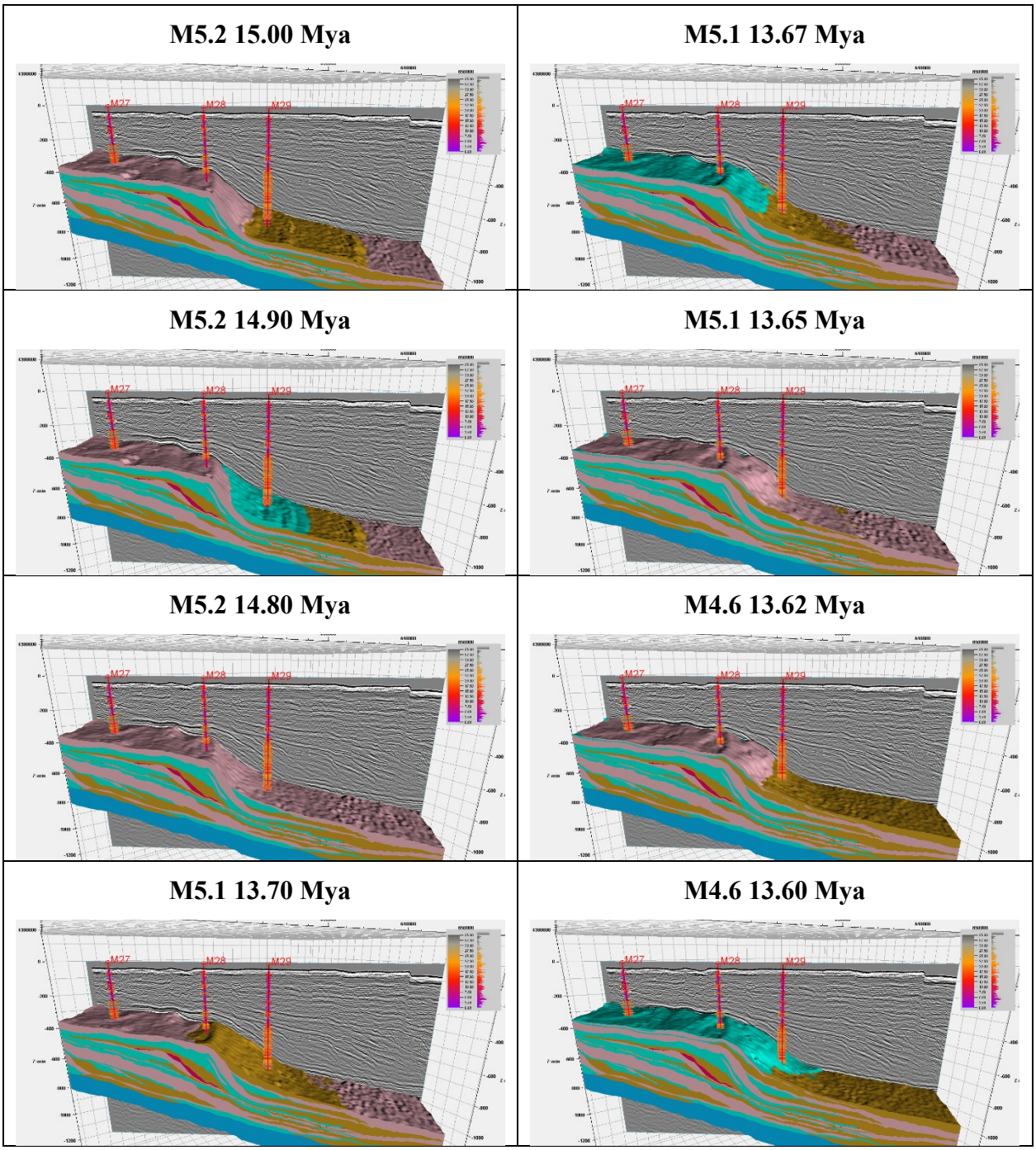
M5.2 15.00 Mya
M5.1 13.67 Mya
M5.2 14.90 Mya
M5.1 13.65 Mya
M5.2 14.80 Mya
M4.6 13.62 Mya
M5.1 13.70 Mya
M4.6 13.60 Mya
M27
M28
M29
Falling Stage Systems Tract
Highstand Systems Tract
Transgressive Systems Tract
Lowstand Systems Tract
Clay
Sand

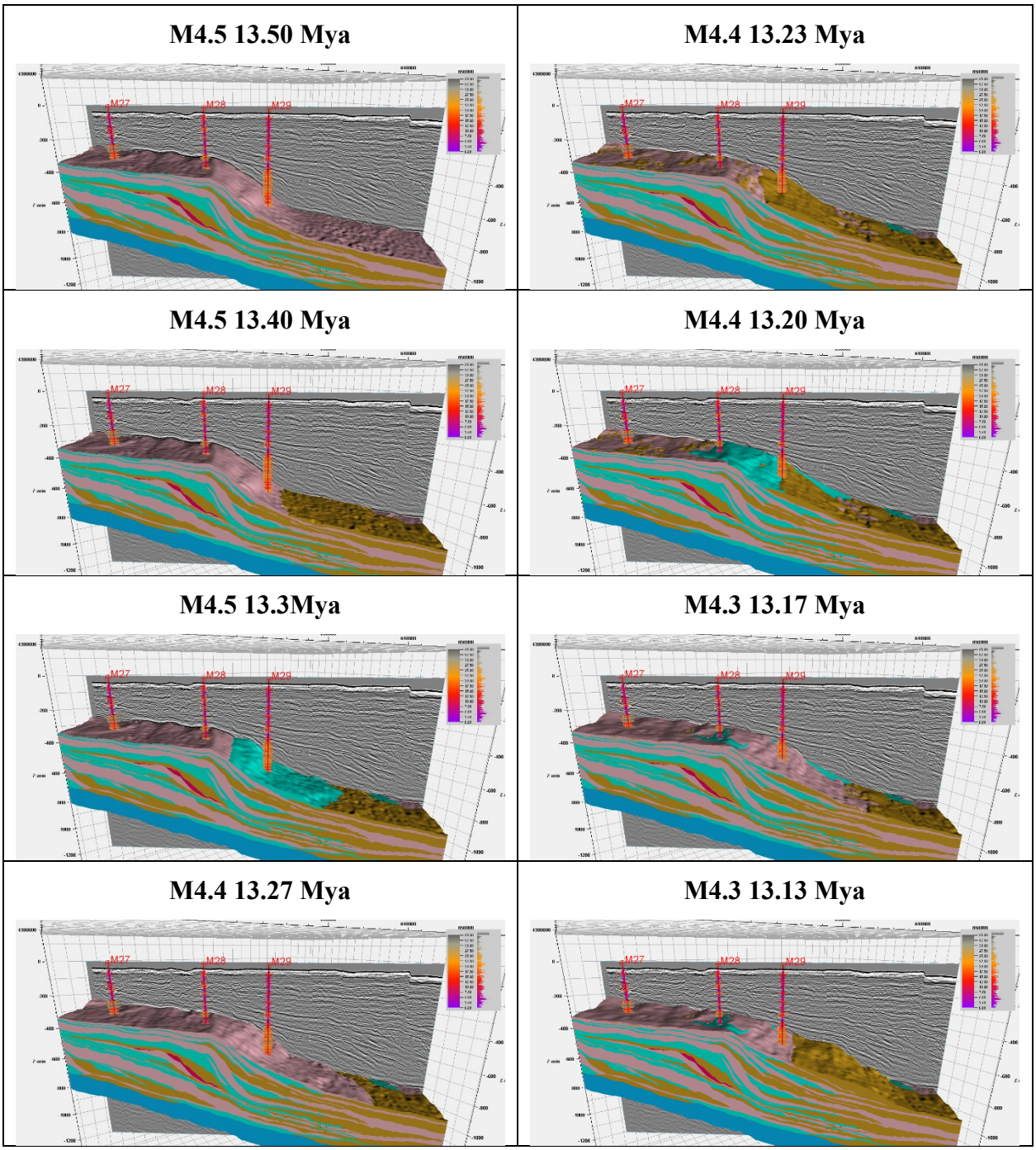
M4.5 13.50 Mya
M4.4 13.23 Mya
M4.5 13.40 Mya
M4.4 13.20 Mya
M4.5 13.3Mya
M4.3 13.17 Mya
M4.4 13.27 Mya
M4.3 13.13 Mya
M27
M28
M29
Falling Stage Systems Tract
Highstand Systems Tract
Transgressive Systems Tract
Lowstand Systems Tract
Clay
Sand

M4.3 13.10 Mya

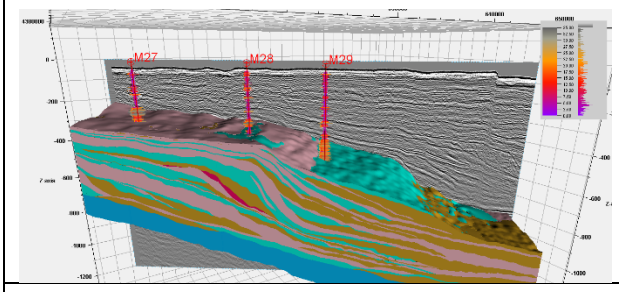

M4.2 13.02 Mya

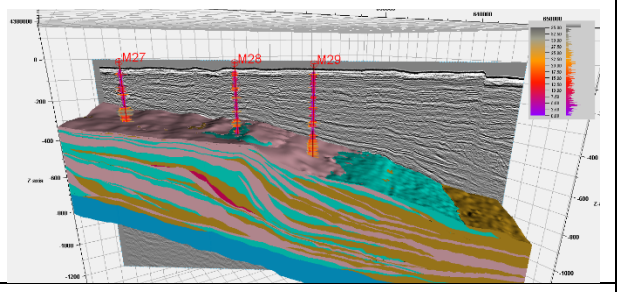

M4.2 13.08 Mya

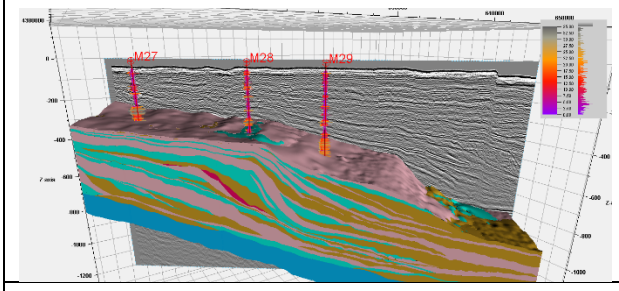

M4.2 13.00 Mya

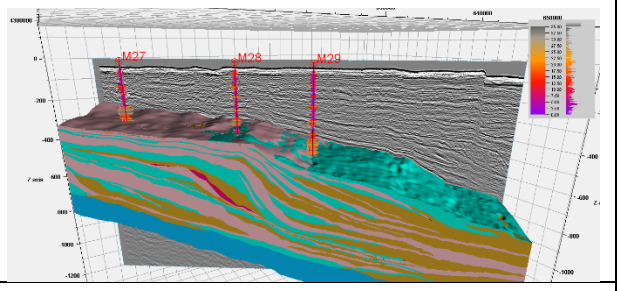

M4.2 13.06 Mya

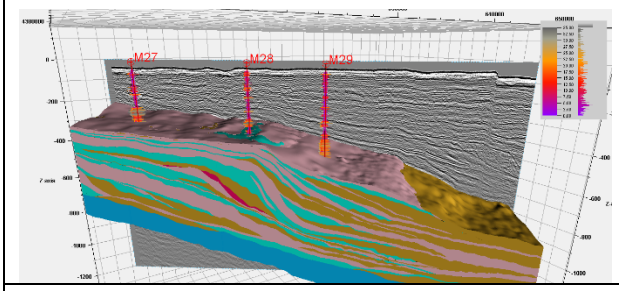

M4 12.98 Mya

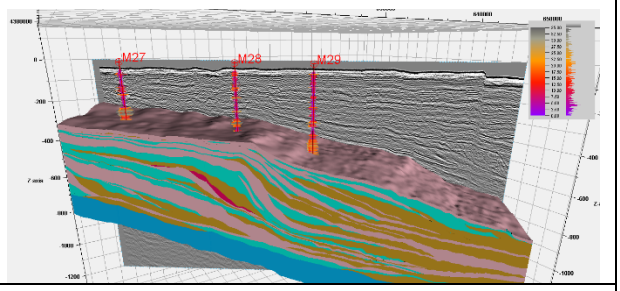

M4.2 13.04 Mya

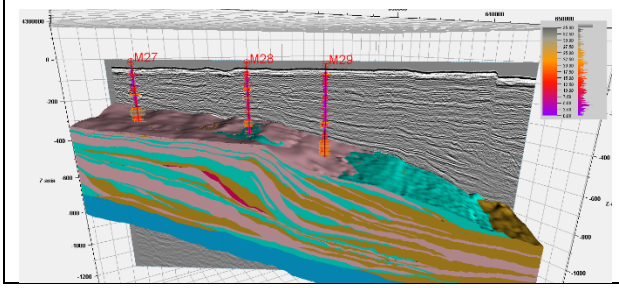

M4 12.95 Mya

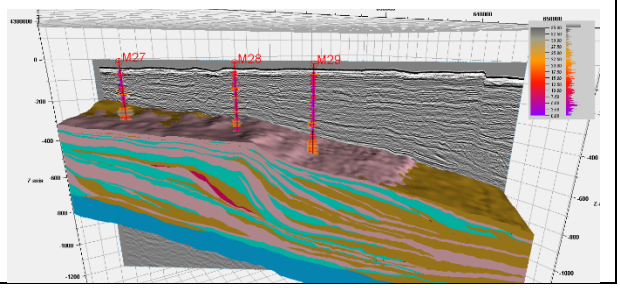

Falling Stage Systems Tract
Highstand Systems Tract
Transgressive Systems Tract
Lowstand Systems Tract

Clay
Sand

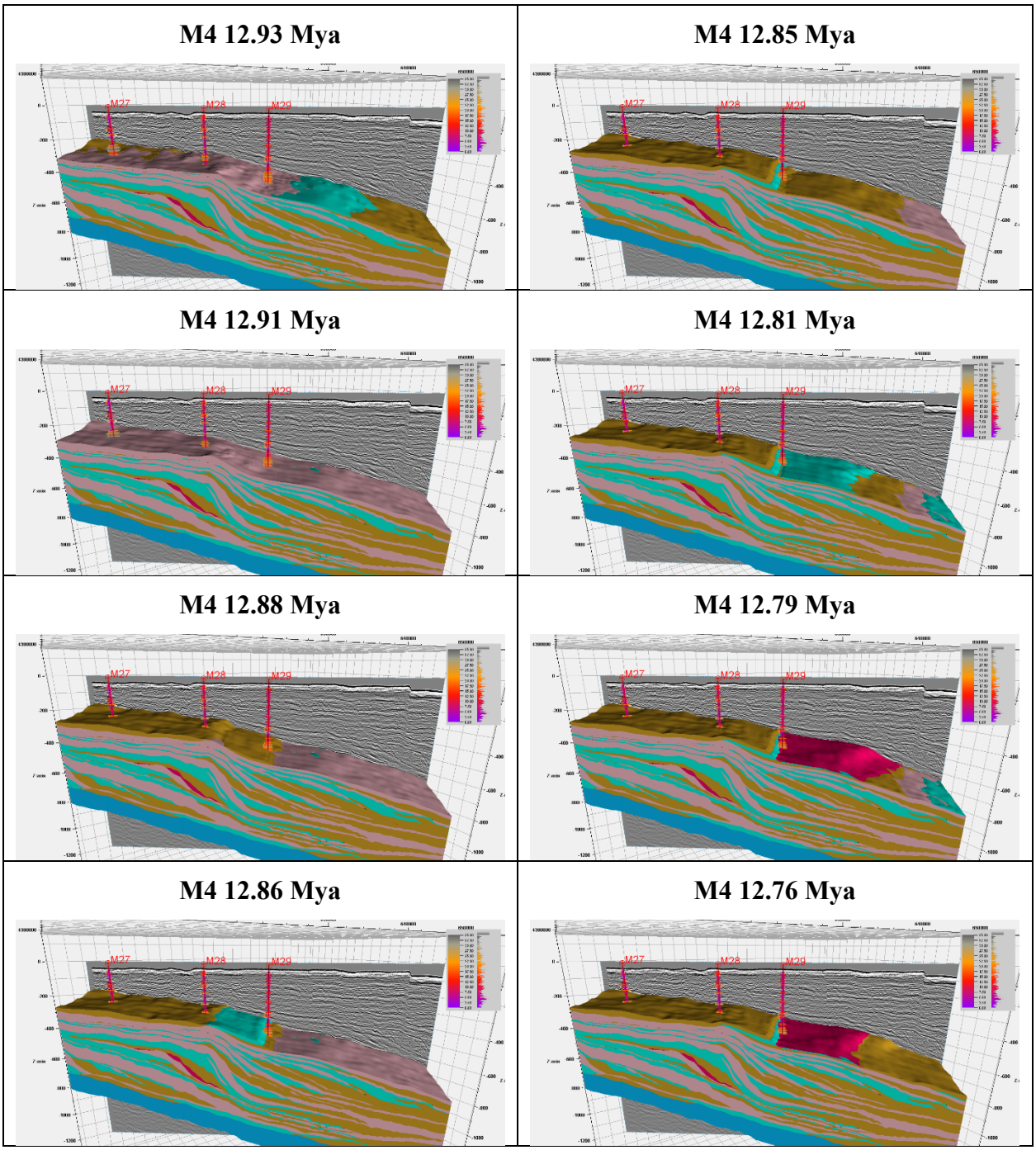
M4 12.93 Mya
M4 12.85 Mya
M4 12.91 Mya
M4 12.81 Mya
M4 12.88 Mya
M4 12.79 Mya
M4 12.86 Mya
M4 12.76 Mya
M27
M28
M29
Falling Stage Systems Tract
Highstand Systems Tract
Transgressive Systems Tract
Lowstand Systems Tract
Clay
Sand

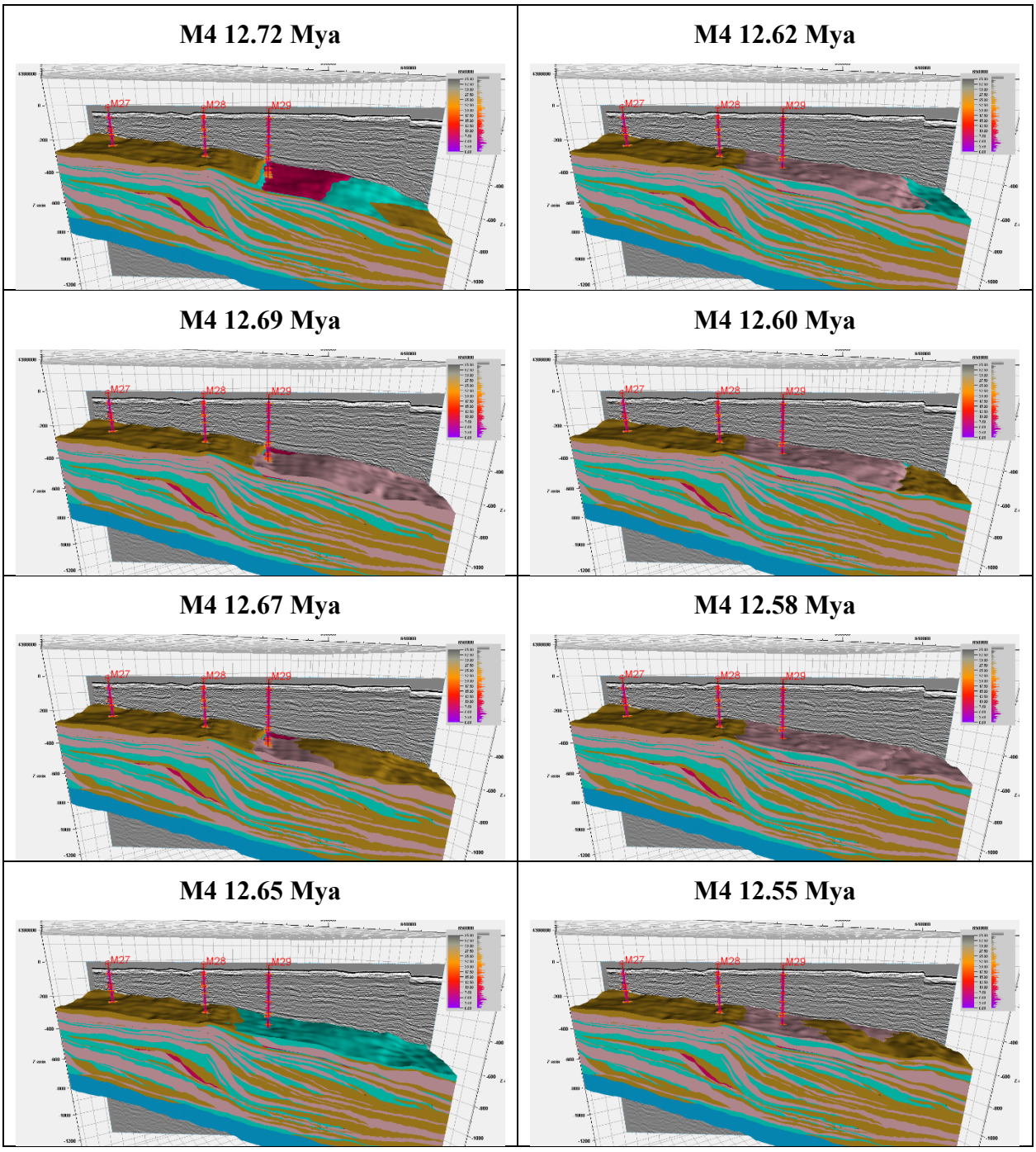
M4 12.72 Mya
M4 12.62 Mya
M4 12.69 Mya
M4 12.60 Mya
M4 12.67 Mya
M4 12.58 Mya
M4 12.65 Mya
M4 12.55 Mya
M27
M28
M29
Falling Stage Systems Tract
Highstand Systems Tract
Transgressive Systems Tract
Lowstand Systems Tract
Clay
Sand